UNIFORMED SERVICES UNIVERSITY OF THE HEALTH SCIENCES
F. EDWARD HÉBERT SCHOOL OF MEDICINE
4301 JONES BRIDGE ROAD
BETHESDA, MARYLAND 20814-4799

August 10, 2006

APPROVAL SHEET

Title of Dissertation: "The Molecular Basis of Canavan Disease: Aspartoacylase Enzyme Characteristics"

Name of Candidate: Jeremy Hershfield
Doctor of Philosophy Degree
15 September 2006

Dissertation and Abstract Approved:

_____   _____9/25/06_____
Teresa Dunn, Ph.D.   Date
Department of Biochemistry & Molecular Biology
Committee Chairperson

_____   _____9/15/06_____
Aryan Namboodiri, Ph.D.   Date
Department of Anatomy, Physiology & Genetics
Committee Member
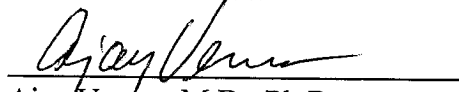
_____   _____9-15-06_____
Thomas Cote, Ph.D.   Date
Department of Pharmacology
Committee Member

_____   _____9-15-06_____
Ajay Verma, M.D., Ph.D.   Date
Department of Neurology
Committee Member

_____   _____9-15-06_____
T. John Wu, Ph.D.   Date
Department of Obstetrics & Gynecology
Committee Member

Report Documentation Page		*Form Approved* *OMB No. 0704-0188*
Public reporting burden for the collection of information is estimated to average 1 hour per response, including the time for reviewing instructions, searching existing data sources, gathering and maintaining the data needed, and completing and reviewing the collection of information. Send comments regarding this burden estimate or any other aspect of this collection of information, including suggestions for reducing this burden, to Washington Headquarters Services, Directorate for Information Operations and Reports, 1215 Jefferson Davis Highway, Suite 1204, Arlington VA 22202-4302. Respondents should be aware that notwithstanding any other provision of law, no person shall be subject to a penalty for failing to comply with a collection of information if it does not display a currently valid OMB control number.		

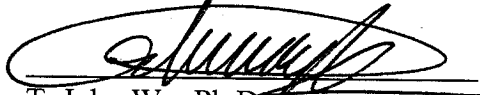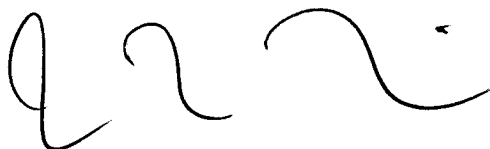| 1. REPORT DATE **2006**	2. REPORT TYPE	3. DATES COVERED **00-00-2006 to 00-00-2006**
4. TITLE AND SUBTITLE **The Molecular Basis of Canavan Disease: Aspartoacylase Enzyme Characteristics**		5a. CONTRACT NUMBER
		5b. GRANT NUMBER
		5c. PROGRAM ELEMENT NUMBER
6. AUTHOR(S)		5d. PROJECT NUMBER
		5e. TASK NUMBER
		5f. WORK UNIT NUMBER
7. PERFORMING ORGANIZATION NAME(S) AND ADDRESS(ES) **Uniformed Services University of the Health Sciences,F. Edward Hebert School of Medicine,4301 Jones Bridge Road,Bethesda,MD,20814-4799**		8. PERFORMING ORGANIZATION REPORT NUMBER
9. SPONSORING/MONITORING AGENCY NAME(S) AND ADDRESS(ES)		10. SPONSOR/MONITOR'S ACRONYM(S)
		11. SPONSOR/MONITOR'S REPORT NUMBER(S)

12. DISTRIBUTION/AVAILABILITY STATEMENT **Approved for public release; distribution unlimited**
13. SUPPLEMENTARY NOTES **The original document contains color images.**
14. ABSTRACT
15. SUBJECT TERMS

16. SECURITY CLASSIFICATION OF:			17. LIMITATION OF ABSTRACT	18. NUMBER OF PAGES **199**	19a. NAME OF RESPONSIBLE PERSON
a. REPORT **unclassified**	b. ABSTRACT **unclassified**	c. THIS PAGE **unclassified**			

Standard Form 298 (Rev. 8-98)
Prescribed by ANSI Std Z39-18

COPYRIGHT STATEMENT

The author hereby certifies that the use of any copyrighted material in the thesis

manuscript entitled:

"The Molecular Basis of Canavan Disease: Aspartoayclase Enzyme Characteristics"

is appropriately acknowledged and, beyond brief excerpts, is with the permission of the

copyright owner.

Jeremy Ray Hershfield
Molecular and Cell Biology Program
Uniformed Services University of the Health Sciences

ABSTRACT

Title of Dissertation: "The Molecular Basis of Canavan Disease: Aspartoacylase
                            Enzyme Characteristics"

Author: Jeremy Ray Hershfield, Ph.D., 2006

Dissertation Directed By: Aryan M.A. Namboodiri, Ph.D.
                           Associate Professor
                           Department of Anatomy, Physiology, and Genetics

Mutations in the gene for aspartoacylase (EC 3.5.1.15; ASPA), which catalyzes deacetylation of N-acetyl-L-aspartate (NAA), correlate with Canavan Disease (CD), a neurodegenerative disorder usually fatal during childhood. Defective ASPA activity has been linked to characteristically elevated NAA levels in the urine of CD patients, and ASPA knockout mice and ASPA deletion rats display CD-like symptoms. While efforts have focused on treating CD, there is limited evidence to support ASPA protein regulation.

The ASPA enzyme is thought to be cytoplasmic. In this dissertation, we used immunohistochemistry to show ASPA within nuclei of rat brain oligodendrocytes, in rat kidney proximal tubule cells, and in cultured mouse and rat oligodendrocytes. Subcellular fractionation analysis from wild-type rats revealed low enzyme activity against NAA in nuclear fractions. While two recent reports have indicated that ASPA is a dimer, size-exclusion chromatography of both nuclear and cytoplasmic fractions showed ASPA is an active monomer. Since ASPA is small enough to passively diffuse through the nuclear pore complex, we constructed, expressed, and detected in COS-7 cells a green fluorescent protein-human ASPA fusion protein. The mixed nuclear-

cytoplasmic localization of GFP-hASPA demonstrated that the subcellular localization of ASPA is regulated.

We then investigated regulation of the ASPA protein at the structural level. A recent alignment study identified ASPA as a member of the carboxypeptidase A (CPA) family. Therefore, we developed and tested a three-dimensional homology model of ASPA based on CPA. Mutations of the putative zinc-binding residues (H21G, E24D, and H116G), the general proton donor (E178A), and mutants designed to switch the order of the zinc-binding residues (H21E/E24H and E24H/H116E) were created and expressed in COS-7 cells. Each mutation yielded wild-type ASPA protein levels, but undetectable ASPA activity. Finally, the analysis of several CD-associated ASPA missense mutations provided a molecular basis for how mutations result in ASPA deficiency.

In summary, we have shown that the ASPA enzyme is regulated by its subcellular localization, multimeric state, and innate structure. These studies provide insight into the physiology of the ASPA reaction and the molecular basis of CD.

The Molecular Basis of Canavan Disease:

Aspartoacylase Enzyme Characteristics

By

Jeremy Ray Hershfield

Dissertation submitted to the Faculty of the

Molecular and Cell Biology Program

Uniformed Services University of the Health Sciences

In partial fulfillment of the requirements for the degree of

Doctor of Philosophy, 2006

DEDICATION

I dedicate this dissertation to my sister, Beryl, whose life was tragically cut short by Canavan Disease, and to my late grandmother, Ada Alderman, whose love and friendship guided me throughout my life.

ACKNOWLEDGMENTS

This dissertation is the amalgamation of the extraordinary efforts of several individuals who helped me to survive graduate school and who assisted me with the science and the means to produce this written document.

First, I would like to thank my mentor, Dr. Namboodiri for guiding me through several projects and allowing me to participate in national conferences. Most importantly, I would like to thank him for acquiring the assistance of others to help submit and publish the work presented in this dissertation. A fair amount of work toward the first manuscript had been done before my arrival in the lab, most notably by Drs. Murtie, Armstrong, Jacobowitz, and Madhavarao. I spent many hours corresponding by e-mail, and in person, with Dr. Garbern, our collaborator at Wayne State University, whose help guaranteed publication of the first manuscript. The same approach with Pat, our structural biologist collaborator from Georgetown University, enabled me to rapidly complete and submit the second manuscript. In addition, I am forever indebted to Drs. Arun and Madhavarao for helping me learn the inner workings of the lab and, in particular to Madhav, for teaching me several invaluable bench and scientific techniques.

I am grateful to the members of my thesis committee, Drs. Dunn, Wu, Cote, Verma, and Namboodiri, for pushing me toward graduation in the allotted time. In particular, I would have been unable to complete my dissertation requirements without Dr. Wu's tireless efforts with methods, data interpretation, editing this written document, and many hours of frank discussion about what it means to be a Ph.D.

While several people helped me to earn my Ph.D., my acknowledgements would not be complete without thanking friends and family who helped me survive my time as a graduate student. By way of sweeping generalization, I'd like to thank the Lymphomaniacs, DH5-α, the lunch table gangs, the rest of my MCB class, and various friends from WWPHS and Cornell. Separately, I'd like to thank Nicole Flint and Ashley Stone, who physically edited this entire document *twice*! Lastly, I thank my lovely girlfriend, Megan Rose Masterson, who fell in love with me when times were at their worst: experiments were failing, my time was short, and I contracted shingles *and* scabies. This woman is an absolute godsend to me and not a day goes by that I don't thank God for us meeting and falling in love here at USUHS.

In closing, I'd like to thank my mother and father, both Ph.D.s in their own right, for raising yet another Jewish doctor by instilling in me academic diligence and for helping me with the decisions that will hopefully propel me to a successful career in research. I would also like to thank my older brother, Mark. I was the Robin to his Batman when we were kids and now he makes a great "little brother" and housemate to me in our early adult years.

TABLE OF CONTENTS

LIST OF TABLES AND FIGURES

Chapter 1

Chapter 2

Chapter 3

Chapter 4

LIST OF ABBREVIATIONS

α-βT	monoclonal antibody against β-tubulin
αASPA	polyclonal antibody against full-length recombinant murine ASPA
ACOG	American College of Obstetricians and Gynecologists
Asp-NAT	aspartate-*N*-acetyl transferase
ASPA	aspartoacylase
ATT	aspartate aminotransferase
BDNF	brain-derived neurotrophic factor
BSA	bovine serum albumin
CD	Canavan Disease
CNS	central nervous system
CPA	carboxypeptidase A
DAPI	4',6'-diamidino-2-phenylindole
DMEM	Dulbecco's modified Eagle medium
DTT	dithiothreitol
EC	enzyme classification
ER	endoplasmic reticulum
ES	embryonic stem
FBS	fetal bovine serum
GABA	γ-aminobutyric acid
GFP	green fluorescent protein
GFP-hASPA	N-terminal GFP-hASPA fusion protein
GTA	glycerol triacetate
hASPA	native untagged human ASPA
HB	homogenization buffer
HEK	human embryonic kidney
HPLC	high performance liquid chromatography
LDH	lactate dehydrogenase
mASPA	native untagged murine ASPA
MOG	myelin oligodendrocyte glycoprotein

NAA	N-acetyl-L-aspartate
NAAG	*N*-acetylaspartylglutamate
NaDC3	sodium dicarboxylate
NIM	nuclear isolation medium
NLS	nuclear localization signal
NPC	nuclear pore complex
nuc-GFP	nuclear GFP
OL	oligodendroycte
OP	orthophenantroline
PBS	phosphate buffered saline
pepASPA	polyclonal antibody against a conserved ASPA peptide
PNGase F	peptide N-glycosidase F
PCR	polymerase chain reaction
TLC	thin-layer chromatography
UTR	untranslated region
WGA	wheat germ agglutin
WT	wild-type
ZnCPA	zinc-dependent carboxypeptidase A

CHAPTER 1

Introduction

Central Hypothesis and Specific Aims

Canavan Disease (CD), also known as spongy degeneration of the central nervous system (CNS), is a fatal neurodegenerative autosomal recessive disorder linked to defects in the enzyme aspartoacylase (EC 3.5.1.15; ASPA) (3, 4). The carrier rate of CD among Ashkenazi (Eastern European) Jews is between 1/41 and 1/57 (5-7), and several ASPA mutations have been associated with CD with increasing frequency in other populations (8-16).
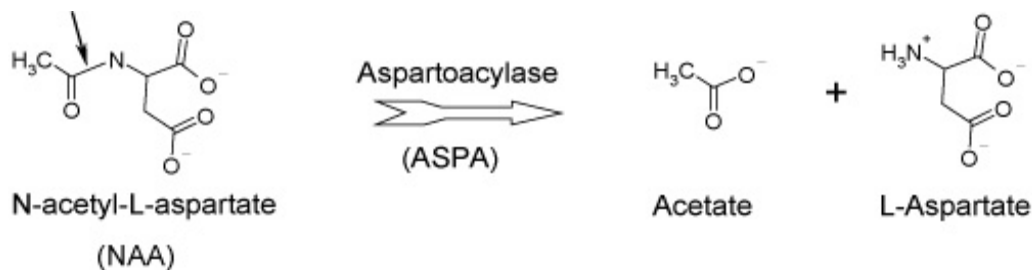
Figure 1. **The ASPA reaction.** ASPA catalyzes hydrolysis of NAA to yield free acetate and aspartate. The arrow depicts the hydrolyzed C-N peptide bond.

The ASPA enzyme catalyzes the deacetylation of *N*-acetyl-L-aspartate (NAA) to generate acetate and aspartate (Figure 1) (3). Deficient ASPA activity is the only known mechanism to account for CD. Further support for ASPA's role in CD comes from animal models in which mice and rats with this deficiency display CD-like symptoms (17, 18).   Characteristic CD pathology is marked by early onset and progressive

macrocephaly (head enlargement), brain vacuolization, and symptoms related to dysmyelination, including head-lag, ataxia, and severe psychomotor retardation (6). While a typical disease progression for CD results in childhood mortality, there are several reports of clinically protracted disease courses (5, 7, 8, 10-14, 16).

Even though the biochemical link between CD and ASPA deficiency is well-established (4), much work is needed to elucidate the physiological role of ASPA and its role in CD etiology. The ASPA protein has been purified from several sources and its enzyme kinetics and specificity have been well-characterized (19-23). However, there is limited evidence pertaining to ASPA protein regulation.

The ASPA protein is likely regulated by its localization within tissues and within cells. The ASPA enzyme and the NAA substrate are found in different cell types within the CNS. Located primarily in neurons of the CNS (24), NAA is the second most abundant free amino acid or amino acid derivative in the CNS (25), and it is believed to function as a storage molecule for free aspartate and acetate (26), as well as a molecular water pump in the brain (27). As a negatively charged molecule (Figure 1), NAA is surrounded by a hydration shell. Therefore, the concomitant accumulation of NAA and water might play a role in brain vacuolization observed in CD.

The ASPA enzyme is found primarily in oligodendrocytes (OLs) (28-31). Although the OL-specific localization of ASPA helps explain the dysmyelination that is observed in CD, the basis of this cellular restriction is unknown. Furthermore, the function of the ASPA enzyme outside the CNS is unknown.

Although NAA normally is undetectable in peripheral tissues (32-34), the expression of the ASPA enzyme is much higher in the kidney than in the CNS. One possible explanation is that NAA hydrolysis in the kidney is very efficient and is carried out at a higher rate. In support of this theory, NAA levels are highly elevated in the urine of CD patients (35). The abundance of ASPA enzyme in the kidney makes this an important model for analyzing ASPA protein characteristics and for elucidating its possible functions outside the CNS.

The subcellular localization of the ASPA enzyme is also unclear. Although previous activity analyses have shown that ASPA is strictly cytoplasmic (36) or partially membrane-bound (20, 37), there have not been detailed antibody-based studies to clarify where ASPA protein resides within cells. The ASPA enzyme might also be regulated by its multimeric state, which could influence its subcellular localization. Although there is some evidence to suggest that ASPA exists as a dimer (21, 22, 28), there is no evidence that shows that ASPA is active as such.

While much research has focused on treating ASPA deficiency, efforts to elucidate the molecular basis of CD have been scarce. ASPA has consistently been referred to as a serine hydrolase of the α/β-hydrolase superfamily of enzymes (1, 38, 39), but alignment studies show there is little homology of ASPA with serine proteases (38, 40). It has also been conjectured that ASPA is functionally and structurally similar to members of the carboxypeptidase A (CPA) family of enzymes (40), but this hypothesis has not been tested. Without a known structure, it is unclear how various ASPA mutations disrupt ASPA function. Although the ASPA gene was cloned and localized to

human chromosome 17p13-ter in the early 1990's (1, 2), subsequent molecular studies have been limited to identification and *in vitro* enzyme activity analyses of ASPA mutants that are associated with CD. There are few studies which have investigated the protein characteristics of mutant ASPA.

Central Hypothesis:

Regulation of the ASPA enzyme by its localization, multimeric state, and structure will help to elucidate its roles in the normal phsyiology and etiology of CD.

Aim 1: Investigate regulation of the ASPA enzyme through its subcellular localization and multimeric state.

The sub-aims are to explore the subcellular localization of ASPA in rodent tissues and cells, analyze the biochemical properties of ASPA within subcellular fractions, and demonstrate that the subcellular localization of ASPA is regulated. Immunohistochemistry and immunocytochemistry with polyclonal antibodies against ASPA will be used to detect ASPA protein within cells. Sucrose density gradient separation of nuclei from cytoplasm, followed by chromatographic separation, activity analysis, and immunoblotting, will be used to assess the properties of ASPA within subcellular compartments. Finally, transient transfection of fluorescently tagged ASPA protein in COS-7 cells will be used to determine if the subcellular localization of ASPA is regulated.

Aim 2: Investigate how the structure of the ASPA enzyme regulates its physiological role and influences how various ASPA missense mutations result in CD.

The sub-aims are to generate a homology model for ASPA using CPA as a template, analyze mutations of various putative catalytic residues to assess the model, and determine how various CD-associated ASPA missense mutations result in ASPA deficiency. Computer programs will be used to generate a 3-D homology model of ASPA based on CPA. Site-directed mutagenesis will be used to recreate various missense mutations in the ASPA gene. Transient transfection into COS-7 cells, followed by activity analysis and immunoblotting, will be used to assess the overall homology model and the effects of various ASPA mutations.

At the conclusion of this dissertation, the subcellular localization, multimeric state, and structure of functional ASPA enzyme will be more apparent. In addition, the impact of these protein features on normal ASPA physiology and CD etiology will be discussed.

Background

Brief History of CD

In 1931, Dr. Myrtelle Canavan first described the brain pathology of a child misdiagnosed with Schilder's encephalitis periaxialis diffusa (41), an extremely rare childhood variant of Multiple Sclerosis that is characterized by demyelination and its associated neurological defects. The symptoms of the child in Dr. Canavan's report included a failure to meet developmental milestones, such as the ability to grasp objects or hold up its head; progressive macroencephaly; and hypotonia, followed by hyper-

5

reflexia. A brain autopsy after the child's death at 16 months revealed a severe loss of myelin and extensive edema (fluid buildup) of white matter, which contains myelinated nerve fibers (6). Along with an earlier report in 1928 by Globus and Strauss (35), Dr. Canavan's clinical report is considered to be among the first to combine demyelination with macrocephaly and spongiform brain pathology, which is the result of extensive vacuolization that renders the brain sponge-like. This unique combination would lead to a separate disease classification, and in 1949, what had become known as "Canavan's Disease" was characterized as a distinct autosomal recessive disorder (42).

The link between CD and ASPA was first determined in the 1980's. Three separate groups came to this conclusion by observing that children with certain neurodegenerative conditions also had *N*-acetylaspartic aciduria, abnormally high levels of NAA in the urine. In the late 1980's, *N*-acetylaspartic aciduria and deficient ASPA activity in cultured fibroblasts were linked to cases of cerebral atrophy but not specifically to infantile spongy degeneration (43, 44). In 1988, ASPA deficiency was linked to CD, a unique disorder that combines macrocephaly; leukodystrophy, which is a white matter disease; and spongy brain deterioration (4, 45). In 1993, the ASPA gene was first cloned, and a common ASPA mutation among Ashkenazim was correlated with CD (1). Subsequently, CD-associated ASPA mutations were found in other European ethnicities (10, 12). As further support for the importance of the ASPA gene in CD, it was found that small-scale and entire deletions of murine and rodent ASPA genes, respectively, lead to CD-like phenotypes in these animal models (17, 18).

CNS Cell Types, Myelination, and the ASPA Reaction

The organization of the CNS and the process of myelination are important to understand when studying ASPA and CD. The substrate for the ASPA reaction, NAA, is localized to the key cells of the CNS, neurons, which transmit chemical signals to control the motor and sensory nervous systems. However, because of their immense size, neurons are the least numerous cells of the CNS. The most numerous cell types of the CNS are glia, which consist of astrocytes, microglia, and OLs (46). Astrocytes, the largest and most numerous glial cells, are irregularly shaped with many long processes, including those which form the glial membrane and contribute to the blood-brain barrier (46). Astrocytes also regulate the extracellular ionic and chemical environments of the CNS and assist in injury responses along with microglia, which are small cells with few processes that are scattered throughout the CNS (46). Microglia have ameboid and phagocytic activity at sites of neuronal damage or inflammation and have also been implicated in cytokine and growth factor secretion, in antigen presentation, and in CNS development and remodeling (47). While ASPA might play a role in astrocytes, there is no evidence to suggest that ASPA is found within microglia.

Therefore, the dysmyelination observed in CD is probably related to the localization of ASPA within OLs. The primary functions of OLs are to synthesize and to maintain the myelin sheath. OLs myelinate the axons found in the white matter tracts of the CNS and are the targets of severe developmental defects, such as Pelizaeus-Merzbacher disease, and degenerative diseases, such as Multiple Sclerosis (48). Their lineage consists of migratory / mitotic hematopoietic neural precursors, which lead to OL

progenitors, which lead to post-mitotic immature OLs, which lead to myelin-synthesizing mature OLs (49).

The myelin sheath, which consists of a single sheet of OL plasma double membrane tightly wrapped into stacks around an axonal segment (46, 49), is disrupted in CD pathology. Myelin is an evolutionary solution to the problem of packing billions of poorly conducting thin axons into a vertebrate brain (46). Myelin comprises ~40-50% of brain white matter and is itself comprised of 70% lipid and 30% protein (49, 50). The major CNS myelin proteins are myelin basic protein and the proteolipid protein (PLP/DM-20), which together account for ~80% of myelin protein. Two minor myelin proteins, often used as markers, are 2',3'-cyclic nucleotide-3'-phosphohydrolase and myelin-associated glycoprotein, which together account for ~5% of myelin protein.

Myelination is a vital developmental process that has been linked to the developmental expression of the NAA substrate and the ASPA enzyme. Myelination consists of OL migration, axon contact, process adhesion, and plasma membrane extension around axons (49). OLs of the CNS myelinate at least 20-30 internodes (myelinated axonal sections) of neighboring axonal segments at once (50). The majority of brain myelination occurs before the age of one in humans, whereas in rodents, it peaks at 18 days and concludes by 60 days (49). Finally, myelination correlates with the activity of several lipid biosynthetic enzymes (49). This is important because ASPA might play a role in fatty acid synthesis during myelination.

Both NAA and ASPA levels increase during myelination. Specifically, NAA concentration and synthesis in rat brain best correlate between days 7 and 21 (33, 51) and

peak at day 22 (32). The levels of NAA in the brain generally increase with age, peaking at 14 days in the corpus collosum and dramatically increasing after 7 days in the optic nerve (52). Meanwhile, ASPA specific activity peaks from 7-21 days in the optic nerve, brain stem, corpus callosum, and, to a lesser extent, cerebellum (53). The most rapid increases in ASPA mRNA, protein, and specific activity in the brain occur during peak myelination, between 14 and 28 days, and are followed by a general increase in ASPA protein and specific activity that continues into adulthood (28, 36, 37, 51, 54-56). The involvement of NAA and ASPA in the myelination process provides a basis for understanding the etiology of CD.

Clinical Aspects of CD

Etiology and Pathology

It is believed that the loss of functional ASPA enzyme leads to an accumulation of the NAA substrate and the resulting deficiency in acetate and aspartate products. In fact, specific mutations in the ASPA gene have been shown to lead to a disruption of enzyme function and have been correlated with CD and its pathological features (Table 1) (1).

Two common features of CD are brain vacuolization and macrocephaly. One hypothesis to explain the mechanism of brain vacuolization in CD involves water accumulation. Because of a hydration shell that surrounds the two negative charges of NAA, water is thought to accumulate along with excess NAA in the extracellular space when ASPA is deficient. Ultrastructural studies have demonstrated a fluid buildup that

causes large spaces within myelin sheaths, swollen astrocytes with distorted elongated mitochondria, and the loss of demarcation between white and gray matter in the cortex leading to intramyelinic edema, vacuolization and overall spongiform pathology (6, 31, 35, 57, 58). The vacuolization of the white matter appears to be most pronounced in the cerebellum and the brain stem (6). In addition, CD patients also have elevated cerebral spinal fluid pressure because excess NAA is excreted into both plasma and the cerebral spinal fluid on its way to the urine (25, 27). Finally, there is some evidence which suggests that excess NAA causes seizures. When intracerebroventricularly injected into Wistar rats, NAA dose-dependently induced EEG abnormalities and seizures (59). Therefore, substrate accumulation might account for seizures that are commonly observed in CD patients.

CD Trait	Description
Enzyme	ASPA catalyzes: NAA→Acetate + L-Aspartate (Figure 1)
Cause	ASPA deficiency
Etiology	Excess NAA causing brain edema Lack of NAA-derived acetate for myelin lipid synthesis
Pathology	Vacuolization of white matter and spongiform deterioration of brain Dysmyelination Breakdown of motor nervous system
Symptoms	Macrocephaly, hypotonia, optic atrophy, seizures, death by ~5-10 years
Diagnosis	Deficient ASPA activity in fibroblasts, amniocytic fluid Elevated NAA leves in brain, urine PCR for common ASPA mutations
Treatment	Symptomatic Gene therapy Acetate supplementation

Table 1. Summary of CD features.

Product deficiency might play a separate role in CD etiology. The fundamental features of CD—dysmyelination, macrocephaly, and spongy degeneration of the CNS—do not implicate deficient aspartate as an etiological agent. There are several other biochemical pathways that provide aspartate, including the citric acid cycle. In contrast, deficiency of the acetate product is likely to play a direct etiological role in the dysmyelination phenotype of CD. Acetate deficiency has been experimentally linked to deficient fatty acid and steroid synthesis during myelin lipid formation (60). The rampant deterioration of the motor function of the CNS and its subsequent effects on balance and coordination are believed to result from ASPA deficiency rather than NAA accumulation because they relate to dysmyelination (29, 61).

Symptoms and Disease Progression

The primary cause of CD is thought to be ASPA deficiency in the CNS. Secondary disease progression is thought to relate to degeneration of the CNS and tertiary disease progression is thought to relate to deterioration of peripheral functions.

The role of ASPA in myelination and the accumulation of NAA delineate when symptoms of CD become evident. Most CD patients present with symptoms at the onset of the myelination process, typically between 6 and 12 months of age, at which point macrocephaly is usually detectable (62). Children with CD are unable to attain developmental milestones such as sitting, standing, walking, and talking, though they can interact with people, laugh, smile, grasp objects, and are initially able to lift their heads while lying down (39).

Secondary neurological progression in CD includes epilepsy, hypotonia giving way to rigidity; spasticity, which is common in cerebral palsy; choreoathetosis, defined as aimless muscle movements and involuntary motions; and eye disorders, such as nystagmus, optic atrophy, and retinal degeneration (6, 62, 63). Approximately 50% of all CD patients have convulsive, rather than absence-like, seizures (17). In addition, while CD patients might have optic atrophy, they usually do not go blind (39, 64). Most current treatments for CD are designed to alleviate these secondary symptoms. A typical disease management consists of physiotherapy; nutritional supplements; and palliative drug regimens, such as anti-epileptics, anxiolytics, and diuretics (6). CD patients commonly miss developmental milestones and most can never walk. Therefore, it is also common for children with CD to be confined to specialized immobilizing wheelchairs from diagnosis until death.

Tertiary disease progression, which is often subsequent to diagnosis, includes frequent vomiting, irritability, and frequent fevers (62, 63). In a typical course of CD, breakdown of the motor nervous system results in gastroesophageal reflux, which leads to feeding difficulties. Therefore, feeding tubes, inserted either through the nose (nasogastric) or through a permanent incision in the stomach (gastrostomy), often become necessary (63). Pathology found outside the CNS also can include pharyngeal hypotonia, macroglossia, oropharyngeal narrowing, and bronchial asymmetry of the upper airway system (65).

As spongy degeneration of the brain becomes absolute, loss of control of nervous function occurs along with general paralysis, an inability to breathe unaided, and death by

the age of 5 to 10. Likely as a result of the tertiary breakdown of the immune system due to the deterioration of the motor nervous system, children with CD commonly die of pneumonia (64).

Diagnosis

While some symptoms of CD are found in other leukodystrophies and neurodegenerative disorders, *N*-acetylaspartic aciduria is exclusive to CD. Slightly elevated NAA levels in the brain, but not the urine, are found in other leukodystrophies (39). In addition, common CD symptoms, such as hypotonia, macrocephaly, and mental retardation, are individually found in other leukodystrophies and neurodegenerative disorders such as metachromic leukodystrophy, glutaric academia, Tay-Sachs, and Alexander disease (6, 39, 63). Specifically, white matter involvement is lacking in Tay-Sachs, a more common disease among the Ashkenazim (63). Before CD was associated with ASPA mutations, cerebral palsy and hypoxic-ischemic encephalopathy were also common misdiagnoses (39). Moreover, spongiform brain degeneration is found following exposure to certain toxins, in response to certain viral infections, in some mitochondrial diseases, and in some metabolic diseases (6, 63). Therefore, to distinguish CD from other conditions, clinical diagnosis must be precise.

Diagnosis of CD usually entails the combination of detecting elevated NAA levels and significantly reduced ASPA activity. In the brain, NAA levels are measured using magnetic resonance spectroscopy. However, they tend to be only slightly increased relative to controls (Table 2). Elevated NAA levels can be detected in blood plasma and in cerebral spinal fluid, but the range is large enough to render this diagnosis insufficient

by itself (43). Diagnostic imaging, which detects elevated NAA levels in the brains of children displaying classic symptoms of a leukodystrophy (combination of hypotonia, head lag, macrocephaly), is sufficient to warrant biochemical and molecular tests for CD (39). More importantly, the most effective diagnostic feature of CD is elevated urinary NAA excretion (12, 63). In the urine, where NAA is measured by gas chromatography-mass spectroscopy, NAA levels are usually elevated greater than 50-fold relative to unaffected children (Table 2) (35). Due to variation in elevated levels, NAA in the urine should be at least 10 times higher than normal for accurate diagnosis (32, 58, 66). In addition, although NAA levels in amniotic fluid are used for prenatal diagnosis, they fluctuate between homozygote and heterozygote values and are unreliable for accurate diagnosis (67, 68).

Subjects	n	Urine NAA (µmol/mmol creatinine)	n	Brain NAA (µmol/mg protein)
CD	95	135.0 – 3685.9	11	0.12 – 0.39
Unaffected	54	4.1 – 59.2	5	0.00 – 0.03

Table 2. Mean NAA levels for diagnosis of CD. Values are depicted as a range (35). NAA levels from CD and control patients were determined by gas chromatography—mass spectrometry. Due to high variability in urinary NAA excretion, NAA levels should be increased ~50-fold for accurate diagnosis of CD.

As ASPA activity is undetectable in the blood (63), fibroblasts are commonly used for ASPA activity analysis and for accurate diagnosis of CD (68). Significantly reduced ASPA activity (less than 10% activity compared with normal) in fibroblasts is characteristic of children with CD (4, 12, 43). By comparison, phenotypically unaffected carriers have 30-50% of normal ASPA activity (35, 69). The *in utero* combination of increased NAA levels in amniotic fluid and ASPA deficiency in chorionic villi and fetal

fibroblasts provides accurate diagnosis of CD during the first trimester (67, 68, 70). However, PCR-based genetic testing for the common CD-associated ASPA mutations for Ashkenazim and non-Ashkenazim Europeans is the most trusted diagnostic tool for prenatal and carrier testing (6, 39). The American College of Obstetricians and Gynecologists (ACOG) recommends carrier screening for CD if both parents are of Ashkenazi descent (71). If only one parent is Ashkenazi or has a family history of CD, the ACOG recommends testing the parent of Ashkenazi descent first, and if they are found to be a carrier, testing the other parent.

The clinical aspects of CD are invariably linked to the biochemical basis of the disease: the inability of the ASPA enzyme to hydrolyze NAA in the CNS.

Characteristics of NAA

While low NAA concentrations typically signify mental retardation and developmental abnormalities, including substantial disintegration and extensive loss of viable neural tissue in infarcted brain tissue following a stroke, Alzheimer's disease, during the early stages of HIV infection, Amyotrophic Lateral Sclerosis, Huntington's disease, Multiple Sclerosis, and various seizure disorders (32, 72), CD is the only known neurological disease where NAA levels in the brain are elevated.

Localization

The NAA molecule was the first acetylated amino acid to be isolated from the

brain. It accounts for ~1% of brain dry weight (33, 73) and up to 0.1% of brain wet weight (32). The concentration of NAA in whole mammalian brain is very high (~6-7 μmol/g, or 13-18 mM) and is second to glutamate in terms of free amino acid or amino acid derivative concentration (24, 25). NAA is absent from Schwann cells of the peripheral nervous system (74), possibly explaining why CD pathology is mostly CNS-specific. In peripheral tissues, such as liver, kidney, and heart, NAA levels are ~1% of those in the brain (32-34). Finally, although they are elevated in CD patients, NAA levels in the urine are normally very low (33).

Within the CNS, significantly greater levels of NAA have been detected in the neuron-rich gray matter versus the OL-rich white matter (20, 74). Overall, it appears that NAA levels are highest in cortical neurons and dorsal root ganglia, and lowest in the corpus callosum and optic nerve (53, 60, 74). The localization of NAA is restricted to cell bodies and basal dendrites in pyramidal, granule, and polymorphic cells of the hippocampus and in substantia nigra, midbrain, and hindbrain of the brainstem (24), which are mostly gray-rich regions of the brain. In the optic nerve and the eyeball, NAA levels are high in neuronal axons (52). Cultured OL progenitors contain NAA, though their levels diminish with differentiation (32, 75). This is consistent with the observation that NAA is absent from mature OLs. Finally, NAA has not been detected in neonatal or mature astrocytes (25).

Synthesis and Transport

The NAA molecule consists of L-aspartic acid with an acetyl group linked to its amino group in a C-N peptide bond (Figure 1). NAA is synthesized from acetyl-CoA and

L-aspartate by aspartate-*N*-acetyl transferase (E.C. 2.3.1.17, Asp-NAT) in neuronal mitochondria (24, 32, 34, 51, 76-78). The biosynthesis of NAA uses glutamate as the transamination source for aspartate and either pyruvate or 3-hydroxybutyrate as the acetyl-CoA source (25). A recently published model for NAA energics (Figure 2) shows that acetylation via the Asp-NAT enzyme removes aspartate from mitochondria and favors both α-ketoglutarate formation from glutamate and energy production using the citric acid cycle (60). The NAA molecule serves as an acetate carrier between neurons and OLs, where NAA-derived acetate and aspartate enter metabolic pathways by ASPA hydrolysis.

The mechanism of NAA transport from neurons to OLs is unknown but has been investigated using astrocytes as a model. Based on NAA's structural similarity to dicarboxylated molecules such as α-ketoglutarate, fumarate, malate, oxaloacetate, and succinate, the sodium dicarboxylate (NaDC3) transporter was investigated as a potential transport system for the uptake of NAA into astrocytes (79). The NaDC3 transporter mRNA has been detected within meningeal layers (supporting tissue surrounding brain), throughout the cerebral cortex, the hippocampus, the cerebellum, and in white matter tracts of the optic nerve (79, 80). Uptake of several *N*-acetylated amino acids via the NaDC3 transporter into primary cortical astrocyte cultures was found to be temperature and Na^+-dependent and Ca^{2+}-independent (79, 81). Neither the neuronal release of NAA into brain interstitial space, nor the transport of NAA into OLs has been investigated. If the NaDC3 transporter is physiologically responsible for NAA transport, then its defective function should result in dysmyelination similar to that of CD. The *in vivo* significance of NaDC3 for NAA uptake and transport remains unknown.
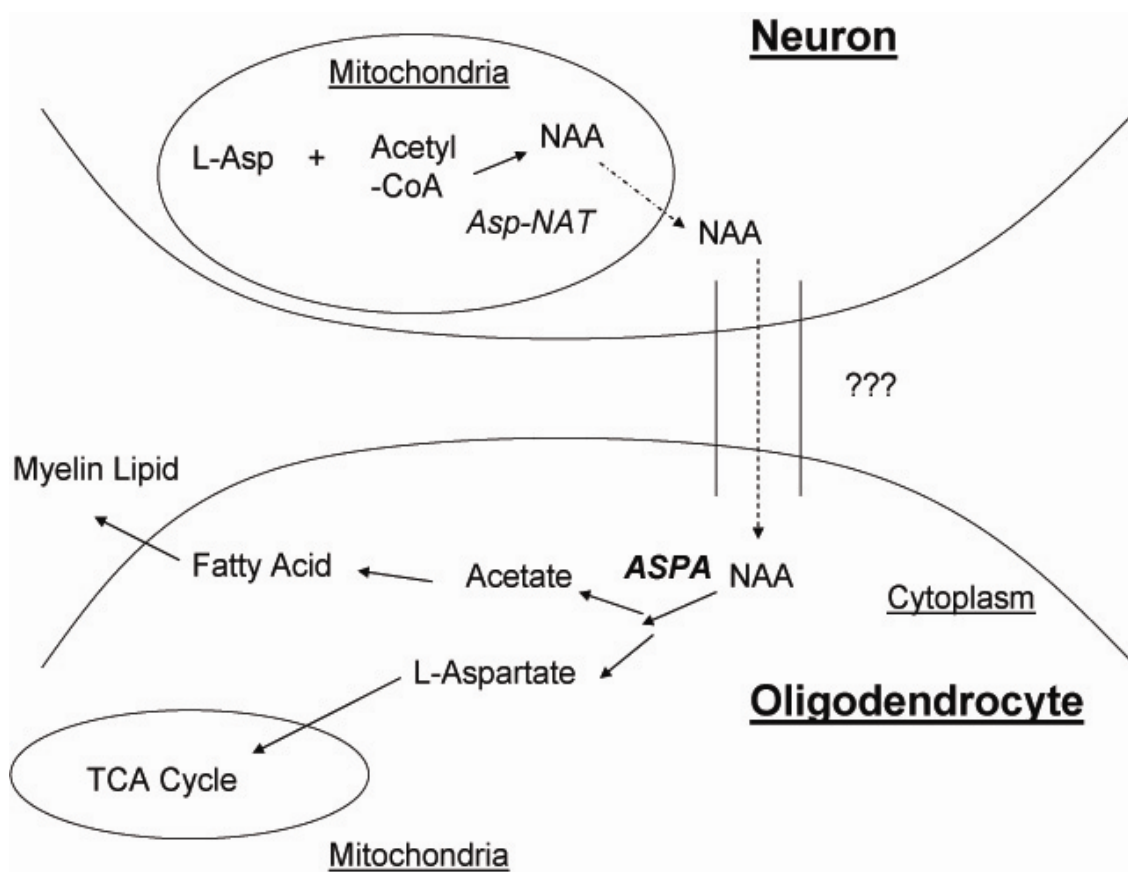
Figure 2. **Localization of ASPA and NAA in the CNS.** NAA is synthesized by Asp-NAT in mitochondria of neurons and transported by an unknown mechanism into OLs. Acetate derived from ASPA-mediated NAA hydrolysis in the cytoplasm of OLs is incorporated into fatty acids of lipids in the myelin sheath. ASPA-derived aspartate likely enters the tricarboxylate acid cycle within mitochondria of OLs.

Localization of the ASPA Enzyme

One of the most interesting features of CD is that the deficient ASPA enzyme and its NAA substrate are localized to separate regions and cell types of the CNS (Figure 2). While NAA is found in neurons of the gray matter, ASPA is found in OLs of the white matter. This implies that NAA hydrolysis is spatially and temporally regulated. The

18

localization of the ASPA enzyme must be addressed in order to understand the physiological significance of the ASPA reaction.

Tissue and Cellular Localization

While it is believed that the ASPA reaction is significant only in the CNS, ASPA is also found in other parts of the body. Specifically, ASPA is expressed predominantly in the skeletal muscle, followed by the kidney and the brain (1). ASPA specific activity in rat and chicken kidney homogenates is ~6- to 14-fold higher than in brain homogenates (36, 37).

Several studies have investigated the localization of ASPA within the CNS. The ASPA reaction appears to be highly regulated in the CNS as NAA and ASPA are found within different cell types. ASPA specific activity is elevated ~3-15-fold in white versus gray matter (20, 36) and is enriched in the brain stem versus the whole brain (82), confirming its specificity to myelin-rich brain regions. While ASPA activity has not been detected in whole eye homogenate (82), it is lowest in the myelin-poor cortex and highest in the myelin-rich optic nerve (53). Immunohistochemistry and *in situ* hybridization using rat tissues detected ASPA in OLs of the white matter tracts, including the corpus collosum, anterior commissure, optic chiasm, thalamus, cortex, corticospinal tract, ensheathing cells of the olfactory bulb, and myelin-associated cerebellum (20, 28, 29, 56, 60). Staining for ASPA co-localized with staining for CC1, an OL cell body marker, in the Purkinje cell layer and axonal fiber layer of the cerebellum, corpus collosum, layer 2 of primary somatosensory cortex (30). This co-staining was strongest in OLs of the medulla and in the spinal cord white matter (30). The expression of ASPA in cerebral

white matter fiber tracts, axonal bundles, cerebellar tracts, and optic tract could account for all aspects of CD including delayed motor skill acquisition, developmental milestones, balance and coordination problems, and optic atrophy (29). As ASPA is mostly absent from neurons, astrocytes, and microglia (29, 30, 82), it is a good marker for OLs (28).

There is some debate as to whether functional ASPA exists in the myelin sheath. In one study, significant ASPA activity was recovered following treatment of purified myelin from rat brain with 0.5 M NaCl or 0.1% taurochlorate to release membrane-bound proteins (82). However, a more recent study showed that staining for ASPA does not co-localize with Rip, a myelin marker and that ASPA protein and activity were not detected in sucrose density gradient-purified myelin (30).

There is further debate as to whether astrocytes contain functional ASPA. Notably, ASPA specific activity is enriched in cultured primary OLs compared with crude rat brain homogenate (83). In addition, ASPA specific activity increases with OL differentiation (31, 53). Furthermore, significant ASPA activity was not detected in cultured astrocytes (31, 83), though a third study detected it in Type-2 cultured astrocytes (53). It should be noted that Type-2 astrocytes have only been detected *in vitro* and are considered to be culture artifacts that occur when OL progenitor cells are grown in the presence of serum (84). There are two possible explanations to resolve the discrepancy among these studies of ASPA activity in astrocytes. First, ASPA activity detected in Type-2 astrocytes could be due to the activity of aminoacylase I, an ASPA homologue (see below). Second, the ASPA activity in Type-2 astrocytes could have come from the

initial OL progenitor cells. In conclusion, the current data suggest that ASPA is most likely absent from astrocytes.

Subcellular Localization

A recently published study used immunohistochemisty with a polyclonal anti-ASPA antibody to detect OLs with immunoreactivity in both the cytoplasm and the nucleus (30). Combined with previous studies, this suggests that ASPA is strictly cytoplasmic, partially membrane-bound, or nuclear-cytoplasmic. In one study, ASPA specific activity derived from the 105,000 g soluble cytosolic fraction was 100-120% higher than from total rat brain homogenate (36). In other studies, non-ionic detergents such as NP-40, Triton X, and Tween-20 significantly increased by 20-70% chicken tissue homogenate (37) and purified bovine brain ASPA specific activity (20). Various pellet fractions from rat brain homogenate also showed significant ASPA activity (82). Although no reports have identified transmembrane domains in ASPA, protein-lipid or protein-membrane interactions might account for membrane-association. Further antibody-based studies are needed to clarify the subcellular localization of the ASPA enzyme.

<u>Functional Roles of the ASPA Reaction</u>

There are two theories pertaining to the physiological role of the ASPA reaction in the CNS that are consistent with the compartmentalized localizations of NAA and ASPA within the CNS (Figure 3). The "lipogenesis hypothesis," which focuses on

acetate deficiency, and the "osmolyte hypothesis," which focuses on substrate accumulation, can account for dysmyelination and spongiform brain deterioration, respectively, which are both observed in CD pathology.
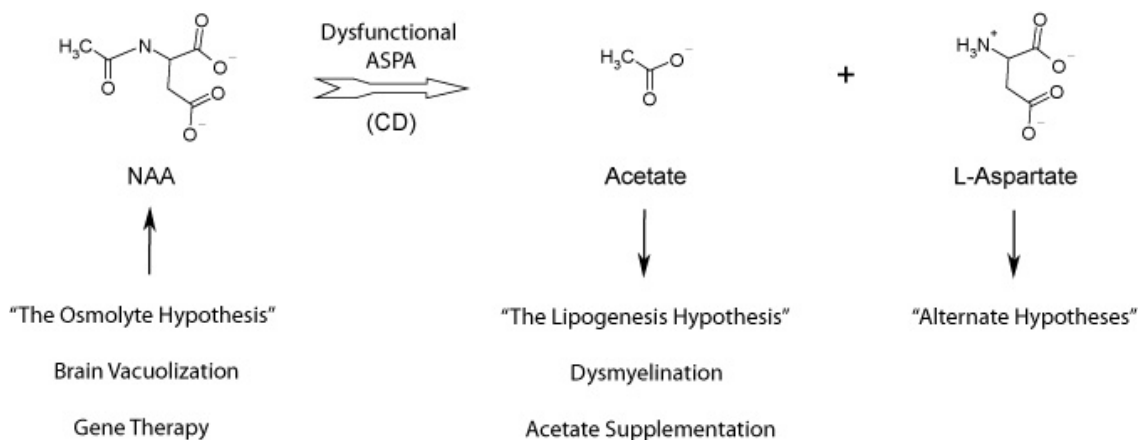
Figure 3. **Functional roles of the ASPA reaction.** Accumulation of NAA substrate (depicted by up arrow) as an etiological agent for CD spongiform deterioration is the crux of the osmolyte hypothesis. Deficiency of ASPA-derived acetate product (depicted by down arrow) as an etiological agent for CD dysmyelination is the crux of the lipogenesis hypothesis. Aspartate deficiency does not appear to play a role in CD etiology.

Several studies have shown that ASPA in the CNS is localized primarily within OLs, which function to myelinate axons in order to facilitate signal transduction throughout the CNS. A role for ASPA in myelination is sometimes known as the lipogenesis hypothesis because ASPA catalyzes the release of acetate from NAA. Acetate that is derived from NAA has been shown to incorporate into myelin lipids (60).

There is a great amount of experimental data that supports the lipogenesis hypothesis. Although there is less experimental support for the osmolyte hypothesis, this proposed function of NAA has received more attention in the CD research field.

Osmolyte Hypothesis

The osmolyte hypothesis states that NAA functions as an osmolyte for the maintenance of water homeostasis in the brain. The characteristic CD-related spongiform degeneration of the brain is partially attributable to edema in extracellular spaces (4, 6, 85). The osmolyte hypothesis is based on the hydration shell that surrounds the two negative charges of NAA at physiological pH. The NAA molecule accounts for ~3-4% of total brain osmolarity (73) and builds a high gradient in the extracellular space between the site of its synthesis (neurons) and its hydrolysis (OLs) (Figure 2). Therefore, when ASPA is deficient, NAA and its concomitant water might be released from neurons and accumulate in the extracellular space. In a sense, ASPA would then function as a molecular water pump, the three properties of which are the use of an energy gradient for passing an osmolyte across a membrane, a high affinity of the osmolyte for water, and the rapid elimination of water by a recycling mechanism (57).

Several factors suggest that the clearance of extracellular NAA by ASPA is not NAA's primary role. Although NAA might function as a molecular water pump, it is not the only anion regulating water homeostasis in the brain as there are other anions with known transporters such as bicarbonate (27). Also, a child with undetectable NAA levels in the brain displays little neurodegeneration, which implyies there are redundant cellular water pumps (57, 72).

Aside from concomitant water accumulation, there are other aspects of NAA accumulation that address the spongiform brain deterioration of CD. Excess NAA might result in accumulation of *N*-acetylaspartylglutamate (NAAG), which tends to be

moderately elevated in the urine of CD patients (66). Excess NAAG, a partial agonist for NMDA and mGluR3 receptors at synaptic junctions (73), might also lead to excess excitatory glutamate via its hydrolysis by carboxydipeptidase (EC 3.4.13.21). This increase might overload synapses and cause neuronal death (66, 71). Indeed, high NAA concentrations of 3 and 10 mM elicited sharp intracellular Ca^{2+} increases counteracted by NMDA inhibitors (86). A prolonged Ca^{2+} influx is also associated with neurotoxicity.

The possibility of NAA cytotoxicity remains controversial. While NAA is detectable throughout the entire rat brain, NAAG has been detected mostly in specific areas, such as the brain stem and the optic nerve (52). Also, enzymatic NAAG synthesis from NAA and glutamate has not been conclusively demonstrated (34, 87, 88). Therefore, NAAG excitotoxicity might not be directly related to NAA accumulation. Furthermore, dose-response studies showed that NAA is less excitatory to neurons than glutamate and that physiologically normal NAA concentrations of 0.1 and 1 mM have no excitatory effect (43, 86). Finally, while some glial cells might be susceptible to toxicity by excess glutamate excitation, OLs were unaffected by the addition of up to 5 mM NAA in culture (53). Although NAA at extremely high concentrations might be neurotoxic, the importance of these findings towards understanding normal NAA function and CD pathology is unknown.

According to the osmolyte hypothesis, the goal of one possible treatment for CD is to clear excess NAA from the extracellular space by restoring ASPA activity to levels observed in phenotypically normal carriers (6). As a monogenic fatal disorder without life-saving treatment, CD has been a prime target for gene therapy trials. The clinical

analysis of a CD patient who received an intraventricular injection into the brain of recombinant human ASPA in a neuron-specific vector indicated variable decreases in NAA levels, increased ASPA expression for ~1 year, new myelination of corpus collosum, basal ganglia, posterior limb of internal capsule, and improved motor function and skill development (89). While current gene therapy trials that target neurons for gene delivery are based on the hypothesis that excess NAA is the major etiological agent for CD pathology, ASPA is found primarily in OLs, not neurons. Therefore, future gene therapy trials would benefit from using a glia-specific vector in order to recapitulate normal ASPA biology (29, 60, 61).

Although NAA is more abundant in gray matter than in white matter, gray matter is largely spared degeneration in CD pathology. Therefore, the impact of excess NAA on CD pathology is probably secondary to the impact of dysmyelination due to deficiency of acetate product.

Lipogenesis Hypothesis

The second theory pertaining to the physiological role of ASPA in the CNS focuses on dysmyelination observed in CD patients. The compartmentalized localizations of ASPA and NAA suggest that neurons transfer intact NAA to OLs, where ASPA liberates acetate for myelin lipid synthesis (4, 30, 43). Several reports based on incorporation of [^{14}C]-acetyl NAA versus [^{14}C]-acetate have shown that acetate released from NAA by ASPA contributes to fatty acid synthesis during myelination (Figure 2). One study showed that fatty acids incorporated 3-times as much acetyl groups from NAA injection versus acetate injection (90). A second study showed the incorporation of the

acetyl group of NAA into fatty acids doubled during myelination, which was similar to the incorporation of acetate during myelination (54). Another study found that lipids incorporated more acetyl groups from NAA than from acetate over time and that proteins did the reverse (51, 82). This differential uptake of NAA-derived acetate into lipids versus free acetate into proteins was specific to the CNS (26, 56, 82).

In addition to acetate derived from ubiquitous metabolic pathways, free acetate derived from NAA by ASPA hydrolysis is believed be a CNS-specific means of providing acetate for fatty acid synthesis during myelination formation (24, 51, 58). Because OLs myelinate several axons at once, they require vast amounts of acetyl-CoA that cannot be provided by the citric acid cycle and citrate lysase systems (56). NAA has one more negative charge than acetate, which improves its storage efficiency within cells and makes it a better acetyl-CoA source when available (26). A deficiency of NAA-derived acetate by means other than dysfunctional ASPA hydrolysis should also result in dysmyelination. A child without NAA has aberrant myelination, which supports this hypothesis (72).

The lipogenesis hypothesis was recently tested in the CD knockout mouse (Table 4) (60). Using tritiated water injections, total myelin lipid synthesis was significantly decreased in knockouts versus control mice. Specifically, the following classes of lipids were significantly decreased in the myelin lipid fraction of knockout versus control mice: cholesterol (~22%), cholesteryl fatty acids (~35%), glycerol-1-fatty acids (~35%), glycerol trifatty acids (~21%), phospholipids and sulfatides (~38%), and phosphatidyl ethanolamine/galatactocerebroside/hydroxyl fatty acid ceramide (~35%). This study also

analyzed lipids postmortem from a human CD patient and found decreased complex glycolipids, cerebrosides, and sulfatides, but not sphingomyelin. It is important to note that only certain lipids, and not total myelination, are disrupted in CD pathology because other metabolic machinery provides acetyl-CoA for lipid synthesis (56). Nonetheless, this study demonstrated the plausibility of the lipogenesis hypothesis (60).

A CD treatment that is consistent with the lipogenesis hypothesis is acetate supplementation. In an early clinical report of CD, a ketogenic diet was administered for 5 months as an alternative substrate for fatty acid synthesis (43). NAA levels did not change and the patient showed no signs of clinical improvement. More recently, acetate supplementation to milk offered a simple, noninvasive, and inexpensive treatment for CD. Calcium acetate (15-30 mg/kg/day), administered to chelate hyperphosphatemia, and acetazolamide (5-7 mg/kg/day), a diuretic designed to decrease white matter extracellular fluid, have been associated with significant neurological function improvements in CD patients (6). An acetate-heavy diet administered soon after CD diagnosis might provide infants the acetate needed for rapid myelination during early postnatal neural development (60).

Recently, acetate supplementation was shown to increase overall brain acetate levels in a proof-of-principle study (91). Glycerol triacetate (GTA), a nontoxic glyceryl tri-ester of acetic acid widely used in perfumes, tanning, dyes, cosmetics, food additives, and external medicine, increased acetate levels in the brains of wild-type (WT) C57BL/6 mice, but it did not increase overall NAA levels. This is significant because the brain vacuolization of CD pathology is most likely the result of excess NAA in the

extracellular space (6). Other than a slight, significant weight gain, there were no obvious side effects of GTA when compared with controls (91).

Alternate Hypotheses for the ASPA Reaction in the CNS

In addition to the osmolyte (NAA substrate accumulation) and lipogenesis (acetate product deficiency) hypotheses, which link ASPA deficiency to clinical CD symptoms, other suggested functions for NAA-derived acetate include acetate as a precursor for acetylcholine synthesis, other acetylation-related processes (26, 32), and adult myelin repair (53). However, the role of NAA-derived acetate in protein acetylation does not appear to be significant (82).

The destination of NAA-derived aspartate is less clear than that of NAA-derived acetate. Unlike aspartate itself, NAA does not act as a neurotransmitter and is inactive in electrophysiological and secondary messenger studies (25). In the past, NAA was thought to function as an intracellular anion pool, an initiator of neuronal protein synthesis, or a storage form of aspartate (32, 35, 51, 92). A lack of NAA-derived aspartate might affect arginine biosynthesis and oxaloacetate through decreased transamination reactions and might cause cell death by disruption of general cellular metabolism (6, 26, 35). Since aspartate itself is a neurotransmitter, defective NAA hydrolysis resulting in decreased aspartate at neuronal junctions might account for some neurological disturbances observed in CD pathology (4). These hypotheses have not been investigated.

Finally, ASPA has recently been implicated in negative transcriptional regulation of brain-derived neurotrophic factor (BDNF) (55). *In situ* hybridization showed that the addition of 100 μM NAA to WT cortical neurons co-cultured with either *Tremor* rat or WT OL progenitor cells caused a ~1.4-fold reduction in BDNF secretion in WT cells compared with a ~1.3-fold increase in *Tremor* rats. When transduced with an rAAV-ASPA vector, *Tremor* rat cultures seemed to reverse phenotype and responded like WT cultures to extracellular NAA. Therefore, increased BDNF expression in the P17 *Tremor* rat brain might be due to the absence of ASPA in OLs. These preliminary results indicate that NAA participates in intracellular signaling by identifying BDNF as a downstream target of ASPA hydrolysis. Further studies are necessary to corroborate this claim.

Role of the ASPA Enzyme in Peripheral Tissues

Secondary CD pathology is typically confined to the CNS, so the main physiological roles for NAA hydrolysis do not address peripheral tissues. Whereas NAA is barely detectable outside the CNS, ASPA is very active in the skeletal muscle and in the kidney. There have been few reports of CD pathology in these tissues. Therefore, it has been suggested that ASPA outside the CNS functions as a scavenger of NAA released from the CNS into the body fluid (1). On the other hand, due to low NAA levels and high ASPA activity in the kidney, the primary substrate of the ASPA enzyme here might be a modified form of NAA (85).

A few studies indicate an active, rather than a "housekeeping" (58), role for ASPA outside the CNS. Fresh tissue slices incorporated greater than 95% and ~18% of radiolabeled NAA into the kidney and the heart, respectively, and ~80% into the liver,

and ~32% into the mammary glands (76), which suggests that NAA usage is not CNS-specific. However, NAA in peripheral tissues is not used for myelin lipid synthesis, and so its role outside the CNS is unclear. While the mammary glands incorporated NAA into fatty acids similarly to acetate, the liver showed only ~15% incorporation (26, 76). Radiolabeled NAA was nearly completely converted to CO_2 in fresh kidney slices (76). Consistent with low levels of endogenous NAA outside the CNS, free acetate levels were unchanged in the liver and kidney of CD knockout mice compared with control mice (60). Further studies are required to clarify the role of the ASPA reaction in peripheral tissues.

ASPA Genetics and Molecular Studies

Since the link between deficient ASPA activity and CD was first reported, investigations have focused on the physiological role of ASPA (4). The cloning of human ASPA cDNA in 1993 (1) paved the way for understanding ASPA gene structure, identifying CD-associated ASPA mutations, and addressing the possibility of a genotype / phenotype correlation for CD.
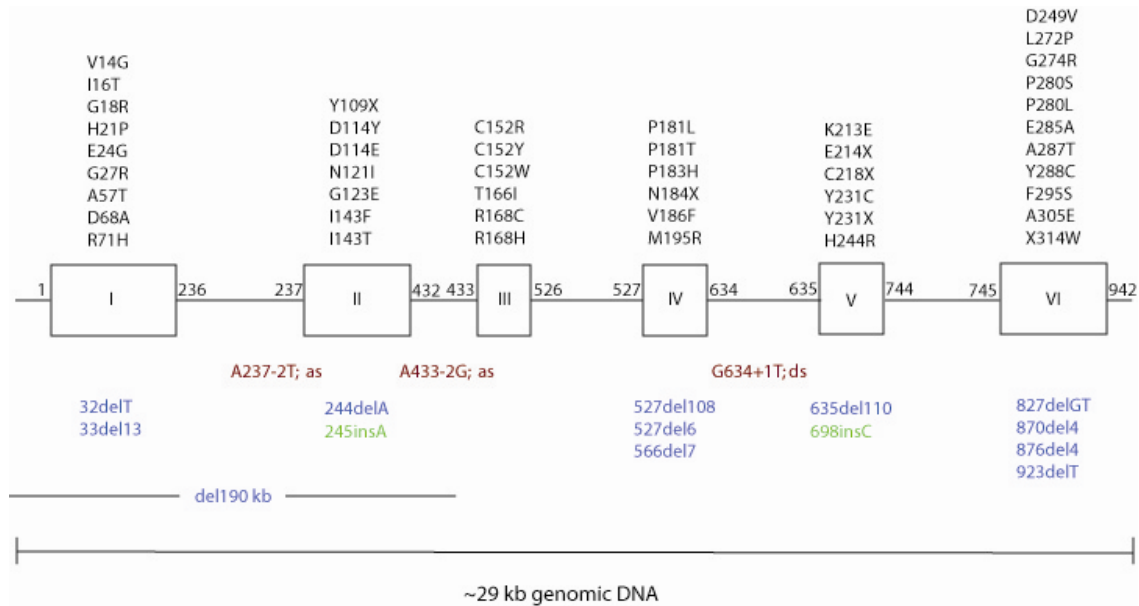
Figure 4. **Organization of the human ASPA gene.** The human ASPA gene spans 29 kb of genomic DNA and consists of 6 exons and 5 introns (2). The first and last cDNA nucleotides for each exon are listed. Mutations in the ASPA gene that are associated with CD are depicted. Missense and nonsense mutations, denoted by the affected amino acid residue, are listed (black text) above their respective exons. Splice site mutations are depicted (red text) either preceding an exon—i.e. "A237-2T; as" refers to an A→T substitution 2 nucleotides upstream of cDNA nucleotide 237 at a splice acceptor site—or directly following an exon—i.e. "G634+1T; ds" refers to a G→T substitution 1 nucleotide downstream of cDNA nucleotide 634 at a splice donor site. Insertions (green text) and deletions (blue text) are depicted beneath the affected exon(s) such that, for example, "245insA" refers to the insertion of an adenine as cDNA nucleotide 245 and "33del13" refers to the deletion of 13 bp beginning with cDNA nucleotide 33. See Table 3 for further mutation details.

Characteristics of the ASPA Gene

The ASPA gene, which spans ~29 kb of genomic DNA and consists of 6 exons and 5 introns (Figure 4), was localized by fluorescence *in situ* hybridization to the short arm of chromosome 17 (17p13-ter) (2). Greater than 90% sequence homology between human and bovine ASPA, as well as cross-hybridization of human ASPA with chicken, dog, monkey, mouse, rabbit, and yeast genomic DNA via Southern blotting, indicate

ASPA has a conserved, significant biological role (2).

Genomic ASPA DNA is processed to cDNA that is ~1,417 bp long, consisting of a 942 bp open reading frame, ~158 bp of 5' untranslated region (UTR), and 316 bp of 3' UTR (Figure 5) (1). There are no published reports on the promoter for the ASPA gene or on its transcriptional regulation. Analysis of ASPA mRNA by Northern blot found 1.44 kb and 5.4 kb bands, which confirms that ASPA expression in several types of human tissues (in decreasing intensity: skeletal muscle, kidney, brain, and liver) and implies gene regulation through either multiple polyadenylation sites or the existence of multiple splice variants (1). Although there is no evidence for regulated splicing of ASPA mRNA, nucleotide A746 in position +2 next to the intron 5 / exon 6 junction might result in splice deficiency upon mutation (93).

Figure 5. **Organization of the human ASPA cDNA.** Human ASPA cDNA is ~1,417 bp long, consisting of a 942 bp open reading frame, ~158 bp of 5' UTR, and 316 bp of 3' UTR, encoding 313 amino acids (1). Numbers along the left side refer to cDNA position (top) and amino acid residue (bottom). The open reading frame (942 bp) is flanked by UTRs that are depicted in green and numbered separately in blue text. Individual codons (313 amino acids) are differentiated by alternating yellow shading. Individual exons (6) are numbered along with the cDNA position and differentiated by alternating gray versus blue text. Predicted sites of post-translational modification (1): five putative phosphorylated residues (S83, S105, S108, S146, and T264) are in underlined red text with a single red star beneath each residue; the putative N-glycosylated residue (N117) is in purple text with two purple stars beneath it.

5' UTR

```
  1 TTGTAACAGAAAATTAAAATATACTCCACTCAAGGGGAATTCTGTACTTTGCCCTTTGGGTAAAGTCTCATTTACA
    ..........................................................................
 76 TTTCTAAACCTTTCTTAAGAAAATCGAATTTCCTTTGATCTCTCTTCTGAATTGCAGAAATCAGATAAAAACTAC
    ..........................................................................
151 TTGGTGAA
```

Exon I (1)

```
  1 ATGACTTCTTGTCACATTGCTGAAGAACATATACAAAAGGTTGCTATCTTTGGAGGAACCCATGGGAATGAGCTA
  1 -M--T--S--C--H--I--A--E--E--H--I--Q--K--V--A--I--F--G--G--T--H--G--N--E--L-

 76 ACCGGAGTATTTCTGGTTAAGCATTGGCTAGAGAATGGCGCTGAGATTCAGAGAACAGGGCTGGAGGTAAAACCA
 26 -T--G--V--F--L--V--K--H--W--L--E--N--G--A--E--I--Q--R--T--G--L--E--V--K--P-

151 TTTATTACTAACCCCAGAGCAGTGAAGAAGTGTACCAGATATATTGACTGTGACCTGAATCGCATTTTTGACCTT
 51 -F--I--T--N--P--R--A--V--K--K--C--T--R--Y--I--D--C--D--L--N--R--I--F--D--L-
```

Exon II (237)

```
226 GAAAATCTTGGCAAAAAAATGTCAGAAGATTTGCCATATGAAGTGAGAAGGGCTCAAGAAATAAATCATTTATTT
 76 -E--N--L--G--K--K--M--S--E--D--L--P--Y--E--V--R--R--A--Q--E--I--N--H--L--F-
                               S
                               *

301 GGTCCAAAAGACAGTGAAGATTCCTATGACATTATTTTTGACCTTCACAACACCACCTCTAACATGGGGTGCACT
101 -G--P--K--D--S--E--D--S--Y--D--I--I--F--D--L--H--N--T--T--S--N--M--G--C--T-
                    S           S                           N
                    *           *                           **
```

Exon III (433)

```
376 CTTATTCTTGAGGATTCCAGGAATAACTTTTTTAATTCAGATGTTTCATTACATTAAGACTTCTCTGGCTCCACTA
126 -L--I--L--E--D--S--R--N--N--F--L--I--Q--M--F--H--Y--I--K--T--S--L--A--P--L-
                                                               S
                                                               *

451 CCCTGCTACGTTTATCTGATTGAGCATCCTTCCCTCAAATATGCGACCACTCGTTCCATAGCCAAGTATCCTGTG
151 -P--C--Y--V--Y--L--I--E--H--P--S--L--K--Y--A--T--T--R--S--I--A--K--Y--P--V-
```

Exon IV (527)

```
526 GGTATAGAAGTTGGTCCTCAGCCTCAAGGGGTTCTGAGAGCTGATATCTTGGATCAAATGAGAAAAATGATTAAA
176 -G--I--E--V--G--P--Q--P--Q--G--V--L--R--A--D--I--L--D--Q--M--R--K--M--I--K-
```

Exon V (635)

```
601 CATGCTCTTGATTTTATACATCATTTCAATGAAGGAAAAGAATTTCCTCCCTGCGCCATTGAGGTCTATAAAATT
201 -H--A--L--D--F--I--H--H--F--N--E--G--K--E--F--P--P--C--A--I--E--V--Y--K--I-
```

Exon VI (745)

```
676 ATAGAGAAAGTTGATTACCCCCGGGATGAAAATGGAGAAATTGCTGCTATCATCCATCCTAATCTGCAGGATCAA
226 -I--E--K--V--D--Y--P--R--D--E--N--G--E--I--A--A--I--I--H--P--N--L--Q--D--Q-

751 GACTGGAAACCACTGCATCCTGGGGATCCCATGTTTTTAACTCTTGATGGGAAGACGATCCCACTGGGCGGAGAC
251 -D--W--K--P--L--H--P--G--D--P--M--F--L--T--L--D--G--K--T--I--P--L--G--G--D-
                                                   T
                                                   *

826 TGTACCGTGTACCCCGTGTTTGTGAATGAGGCCGCATATTACGAAAAGAAAGAAGCTTTTGCAAAGACAACTAAA
276 -C--T--V--Y--P--V--F--V--N--E--A--A--Y--Y--E--K--K--E--A--F--A--K--T--T--K-

901 CTAACGCTCAATGCAAAAAGTATTCGCTGCTGTTTACATTAG
301 -L--T--L--N--A--K--S--I--R--C--C--L--H--*-
```

3' UTR

```
  1 AAATCACTTCCAGCTTACATCTTACACGGTGTCTTACAAATTCTGCTAGTCTGTAAGCTCCTTAAGAGTAGGGTT
    ..........................................................................
 76 GTGCCTTATTCAACTGCATACATAGCTCCTAGCACAGTGCCTTATTCGGTAGGCATCTAAGCACATTTCTTAAAT
    ..........................................................................
151 TAATTAATATATCTTTAAAGATATCATATTTTTATGTATGTAGCTTATTCAAAGAAGTGTTTCCTATTTCTATATA
    ..........................................................................
226 GTTTATTATACATGATACTTGGGTAGCTCAACATTCTTAATAAACAGCCTTTGTATTCAGAATATAAAATTGAAA
    ..........................................................................
301 TAGATATATATAAAGTT
    ................
```

33

CD Mutations and Population Genetics

There are 56 known mutations in the ASPA gene that are correlated with CD, including 44 missense / nonsense mutations (Table 3) that variably span all 6 exons and various deletions and insertions (Figure 4) (94). Among Ashkenazim, the Glu→Ala mutation at amino acid residue 285 (E285A, nucleotide A854C, exon VI; see Table 3; for the purpose of this dissertation, mutations will be defined as amino acid substitutions unless otherwise preceded by "nucleotide") is the most common (5, 7, 10, 11, 95), and the most common mutation among other populations is A305E (8, 10-16).

The frequency of CD among Ashkenazim is between 57.5% and 67.0% of all CD cases (35, 62, 63). The most common CD mutations primarily affect Ashkenazim whose ancestry is traceable to the Vilnius region of Lithuania (5, 10, 35). The E285A missense mutation and the Y231X nonsense mutation account for about 97% of 104 Ashkenazi CD cases (1, 11). In total, the E285A mutation accounts for roughly 86% of all CD cases and the Y231X mutation accounts for the other 14% (1, 10, 58).

In addition to the CD-associated nucleotide C693A (Y231X) point mutation, there is a C693T polymorphism that is believed to be linked to the CD-associated nucleotide A854C (E285A) point mutation (10, 96). Molecular analysis of 101 Israeli CD patients at position 693 found 57 who were C/C (unaffected), 37 who were C/T (heterozygous), and 7 who were T/T (polymorphic) (96). These findings correspond to allele frequencies of C = 0.75 and T = 0.25, which is consistent with the Hardy-Weinburg equilibrium (96). The authors of the study then investigated position 693 of 7 known A854C carriers and

two homozygous A854C CD patients and found that 3 carriers were C/T and 4 were T/T.

Both CD patients in the study were determined to be T/T.

Nucleotide	Exon	Amino Acid	Relative Activity	Ethnicity	Citations
T416	I	V14G	Untested	German, Polish, Dutch	(15)
T47C	I	I16T	0.38%	Dutch, Greek, Italian	(8, 11, 16)
G52C/A	I	G18R	Untested	Persian	(15)
A62C	I	H21P	Untested	Dutch	(13)
A71G	I	E24G	Undetectable activity	German	(16)
G79A	I	G27R	3.07%	German, Italian, Dutch	(8, 11, 13, 16)
G169A	I	A57T	Untested	German	(13)
A203C	I	D68A	Undetectable activity	British	(16)
G212A	I	R71H	Undetectable activity	N/A	(9)
T327G	II	Y109X	Untested	Spanish	(8)
G340T	II	D114Y	Untested	Norwegian	(93)
C342A	II	D114E	0.35%	Turkish	(11, 16)
A362T	II	N121I	Untested	German, Polish	(15)
G368A	II	G123E	26.9%	Canadian, European	(11, 16)
A427T	II	I143F	Untested	Guatemalan	(15)
T428C	II	I143T	Untested	Japanese	(97)
T454C	III	C152R	Undetectable activity	Arab	(98)
G455A	III	C152Y	0.16%	Ireland	(11)
C456G	III	C152W	Undetectable activity	Yemenite	(16)
C497T	III	T166I	Untested	Mexican	(15)
C502T	III	R168C	Undetectable activity	Turkish, Italian	(11, 15)
G503A	III	R168H	Untested	British, Belgian	(13)
C541A	IV	P181T	Untested	German, French, Dutch, Turkish, Polish	(13, 15, 16)
C542T	IV	P181L	Untested	Dutch, German	(15)
C548A	IV	P183H	Untested	French	(8)
C550T	IV	Q184X	Untested	German, British	(16)
G556T	IV	V186F	Untested	Guadelopian	(8)
T584G	IV	M195R	Untested	Algerian	(8)
A637G	V	K213E	Untested	Greek	(99)
G640T	V	E214X	Untested	German, British, Italian	(15, 16)
C654A	V	C218X	Untested	Gypsy	(12)
A692G	V	Y231C	Untested	Turkish	(100)
C693X	V	Y231X	Undetectable activity	Ashkenazi Jewish	(5, 10, 13)
A731G	V	H244R	Undetectable activity	Italian	(15, 16)
A746T	VI	D249V	Undetectable activity	British, Norwegian, Swedish	(16, 93)
T815C	VI	L272P	Untested	Italian	(15)
G820A	VI	G274R	Untested	Turkish, Greek	(8, 12, 99)
C838T; C839T	VI	P280S; P280L	Untested	French, Italian	(8)
A854C	VI	E285A	2.5%	Ashkenazi Jewish	(1, 10, 11, 15, 16)
G859A	VI	A287T	Untested	German	(8, 15, 16)
A863G	VI	Y288C	Polymorphism (100%)	Canada, Greek	(14, 99, 101)
T884C	VI	F295S	Untested	Greek, Turkish	(8, 12, 99)
C914A	VI	A305E	Undetectable activity	Pan-European	(8-12, 14-16)
A941G	VI	X314W	Untested	Guam	(15, 16)

Table 3. CD-linked missense / nonsense mutations in the ASPA gene. See Figure 4 and text for more details.

Even though the sample size was small, the authors hypothesized that the most common CD mutation among Ashkenazim, A854C, arose on the C693T polymorphic allele (96). A later study with a larger sample size found an allele frequency among 24 A854C carriers of T = 0.67 and C = 0.33 (7). In addition, the study found that 14 of 16 C/T alleles at position 693 carried both the C693T polymorphism and the A854C mutation on the same allele, which reflect a disequilibrium linkage of the C693T polymorphism and the A854C mutation. Therefore, the E285A mutation is likely the result of an ancestral Ashkenazi Jewish founder effect (1, 7).

As there are only two known CD-associated ASPA missense / nonsense mutations associated with the Ashkenazim, CD is a prime candidate for genetic counseling based on carrier testing. The carrier rate of the E285A mutation among Israeli Ashkenazim is 1/59, corresponding to a frequency of E285A homozygotes in 1 out of every 14,000 live births (95). An analysis of 4,000 blood specimens from healthy American Ashkenazim for both the E285A and Y231X mutations later found 106 carriers, which equates to a 1/37.7 carrier rate, or a frequency of 1 in 5,000 live births (63). Samples taken from 449 unaffected Ashkenazim in the New York metropolitan area as part of a carrier-screening program for other common Ashkenazi genetic diseases—Gaucher disease, cystic fibrosis, and Tay-Sachs disease—yielded a carrier rate of 1/41, corresponding to 1 out 6,700 births, with 10 E285A and one Y231X carriers (5). More recently, a comprehensive population screening program for the E285A and Y231X mutations conducted using 1,423 Ashkenazi Jews in the Toronto area detected a combined carrier frequency of 1/57, which corresponds to a CD instance rate of 1 out of 12,996 live births (7). This was consistent with the 2 cases of CD that had been reported in the Toronto area over a 20-

year period (7). Overall, the incidence of CD among Ashkenazim is roughly 1 in 10,000 live births based on a ~1/50 carrier rate.

Although CD is a rare genetic disease thought to be specific to the Ashkenazim, its detection among non-Ashkenazim has increased in recent years. While the E285A mutation is not usually detected among non-Ashkenazim (10, 12, 13), the A305E missense mutation is virtually exclusive to non-Ashkenazim (7) and accounts for ~40% to 60% of CD cases among European non-Ashkenazim (8, 10-13). This number is somewhat lower when factoring in a more ethnically diverse and less European population (16). Because CD is associated with mutations in the ASPA gene, there are several instances of compound heterozygous mutations, the majority of which involve the A305E mutation paired with a less common mutation (9, 11, 13, 14). Other missense / nonsense mutations that affect children from varying backgrounds are summarized in Table 3. Most of these mutations are family-specific or the apparent result of local founder effects (11), such as the D114Y missense mutation, which is localized to a small geographic region in Norway (93).

In addition to these missense mutations, several other molecular events, such as deletions, insertions, and splice junction mutations (Figure 4), have been implicated as causative agents for CD.

There are a few examples of intronic mutations that are thought to affect splicing of ASPA mRNA. Among Ashkenazim, an infrequent mutation (~1.1%) is the A$\rightarrow$G substitution at the nucleotide 433 -2 acceptor site in intron 2 (A433-2G; as), which might result in skipping of exon 3 and a 94 bp frameshift (10). In a non-Jewish Turk, there was

a G$\rightarrow$T substitution at the nucleotide 634 +1 donor site for intron 4 (G634+1T; ds) (102).
Finally, in a German patient, there was an A$\rightarrow$T substitution at the nucleotide 237 -2
acceptor site of intron 1 (A237 -2T; as) (16).

There are also examples of insertions and deletions in the ASPA gene that have
been linked to CD. In a Norwegian patient, there was an insertion of an adenine at
nucleotide 245 (245insA) (93). In a Yemenite patient, there was an insertion of a
cytosine at nucleotide 698 (698insC) (16). In two non-Jewish Mexican siblings, there
was a ~190 kb deletion (del190 kb) spanning from upstream of the start codon to within
the second intron of the ASPA gene (103). In a non-Jewish Turk, there was a deletion of
exon 4 (527del108) (13). In a Pakistani patient, there was a homozygous deletion of
exon 5 (635del110) (8). Finally, in the only known case of CD among African
Americans, there was a frameshift deletion of thymidine at nucleotide 32 (32delT) (11).
Other deletions are depicted in Figure 4.

Genotype / Phenotype Correlation

The identification of greater than 50 CD-associated mutations in the ASPA gene
has enabled researchers to address whether a particular genotype is associated with a
specific phenotype. There were once three proposed clinical variants for CD progression:
congenital (disease apparent at birth), infantile (most common; symptoms manifest after
first 6 months; high variability in life span), and juvenile (disease manifests after 5 years)
(35, 104). However, these variants were described before biochemical assignment and
might not have referred to actual cases of CD (63). In addition, the high variability of
disease progression, coupled with the fact that symptoms do not become apparent until a

particular aspect of the CNS becomes functional, makes it more likely that the onset of CD is prenatal and that the disease progression is variable (62, 64). Therefore, more appropriate characterizations of CD progression are mild, typical, and severe.

Certain mutations in the ASPA gene have been associated with a particular CD phenotype. The E214X nonsense mutation was found in a patient who presented with symptoms at birth and died before the age of 1, suggesting it is associated with a more severe phenotype (16). Most other putative genotype / phenotype correlations have been contradicted by other types of disease progressions. The most common mutations among Ashkenazim (E285A) and non-Ashkenazi Europeans (A305E) have been found in both mild (9, 12, 62) and typical progressions (10, 13, 16). Because the life expectancy of E285A or A305E homozygotes can vary from 1 to 32 years (63), there does not appear to be a genotype / phenotype correlation for these two mutations (12, 39). In addition, the D114Y missense mutation has been associated with a mild clinical course (43, 93), and the D249V missense mutation has been associated with a severe clinical course (16). However, as both D114Y/D114Y and D249V/D249V homozygotes have shown variable progressions, there is no specific genotype / phenotype correlation for these two mutations (93).

Certain mild CD progressions that involve slightly elevated NAA levels (9, 101) and / or residual ASPA activity (39, 105) might be the results of protective mutations, which might ameliorate a disease course when present as compound mutations with CD-associated mutations which disrupt ASPA activity (64). Rare non-Ashkenazim ASPA mutations, such as the R71H, K213E, and Y288C mutations, have been implicated in

promoting mild phenotypes (9, 14, 99). Specifically, the Y288C mutation might confer a mild CD phenotype for several reasons (14, 99). The Y288C mutation affects a highly conserved amino acid, was not found in a large control population, and has been detected in more than 3 patients with a mild course of the disease. In each case, though NAA levels were increased and ASPA activity was markedly reduced, no other ASPA mutation was found. An alternate hypothesis, independent of a direct genotype / phenotype correlation for a mild course of CD, suggests there are one or several disease-modifying genes elsewhere in the ASPA gene (99).

Individual disease progressions are more likely the result of improved medical and nursing care (9, 62, 95). In conclusion, the current studies have not provided strong evidence for a genotype / phenotype correlation for CD.

Animal Models for CD

A rudimentary understanding of the ASPA gene and the identification of several CD-associated ASPA mutations have led to the generation of animal models for studying CD pathology. In the 1980s there were several reports of naturally occurring animal case studies, such as dogs, mice, and silver foxes, which were found to display spongy degeneration of the brain and macrocephaly (106-108). However, as these reports preceded the biochemical link of ASPA deficiency to CD, biochemical confirmations were never attempted and these animal examples no longer exist (39).

In the absence of a naturally occurring animal model, monogenic disease models

are commonly made by artificially inactivating the gene in question by replacing or disrupting it with other DNA. Knockout models are also useful for discerning the function of an unknown gene because the artificially induced loss of a gene typically induces phenotypic alterations, e.g., appearance, behavior, or various biochemical characteristics, which provide clues to its normal function. Mice are the most common animal model for knockouts because of their high genetic similarity to humans, size, short life-spans, and ease-of-use in the laboratory. It is important to note that knockout mice can give insight only into the possible function of the homologous gene in humans, as species variability must be considered when interpreting knockout mouse data.

	CD Knockout Mouse	*Tremor* Rat
Discovery	Man-made	Genetic mutant of epilepsy rats
Defect	10 bp deletion in exon 4 of ASPA gene	>200 kb deletion including ASPA, olfactory receptor, and vanilloid receptor subtype I genes
Symptoms	Spongiform CNS deterioration Brain vacuolization Macrocephaly Neurological impairment	Spongiform CNS deterioration Brain vacuolization Absence-like seizures Body tremor
Model Usage	CD pathology CD gene therapy trials	CD gene therapy trials Epilepsy ASPA characteristics

Table 4. Animal models for CD.

ASPA (CD) Knockout Mouse

Using creatine kinase-mediated homologous recombination to create a 10 bp deletion in exon 4 of the murine ASPA gene (Table 4), a knockout mouse was generated that allowed CD pathology to be studied in a controlled manner (18, 39). The resulting

truncated ASPA gene was introduced to embryonic stem (ES) cells and Southern blotting was used to detect the ES cells that contained the appropriate construct. The ES cells were micro-injected into mouse blastocysts, which were then surgically implanted in surrogate pregnant mice. The offspring were heterozygous for the normal and disrupted ASPA genes.

Since the ASPA knockout mouse was designed to recreate CD pathology, it is usually referred to as the CD knockout mouse. The CD knockout mouse displays several CD-like symptoms, including decreased body weight; increased brain weight and macrocephaly; neurological impairment, which include ataxia, lethargy, lowered mobility, splayed walk, and tremors; degenerated and vacuolated white matter; hypotonia; deficient ASPA activity; and high NAA levels in the serum and urine (18, 60, 109). Notably, free acetate is also decreased in the brains of knockout mice because it cannot be liberated from NAA via ASPA (60). This is consistent with the lipogenesis hypothesis for the basis of dysmyelination observed in CD pathology (Figure 3).

While measurements of chemical compounds such as acetate have not been made in the brains of CD patients, they, along with measurements of proteins, have been made in the CD knockout mice. CD knockout mice also have low levels of the inhibitory neurotransmitter, γ-aminobutyric acid (GABA), and its precursor, the excitatory neurotransmitter, glutamate, that might contribute to both spasticity and cortical excitability (109, 110). Although these compounds have not been measured in CD patients, they might play a role in secondary CD progression pertaining to neurological deterioration.

In addition to these compounds, proteins have been investigated in the CD knockout mouse. Brain aspartate levels should be decreased when ASPA is inactive (Figure 3). However, they are elevated in the brains of CD knockout mice relative to controls (109). This might be attributed to the reduced activity of the aspartate aminotransferase (ATT) enzyme, which catalyzes the conversion of aspartate to glutamate (109). Activities of other metabolic enzymes, such as alanine aminotransferase and succinic semialdehyde dehydrogenase (which plays a role mental retardation), are unaffected in the brains of CD knockout mice (109).

Finally, a microarray analysis identified 647 genes that differed between WT and CD knockout mice (110). However, 90% of these genes displayed a difference of 10% or less (110). Three markedly altered and potentially CD-relevant genes were EAAT4, a glutamate transporter, GABRA6, a GABA receptor subunit, and Spi2, a serine protease inhibitor (110). The expression of EAAT4 and GABRA6 in CD knockout mice were reduced on average 9.7-fold and 119.1-fold, respectively, relative to WT mice, while Spi2 levels were increased 29.9-fold (110). Decreased EAAT4 and ATT levels are believed to contribute to overall reduced glutamate in knockout brains (109, 110). The significance of these findings towards elucidating the basis of CD remains unclear, though it is important to note that the aforementioned proteins have not been investigated in CD patients.

Gene therapy using recombinant human ASPA cDNA has been attempted in CD knockout mice. Promising results of gene therapy include the ephemeral, partial restoration of ASPA activity in the CNS, and slight decreases of NAA levels, thalamic

vacuolization, and water accumulation localized to the delivery vector injection sites (111). Gene therapy using intracranial injections of neuronal progenitor cells retrovirally transduced with recombinant human ASPA (also known as stem cell therapy) was attempted to potentially introduce functional OLs and ASPA into CD knockout mice (112). Preliminary observations made 4 weeks post-transplantation showed a mild increase in ASPA activity localized to the injection site, but no reversal of CD pathology (112).

In conclusion, the CD knockout mouse has been a valuable model for understanding the basis of CD and for testing gene therapy trials. A second model for studying the etiology of CD is the *Tremor* rat.

ASPA Deletion (*Tremor*) Rat

The *Tremor* rat was discovered as a genetic mutant of epileptic rats (113). Genome shift, exon trapping, sequencing, Northern, Southern, and Western blots, and RT-PCR detected a greater than 200 kb deletion that includes the entire ASPA gene, and the absence of both ASPA mRNA and protein in all tissues of the *Tremor* rat (Table 4) (17, 28). The other deleted genes in the *Tremor* rat are the olfactory receptor gene and the vanilloid receptor subtype I gene, both of which are unlikely to account for the absence-like seizures and spongiform degeneration (17). ASPA activity is undetectable in whole brain homogenate, and NAA levels are significantly elevated in all brain regions, particularly in the pons and the thalamus, which are regions marked by severe spongiform deterioration (17).

Similar to CD pathology, *Tremor* rats display spongiform CNS deterioration and brain vacuolization accompanied by hypomyelination in the pons, cerebellum, thalamus, and white matter of the spinal cord by 3 weeks of age (17). By 12 weeks, the degeneration spreads to the hypothalamus, cerebral cortex, and gray matter of the spinal cord. *Tremor* rat characteristics that are specific to rats include body tremor, curled whiskers, waved hair, and dysgenesis of gonads in both sexes (17). *Tremor* rat heterozygotes more closely resemble CD patients and have absence-like seizures, though less frequently and later in life than humans (17).

Like the CD knockout mouse, the *Tremor* rat is a model for ASPA gene therapy trials. Initial results from an experiment that used recombinant rat ASPA targeted to neurons included an ephemeral decrease in the incidence and duration of absence-like seizures (114, 115). A subsequent study delivered recombinant human ASPA targeted to neurons of male and female *Tremor* rats between 16 and 30 weeks of age (116). This treatment increased ASPA activity to 37% of heterozygotes, whom have 50% of WT activity, and decreased NAA levels in the brain by 23% (116). *Tremor* rats that received gene therapy were unable to complete the rotorod task, an indirect measure of locomotor pathway function. The most recent gene therapy trial delivered recombinant human ASPA targeted to neurons of male and female *Tremor* rats between 21 and 24 days of age and resulted in the restoration of normal ASPA expression and activity throughout neurons of the entire brain up to 26 weeks post-injection, decreased NAA levels, and attenuated absence-like seizures (61). However, this treatment did not improve vacuolization of the white matter, total myelin integrity, and various behavioral features (61).

Both the CD knockout mouse and the *Tremor* rat are good animal models for studying CD and ASPA biology (Table 4). With only the ASPA gene inactivated, CD knockout mice are useful for studying CD pathology, while *Tremor* rats, with the entire ASPA gene deleted, are more useful for studying ASPA protein characteristics.

ASPA Protein Characteristics

Aminoacylase Enzyme Family

The enzyme classification (EC) system of the International Union of Biochemistry uses six classes of enzymes—oxidoreductases (1), transferases (2), hydrolases (3), lyases (4), isomerases (5), and ligases (6)—based on the enzyme's substrate specificity. The E.C. number, 3.5.1.15, of the ASPA enzyme refers to the hydrolysis (3) of a carbon-nitrogen, non-polypeptide (3.5), linear amide (3.5.1) bond. The final E.C. number was assigned based on chronology: ASPA was classified as aminoacylase II along with aminoacylase I (EC 3.5.1.14) in 1952 (3, 19).

Aminoacylases are classified based on their substrates. They are predominantly kidney enzymes that catalyze the deacylation of *N*-acyl-L-amino acids to yield fatty acids and amino acids as products (117). There are two other aminoacylase family members, homologues of ASPA that have similar protein characteristics and similar substrate specificities, which are relevant when studying ASPA in the kidney.

While aminoacylase I hydrolyzes chloroacetyl moieties most effectively, it has a broad substrate specificity that primarily acts upon acyl derivatives of amino acids with aliphatic side chains, such as isoleucine, leucine, and valine (19, 43). Although there is virtually no homology between human ASPA and aminoacylase I cDNA (1), purified aminoacylase I displays ~5% as much activity as ASPA towards NAA in the kidney (19).

Aminoacylase III (E.C. undetermined), active as a ~140 kDa homotetramer, hydrolyzes haloalkene-derived mercapturates (S-substituted *N*-acetyl-L-cysteines)— terminal metabolites formed by the glutathione-dependent metabolism of electrophilic xenobiotics—and other *N*-acyl aromatic amino acids (117-119). Unlike purified aminoacylase I, purified aminoacylase III does not show detectable activity towards NAA (117, 118). Cyanogen bromide-degraded aminoacylase III that was partially purified from rat kidney yielded 20 and 40 amino acid peptide sequences with 70% and 42% identity to amino acids 87-103 and 220-259 of human ASPA, respectively (117). These peptide fragments signify local homology between aminoacylase III and ASPA (117). Overall, murine aminoacylase III cDNA is ~43% identical to murine ASPA cDNA (118).

It is important to know the localization of aminoacylases I and III within the kidney to distinguish them from ASPA. Immunohistochemistry and immunoblotting suggested aminoacylase III is partially membrane-bound in glomeruli and proximal and distal convoluted tubules of kidney (117, 118). While ASPA is predominantly expressed in the skeletal muscle, followed by the kidney and the brain, aminoacylase III is expressed primarily in the kidney, followed by the liver, heart, small intestine, brain, lung, testis, and stomach (118). Finally, both aminoacylases I and III have been detected

in the gray matter of the brain (cortex, neuronal cell bodies) but not in the white matter (117), indicating that ASPA is a white matter-specific aminoacylase.

Size and Structure

The size, subunit composition, and structure of the ASPA enzyme, a unique member of the aminoacylase enzyme family, are crucial to its function. The human ASPA enzyme consists of 313 amino acids, is predicted to weigh ~36 kDa, and is ~86% and ~92% identical to bovine and murine ASPA, respectively (1, 23). The predicted size agrees with the experimentally determined molecular weight. Subtracting the size of molecular tags, both mouse and human ASPA have been shown to be 36-38 kDa when expressed in *E. coli* (23, 28). In addition, a 37 kDa ASPA band has been detected by immunoblotting in rat brain homogenate (30).

While aminoacylase III has been shown to be active as a tetramer, there is some debate as to whether ASPA functions as a monomer or a dimer. Initial reports suggested a 58 kDa protein in bovine and human brain, and in cultured human skin fibroblasts (20). However, when the cloning of the ASPA gene revealed a smaller protein, the quality of the antibody in the earlier study came into question. Two more recent analyses using mass spectroscopy and dynamic light scattering showed that the majority of recombinant human ASPA purified from both *E. coli* and *P. pastoris* existed in solution as a dimer (21, 22). Although the size of the purported dimer band (84 kDa) was larger than the predicted size (72 kDa), this conclusion was also reached by immunoblotting using polyclonal antiserum against human ASPA (28). Since denaturing SDS-PAGE conditions of immunoblotting break most native ionic interactions, this upper band

probably reflected covalent dimerization or cross-reactivity with another antigen. In addition, protein aggregates are common when expressing proteins in bacteria, so studies using mass spectroscopic analysis of proteins purified from *E. coli* (22) might have detected artificial dimers. The multimeric state of functional ASPA remains unclear.

The three-dimensional structure of any aminoacylase is also unknown and the functional domains of ASPA, including hydrolytic sites and binding sites, have not been characterized. Current indications of the structure of the ASPA enzyme have been inferred from CD-associated ASPA mutations. For example, the D114E missense mutation, which *in vitro* reduced ASPA activity to 0.35% of WT enzyme (11), extends the length of the side chain by a single methylene group, suggesting Asp114 is important for ASPA structure and function (93).

Furthermore, CD-associated mutations at Cys152 have intimated the presence of an intramolecular disulfide bond in ASPA (11, 16, 98). Low amounts of dithiothreitol (DTT; up to 0.5 mM) are required to maintain ASPA activity whereas higher concentrations (5-10 mM) significantly ablate activity (20, 83). Specifically, the protein secondary structure prediction method of Chou-Fasman indicated that Cys61 and Cys152 lie in β-sheet regions and might form an intramolecular disulfide bond (98). Briefly, the Chou-Fasman algorithm assigns amino acid residues conformational potentials to form or break α-helices or β-sheets and assumes that nucleation for a particular local conformation begins at a region of maximum potential and ends at a region of low potential (120). Aside from this bioinformatics observation, there is no experimental evidence to suggest that Cys61 and Cys152 form a disulfide bond.

Post-Translational Modifications

The structures of many enzymes are regulated during various cell signaling processes by post-translational modifications, such as acetylation, prenylation, glycosylation, and phosphorylation. ASPA, which mostly during myelination is found in OLs of the CNS, might be regulated by post-translational modifications. After human and bovine ASPA genes were cloned in 1993, they were hypothesized to contain one potential *N*-glycosylation site (Asn117) and 5 potential phosphorylation sites (Ser83, Ser105, Ser108, Ser146, and Thr264) (Figure 5) (1).

While there are no reported investigations of ASPA phosphorylation, a recent study using recombinant human ASPA purified from yeast investigated post-translational modification by glycosylation (21). Yeast-expressed human ASPA was found to be 150-fold more active and much more stable than bacterially-expressed human ASPA (21, 22). This eukaryotic-specific stability and enhanced activity was attributed to glycosylation. An hour incubation with peptide N-glycosidase F (EC 3.5.1.52; PNGase F), an amidase that cleaves between the innermost N-acetylglucosamine and asparagine residues of high mannose, hybrid, and complex oligosaccharides from N-linked glycoproteins, reduced ASPA specific activity by greater than 80%. Mass spectroscopic analysis of this released carbohydrate identified a monosialylated oligosaccharide with 6 hexoses, 6 *N*-acetylhexosamines, and 1 *N*-acetylneuraminic acid (sialic acid) (21). The predicted glycosylation site, Asn117, was mutated to Gln to remove the possibility of glycosylation and simultaneously retain the same side-chain functionality (21). The stability and specific activity of purified N117Q resembled that of the deglycosylated enzyme, but the

K_M (see below) remained the same as for the native enzyme (21). Because the specific activity of N117Q was unaffected by PNGase F treatment and because the mass difference between N117Q and the native enzyme was equal to that of a single monosialyated oligosaccharide, Asn117 is likely the only glycosylation site in the ASPA enzyme (21). While this modification might protect ASPA from aggregation by shielding a hydrophobic region, the biological relevance of glycosylation at Asn117 remains unclear.

Kinetics and Catalysis

The final structure of the ASPA enzyme, including any of its post-translational modifications, is responsible for its catalytic function. Several reports have shown that efficient ASPA catalysis is specific to NAA. Two common parameters that define catalytic efficiency are the Michaelis-Menten constant, K_M, and the maximal velocity, V_{max}, of the reaction. The K_M value is the substrate concentration at which the reaction velocity is half of the maximum. The reported K_M of purified ASPA is between 0.3 and 0.85 mM (10, 20, 21, 23), and the V_{max} is 43 μmol/min/mg (20). The reported specific activity of human ASPA purified from yeast (10-15 units/mg) is comparable to that of purified ASPA from bovine brain (20 units/mg) (21). Meanwhile, the reported K_M value of recombinant human ASPA expressed in *E. coli* (0.5-0.7 mM) is comparable to that of recombinant murine ASPA expressed in *E. coli* (0.3-0.5 mM) (22). Although the ASPA enzyme is highly specific for NAA, one study found it displayed even higher activity against *N*-formylaspartate (22). Purified ASPA specific activity was inhibited by ~60% using 1.25 mM concentrations of D-aspartate derivatives, further confirming its

specificity for L-aspartate derivatives (20). Finally, while purified human and murine ASPA displayed ~10% activity against *N*-acetylasparagine (23), this result was not corroborated (22).

How the ASPA enzyme specifically catalyzes the hydrolysis of NAA is unknown. While its functional domains remain uncharacterized, ASPA has consistently been referred to as a serine hydrolase of the α/β-hydrolase superfamily of enzymes due to its inhibition by diisopropyl fluorophosphates, which suggests a catalytic serine, and because of local sequence homology to catalytic cores in esterases (1, 38, 39). These highly conserved putative catalytic cores are 18-GGTHGNE-24, 275-DCTV-278, and 283-VNEAAYY-289, similar to the consensus sequences, GXXHG/AXE/D, DXXF/V, and VXEXXXY, which are involved in esterase catalysis (1, 2, 23, 38). Citing this hypothesis, the H21P, E24G and E285A CD-associated mutations in the first and third of these proposed regions in the ASPA protein have been suggested to ablate ASPA activity by disrupting a single critical catalytic domain (1, 13, 16). However, an alignment study showed that there is little homology of ASPA with serine proteases and that ASPA lacks an invariant serine as a candidate for a catalytic residue (40).

It has been suggested that the catalytic mechanism of ASPA might involve a catalytic triad of His, Glu, and Ser residues (1). The carbon backbone of NAA has been suggested to interact with ASPA's active site because substrates with more electronegative carbonyl groups are better substrates for ASPA-mediated hydrolysis (20, 35). A nucleophilic attack, which is similar to the mechanism of metalloproteases, then might occur at the carbonyl carbon, irrespective of the α and β-carboxyl groups (22). The

52

details of this putative mechanism have not been made clear.

ASPA As a CPA Family Member

Based on its substrate specificity, ASPA was initially characterized as a member of the aminoacylase enzyme family (3). However, the catalytic mechanism of ASPA more likely resembles that of a suitable structurally homologous enzyme. Although various studies have referred to ASPA as a serine hydrolase, a recent report suggested that ASPA shares significant local and functional homology to the CPA family (40). Members of the CPA enzyme family utilize a single zinc atom for catalysis.

Biological Roles of Zinc in Enzymes

Zinc, unlike copper and iron, is a stable metal ion with a filled d-shell that prevents it from undergoing oxidation or reduction in a biological medium (121, 122). Zinc ligates nitrogen and oxygen compounds as readily as it ligates sulfur. Its exceptionally flexible coordination sphere allows it to transiently accept different coordination geometries of proteins and other biological macromolecules without impeding catalysis (122). This property allows for the expansion of the coordination sphere at one step of catalysis and its contraction at another step (121). Biological roles for zinc include stabilizing protein and nucleic acid structure (zinc finger transcription factors), preserving the integrity of subcellular organelles, participating in transport processes, and playing important roles in viral and immune phenomena (122).

There are three major classifications for zinc-dependent proteins: structural, co-catalytic, and catalytic. The only amino acids known to serve as zinc-binding ligands in enzymes are aspartate, glutamate, cysteine, and histidine (123). Structural zincs, which do not bind water, bind four protein ligands, most commonly cysteine (121, 122). Co-catalytic zinc enzymes have two atoms of zinc in close proximity, with each metal bridged by a side chain moiety of aspartate, glutamate, histidine, or water (121, 124). Finally, catalytic zincs have a single zinc atom bound to water and any three nitrogen, oxygen, and sulfur donors from a nearby amino acid side chain, with histidine being the most common (121, 122, 124, 125).

For catalytic zinc sites, the identity of the three amino acid ligands (Asp, Glu, His), their spacing, and their secondary interactions with neighboring amino acids are believed to be crucial for zinc-mediated catalysis (121). Although zinc is the only transition metal essential to the function of members of each of the six enzyme classes, it is most commonly required among the hydrolases (121, 125). The only shared feature of the zinc hydrolase superfamily, which consists of divergently related proteins that include aminopeptidases, carboxypeptidases, and deacetylases, is the use of zinc in the catalytic mechanism (124). Two histidines are characteristic of carboxypeptidases A and B, thermolysin, phospholipase C, and alkaline phosphatase, while three histidines are characteristic of carbonic anhydrase I/II, B-lactamase, and DD-carboyxpeptidase of Streptomyces albus G (125). The only catalytic zinc enzyme with just one histidine is alcohol dehydrogenase, which is also the only catalytic zinc enzyme that contains two cysteine ligands (125).

For several enzymes, the first two ligands are separated by 1-3 amino acids, and the second and third ligands are separated by 20 to 120 amino acids (125). In addition to providing stability to zinc coordination, this long spacer arm might participate in alignment of the active site, bringing catalytic and substrate-binding groups into apposition (122). In contrast to spacing in catalytic zinc enzymes, the interligand distances in structural zinc sites are short, and are consistent with a role for zinc in protein stability analogous to disulfide bonding (125).

ASPA As a Metalloenzyme

Several studies have indicated that zinc has an important role in ASPA catalysis. The divalent cation chelators, EDTA and EGTA, have been shown to drastically reduce ASPA specific activity in bovine brain homogenate (20) and in dialyzed recombinant human ASPA purified from *E. coli* (22). Zinc chloride slightly increased purified bovine brain ASPA specific activity (~120%) at low concentrations (0.001 mM) and inhibited specific activity at higher concentrations (20). Following dialysis and denaturation of recombinant human ASPA expressed in *E. coli*, roughly two atoms of zinc were detected per enzyme subunit by ion-coupled plasma spectroscopy as the only significant metal ion present (22).

A recent report inspected the relationship of zinc content and activity in recombinant human ASPA purified from *P. pastoris* (21). First, dialysis alone did not remove zinc, which explains why up to 5 mM EDTA and EGTA had no effect on purified brain ASPA specific activity in a previous study (20). This also explained why zinc-treated ASPA was similarly active to native ASPA refolded without additional metal

ions (22). Second, dialysis against 5 mM orthophenantroline (OP), which is more specific to zinc than EDTA and EGTA, for 72 hours resulted in ~14% residual ASPA activity compared with dialysis against buffer lacking OP, concomitantly decreasing zinc content from 1.3 to 0.2 atoms per subunit (21). The addition of up to 3 μM $ZnCl_2$ restored full activity while higher levels led to inhibition. Finally, glycosylation did not affect metal binding as the zinc content of the N117Q mutant was 1.1 atoms per subunit. These experiments showed that ASPA is a zinc-dependent metalloenzyme with a single zinc atom that is required for catalysis, but did not explore the nature of its zinc binding ligands.

ASPA and CPA

ASPA is a potential member of the zinc-dependent CPA enzyme family (40). Carboxypeptidases complement the actions of chymotrypsin, pepsin, and trypsin by catalyzing the degradation of food-derived polypeptides to amino acids such as Arg, Lys, Phe, and Trp (121). Specifically, CPA (EC 3.4.17.1) is a 307 amino acid, 34.5 kDa metalloexopeptidase that hydrolyzes C-terminal amino acids from polypeptide substrates (126). The zinc-binding site of the CPA family is characterized by a unique short zinc binding motif containing the first two ligands, histidine and glutamate (127). The third zinc ligand is a histidine that is located 108-135 amino acids C-terminal to this motif (127). Although the carboxypeptidase superfamily includes some enzymes that bind two zinc atoms, CPA family members have been shown to bind a single zinc atom (40, 126).

The nature of the active site and the catalytic mechanism of the carboxypeptidases might help elucidate structure and function relationships in ASPA. There are numerous

existing crystal structures of CPA family members (126, 128-135). The catalytic zinc site of CPA, referred to as the S1 pocket, consists of the δ1 nitrogen of His69, the ε1 and ε2 oxygens of Glu72, the δ1 nitrogen of His196, and a water molecule (Figure 6) (126, 128). The first 2 ligands, separated by the "short spacer," reside in a seven amino acid loop region between a β-sheet and an α-helix, while His196, separated from Glu72 by a "long spacer," is the last residue in a β-pleated sheet (121, 125). Along with Glu270 and Arg145 (other residues essential for catalysis), these zinc binding ligands are highly conserved among 8 CPAs and carboxypeptidase Bs from cow, crayfish, human, mouse, and rat (122, 125). The S1' pocket contains the C-terminal carboxylate of the peptide substrate, hydrogen-bonded by a salt link to the positively charged guanidinium moiety of Arg145, hydrogen-bonded to Tyr248, and hydrogen-bonded to the amide group of Asn144 (126, 128, 136). Tyr248 appears to be involved in substrate binding but not in catalysis (126, 137).

Like its structure, the catalytic mechanism of CPA is well-characterized (40, 124, 136, 137). It is believed that carboxypeptidases operate by a similar general base mechanism (124, 138). Here, zinc is a classical electrophilic catalyst providing electrostatic stabilization for negatively charged intermediates formed during the reaction course (126). An alternate hypothesis, known as the covalent acyl enzyme intermediate mechanism (characteristic of serine proteases), involves the COO^- of Glu270 forming a covalent bond (anhydride) with the COOH of the substrate. There is little support for this hypothesis.

A detailed reaction mechanism for CPA (Figure 6) has recently been described (128). First, the positive charge distribution at the active site, specifically facilitated by Asn144, Arg145, and Tyr248, assists in binding the negatively charged C-terminus of the substrate (Figure 6A). The scissile (easily split) carbonyl oxygen then becomes the 6th zinc ligand (Glu72 bidentate, His69, His196, water). Along with the approaching guanidinium ($CHCO_2^-NH_3^+$) group of Arg127, the substrate's scissile carbonyl oxygen makes the zinc-bound water molecule more acidic so its proton moves to the COO^- of Glu270 (Figure 6B). The remaining zinc-bound hydryoxyl (OH^-) group then performs a nucleophilic attack on the scissile carbonyl carbon, which creates the negatively charged transition state (Figure 6C). This gem-diolate anion (referring to twin O^- groups) is stabilized by the guanidinium group of Arg127 and bidentate coordination with zinc. Once the gem-diolate collapses to form the products, the released amino acid obtains protons from Glu270 and water (Figure 6D). The positively charged ammonium groups of the arginines in the active site then help to expel the product. Product efflux from the active site is accompanied by an influx of water. In summary, CPA catalysis involves Glu270 accepting a proton from a water molecule so that it can perform a nucleophilic attack on the carbonyl carbon of the substrate's scissile bond, followed by proton transfer to the leaving amino group of the peptide substrate, with a single zinc ion involved in water polarization and stabilization of the tetrahydral substrate intermediate (40, 124, 136, 137).

Several residues involved in CPA catalysis are conserved in human and murine ASPA (23, 40) and are equivalent to those involved in zinc coordination (His21, Glu24, His116), substrate-binding cavity shaping (Asp68), substrate binding (Arg71), transition

state stability (Arg63), and catalysis (Glu178) (40). Notably, missense mutations at His21, Glu24, Asp68, and Arg71 have been detected in CD patients (9, 13, 16). While there are no existing CD mutations at Glu178, there are nearby CD mutations at Pro181, Pro183, and Val186 (8, 13, 16), suggesting Glu178 might be an important catalytic residue. The biological significance of the similarities between ASPA and CPA has not been established.
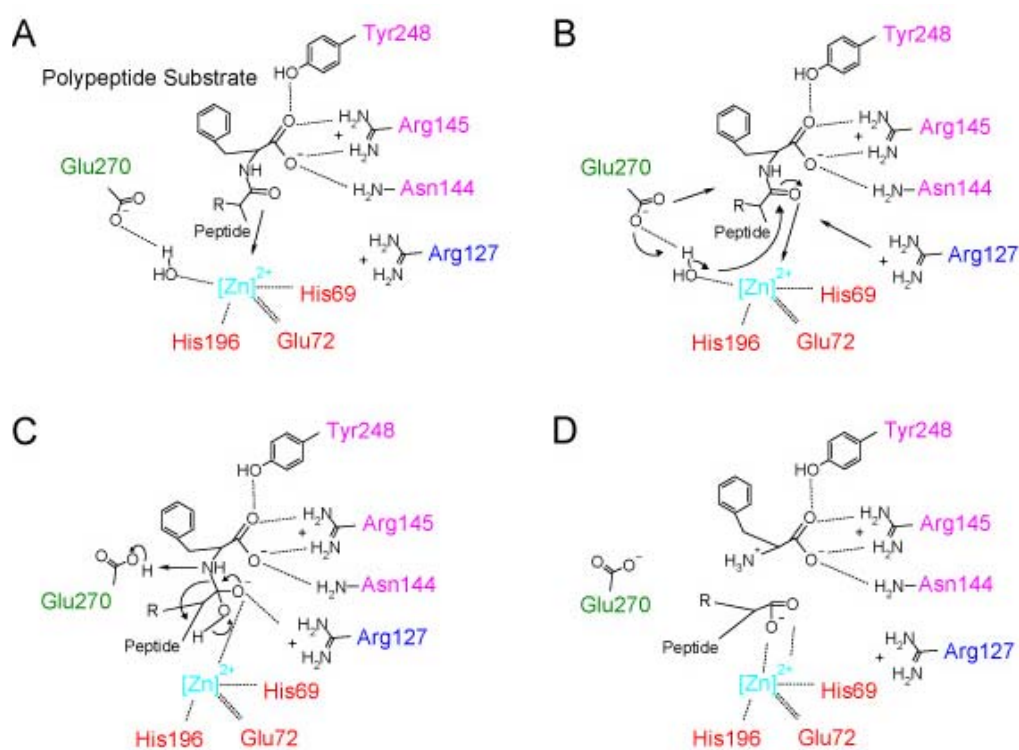

Figure 6. **Catalytic mechanism of CPA.** The catalytic zinc atom is in cyan blue. The catalytic proton donor is in green. Zinc-binding ligands are in red. Substrate binding ligands are in magenta. A transition state stabilizing residue is in blue. *A*, Substrate binding. *B*, Nucleophilic attack. *C*, Transition-state intermediate. *D*, Product formation

References

1.   Kaul, R., Gao, G. P., Balamurugan, K., and Matalon, R. (1993) Cloning of the human aspartoacylase cDNA and a common missense mutation in Canavan disease. *Nat Genet* **5**, 118-123

2.   Kaul, R., Balamurugan, K., Gao, G. P., and Matalon, R. (1994) Canavan disease: genomic organization and localization of human ASPA to 17p13-ter and conservation of the ASPA gene during evolution. *Genomics* **21**, 364-370

3.   Birnbaum, S. M., Levintow, L., Kingsley, R. B., and Greenstein, J. P. (1952) Specificity of amino acid acylases. *J Biol Chem* **194**, 455-470

4.   Matalon, R., Michals, K., Sebesta, D., Deanching, M., Gashkoff, P., and Casanova, J. (1988) Aspartoacylase deficiency and N-acetylaspartic aciduria in patients with Canavan disease. *Am J Med Genet* **29**, 463-471

5.   Kronn, D., Oddoux, C., Phillips, J., and Ostrer, H. (1995) Prevalence of Canavan disease heterozygotes in the New York metropolitan Ashkenazi Jewish population. *Am J Hum Genet* **57**, 1250-1252

6.   Leone, P., Janson, C. G., McPhee, S. J., and During, M. J. (1999) Global CNS gene transfer for a childhood neurogenetic enzyme deficiency: Canavan disease. *Curr Opin Mol Ther* **1**, 487-492

7.   Feigenbaum, A., Moore, R., Clarke, J., Hewson, S., Chitayat, D., Ray, P. N., and Stockley, T. L. (2004) Canavan disease: carrier-frequency determination in the Ashkenazi Jewish population and development of a novel molecular diagnostic assay. *Am J Med Genet* **124A**, 142-147

8.   Elpeleg, O. N., and Shaag, A. (1999) The spectrum of mutations of the aspartoacylase gene in Canavan disease in non-Jewish patients. *J Inherit Metab Dis* **22**, 531-534

9.   Janson, C. G., Kolodny, E. H., Zeng, B. J., Raghavan, S., Pastores, G., Torres, P., Assadi, M., McPhee, S., Goldfarb, O., Saslow, B., Freese, A., Wang, D. J., Bilaniuk, L., Shera, D., and Leone, P. (2006) Mild-onset presentation of Canavan's disease associated with novel G212A point mutation in aspartoacylase gene. *Ann Neurol* **59**, 428-431

10.   Kaul, R., Gao, G. P., Aloya, M., Balamurugan, K., Petrosky, A., Michals, K., and Matalon, R. (1994) Canavan disease: mutations among Jewish and non-jewish patients. *Am J Hum Genet* **55**, 34-41

11.   Kaul, R., Gao, G. P., Matalon, R., Aloya, M., Su, Q., Jin, M., Johnson, A. B., Schutgens, R. B., and Clarke, J. T. (1996) Identification and expression of eight novel mutations among non-Jewish patients with Canavan disease. *Am J Hum Genet* **59**, 95-102

12.   Shaag, A., Anikster, Y., Christensen, E., Glustein, J. Z., Fois, A., Michelakakis, H., Nigro, F., Pronicka, E., Ribes, A., Zabot, M. T., and et al. (1995) The molecular basis of canavan (aspartoacylase deficiency) disease in European non-Jewish patients. *Am J Hum Genet* **57**, 572-580

13.   Sistermans, E. A., de Coo, R. F., van Beerendonk, H. M., Poll-The, B. T., Kleijer, W. J., and van Oost, B. A. (2000) Mutation detection in the aspartoacylase gene in 17 patients with Canavan disease: four new mutations in the non-Jewish population. *Eur J Hum Genet* **8**, 557-560

14.   Yalcinkaya, C., Benbir, G., Salomons, G. S., Karaarslan, E., Rolland, M. O., Jakobs, C., and van der Knaap, M. S. (2005) Atypical MRI findings in Canavan disease: a patient with a mild course. *Neuropediatrics* **36**, 336-339

15.   Zeng, B. J., Pastores, G. M., Leone, P., Raghavan, S., Wang, Z. H., Ribeiro, L. A., Torres, P., Ong, E., and Kolodny, E. H. (2006) Mutation analysis of the aspartoacylase gene in non-Jewish patients with Canavan disease. *Adv Exp Med Biol* **576**, 165-173; discussion 361-163

16. Zeng, B. J., Wang, Z. H., Ribeiro, L. A., Leone, P., De Gasperi, R., Kim, S. J., Raghavan, S., Ong, E., Pastores, G. M., and Kolodny, E. H. (2002) Identification and characterization of novel mutations of the aspartoacylase gene in non-Jewish patients with Canavan disease. *J Inherit Metab Dis* **25**, 557-570

17. Kitada, K., Akimitsu, T., Shigematsu, Y., Kondo, A., Maihara, T., Yokoi, N., Kuramoto, T., Sasa, M., and Serikawa, T. (2000) Accumulation of N-acetyl-L-aspartate in the brain of the tremor rat, a mutant exhibiting absence-like seizure and spongiform degeneration in the central nervous system. *J Neurochem* **74**, 2512-2519

18. Matalon, R., Rady, P. L., Platt, K. A., Skinner, H. B., Quast, M. J., Campbell, G. A., Matalon, K., Ceci, J. D., Tyring, S. K., Nehls, M., Surendran, S., Wei, J., Ezell, E. L., and Szucs, S. (2000) Knock-out mouse for Canavan disease: a model for gene transfer to the central nervous system. *J Gene Med* **2**, 165-175

19. Birnbaum, S. M. (1955) Amino acid acylases I and II from hog kidney. *Methods in Enzymology* **2**, 115-119

20. Kaul, R., Casanova, J., Johnson, A. B., Tang, P., and Matalon, R. (1991) Purification, characterization, and localization of aspartoacylase from bovine brain. *J Neurochem* **56**, 129-135

21. Le Coq, J., An, H. J., Lebrilla, C., and Viola, R. E. (2006) Characterization of human aspartoacylase: the brain enzyme responsible for canavan disease. *Biochemistry* **45**, 5878-5884

22. Moore, R. A., Le Coq, J., Faehnle, C. R., and Viola, R. E. (2003) Purification and preliminary characterization of brain aspartoacylase. *Arch Biochem Biophys* **413**, 1-8

23. Namboodiri, M. A., Corigliano-Murphy, A., Jiang, G., Rollag, M., and Provencio, I. (2000) Murine aspartoacylase: cloning, expression and comparison with the human enzyme. *Brain Res Mol Brain Res* **77**, 285-289

24. Moffett, J. R., Namboodiri, M. A., Cangro, C. B., and Neale, J. H. (1991) Immunohistochemical localization of N-acetylaspartate in rat brain. *Neuroreport* **2**, 131-134

25. Clark, J. B. (1998) N-acetyl aspartate: a marker for neuronal loss or mitochondrial dysfunction. *Dev Neurosci* **20**, 271-276

26. Mehta, V., and Namboodiri, M. A. (1995) N-acetylaspartate as an acetyl source in the nervous system. *Brain Res Mol Brain Res* **31**, 151-157

27. Baslow, M. H. (1999) Molecular water pumps and the aetiology of Canavan disease: a case of the sorcerer's apprentice. *J Inherit Metab Dis* **22**, 99-101

28. Klugmann, M., Symes, C. W., Klaussner, B. K., Leichtlein, C. B., Serikawa, T., Young, D., and During, M. J. (2003) Identification and distribution of aspartoacylase in the postnatal rat brain. *Neuroreport* **14**, 1837-1840

29. Kirmani, B. F., Jacobowitz, D. M., Kallarakal, A. T., and Namboodiri, M. A. (2002) Aspartoacylase is restricted primarily to myelin synthesizing cells in the CNS: therapeutic implications for Canavan disease. *Brain Res Mol Brain Res* **107**, 176-182

30. Madhavarao, C. N., Moffett, J. R., Moore, R. A., Viola, R. E., Namboodiri, M. A., and Jacobowitz, D. M. (2004) Immunohistochemical localization of aspartoacylase in the rat central nervous system. *J Comp Neurol* **472**, 318-329

31. Baslow, M. H., Suckow, R. F., Sapirstein, V., and Hungund, B. L. (1999) Expression of aspartoacylase activity in cultured rat macroglial cells is limited to oligodendrocytes. *J Mol Neurosci* **13**, 47-53

32. Tsai, G., and Coyle, J. T. (1995) N-acetylaspartate in neuropsychiatric disorders. *Prog Neurobiol* **46**, 531-540

33. Tallan, H. H., Moore, S., and Stein, W. H. (1956) N-Acetyl-L-aspartic acid in brain. *J Biol Chem* **219**, 257-264

34.   Truckenmiller, M. E., Namboodiri, M. A., Brownstein, M. J., and Neale, J. H. (1985) N-Acetylation of L-aspartate in the nervous system: differential distribution of a specific enzyme. *J Neurochem* **45**, 1658-1662

35.   Matalon, R., Kaul, R., and Michals, K. (1993) Canavan disease: biochemical and molecular studies. *J Inherit Metab Dis* **16**, 744-752

36.   D'Adamo, A. F., Jr., Smith, J. C., and Woiler, C. (1973) The occurrence of N-acetylaspartate amidohydrolase (aminoacylase II) in the developing rat. *J Neurochem* **20**, 1275-1278

37.   D'Adamo, A. F., Jr., Wertman, E., Foster, F., and Schneider, H. (1978) A radiochemical assay for N-acetyl-L-aspartate amidohydrolase (EC 3.5.1.15) and its occurrence in the tissues of the chicken. *Life Sci* **23**, 791-795

38.   Cygler, M., Schrag, J. D., Sussman, J. L., Harel, M., Silman, I., Gentry, M. K., and Doctor, B. P. (1993) Relationship between sequence conservation and three-dimensional structure in a large family of esterases, lipases, and related proteins. *Protein Sci* **2**, 366-382

39.   Matalon, R., and Michals-Matalon, K. (1999) Recent advances in Canavan disease. *Adv Pediatr* **46**, 493-506

40.   Makarova, K. S., and Grishin, N. V. (1999) The Zn-peptidase superfamily: functional convergence after evolutionary divergence. *J Mol Biol* **292**, 11-17

41.   Canavan, M. (1931) Schilder's encephalitis periaxialis diffusa. *Arch Neurol Psychiatry.* **25**, 299-308

42.   van Bogaert L, B. I. (1949) Sur une idote familiale avec degenerescence sponglieuse de neuraxe (note preliminaire). *Acta Neurol Belg.* **49**, 572-587

43.   Hagenfeldt, L., Bollgren, I., and Venizelos, N. (1987) N-acetylaspartic aciduria due to aspartoacylase deficiency--a new aetiology of childhood leukodystrophy. *J Inherit Metab Dis* **10**, 135-141

44.   Kvittingen, E. A., Guldal, G., Borsting, S., Skalpe, I. O., Stokke, O., and Jellum, E. (1986) N-acetylaspartic aciduria in a child with a progressive cerebral atrophy. *Clin Chim Acta* **158**, 217-227

45.   Divry, P., Vianey-Liaud, C., Gay, C., Macabeo, V., Rapin, F., and Echenne, B. (1988) N-acetylaspartic aciduria: report of three new cases in children with a neurological syndrome associating macrocephaly and leukodystrophy. *J Inherit Metab Dis* **11**, 307-308

46.   Squire, L., Bloom, F., McConnell, S., Roberts, J., Spitzer, N., and Zigmond, M. (2003) *Fundamental Neuroscience* Vol. 2, Academic Press, New York

47.   Streit, W. J., Conde, J. R., Fendrick, S. E., Flanary, B. E., and Mariani, C. L. (2005) Role of microglia in the central nervous system's immune response. *Neurol Res* **27**, 685-691

48.   Wegner, M. (2001) Expression of transcription factors during oligodendroglial development. *Microsc Res Tech* **52**, 746-752

49.   Baumann, N., and Pham-Dinh, D. (2001) Biology of oligodendrocyte and myelin in the mammalian central nervous system. *Physiol Rev* **81**, 871-927

50.   Compston, A., Zajicek, J., Sussman, J., Webb, A., Hall, G., Muir, D., Shaw, C., Wood, A., and Scolding, N. (1997) Glial lineages and myelination in the central nervous system. *J Anat* **190 (Pt 2)**, 161-200

51.   Burri, R., Steffen, C., and Herschkowitz, N. (1991) N-acetyl-L-aspartate is a major source of acetyl groups for lipid synthesis during rat brain development. *Dev Neurosci* **13**, 403-411

52.   Florian, C. L., Williams, S. R., Bhakoo, K. K., and Noble, M. D. (1996) Regional and developmental variations in metabolite concentration in the rat brain and eye: a study using 1H NMR spectroscopy and high performance liquid chromatography. *Neurochem Res* **21**, 1065-1074

53.   Bhakoo, K. K., Craig, T. J., and Styles, P. (2001) Developmental and regional distribution of aspartoacylase in rat brain tissue. *J Neurochem* **79**, 211-220

54.   D'Adamo, A. F., Jr., Gidez, L. I., and Yatsu, F. M. (1968) Acetyl transport mechanisms. Involvement of N-acetyl aspartic acid in de novo fatty acid biosynthesis in the developing rat brain. *Exp Brain Res* **5**, 267-273

55.   Francis, J. S., Olariu, A., McPhee, S. W., and Leone, P. (2006) Novel role for aspartoacylase in regulation of BDNF and timing of postnatal oligodendrogenesis. *J Neurosci Res*

56.   Kirmani, B. F., Jacobowitz, D. M., and Namboodiri, M. A. (2003) Developmental increase of aspartoacylase in oligodendrocytes parallels CNS myelination. *Brain Res Dev Brain Res* **140**, 105-115

57.   Baslow, M. H. (2002) Evidence supporting a role for N-acetyl-L-aspartate as a molecular water pump in myelinated neurons in the central nervous system. An analytical review. *Neurochem Int* **40**, 295-300

58.   Matalon, R., and Michals-Matalon, K. (1999) Biochemistry and molecular biology of Canavan disease. *Neurochem Res* **24**, 507-513

59.   Akimitsu, T., Kurisu, K., Hanaya, R., Iida, K., Kiura, Y., Arita, K., Matsubayashi, H., Ishihara, K., Kitada, K., Serikawa, T., and Sasa, M. (2000) Epileptic seizures induced by N-acetyl-L-aspartate in rats: in vivo and in vitro studies. *Brain Res* **861**, 143-150

60.   Madhavarao, C. N., Arun, P., Moffett, J. R., Szucs, S., Surendran, S., Matalon, R., Garbern, J., Hristova, D., Johnson, A., Jiang, W., and Namboodiri, M. A. (2005) Defective N-acetylaspartate catabolism reduces brain acetate levels and myelin lipid synthesis in Canavan's disease. *Proc Natl Acad Sci U S A* **102**, 5221-5226

61.   Klugmann, M., Leichtlein, C. B., Symes, C. W., Serikawa, T., Young, D., and During, M. J. (2005) Restoration of aspartoacylase activity in CNS neurons does not ameliorate motor deficits and demyelination in a model of Canavan disease. *Mol Ther* **11**, 745-753

62.   Traeger, E. C., and Rapin, I. (1998) The clinical course of Canavan disease. *Pediatr Neurol* **18**, 207-212

63.   Matalon, R., Michals, K., and Kaul, R. (1995) Canavan disease: from spongy degeneration to molecular analysis. *J Pediatr* **127**, 511-517

64.   Zelnik, N., Luder, A. S., Elpeleg, O. N., Gross-Tsur, V., Amir, N., Hemli, J. A., Fattal, A., and Harel, S. (1993) Protracted clinical course for patients with Canavan disease. *Dev Med Child Neurol* **35**, 355-358

65.   Francois, J., and Manaligod, J. M. (2002) Upper airway abnormalities in Canavan disease. *Int J Pediatr Otorhinolaryngol* **66**, 303-307

66.   Burlina, A. P., Ferrari, V., Divry, P., Gradowska, W., Jakobs, C., Bennett, M. J., Sewell, A. C., Dionisi-Vici, C., and Burlina, A. B. (1999) N-acetylaspartylglutamate in Canavan disease: an adverse effector? *Eur J Pediatr* **158**, 406-409

67.   Besley, G. T., Elpeleg, O. N., Shaag, A., Manning, N. J., Jakobs, C., and Walter, J. H. (1999) Prenatal diagnosis of Canavan disease--problems and dilemmas. *J Inherit Metab Dis* **22**, 263-266

68.   Rolland, M. O., Divry, P., Mandon, G., Thoulon, J. M., Fiumara, A., and Mathieu, M. (1993) First-trimester prenatal diagnosis of Canavan disease. *J Inherit Metab Dis* **16**, 581-583

69.   Barash, V., Flhor, D., Morag, B., Boneh, A., Elpeleg, O. N., and Gilon, C. (1991) A radiometric assay for aspartoacylase activity in human fibroblasts: application for the diagnosis of Canavan's disease. *Clin Chim Acta* **201**, 175-181

70.   Matalon, R., Michals, K., Gashkoff, P., and Kaul, R. (1992) Prenatal diagnosis of Canavan disease. *J Inherit Metab Dis* **15**, 392-394

71.   Gordon, N. (2001) Canavan disease: a review of recent developments. *Eur J Paediatr Neurol* **5**, 65-69

72. Martin, E., Capone, A., Schneider, J., Hennig, J., and Thiel, T. (2001) Absence of N-acetylaspartate in the human brain: impact on neurospectroscopy? *Ann Neurol* **49**, 518-521

73. Baslow, M. H. (2000) Functions of N-acetyl-L-aspartate and N-acetyl-L-aspartylglutamate in the vertebrate brain: role in glial cell-specific signaling. *J Neurochem* **75**, 453-459

74. Bhakoo, K. K., Williams, I. T., Williams, S. R., Gadian, D. G., and Noble, M. D. (1996) Proton nuclear magnetic resonance spectroscopy of primary cells derived from nervous tissue. *J Neurochem* **66**, 1254-1263

75. Bhakoo, K. K., and Pearce, D. (2000) In vitro expression of N-acetyl aspartate by oligodendrocytes: implications for proton magnetic resonance spectroscopy signal in vivo. *J Neurochem* **74**, 254-262

76. Benuck, M., and D'Adamo, A. F., Jr. (1968) Acetyl transport mechanisms. Metabolism of N-acetyl-L-aspartic acid in the non-nervous tissues of the rat. *Biochim Biophys Acta* **152**, 611-618

77. Goldstein, F. B. (1959) Biosynthesis of N-acetyl-L-aspartic acid. *Biochim Biophys Acta* **33**, 583-584

78. Madhavarao, C. N., Chinopoulos, C., Chandrasekaran, K., and Namboodiri, M. A. (2003) Characterization of the N-acetylaspartate biosynthetic enzyme from rat brain. *J Neurochem* **86**, 824-835

79. Huang, W., Wang, H., Kekuda, R., Fei, Y. J., Friedrich, A., Wang, J., Conway, S. J., Cameron, R. S., Leibach, F. H., and Ganapathy, V. (2000) Transport of N-acetylaspartate by the Na(+)-dependent high-affinity dicarboxylate transporter NaDC3 and its relevance to the expression of the transporter in the brain. *J Pharmacol Exp Ther* **295**, 392-403

80. George, R. L., Huang, W., Naggar, H. A., Smith, S. B., and Ganapathy, V. (2004) Transport of N-acetylaspartate via murine sodium/dicarboxylate cotransporter NaDC3 and expression of this transporter and aspartoacylase II in ocular tissues in mouse. *Biochim Biophys Acta* **1690**, 63-69

81. Sager, T. N., Thomsen, C., Valsborg, J. S., Laursen, H., and Hansen, A. J. (1999) Astroglia contain a specific transport mechanism for N-acetyl-L-aspartate. *J Neurochem* **73**, 807-811

82. Chakraborty, G., Mekala, P., Yahya, D., Wu, G., and Ledeen, R. W. (2001) Intraneuronal N-acetylaspartate supplies acetyl groups for myelin lipid synthesis: evidence for myelin-associated aspartoacylase. *J Neurochem* **78**, 736-745

83. Madhavarao, C. N., Hammer, J. A., Quarles, R. H., and Namboodiri, M. A. (2002) A radiometric assay for aspartoacylase activity in cultured oligodendrocytes. *Anal Biochem* **308**, 314-319

84. Rao, M. S. (1999) Multipotent and restricted precursors in the central nervous system. *Anat Rec* **257**, 137-148

85. Namboodiri, A. M., Peethambaran, A., Mathew, R., Sambhu, P. A., Hershfield, J., Moffett, J. R., and Madhavarao, C. N. (2006) Canavan disease and the role of N-acetylaspartate in myelin synthesis. *Mol Cell Endocrinol*

86. Rubin, Y., LaPlaca, M. C., Smith, D. H., Thibault, L. E., and Lenkinski, R. E. (1995) The effect of N-acetylaspartate on the intracellular free calcium concentration in NTera2-neurons. *Neurosci Lett* **198**, 209-212

87. Arun, P., Madhavarao, C. N., Hershfield, J. R., Moffett, J. R., and Namboodiri, M. A. (2004) SH-SY5Y neuroblastoma cells: a model system for studying biosynthesis of NAAG. *Neuroreport* **15**, 1167-1170

88. Tyson, R. L., and Sutherland, G. R. (1998) Labeling of N-acetylaspartate and N-acetylaspartylglutamate in rat neocortex, hippocampus and cerebellum from [1-13C]glucose. *Neurosci Lett* **251**, 181-184

89. Leone, P., Janson, C. G., Bilaniuk, L., Wang, Z., Sorgi, F., Huang, L., Matalon, R., Kaul, R., Zeng, Z., Freese, A., McPhee, S. W., Mee, E., During, M. J., and Bilianuk, L. (2000) Aspartoacylase gene transfer to the mammalian central nervous system with therapeutic implications for Canavan disease. *Ann Neurol* **48**, 27-38

90. D'Adamo, A. F., Jr., and Yatsu, F. M. (1966) Acetate metabolism in the nervous system. N-acetyl-L-aspartic acid and the biosynthesis of brain lipids. *J Neurochem* **13**, 961-965

91. Mathew, R., Arun, P., Madhavarao, C. N., Moffett, J. R., and Namboodiri, M. A. (2005) Progress toward acetate supplementation therapy for Canavan disease: glyceryl triacetate administration increases acetate, but not N-acetylaspartate, levels in brain. *J Pharmacol Exp Ther* **315**, 297-303

92. Baslow, M. H. (2003) N-acetylaspartate in the vertebrate brain: metabolism and function. *Neurochem Res* **28**, 941-953

93. Olsen, T. R., Tranebjaerg, L., Kvittingen, E. A., Hagenfeldt, L., Moller, C., and Nilssen, O. (2002) Two novel aspartoacylase gene (ASPA) missense mutations specific to Norwegian and Swedish patients with Canavan disease. *J Med Genet* **39**, e55

94. Stenson, P. D., Ball, E. V., Mort, M., Phillips, A. D., Shiel, J. A., Thomas, N. S., Abeysinghe, S., Krawczak, M., and Cooper, D. N. (2003) Human Gene Mutation Database (HGMD): 2003 update. *Hum Mutat* **21**, 577-581

95. Elpeleg, O. N., Anikster, Y., Barash, V., Branski, D., and Shaag, A. (1994) The frequency of the C854 mutation in the aspartoacylase gene in Ashkenazi Jews in Israel. *Am J Hum Genet* **55**, 287-288

96. Propheta, O., Magal, N., Shohat, M., Eyal, N., Navot, N., and Horowitz, M. (1998) A benign polymorphism in the aspartoacylase gene may cause misinterpretation of Canavan gene testing. *Eur J Hum Genet* **6**, 635-637

97. Kobayashi, K., Tsujino, S., Ezoe, T., Hamaguchi, H., Nihei, K., and Sakuragawa, N. (1998) Missense mutation (I143T) in a Japanese patient with Canavan disease. *Hum Mutat* **Suppl 1**, S308-309

98. Kaul, R., Gao, G. P., Michals, K., Whelan, D. T., Levin, S., and Matalon, R. (1995) Novel (cys152 > arg) missense mutation in an Arab patient with Canavan disease. *Hum Mutat* **5**, 269-271

99. Tacke, U., Olbrich, H., Sass, J. O., Fekete, A., Horvath, J., Ziyeh, S., Kleijer, W. J., Rolland, M. O., Fisher, S., Payne, S., Vargiami, E., Zafeiriou, D. I., and Omran, H. (2005) Possible genotype-phenotype correlations in children with mild clinical course of Canavan disease. *Neuropediatrics* **36**, 252-255

100. Rady, P. L., Vargas, T., Tyring, S. K., Matalon, R., and Langenbeck, U. (1999) Novel missense mutation (Y231C) in a turkish patient with canavan disease. *Am J Med Genet* **87**, 273-275

101. Surendran, S., Bamforth, F. J., Chan, A., Tyring, S. K., Goodman, S. I., and Matalon, R. (2003) Mild elevation of N-acetylaspartic acid and macrocephaly: diagnostic problem. *J Child Neurol* **18**, 809-812

102. Rady, P. L., Penzien, J. M., Vargas, T., Tyring, S. K., and Matalon, R. (2000) Novel splice site mutation of aspartoacylase gene in a Turkish patient with Canavan disease. *Eur J Paediatr Neurol* **4**, 27-30

103. Tahmaz, F. E., Sam, S., Hoganson, G. E., and Quan, F. (2001) A partial deletion of the aspartoacylase gene is the cause of Canavan disease in a family from Mexico. *J Med Genet* **38**, E9

104. Adachi, M., Schneck, L., Cara, J., and Volk, B. W. (1973) Spongy degeneration of the central nervous system (van Bogaert and Bertrand type; Canavan's disease). A review. *Hum Pathol* **4**, 331-347

105. von Moers, A., Sperner, J., Michael, T., Scheffner, D., and Schutgens, R. H. (1991) Variable course of Canavan disease in two boys with early infantile aspartoacylase deficiency. *Dev Med Child Neurol* **33**, 824-828

106. Azzam, N. A., Bready, J. V., Vinters, H. V., and Cancilla, P. A. (1984) Spontaneous spongy degeneration of the mouse brain. *J Neuropathol Exp Neurol* **43**, 118-130

107. Hagen, G., and Bjerkas, I. (1990) Spongy degeneration of white matter in the central nervous system of silver foxes (Vulpes vulpes). *Vet Pathol* **27**, 187-193

108. Zachary, J. F., and O'Brien, D. P. (1985) Spongy degeneration of the central nervous system in two canine littermates. *Vet Pathol* **22**, 561-571

109. Surendran, S., Matalon, K. M., Szucs, S., Tyring, S. K., and Matalon, R. (2003) Metabolic changes in the knockout mouse for Canavan's disease: implications for patients with Canavan's disease. *J Child Neurol* **18**, 611-615

110. Surendran, S., Rady, P. L., Michals-Matalon, K., Quast, M. J., Rassin, D. K., Campbell, G. A., Ezell, E. L., Wei, J., Tyring, S. K., Szucs, S., and Matalon, R. (2003) Expression of glutamate transporter, GABRA6, serine proteinase inhibitor 2 and low levels of glutamate and GABA in the brain of knock-out mouse for Canavan disease. *Brain Res Bull* **61**, 427-435

111. Matalon, R., Surendran, S., Rady, P. L., Quast, M. J., Campbell, G. A., Matalon, K. M., Tyring, S. K., Wei, J., Peden, C. S., Ezell, E. L., Muzyczka, N., and Mandel, R. J. (2003) Adeno-associated virus-mediated aspartoacylase gene transfer to the brain of knockout mouse for canavan disease. *Mol Ther* **7**, 580-587

112. Surendran, S., Shihabuddin, L. S., Clarke, J., Taksir, T. V., Stewart, G. R., Parsons, G., Yang, W., Tyring, S. K., Michals-Matalon, K., and Matalon, R. (2004) Mouse neural progenitor cells differentiate into oligodendrocytes in the brain of a knockout mouse model of Canavan disease. *Brain Res Dev Brain Res* **153**, 19-27

113. Yamada, J., Serikawa, T., Ishiko, J., Inui, T., Takada, H., Kawai, Y., and Okaniwa, A. (1985) Rats with congenital tremor and curled whiskers and hair. *Jikken Dobutsu* **34**, 183-188

114. Seki, T., Matsubayashi, H., Amano, T., Kitada, K., Serikawa, T., Sakai, N., and Sasa, M. (2002) Adenoviral gene transfer of aspartoacylase into the tremor rat, a genetic model of epilepsy, as a trial of gene therapy for inherited epileptic disorder. *Neurosci Lett* **328**, 249-252

115. Seki, T., Matsubayashi, H., Amano, T., Kitada, K., Serikawa, T., Sasa, M., and Sakai, N. (2004) Adenoviral gene transfer of aspartoacylase ameliorates tonic convulsions of spontaneously epileptic rats. *Neurochem Int* **45**, 171-178

116. McPhee, S. W., Francis, J., Janson, C. G., Serikawa, T., Hyland, K., Ong, E. O., Raghavan, S. S., Freese, A., and Leone, P. (2005) Effects of AAV-2-mediated aspartoacylase gene transfer in the tremor rat model of Canavan disease. *Brain Res Mol Brain Res* **135**, 112-121

117. Uttamsingh, V., Baggs, R. B., Krenitsky, D. M., and Anders, M. W. (2000) Immunohistochemical localization of the acylases that catalyze the deacetylation of N-acetyl-L-cysteine and haloalkene-derived mercapturates. *Drug Metab Dispos* **28**, 625-632

118. Pushkin, A., Carpenito, G., Abuladze, N., Newman, D., Tsuprun, V., Ryazantsev, S., Motemoturu, S., Sassani, P., Solovieva, N., Dukkipati, R., and Kurtz, I. (2004) Structural characterization, tissue distribution, and functional expression of murine aminoacylase III. *Am J Physiol Cell Physiol* **286**, C848-856

119. Suzuki, Y., Yamashita, R., Nakai, K., and Sugano, S. (2002) DBTSS: DataBase of human Transcriptional Start Sites and full-length cDNAs. *Nucleic Acids Res* **30**, 328-331

120. Persson, B. (2000) Bioinformatics in protein analysis. *Exs* **88**, 215-231

121. Auld, D. S. (2001) Zinc coordination sphere in biochemical zinc sites. *Biometals* **14**, 271-313

122. Vallee, B. L., and Auld, D. S. (1990) Zinc coordination, function, and structure of zinc enzymes and other proteins. *Biochemistry* **29**, 5647-5659

123. Medina, J. F., Wetterholm, A., Radmark, O., Shapiro, R., Haeggstrom, J. Z., Vallee, B. L., and Samuelsson, B. (1991) Leukotriene A4 hydrolase: determination of the three zinc-binding ligands by site-directed mutagenesis and zinc analysis. *Proc Natl Acad Sci U S A* **88**, 7620-7624

124. Wouters, M. A., and Husain, A. (2001) Changes in zinc ligation promote remodeling of the active site in the zinc hydrolase superfamily. *J Mol Biol* **314**, 1191-1207

125. Vallee, B. L., and Auld, D. S. (1990) Active-site zinc ligands and activated H2O of zinc enzymes. *Proc Natl Acad Sci U S A* **87**, 220-224

126. Christianson, D. W., and Lipscomb, W. N. (1986) X-ray crystallographic investigation of substrate binding to carboxypeptidase A at subzero temperature. *Proc Natl Acad Sci U S A* **83**, 7568-7572

127. Hooper, N. M. (1994) Families of zinc metalloproteases. *FEBS Lett* **354**, 1-6

128. Jensen, F., Bukrinsky, T., Bjerrum, J., and Larsen, S. (2002) Three high-resolution crystal structures of cadmium-substituted carboxypeptidase A provide insight into the enzymatic function. *J Biol Inorg Chem* **7**, 490-499

129. Rees, D. C., Lewis, M., and Lipscomb, W. N. (1983) Refined crystal structure of carboxypeptidase A at 1.54 A resolution. *J Mol Biol* **168**, 367-387

130. Bukrinsky, J. T., Bjerrum, M. J., and Kadziola, A. (1998) Native carboxypeptidase A in a new crystal environment reveals a different conformation of the important tyrosine 248. *Biochemistry* **37**, 16555-16564

131. Shoham, G., Rees, D. C., and Lipscomb, W. N. (1984) Effects of pH on the structure and function of carboxypeptidase A: crystallographic studies. *Proc Natl Acad Sci U S A* **81**, 7767-7771

132. van Aalten, D. M., Chong, C. R., and Joshua-Tor, L. (2000) Crystal structure of carboxypeptidase A complexed with D-cysteine at 1.75 A - inhibitor-induced conformational changes. *Biochemistry* **39**, 10082-10089

133. Gomez-Ortiz, M., Gomis-Ruth, F. X., Huber, R., and Aviles, F. X. (1997) Inhibition of carboxypeptidase A by excess zinc: analysis of the structural determinants by X-ray crystallography. *FEBS Lett* **400**, 336-340

134. Greenblatt, H. M., Feinberg, H., Tucker, P. A., and Shoham, G. (1998) Carboxypeptidase A: native, zinc-removed and mercury-replaced forms. *Acta Crystallogr D Biol Crystallogr* **54**, 289-305

135. Kilshtain-Vardi, A., Glick, M., Greenblatt, H. M., Goldblum, A., and Shoham, G. (2003) Refined structure of bovine carboxypeptidase A at 1.25 A resolution. *Acta Crystallogr D Biol Crystallogr* **59**, 323-333

136. Kim, H., and Lipscomb, W. N. (1990) Crystal structure of the complex of carboxypeptidase A with a strongly bound phosphonate in a new crystalline form: comparison with structures of other complexes. *Biochemistry* **29**, 5546-5555

137. Matthews, B. W. (1988) Structural Basis of the Action of Thermolysin and Related Zinc Peptidases. *Accelerated Chemical Research* **21**, 333-340

138. Kim, H., and Lipscomb, W. N. (1991) Comparison of the structures of three carboxypeptidase A-phosphonate complexes determined by X-ray crystallography. *Biochemistry* **30**, 8171-8180

Aspartoacylase is a regulated nuclear-cytoplasmic enzyme

Jeremy R. Hershfield,* Chikkathur N. Madhavarao,* John R. Moffett,* Joyce A. Benjamins,† James Y. Garbern,†,‡ and Aryan Namboodiri*,1

*Department of Anatomy, Physiology, and Genetics, The Uniformed Services University of the Health Sciences, Bethesda, Maryland, USA; †Department of Neurology, Wayne State University School of Medicine, Detroit, Michigan, USA; ‡Center for Molecular Medicine and Genetics, Wayne State University School of Medicine, Detroit, Michigan, USA

ABSTRACT Mutations in the gene for aspartoacylase (ASPA), which catalyzes deacetylation of *N*-acetyl-L-aspartate in the central nervous system (CNS), result in Canavan Disease, a fatal dysmyelinating disease. Consistent with its role in supplying acetate for myelin lipid synthesis, ASPA is thought to be cytoplasmic. Here we describe the occurrence of ASPA within nuclei of rat brain and kidney, and in cultured rodent oligodendrocytes. Immunohistochemistry showed cytoplasmic and nuclear ASPA staining, the specificity of which was demonstrated by its absence from tissues of the *Tremor* rat, an ASPA-null mutant. Subcellular fractionation analysis revealed low enzyme activity against NAA in nuclear fractions from normal rats. Whereas two recent reports have indicated that ASPA exists as a dimer, size-exclusion chromatography of subcellular fractions showed ASPA is an active monomer in both subcellular fractions. Western blotting detected ASPA as a single 38 kD band. Because ASPA is small enough to passively diffuse into the nucleus, we constructed, expressed, and detected in COS-7 cells a green fluorescent protein-human ASPA (GFP-hASPA) fusion protein larger than the permissible size for the nuclear pore complex. GFP-hASPA was enzymatically active and showed mixed nuclear-cytoplasmic distribution. We conclude that ASPA is a regulated nuclear-cytoplasmic protein that may have distinct functional roles in the two cellular compartments.—Hershfield, J. R., Madhavarao, C. N., Moffett, J. R., Benjamins, J. A., Garbern, J. Y., Namboodiri, A. Aspartoacylase is a regulated nuclear-cytoplasmic enzyme. *FASEB J.* 20, E000–E000 (2006)

Key Words: Canavan Disease · N-acetylaspartate · aminoacylase · kidney · oligodendrocytes · Tremor rat

MUTATIONS IN THE gene encoding aspartoacylase (ASPA, EC 3.5.1.15), which catalyzes deacetylation of *N*-acetyl-aspartate (NAA), result in Canavan Disease (CD), a neurodegenerative disorder most prevalent among Ashkenazi Jews. The pathology of CD is marked by brain vacuolization and dysmyelination, resulting in death during childhood (1, 2). Considerable effort has been devoted to understanding the basis of CD by elucidating the function of ASPA in the CNS. Developmental increases in ASPA and NAA correlate with myelination (3–8) and several studies have shown incorporation of acetate from NAA into myelin lipids (9–13). Overall acetate levels and lipid synthesis have recently been shown to be deficient in brains of CD knockout mice (14), providing strong support for the hypothesis that NAA in the CNS supplies acetyl groups for lipid synthesis during myelination (3, 7, 14). The functions served by ASPA in other tissues such as kidney (17) are currently unknown.

ASPA activity was originally found to be restricted to cultured oligodendrocytes (15). Subsequently, antibodies against recombinant human ASPA (8) and recombinant murine ASPA (16) demonstrated ASPA expression primarily in oligodendrocytes in rat brain by immunohistochemistry. These and earlier studies showing ASPA activity restricted to the cytoplasm (6, 7) and in membrane fractions (11, 17, 18) have implied a specific subcellular localization for ASPA, but this remains to be established definitively. Immunohistochemistry of rat brain sections identified oligodendrocytes expressing ASPA protein and provided initial indications that ASPA is present in the nucleus as well (16). Currently, all hypotheses linking the basis of CD pathology to the function of ASPA refer to a cytoplasmic role for the enzyme. However, in order to completely understand and fully treat the disease, the possibility of nuclear ASPA localization, and the concomitant possibility of specific nuclear functions, warrant investigation.

Recently, separate analyses have suggested that recombinant human ASPA [MW of 35–38 kD (19)] exists as a dimer without posttranslational modifications (8, 19, 20). ASPA purified from *E. coli* was initially characterized as a dimer by mass spectroscopy (20) and later by Western blot (8), implying covalent dimerization. However, neither study investigated whether ASPA is active as a dimer, or whether the dimer band was ASPA-specific.

In this report we investigated ASPA's subcellular localization using rat organs, cultured oligodendrocytes, and transfected cells. Furthermore, we explored the catalytic properties of ASPA in subcellular fractions from rat brain and kidney.

MATERIALS AND METHODS

Rodent oligodendrocyte culture

Primary rat oligodendroglia were cultured from brains of 2 d old Sprague-Dawley rat pups as described previously (21). Maturity was determined by using antibodies against cell type-specific markers (21); specifically, expression of myelin oligodendrocyte glycoprotein (MOG; detected with monoclonal antibody (mAb) 8–18C5; hybridoma cells) (22) was associated with full maturity.

Enriched murine oligodendroglia cultures were prepared from brains of 1 to 2 d-old Balb/C mice (23) by a modification of the shake-off method (24). To improve oligodendrocyte survival, enriched oligodendrocyte cultures were maintained in a 2:1 mixture of (*i*) chemically defined medium with 2% newborn calf serum and (*ii*) astrocyte conditioned medium consisting of Dulbecco's modified Eagle's medium (DMEM) with 10% newborn calf serum. Three days later, fluorodeoxyuridine (5 μg/ml) was added to inhibit proliferation of astrocyte and other cellular contaminants. Cells were analyzed 5–9 d after enrichment and typically contained ~90–95% oligodendrocytes, most of which were mature and positive for MBP and PLP1 staining, as described previously (23).

Aspartoacylase immunocytochemistry

Cultured rat oligodendroglia were fixed with 4% paraformaldehyde (10 min), washed with PBS, and incubated overnight (4°C) with a monoclonal anti-MOG antibody (Ab) (22) (diluted 1:5 in PBS and 3% BSA, BSA) and a polyclonal antibody (pAb) against full-length recombinant murine ASPA (αASPA, diluted 1:500 in PBS). Cells were washed with PBS, preincubated with 5% donkey serum (20 min), and incubated with FITC-conjugated donkey anti mouse (1:200) and Cy3-conjugated donkey anti-rabbit (1:400) secondary antibodies diluted in PBS + 3% BSA (1 h, RT). Cells were washed with PBS and mounted using Vectashield medium with 4′,6′-diam idino-2-phenylidole (DAPI) (Vector Lab, Burlingame, CA).

Briefly, immunocytochemistry on cultured murine oligodendrocytes was performed with a 1:5000 dilution of rabbit sera against a domain conserved in rodent and human ASPA (residues 83–101 SEDLPYEVRRAQEINHLFG; pepASPA) after treating the cells with 0.01% Triton-X. Bound Ab was detected using appropriate fluorescently labeled anti-rabbit IgG. Indirect epifluorescent microscopy was performed using a Nikon TE2000 instrument (Melville, NY).

COS-7 cells were fixed (20 min in 10% formalin) 30–48 h posttransfection, washed with PBS, and incubated 1 h with 1:1000 αASPA or pepASPA in PBS plus 3% BSA. Following PBS washes, cells were incubated 1 h in 1:100 FITC-conjugated goat anti-rabbit secondary Ab (Jackson, West Grove, PA), washed, and mounted on slides using VectaShield Mounting Medium with DAPI. Confocal microscopy and subsequent data analysis were done using the Zeiss Pascal Laser Scanning Confocal Microscope and proprietary software (Thornwood, NY).

Aspartoacylase immunohistochemistry

Confocal microscopy was performed as described above. Peroxidase immunohistochemistry was performed as described previously (16). Briefly, free-floating rat tissue sections were blocked by incubation for 20 min in PBS containing 2% NGS and 0.1% sodium azide. Endogenous peroxidase was blocked by washing sections in PBS and incubating them in a 50:50 mixture of methanol and water containing 1% H_2O_2 for 30 min with agitation. Sections were incubated with 1:5000 crude αASPA for 24 to 48 h at room temperature, with constant rotary agitation. Bound antibodies were visualized by the avidin-biotin complex (ABC) method with horseradish peroxidase as the enzyme marker (Vectastain Elite, Vector) and developed with a Ni and Co enhanced diaminobenzidene chromogen (Pierce, Rockford, IL). Sections were mounted on slides with resin, and images were acquired with an Olympus BX51 microscope and Qcolor5 digital camera.

Subcellular fractionation

Rat brains and kidneys were removed from adult Sprague-Dawley male and female rats, frozen on dry ice, and stored at −80°C until use. All steps were performed on ice. Tissues were minced and homogenates were prepared by 8–10 low-speed up/down strokes with a Potter-Elvejham homogenizer in nuclear isolation medium (NIM; 0.25 M sucrose; 25 mM KCl; 5 mM $MgCl_2$; 10 mM Tris-HCl, pH 7.4) supplemented with protease inhibitor cocktail (15 μl/mL) and phosphatase inhibitors (4.52 nM microcystin-LR, 20 μM (-)-p-bromotetramisole oxalate, 4.59 μM cantharadin, 2 mM imidazole, 4.84 mM sodium tartrate, 1.17 mM sodium molybdate, 1 mM sodium orthovanadate) (Sigma, St. Louis, MO). Following passage through cheesecloth, filtrates were centrifuged (800 g, 10 min, 4°C), resuspended in NIM, and recentrifuged.

A) Resulting supernatants were adjusted to "homogenization buffer" (*HB*; 0.5 mM DTT; 50 mM Tris-HCl, pH 8.0; 50 mM NaCl; 0.05% IGEPAL CA-630; 8% glycerol). Supernatant resulting from the second centrifugation (16,000 *g*, 20 min, 4°C) was used in subsequent analysis as cytoplasmic protein extract.

B) Resulting crude nuclear pellets were resuspended in highly viscous NIM (containing 2.3 M sucrose) and pelleted by swinging bucket rotor ultracentrifugation (100,000 *g*, 80 min, 4°C). An aliquot of the resulting purified nuclei was resuspended in NIM and stained with DAPI to observe characteristic nuclear morphology. Remaining nuclei were resuspended in HB, sonicated, and repelleted (16,000 *g*, 10 min, 4°C). Resulting supernatant was used as nuclear protein extract for subsequent analysis.

Protein concentrations were determined by Bio-Rad's DC protein assay (Hercules, CA) based on the method of Lowry. Cytoplasmic contamination of nuclear extract was assessed by using a commercial lactate dehydrogenase (LDH) assay (Randox, Oceanside, CA).

Anion exchange chromatography

Macroprep diethylaminoethyl (DEAE) weak cellulose resin (Bio-Rad) was used as an anion-exchange matrix to separate ASPA from the bulk of cytoplasmic and nuclear proteins, respectively. Resin (2.5 μl bed vol) was equilibrated with 10 column vol of HB before being mixed gently (1 h, 4°C) with 8.5 μl of sample (33 mg protein). Three unbound fractions were collected immediately, and excess unbound proteins were washed with 10 column vol of HB. Proteins were then eluted by 6 column vol washes of HB containing (*i*) 150 mM NaCl, (*ii*) 250 mM NaCl, and (*iii*) 500 mM NaCl. Fractions

were concentrated, assayed for protein, and analyzed for ASPA activity and content by spectrophotometric (cytoplasmic extract) or radiometric (nuclear extract) assay, as well as by Western blot. Maximal activity was identified in fractions 1 and 2 under 150 mM NaCl elution for cytoplasmic extract. Anion exchange chromatography was performed three times using separate nuclear and cytoplasmic preparations.

Size-exclusion chromatography

The column (TOSOHAAS G3000SW, Thompson, Clear Brook, VA) was equilibrated in HB minus DTT, and a standard curve was prepared using protein standards [ribonuclease A, chymotrypsinogen, carbonic anhydrase, ovalbumin, BSA, alcohol dehydrogenase (ADH), β-amylase (Sigma)]. A 0.5 µl aliquot of anion-exchange chromatography sample was injected into the column and eluted at 0.5 µl/min and collected as ~45 × 0.5 µl fractions. For some experiments, multiple injections resulted in pooled fractions. Fractions were concentrated, assayed for protein, and analyzed for ASPA activity and content by radiometric assay and Western blot.

Aspartoacylase enzyme assays

A coupled spectrophotometric ASPA activity assay based on β-NADH oxidation of ASPA-liberated aspartate (25) was followed as described elsewhere (26). A high-sensitivity radiometric assay involving thin-layer chromatography (TLC)-based product separation and phosphor image-based quantification was followed as described previously (26).

SDS-PAGE and Western blot

Samples were diluted in 5× loading buffer (Quality Biological, Gaithersburg, MD), reduced with 10 mM DTT, and heated (90°C, 5 min) prior to loading onto 10% precast Tris-Glycine gels (Invitrogen, Carlsbad, CA). Following electrophoresis, samples were transferred to Immobilon-P PVDF (Millipore, Bedford, MA) membranes using the XCell II blotting module (Invitrogen). Membranes were blocked (PBS, 0.05% v/v Tween-20, and 5% NGS) for 1 h at room temperature, followed by overnight 4°C incubation with αASPA, pepASPA, monoclonal green fluorescent protein (GFP) Ab (Chemicon, Temecula, CA), or monoclonal β-tubulin Ab (Upstate, Charlottesville, VA). Following brief washing, horseradish peroxidase-conjugated goat anti-rabbit or antimouse secondary Ab was added at dilutions of 1:2500–1:5000. Membranes were washed and developed in Super Fast diaminobenzidine substrate (Sigma).

Plasmid constructs

Full-length human ASPA cDNA was subcloned by polymerase chain reaction (PCR) using primers ATGACTTCTTGTCA-CATTGCT (forward) and CTAATGTAAACAGCAGCGAAT (reverse) from pBAD/Thio-TOPO (Invitrogen) (27) into the TOPO-T/A cloning site of pcDNA3.1/NT-GFP-TOPO. The resulting GFP-hASPA plasmid expresses a fusion protein of cycle 3 GFP fused to the NH_2 terminus of ASPA. Full-length human ASPA cDNA was also subcloned into the TOPO-T/A cloning site of pcDNA3.1/V5-His-TOPO such that the resulting hASPA plasmid expresses untagged, native ASPA. Control plasmids expressing GFP alone and GFP fused to tandem nuclear localization signals (NLS) of SV40 Large T Antigen (nuc-GFP) were obtained from Invitrogen.

Cell culture and transient transfections

COS-7 (American Type Culture Collection, Manassas, VA) cells were grown at 37°C with 5% CO_2, cultured in DMEM containing 10% FBS, grown to confluence, and subcultured every 3–4 d. Transient transfections were performed using Lipofectamine 2000 (Invitrogen). For fluorescence microscopy, 0.8 µg DNA was added to cells grown on coverslips in 24-well plates. For Western blot and enzyme activity analyses, 8 µg DNA was added to cells in 60 mm culture dishes. Transfected COS-7 cells were harvested 24–48 h posttransfection by treatment with 2 mM EDTA (15 min, 37°C), spun down, and washed with PBS. Whole cell extracts were generated by sonicating cell pellets in HB. Cellular debris was then removed (16,000 g, 10 min, 4°C), and protein concentrations were determined.

Statistical analysis

Enzyme activities are presented as means ± SEM. Differences between groups were analyzed by t test for a significance level of $P < 0.05$.

RESULTS

Subcellular localization of ASPA in rodent oligodendrocytes

We recently reported ASPA staining throughout oligodendrocytes in rat brain sections by immunohistochemistry (16). These studies also raised the possibility that ASPA might be expressed in the nucleus as well as the cytoplasm of oligodendrocytes. In the absence of an obvious functional role for ASPA in the nucleus, we have thoroughly examined the occurrence of nuclear ASPA using multiple techniques. Two online subcellular localization prediction programs, LOCTree and PSORTII (http://psort.nibb.ac.jp), based on amino acid sequence, predict that human ASPA is partially nuclear (34.8% cytoplasmic and 17.4% nuclear).

Indirect immunofluorescence of cultured primary rat and mouse oligodendrocytes enabled us to show ASPA merged with DAPI, a DNA stain, in representative cells (**Fig. 1**). Our previous experiment used a pAb against full-length recombinant murine ASPA (αASPA) (16). In Fig. 1*B* we utilized newly generated rabbit serum against a conserved ASPA peptide (pepASPA) to substantiate Ab specificity for ASPA in the nucleus. Among cell types of the CNS, ASPA expression and activity have been found primarily in oligodendrocytes (4, 7, 15, 16). We confirm here that ASPA is highly expressed in mature oligodendrocytes by using a maturity-specific Ab raised against myelin oligodendrocyte glycoprotein (MOG) (see Fig. 1*A*) as well as CC1 (see Fig. 1*B*). Note that in Fig. 1*A*, weak ASPA staining appears in several cells that do not stain positively for MOG. In this representative mature oligodendrocyte cultured from rat brain, MOG was confined to the peripheral cytoplasm and cell processes, while ASPA stained throughout cytoplasm and the nucleus (Fig. 1*A*). This phenomenon was confirmed in murine oli-
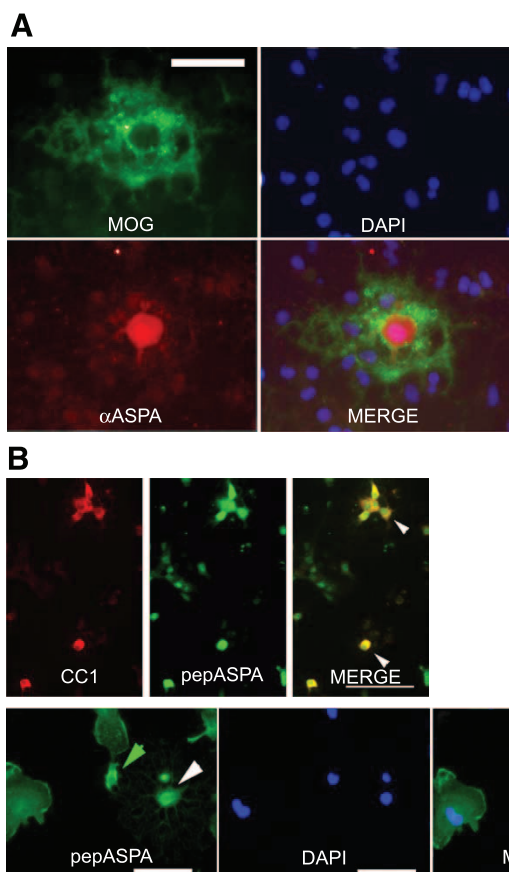
Figure 1. ASPA in cultured oligodendrocytes. *A)* ASPA staining in a representative mature cultured rat oligodendrocyte using an Ab against recombinant murine ASPA (αASPA) (red). Cell processes are highlighted using an Ab against myelin oligodendrocyte protein (MOG) (green). Nuclei are stained with DAPI (blue). Merged field shows ASPA colocalizes with DAPI. Scale bar = 20 μm. *B)* ASPA staining in cultured murine oligodendrocytes using serum against a conserved ASPA peptide (pepASPA) (green). Nuclei are stained with DAPI (blue). Cytoplasm is stained with CC1 oligodendrocyte marker protein (red). *Top panel)* White arrows point to examples of cells where CC1 and ASPA staining correlate very weakly. *Bottom panel)* Perinuclear staining examples in mostly differentiated oligodendrocytes are depicted with green arrows. An example of predominantly nuclear ASPA staining is marked by a white arrow. Merged field shows ASPA colocalizing with DAPI. *Top panel)* scale bar = 100 μm. *Bottom panel)* Scale bar = 20 μm.

godendrocytes using staining for CC1 marker protein (see Fig. 1*B*, top panel). ASPA staining that does not colocalize with cytoplasmic CC1 can be described as nuclear by colocalization with DAPI (Fig. 1*B*, bottom panel).

To address whether ASPA staining observed in Fig. 1 represented true nuclear localization rather than cytoplasmic overlay, Z-series were generated by confocal microscopy, capturing multiple depths of a rat brain section stained with αASPA. The first representative panel (**Fig. 2A**) shows several examples of ASPA and DAPI colocalization, indicative of nuclear ASPA in rat brain oligodendrocytes. Furthermore, ASPA colocalized with DAPI in the same planes, indicating that

fluorescence due to ASPA arises from within the nucleus. ASPA in these oligodendrocytes was both cytoplasmic and nuclear. Additionally, morphometric data show that the area of ASPA staining is larger than, and includes, the area stained for DAPI (nucleus) at several depths of the Z-series (Fig. 2*C*). Thus, it is highly suggestive of ASPA localization in both cytoplasm and nucleus. Also, cells within the same tissue section showed ASPA in the cytoplasm only, as confirmed by cross-sectional depth analysis in the Z-plane (Fig. 2*B*). Our results indicate that ASPA can be found in three distinct configurations within oligodendrocytes: predominantly nuclear, mixed nuclear-cytoplasmic, and predominantly cytoplasmic.

ASPA staining is absent throughout *Tremor* rat brain sections

The *Tremor* rat is a mutant epilepsy model that was found to lack the entire ASPA gene (28, 29). Because ASPA is completely absent in this strain, as opposed to a truncated form in the knockout mouse for CD (30), and because we have consistently analyzed rats (not mice) for NAA and ASPA (3, 7, 16, 31), we used *Tremor* rats as ASPA −/− model systems. We compared wild-type (WT) and *Tremor* rat brain sections by peroxidase immunohistochemistry with αASPA to assess whether nuclear ASPA staining was based on the ASPA gene (**Fig. 3**). As reported previously (16), ASPA protein was found in oligodendrocytes throughout the CNS. Figure 3*A* shows ASPA expression in three brain regions—cortex, corpus callosum, and striatum. ASPA-expressing oligodendrocytes were heavily concentrated in white matter of the corpus callosum, as previously shown (3, 4). In corresponding *Tremor* rat tissue sections, using the same concentration of primary Ab, ASPA staining was completely absent (Fig. 3*B*). Since αASPA displayed no cross-reactivity with antigens in the *Tremor* rat brain, the observed nuclear localization must also be due to ASPA gene product.

Localization of ASPA in rat kidney

Although ASPA was originally purified from hog kidney (32), its cellular localization within this organ has yet to be examined. Peroxidase immunohistochemistry of rat kidney sections in **Fig. 4** shows abundant ASPA expression in kidney. ASPA was selectively localized to kidney cortex and absent from medulla (Fig. 4*A*). Within kidney cortex, ASPA was strongly expressed in proximal tubule cells but was absent from glomeruli (Fig. 4*C*). Using *Tremor* rat kidney sections, again we observed that αASPA did not cross-react with other antigens, indicating that immunoreactivity was selectively localizing ASPA gene product (Fig. 4*D*). At higher magnification in kidney cortex from WT rats, heavy nuclear staining was observed in individual proximal tubule cells (Fig. 4*B*).
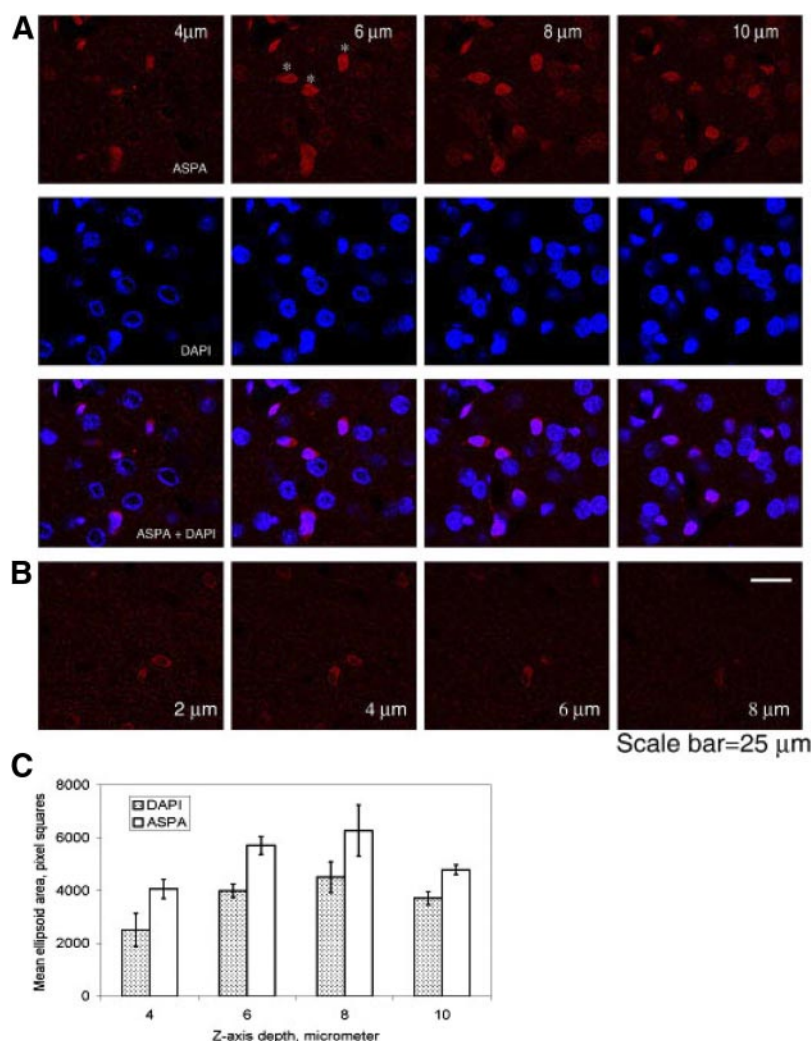
Figure 2. Subcellular localization of ASPA in rat brain sections. *A)* Z-series generated by confocal microscopy capturing multiple depths of a rat brain section stained with αASPA. Examples of predominantly nuclear ASPA (red) colocalizing with DAPI at same depths are shown. *B)* ASPA can also be strictly cytoplasmic. Scale bar = 25 μm. *C)* Cellular morphometric data for ASPA and DAPI staining. The areas corresponding to ASPA (red) and DAPI (blue) were calculated by approximating to an ellipsoid. The exact number of pixels of the long axis and short axis of the ellipse were obtained using Adobe Illustrator software on the raw digital images. Three cells were chosen (identified with asterisks) and compared for the areas of ASPA and DAPI using *t* test with equal variances. Comparisons were made depth-wise (three values), as well as across all depths for each cell (four values); ASPA areas were significantly larger than DAPI areas by at least 500 pixel squares at all the depths and for every cell ($P < 0.05$).

Nuclear ASPA is catalytically active

Nuclei isolated from adult rat organs by sucrose density gradient ultracentrifugation, when resuspended in nonlytic buffer and stained for DNA by DAPI, were plentiful and intact (data not shown). Furthermore, LDH, a cytoplasmic marker, showed specific activity in the nuclear extract that was virtually negligible compared with cytoplasmic extract (~2%).

We utilized a highly sensitive radiometric ASPA assay (26) to analyze subcellular fractions for enzyme activity. For comparison, we analyzed cytoplasmic extracts (**Fig. 5A**) from kidney and brain of WT and ASPA −/− mutant *Tremor* rats (28). As described previously, there was ~10-fold higher activity in kidney than in brain (6, 17, 30). This activity was due to the ASPA gene as it was not present in *Tremor* rat tissue extracts. We then assayed nuclear extracts (Fig. 5B) and noted a similar ratio of elevated kidney-to-brain ASPA activity (~6:1 in cytoplasm, ~3:1 in nucleus). Nuclear ASPA activity was undetectable in *Tremor* rat tissues, confirming it was due to ASPA gene product in WT rats. The percentage of nuclear ASPA activity against NAA substrate relative to
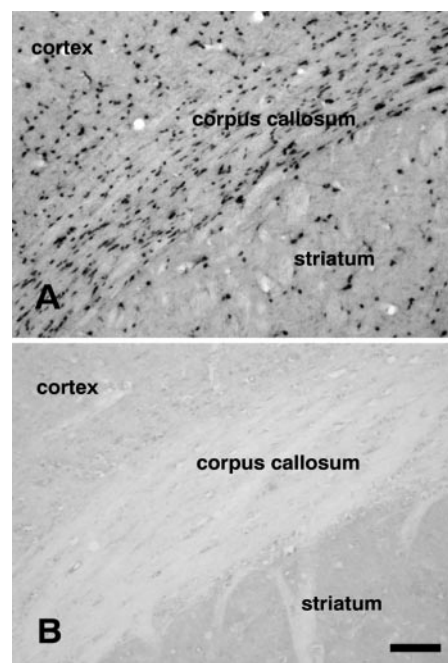

Figure 3. ASPA localization in rat brain sections. *A)* ASPA immunoreactivity in the corpus callosum and adjacent structures of WT rats. *B)* Staining is completely absent from ASPA null *Tremor* rat tissue sections. Scale bar = 120 μm.

Figure 4. ASPA localization in rat kidney sections. *A)* ASPA expression was strong in kidney cortex, but was low in the medulla. *B)* ASPA expression was exceptionally strong in the nuclei of some proximal tubule cells in the cortex. White arrows point to representative nuclei. *C)* ASPA was expressed throughout proximal tubules but was not observed in glomeruli in WT rat kidney cortex (g in panel *C*). *D)* ASPA immunoreactivity was absent from ASPA-null *Tremor* rat kidney sections. Scale bar = 800 μm (*A*), 50 μm (*B*), 200 μm (*C, D*).
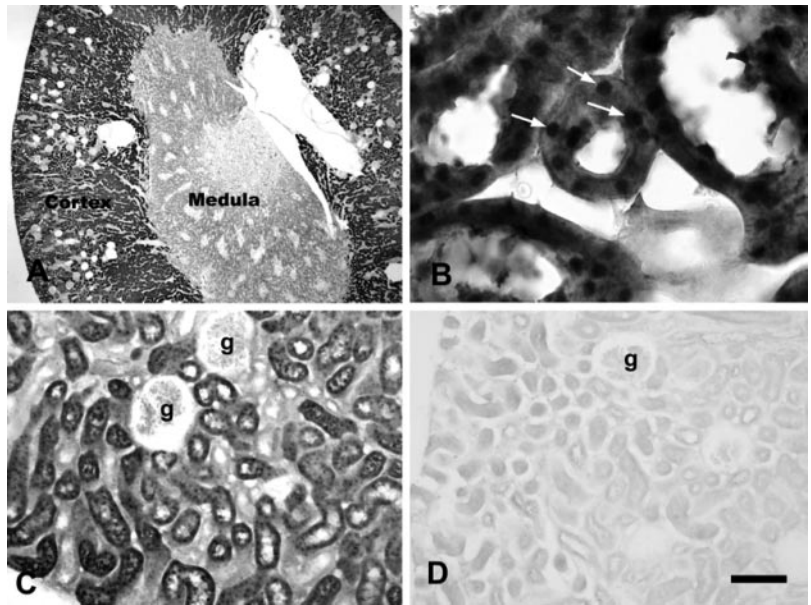
cytoplasmic activity was ~3% in kidney and ~6% in brain extracts.

To qualitatively analyze what proportion of ASPA protein existed in our nuclear extracts, we analyzed kidney extracts by Western blot using both αASPA and pepASPA antibodies (Fig. 5*C*). Previous immunoblotting studies using different ASPA antibodies have identified an ASPA monomer and a putative ASPA dimer (8, 20). The present study is the first to immunoblot ASPA from kidney, where two other aminoacylases exist in great abundance. Therefore, we relied on the *Tremor* rat to determine which band detected by our polyclonal antibodies actually reflected ASPA protein. Both antibodies detected an ASPA monomer band at 38 kD that was missing from *Tremor* rat extract (Fig. 5*C*). This ASPA monomer was detected in nuclear extract at a considerably lower level than in cytoplasmic extract, comparable to its correspondingly lower activity. Thus, it appears that only a small population of ASPA is in the nucleus. Each Ab cross-reacted with some other proteins from *Tremor* rat extracts (see "Mut" lanes). The prominent band detected at 32 kD likely reflects aminoacylase III, which has been characterized as a 32–35 kD protein (33, 34). Consistent with the cytoplasmic localization of both aminoacylase I (35) and aminoacylase III (33), these cross-reacting bands were not detected in our nuclear extracts (Fig. 5*C*). This lack of cross-reactive cytoplasmic bands carrying over from cytoplasmic to nuclear preparations indicates the ASPA monomer band in nuclear extract was not the result of cytoplasmic contamination. Additionally, this supports the observation that low nuclear activity in kidney and brain extracts is not due to cytoplasmic contamination. The putative ASPA dimer band detected by Western blotting of rat brain homogenates using serum against recombinant human ASPA (8) also appeared in our immunoblots of *Tremor* rat extracts (Fig. 5*C*), as well as in WT rat

cytoplasmic extract following incubation with αASPA that was pretreated with its antigen (data not shown), indicating that this band was the result of cross-reactivity rather than dimerization.

Nuclear ASPA displays weaker ionic behavior than cytoplasmic ASPA

To assess the biochemical nature of ASPA within cytoplasm and within nuclei, we partially purified ASPA from each extract and compared column elution properties. ASPA-rich kidney tissue (see Fig. 5) was used as the enzyme source. Our purification plan involved (*i*) anion-exchange chromatography and (*ii*) HPLC size-exclusion chromatography. The methods were each tested separately using crude solubilized enzyme (data not shown) and subsequently combined in the order presented.

DEAE cellulose chromatography was used as the first chromatographic step for enzyme purification; ASPA activity profiles are presented in **Fig. 6**. Elution with 150 mM NaCl was used to recover maximum enzyme activity, rather than 75 mM NaCl elution used for ASPA purification from bovine brain (18). We tested NaCl concentrations up to 1 M in assay buffer and found no effect on ASPA activity in crude rat kidney homogenate (data not shown). For cytoplasmic extracts (Fig. 6*A*), as much as 70% of the enzyme activity was bound to the column and eluted with 150 mM NaCl medium. The remaining ~30% of activity was found in the unbound fraction. ASPA activity was not detected in subsequent elutions with 250 mM and 500 mM NaCl for either extract (data not shown). There was a statistically significant ~6-fold enrichment of ASPA-specific activity in the 150 mM NaCl vs. the unbound fraction (from 250 nmol/h/mg protein to 1500 nmol/h/mg protein). For nuclear extracts (Fig. 6*B*), less than 50% of total
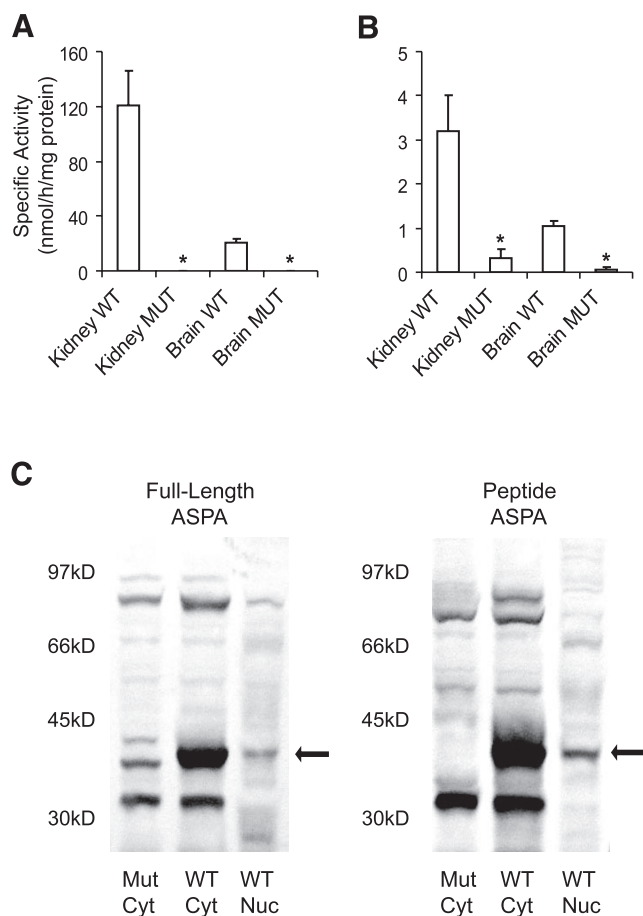
Figure 5. ASPA in cytoplasmic and nuclear extracts. Subcellular fractionation and radiometric enzyme assay are described in Materials and Methods. Specific activities are presented as mean ± SEM for three to four data points. *A)* ASPA activity detected in rat kidney and brain cytoplasmic protein extracts is completely absent in ASPA null *Tremor* rat (MUT) tissues. *B)* ASPA activity detected in rat kidney and brain sucrose density gradient-purified nuclear protein extracts is virtually absent in *Tremor* rat tissues. (*Indicates mutant values differ significantly from WT values, *P < 0.05*). *C)* Western blot of ASPA from fractionated kidney extract. *Left panel)* Western blot (1:2000) with αASPA. *Right panel)* Western blot (1:2000) with pepASPA. *Mut Cyt, Tremor* rat (mutant) cytoplasmic extract. *WT Cyt,* WT cytoplasmic extract. *WT Nuc,* WT nuclear extract. 100 μg protein per lane. Arrows point to the ASPA monomer, which is absent from *Tremor* rat extract.

enzyme activity was bound to the column and eluted with 150 mM NaCl buffer. There was virtually no enrichment of nuclear ASPA specific activity under the described conditions.

Active rat kidney ASPA is a monomer

The first two 150 mM fractions ("150mM" in Fig. 6) containing the majority of cytoplasmic enzyme activity were pooled and concentrated for further purification by size-exclusion chromatography. For comparative purposes, corresponding 150 mM fractions were similarly pooled and concentrated for the nuclear extract. **Figure 7** shows ASPA elution profiles from HPLC

size-exclusion chromatography. To avoid a clumping effect whereby highly concentrated sample resulted in ASPA activity detected both at very high sizes (>300 kD) as well as at a size corresponding to the ASPA monomer (data not shown), a relatively dilute cytoplasmic sample from the 150 mM NaCl DEAE-cellulose elution was separated by gel filtration. Maximum specific and total activities were observed in a size range (between 29 and 43 kD) containing the ASPA monomer (Fig. 7*A*). The MW values calculated from a log plot using MW standard proteins corresponded well (35–38 kD) to the size of the ASPA monomer (data not shown). Nuclear protein samples were found to follow a similar pattern, with peak activity corresponding to the ASPA monomer (Fig. 7*B*). In nuclear extract only, there appeared to be residual activity (~25% peak activity) corresponding to a MW of 67–200 kD, which could reflect a reduced activity corresponding to putative dimerized ASPA (8, 20). This activity might have also existed in the cytoplasmic extract at a low level, undetectable due to the tailing effect from high activity of the monomer.

Maximum total activities recovered from ~450 rat kidneys following two rounds of purification were 236 nmol/h for cytoplasmic ASPA and 8.3 nmol/h for nuclear ASPA, respectively, indicating that only a very small proportion of ASPA activity against NAA (3%) is found in kidney nuclei. However, purification sufficiently enriched the specific activity of nuclear ASPA so that it was higher than that of the initial rat kidney cytoplasmic extract: 185 nmol/h/mg protein vs. ~121
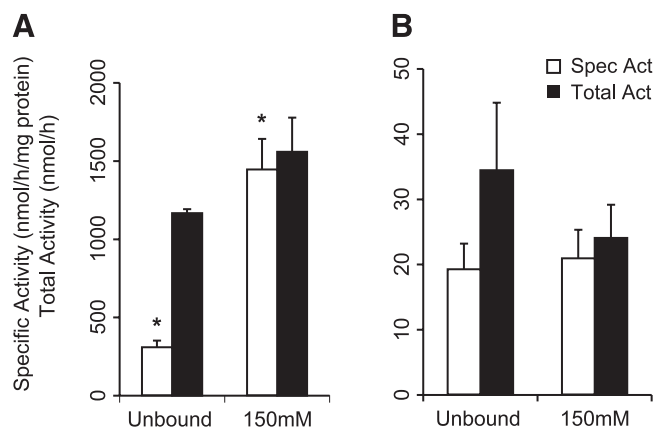

Figure 6. Anion-exchange chromatography ASPA activity elution profiles from rat kidney nuclear and cytoplasmic extracts. Column setup and NaCl elution gradient, as well as spectrophotometric (cytoplasmic extract) and radiometric (nuclear extract) enzyme assays, are described in Materials and Methods. Each fraction represents two pooled fractions with average specific activities and summed total activities. Data are presented as mean ± SEM for three points. *A)* For cytoplasmic extract, specific activity of 150 mM fractions is significantly higher (*P < 0.05*) than that of unbound fractions. Total activity of the 150 mM fractions is also elevated compared to unbound fractions. *B)* For nuclear extract, both specific and total activities are nearly evenly distributed between unbound and 150 mM fractions. No activity was found for cytoplasmic and nuclear extracts with 250 mM and 500 mM NaCl elutions (data not shown).

Figure 7. Determining the size of active rat kidney nuclear and cytoplasmic ASPA. Pooled 150 mM NaCl anion-exchange chromatographed fractions were concentrated and injected into a size-exclusion column. Adjacent fractions corresponding to 500 μl/min elution were pooled and concentrated. *A–B)* Radiometric enzyme assay is described in Materials and Methods. The data are averages of two assays. Peak specific and total ASPA activity from both cytoplasmic (*A*) and nuclear (*B*) 150 mM NaCl anion-exchange fractions occur between fractions 36 and 40, corresponding to a MW of 38 kD as determined by standard curve (data not shown). Sizes (in kDa) of MW marker proteins are indicated by arrows. *C)* Western blot (1:2000 αASPA) of cytoplasmic protein (2.5 μg per lane) in size-exclusion chromatography fractions. *D)* Western blot (1:1000 αASPA) of nuclear protein (8 μg per lane) in size-exclusion chromatography fractions.
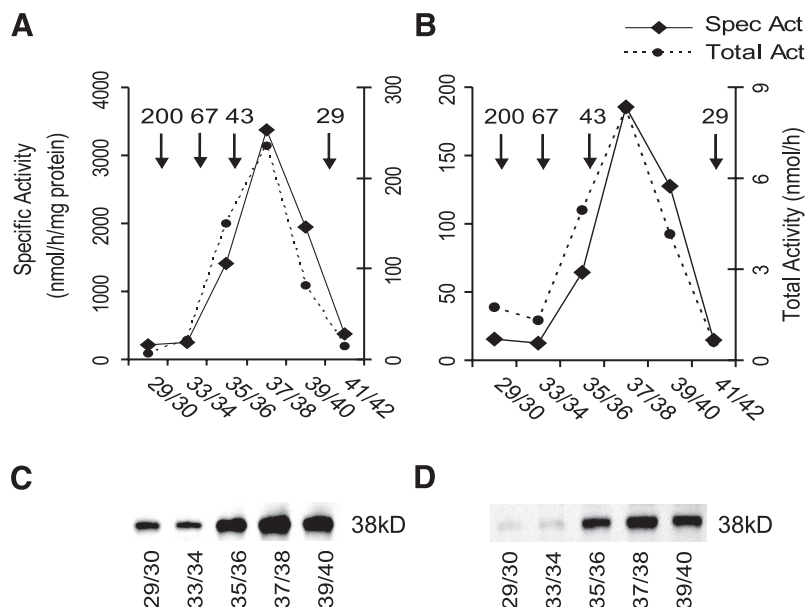
nmol/h/mg protein. Western blot analysis of size-exclusion fractions complemented both activity elution profiles. The ASPA monomer band was present in all cytoplasmic fractions, with peak intensity in fractions with maximal activity (Fig. 7*C*). In contrast, the ASPA monomer band was present only in nuclear fractions where ASPA activity was present, rather than throughout the entire elution (Fig. 7*D*). Careful inspection of the *y*-axes for both extracts reveals relatively significant residual activity in fractions corresponding to high MW in cytoplasmic but not nuclear extract, which accounts for the weak ASPA bands in these cytoplasmic fractions.

Generation and confirmation of GFP-hASPA

ASPA is small enough to passively diffuse through the nuclear pore complex (NPC). Therefore, we tagged ASPA with GFP so the size of the fusion protein would exceed the 40–60 kD size cutoff for passive diffusion through the NPC (36). GFP was linked to the NH_2 terminus of ASPA (GFP-hASPA) because ASPA's catalytic domain has been tentatively assigned toward its C-terminus (19, 37, 38) and because linking GFP to either terminus of a protein tends to result in identical subcellular distributions (39, 40). Immunoblots of transiently transfected COS-7 cells confirmed that additional linker residues connecting cycle 3 GFP (27 kD) to the hASPA (38 kD) increased the size of GFP-hASPA to 69 kD (**Fig. 8*A***). Western blots of control transfections with GFP alone and native hASPA confirmed their respective individual sizes. As previously reported for other kidney cell lines (8, 20, 38), ASPA was not endogenous to COS-7 cells, allowing us to discern ASPA from background bands at ~50 and ~80 kD ("No DNA" lane in Fig. 8*A*). GFP-hASPA was found to be catalytically active similar to native untagged hASPA (Fig. 8*B*), implying it is useful for studying ASPA's subcellular localization. ASPA activity was undetectable in control GFP and mock transfections.

Subcellular localization of transfected ASPA

The distribution of transiently transfected GFP-hASPA in formalin-fixed COS-7 cells was mostly mixed nuclear-cytoplasmic (see **Fig. 9*A***, "GFP-hASPA"). GFP alone demonstrated mixed nuclear-cytoplasmic fluorescence characteristic of a small, diffuse protein while nuc-GFP (see Materials and Methods) demonstrated predominantly nuclear fluorescence (Fig. 9*A*). The ratio of nuclear to cytoplasmic GFP-hASPA was determined by merging GFP and DAPI images from several fields of transfected COS-7 cells to assess the extent of nuclear, mixed, and cytoplasmic staining. GFP-hASPA's distribution (Fig. 9*B*) was very similar to that predicted for ASPA obtained using PSORTII (http://psort.nibb. ac.jp): 17.4% nuclear and 34.8% cytoplasmic. Finally, we used indirect immunofluorescence with pepASPA and a FITC-conjugated secondary Ab to analyze the subcellular distribution of transfected native hASPA. In Fig. 9*C* we verified that native ASPA is also a mixed nuclear-cytoplasmic protein, as visualized at high magnification by merger with DAPI images.

DISCUSSION

For many years ASPA has been assumed to be a soluble, cytoplasmic enzyme with some partial membrane association (6, 11, 17, 18). However, our recent immunohistochemical localization study raised the possibility that ASPA may also be found in the nucleus of oligodendrocytes (16). In our current report we explored this possibility and have established that ASPA is a nuclear-cytoplasmic enzyme. The occurrence of ASPA in the nucleus was demonstrated using immunofluorescence, confocal microscopy, peroxidase immunohistochemistry, and immunoblotting. Additionally, we have shown that ASPA in the nucleus of rat kidney and brain cells retains low levels of catalytic activity toward NAA.
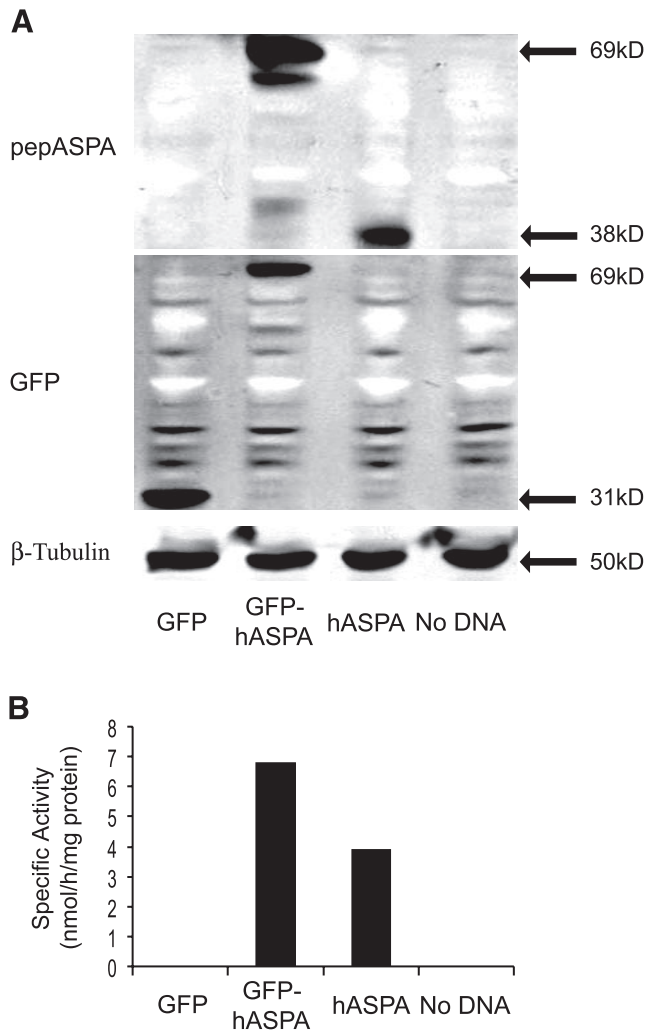
Figure 8. GFP-hASPA fusion protein is enzymatically active. Whole cell extracts were prepared from COS-7 cells transiently transfected with the indicated vectors (see Materials and Methods). *A)* Western blots with pepASPA Ab (1:5000) and a monoclonal GFP Ab (1:5000) reveal native hASPA is 38 kD, GFP alone is 31 kD, and GFP-hASPA is 69 kD. ASPA is not endogenous to COS-7 cells; 30 μg protein per lane. *B)* GFP-hASPA and native untagged hASPA have comparable activities using the radiometric ASPA enzyme assay.

Three additional arguments support this unexpected localization for ASPA. First, both ASPA antibodies, one directed to a conserved peptide region (pepASPA) and the other directed against the whole protein (αASPA), gave the same nuclear pattern of staining in cultured oligodendrocytes from both rat and mouse. Second, specificity of the αASPA signal seen in tissue sections was confirmed using corresponding brain and kidney sections from *Tremor* rats (28) wherein ASPA staining was completely absent. Third, expression of both GFP-tagged and native untagged human ASPA in COS-7 cells showed a mixed nuclear-cytoplasmic distribution.

Analysis of the GFP-hASPA fusion protein, which was larger than the 40–60 kD cutoff for passive diffusion through the NPC (36), demonstrated active import of ASPA into the nucleus. We now consider ASPA a member of a burgeoning family of previously assumed cytoplasmic proteins also capable of nuclear localization, including receptor interacting protein 3 (41), choline acetyltransferase (42), and nardilysin (39).
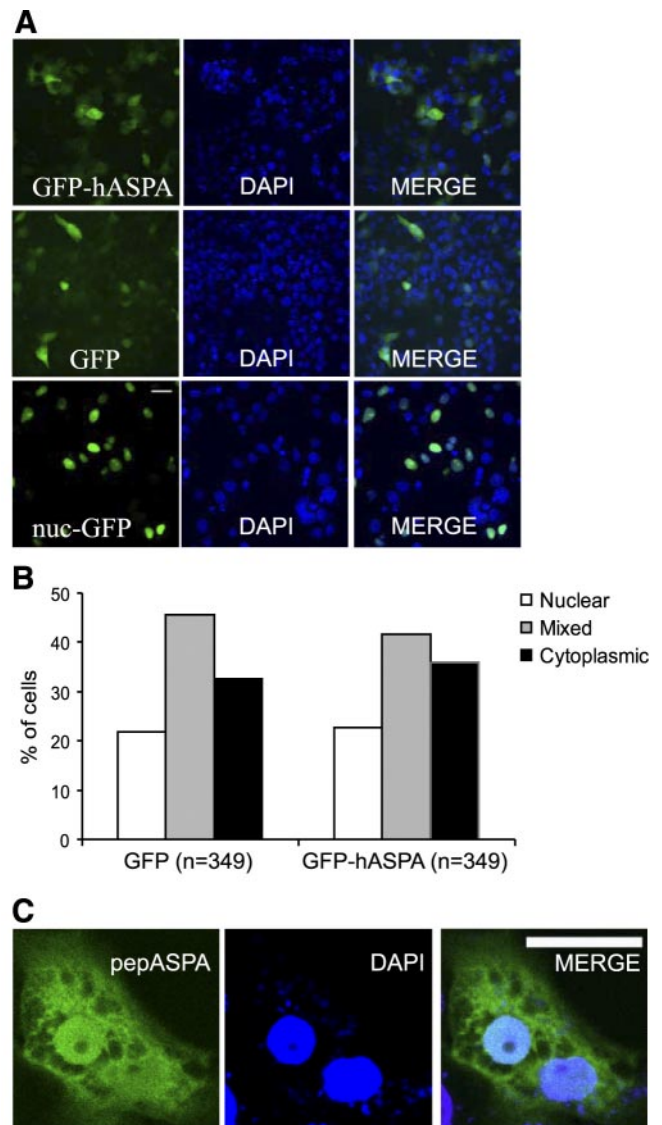

Figure 9. Transfected GFP-hASPA and native hASPA are nuclear-cytoplasmic. COS-7 cells were transiently transfected with the indicated vectors. *A)* Confocal microscopy of representative fields. Cells were grown and fixed on coverslips. GFP-hASPA depicts mostly mixed nuclear-cytoplasmic staining. GFP depicts mixed staining and nuc-GFP (GFP targeted to the nucleus by the SV40 Large T antigen NLS) depicts predominantly nuclear localization. Scale bar = 20 μm. *B)* Quantification of GFP-hASPA subcellular distribution. Several fields of cells grown in 24-well plates and imaged directly by using an inverted fluorescent microscope were scored for mainly nuclear, mixed nuclear-cytoplasmic, and mainly cytoplasmic localization based on merged images with DAPI. GFP-hASPA is predominantly nuclear-cytoplasmic, similar to the GFP control. *C)* Indirect immunofluorescence of native untagged hASPA. Fixed cells were stained using pepASPA Ab (1:1000), visualized by FITC-conjugated secondary Ab, and imaged by confocal microscopy (see Materials and Methods). Representative cells display ASPA distributed throughout cytoplasm while colocalizing with DAPI in two representative fields at high magnification. Scale bar = 10 μm.

Moreover, ASPA appears to be similar to proteins such as proteinase inhibitor 9 (43), histones (36, 44), high mobility group proteins (44), and the 18 kD isoform of fibroblast growth factor 2 (45), which are small enough to passively diffuse through the NPC but have been shown to be actively imported.

The functional significance of nuclear ASPA in brain oligodendrocytes and kidney proximal tubule cells remains unknown, yet highly intriguing. One recently confirmed function of ASPA in brain is to supply acetyl groups from NAA for myelin lipid synthesis (14). This role is consistent with the dysmyelination observed in CD patients with mutations that ablate ASPA's catalytic activity (46). We confirm in this report that ASPA is expressed predominantly in oligodendrocytes in the CNS (8, 15, 16). We observed nuclear ASPA staining only in a subpopulation of predominantly immature oligodendrocytes in cell culture, raising the possibility that ASPA's subcellular localization is regulated during oligodendrocyte development and/or myelination. In the future, a closer examination of ASPA staining during rodent development may provide insight into whether nuclear ASPA follows the same expression pattern as cytoplasmic ASPA, or if pools of ASPA are sequestered in the nucleus in order to regulate free acetyl groups for myelin lipid synthesis.

The functions served by ASPA in the CNS have been fairly well studied; however, the physiological role of ASPA within kidney has yet to be closely examined. Although kidney ASPA was the original source for ASPA purification from hog (47) and is more abundant than brain ASPA and much more active against NAA (6, 19), it has been assigned a simple scavenging function (19). While molecular diagnosis is currently required as confirmation (48), elevated urine NAA remains as the fundamental diagnostic marker of children with CD (46). This raises the possibility that kidney ASPA serves a crucial role in deacetylating NAA retained from the circulation (49). In CD patients, dysfunctional proximal tubule ASPA could result in impaired ability to deacetylate retained NAA, resulting in its accumulation in urine where it is easily detectable. The cause of this accumulation has yet to be investigated and could be due to dysfunctional kidney, increased pathological NAA clearance from the circulation, or both. Curiously, kidney pathology is rarely reported in children with CD (28, 50). It is possible that one function of ASPA in kidney is to retain acetate from small acetylated compounds in the circulation via deacetylation. Loss of ASPA function in the kidney could then exacerbate the reduced acetate availability involved in the pathogenesis of CD (14). There are two other partially characterized aminoacylases in kidney with residual specificity toward NAA (33, 34), which may assist with ASPA's physiological role in kidney. In this report we localized ASPA to proximal tubules of kidney cortex, noting that ASPA was absent from the entire kidney medulla, as well as the cortical glomeruli. Acylases are generally abundant in kidney, and both aminoacylase I and III have been localized to kidney proximal tubules (33,

34), similar to the distribution of ASPA (aminoacylase II) observed in the current study. Acylases purportedly function in the detoxification of xenobiotic compounds. Another possible implication of ASPA localization to these kidney regions is retention of amino acids, a known function of the kidney proximal tubules.

At least two possibilities pertain to the reduced catalytic activity of nuclear ASPA toward NAA. First, a small pool of ASPA is targeted to the nucleus by a hereto unknown regulatory signal and retains catalytic activity against NAA. The mostly cytoplasmic 69 kD form of choline acetyltransferase, which catalyzes synthesis of the neurotransmitter acetylcholine (Ach), was found to retain minimal activity in fractionated nuclei of transiently transfected HEK293 cells (51). Second, when ASPA is targeted to nuclei, either the nuclear environment or some modification to the enzyme causes it to lose most of its specificity toward NAA. Enzymes such as CMP-Neu5Ac-synthetase, which catalyzes the activation of 5-N-acetylneuraminic acid to cytidine-monophosphate N-acetylneuraminic acid (52), and the 82 kD isoform of choline acetyltransferase (42) are believed to have alternate nuclear substrate specificities. This supports the hypothesis that ASPA has an alternate specificity when nuclear. In addition to possibly being active against other N-acetylated amino acids, nuclear ASPA may also be active against N-acetylated proteins such as actin, which in its active form has an acetylated aspartate as its N-terminal residue (53, 54). It is known that actin is present in the nucleus (55) and that its binding activity to myosin is regulated by an N-terminal acetylation/deacetylation mechanism (56). The fact that ASPA activity against NAA was relatively low in nuclear extracts, whereas ASPA immunoreactivity was generally strong in kidney and oligodendrocytes nuclei, further suggests that nuclear ASPA may have different substrate specificities than the cytoplasmic form.

It is difficult to reconcile the low nuclear ASPA expression as shown by Western blot with the strong nuclear staining for ASPA observed by immunohistochemistry in oligodendrocytes and proximal kidney tubule cells. One possibility is that the isolation and preparation of tissue nuclei for Western blotting resulted in poor ASPA yields, thus underestimating the proportion of ASPA that was localized to the nuclear compartment. Another possibility is that nuclear ASPA has a different substrate specificity and may not have high activity against NAA. It is possible that Western blotting and enzyme assays of nuclear extracts underestimated the degree of ASPA protein expression in cell nuclei.

Investigating column elution properties of cytoplasmic and nuclear ASPA elucidated another important finding of our study, which is that ASPA is active as a monomer. In previous studies, ASPA was inferred to be a dimer by mass spectroscopy of recombinant human ASPA purified from *E. coli* (20) and from Western blot analyses (8). Our current study is the first to examine native ASPA from animal tissue by size-exclusion chro-

matography, allowing us to observe that native ASPA is active as a monomer. ASPA is thus distinguished from aminoacylase III, which, through similar means, was demonstrated to be active as a tetramer (33). These data, however, do not rule out the possibility that ASPA also exists as an inactive dimer. Western blot analysis detected the majority of cytoplasmic ASPA in fractions between 29 and 45 kD, indicating that the majority of rat kidney ASPA exists as a monomer. Similarly, although we detected an ~82 to 84 kD band by Western blot analysis as previously reported (8), this band was also detected in extracts from ASPA null *Tremor* rats and in untransfected COS-7 cells, implying it was a cross-reactive protein and was not due to ASPA.

We also observed that nuclear ASPA displays less affinity toward positively charged column resins than cytoplasmic ASPA. Although this may be a trivial reflection of the different ionic environments of the extracts, it suggests that nuclear ASPA is less anionic than cytoplasmic ASPA, possibly signifying differential post-translational modifications. Mass spectroscopy analysis of recombinant human ASPA purified from *E. coli* found no posttranslational modifications (20). However, bacterially expressed proteins often do not undergo posttranslational medications that occur in eukaryotic cells. Thus, it is possible that differential phosphorylation may be involved in the nuclear localization of ASPA. We are currently investigating whether any of five putative phosphorylation target residues (19) affect ASPA activity and subcellular localization.

The mechanism responsible for the nuclear import of ASPA is currently unknown due to the lack of studies on its posttranslational regulation. Traditional protein nuclear import relies on the classical NLS (based on the SV40 large T antigen), whose critical lysine residues facilitate protein binding to importin α/importin β for movement through the NPC (57, 58). However, there are a wealth of less-characterized sequences for nuclear targeting, including a 38 amino acid fragment from hnRNP A1 and A2 (M9 sequence), the KNS sequence from hnRNP K protein, the HNS sequence from the HuR protein, ankyrin repeats from IkBalpha, an acidic amino acid region in FAS associated factor 1, a PPXXR sequence of Sam68, a S/TPXKRL/I sequence of Cdc6, and GR repeats in large FGF-2 isoforms (44). Most notably, an experimental approach to discovering novel NLS's found less than 50% of the classical variety as well as several sequences exhibiting clusters of just 2–3 lysine and/or arginine nonbipartite basic NLS repeats and RTRG repeats (44). Indeed, not all nuclear proteins need an NLS as entry may be afforded by interaction with another protein that does have an NLS (36). Conversely, an NLS does not guarantee nuclear localization as 4.2% of non-nuclear proteins contain a putative NLS (59). Epitope masking, glycosylation, and phosphorylation are other ways for proteins lacking an NLS to enter the nucleus (59). Visual inspection after failing to find a putative or functional NLS has identified a nonclassical C-terminal bipartite NLS in 18 kD fibroblast growth factor-2, characterized by two clusters

of two or three basic amino acids separated by 8–17 amino acids (40). Similarly, we searched ASPA's primary amino acid sequence for clusters of conserved basic amino acids and identified a conserved KKEAFAKTTK C-terminal sequence. This putative NLS resembles a functional nonclassical NLS, PAAKRVKLD (60) and is a condensed version of a nonclassical bipartite NLS found in SIM1 and SIM2 proteins (61). We are currently assessing the importance of this region of ASPA in influencing partial nuclear localization.

In summary, we have shown that ASPA is localized to both cytoplasm and the nucleus in specific cell types in rodent brain and kidney and that this nuclear enzyme is weakly catalytically active against the only known substrate for the cytoplasmic form of the enzyme. Concurrently, we have shown that ASPA is active as a monomer and that nuclear import is not due to simple diffusion. The biological role of nuclear ASPA remains to be established. It is possible that CD mutations in ASPA affect its subcellular localization in addition to its catalytic activity and that variations in the two might play a critical role in determining different CD phenotypes. Thus, regulation of ASPA's nuclear-cytoplasmic shuttling could be highly significant in understanding both the molecular basis for, and the potential treatment of CD. [FJ]

REFERENCES

1. Matalon, R., Michals, K., Sebesta, D., Deanching, M., Gashkoff, P., and Casanova, J. (1988) Aspartoacylase deficiency and N-acetylaspartic aciduria in patients with Canavan disease. *Am. J. Med. Genet.* **29,** 463–471
2. Leone, P., Janson, C. G., McPhee, S. J., and During, M. J. (1999) Global CNS gene transfer for a childhood neurogenetic enzyme deficiency: Canavan disease. *Curr. Opin. Mol. Ther.* **1,** 487–492
3. Kirmani, B. F., Jacobowitz, D. M., and Namboodiri, M. A. (2003) Developmental increase of aspartoacylase in oligodendrocytes parallels CNS myelination. *Brain Res. Dev. Brain Res.* **140,** 105–115
4. Bhakoo, K. K., Craig, T. J., and Styles, P. (2001) Developmental and regional distribution of aspartoacylase in rat brain tissue. *J. Neurochem.* **79,** 211–220
5. D'Adamo, A. F., Jr., Gidez, L. I., and Yatsu, F. M. (1968) Acetyl transport mechanisms. Involvement of N-acetyl aspartic acid in de novo fatty acid biosynthesis in the developing rat brain. *Exp. Brain Res.* **5,** 267–273
6. D'Adamo, A. F., Jr., Smith, J. C., and Woiler, C. (1973) The occurrence of N-acetylaspartate amidohydrolase (aminoacylase II) in the developing rat. *J. Neurochem.* **20,** 1275–1278

7. Kirmani, B. F., Jacobowitz, D. M., Kallarakal, A. T., and Namboodiri, M. A. (2002) Aspartoacylase is restricted primarily to myelin synthesizing cells in the CNS: therapeutic implications for Canavan disease. *Brain Res. Mol. Brain Res.* **107,** 176–182

8. Klugmann, M., Symes, C. W., Klaussner, B. K., Leichtlein, C. B., Serikawa, T., Young, D., and During, M. J. (2003) Identification and distribution of aspartoacylase in the postnatal rat brain. *Neuroreport* **14,** 1837–1840

9. Benuck, M., and D'Adamo, A. F., Jr. (1968) Acetyl transport mechanisms. Metabolism of N-acetyl-L-aspartic acid in the non-nervous tissues of the rat. *Biochim. Biophys. Acta* **152,** 611–618

10. Burri, R., Steffen, C., and Herschkowitz, N. (1991) N-acetyl-L-aspartate is a major source of acetyl groups for lipid synthesis during rat brain development. *Dev. Neurosci.* **13,** 403–411

11. Chakraborty, G., Mekala, P., Yahya, D., Wu, G., and Ledeen, R. W. (2001) Intraneuronal N-acetylaspartate supplies acetyl groups for myelin lipid synthesis: evidence for myelin-associated aspartoacylase. *J. Neurochem.* **78,** 736–745

12. D'Adamo, A. F., Jr., and Yatsu, F. M. (1966) Acetate metabolism in the nervous system. N-acetyl-L-aspartic acid and the biosynthesis of brain lipids. *J. Neurochem.* **13,** 961–965

13. Mehta, V., and Namboodiri, M. A. (1995) N-acetylaspartate as an acetyl source in the nervous system. *Brain Res. Mol. Brain Res.* **31,** 151–157

14. Madhavarao, C. N., Arun, P., Moffett, J. R., Szucs, S., Surendran, S., Matalon, R., Garbern, J., Hristova, D., Johnson, A., Jiang, W., and Namboodiri, M. A. (2005) Defective N-acetylaspartate catabolism reduces brain acetate levels and myelin lipid synthesis in Canavan's disease. *Proc. Natl. Acad. Sci. U. S. A.* **102,** 5221–5226

15. Baslow, M. H., Suckow, R. F., Sapirstein, V., and Hungund, B. L. (1999) Expression of aspartoacylase activity in cultured rat macroglial cells is limited to oligodendrocytes. *J. Mol. Neurosci.* **13,** 47–53

16. Madhavarao, C. N., Moffett, J. R., Moore, R. A., Viola, R. E., Namboodiri, M. A., and Jacobowitz, D. M. (2004) Immunohistochemical localization of aspartoacylase in the rat central nervous system. *J. Comp. Neurol.* **472,** 318–329

17. D'Adamo, A. F., Jr., Wertman, E., Foster, F., and Schneider, H. (1978) A radiochemical assay for N-acetyl-L-aspartate amidohydrolase (EC 3.5.1.15) and its occurrence in the tissues of the chicken. *Life Sci.* **23,** 791–795

18. Kaul, R., Casanova, J., Johnson, A. B., Tang, P., and Matalon, R. (1991) Purification, characterization, and localization of aspartoacylase from bovine brain. *J. Neurochem.* **56,** 129–135

19. Kaul, R., Gao, G. P., Balamurugan, K., and Matalon, R. (1993) Cloning of the human aspartoacylase cDNA and a common missense mutation in Canavan disease. *Nat. Genet.* **5,** 118–123

20. Moore, R. A., Le Coq, J., Faehnle, C. R., and Viola, R. E. (2003) Purification and preliminary characterization of brain aspartoacylase. *Arch. Biochem. Biophys.* **413,** 1–8

21. Armstrong, R. C. (1998) Isolation and characterization of immature oligodendrocyte lineage cells. *Methods* **16,** 282–292

22. Linnington, C., Webb, M., and Woodhams, P. L. (1984) A novel myelin-associated glycoprotein defined by a mouse monoclonal antibody. *J. Neuroimmunol.* **6,** 387–396

23. Benjamins, J. A., Nedelkoska, L., and George, E. B. (2003) Protection of mature oligodendrocytes by inhibitors of caspases and calpains. *Neurochem. Res.* **28,** 143–152

24. McCarthy, K. D., and de Vellis, J. (1980) Preparation of separate astroglial and oligodendroglial cell cultures from rat cerebral tissue. *J. Cell Biol.* **85,** 890–902

25. Fleming, M. C., and Lowry, O. H. (1966) The measurement of free and N-acetylated aspartic acids in the nervous system. *J. Neurochem.* **13,** 779–783

26. Madhavarao, C. N., Hammer, J. A., Quarles, R. H., and Namboodiri, M. A. (2002) A radiometric assay for aspartoacylase activity in cultured oligodendrocytes. *Anal. Biochem.* **308,** 314–319

27. Namboodiri, M. A., Corigliano-Murphy, A., Jiang, G., Rollag, M., and Provencio, I. (2000) Murine aspartoacylase: cloning, expression and comparison with the human enzyme. *Brain Res. Mol. Brain Res.* **77,** 285–289

28. Kitada, K., Akimitsu, T., Shigematsu, Y., Kondo, A., Maihara, T., Yokoi, N., Kuramoto, T., Sasa, M., and Serikawa, T. (2000) Accumulation of N-acetyl-L-aspartate in the brain of the tremor rat, a mutant exhibiting absence-like seizure and spongiform degeneration in the central nervous system. *J. Neurochem.* **74,** 2512–2519

29. Yamada, J., Serikawa, T., Ishiko, J., Inui, T., Takada, H., Kawai, Y., and Okaniwa, A. (1985) Rats with congenital tremor and curled whiskers and hair. *Jikken Dobutsu.* **34,** 183–188

30. Matalon, R., Rady, P. L., Platt, K. A., Skinner, H. B., Quast, M. J., Campbell, G. A., Matalon, K., Ceci, J. D., Tyring, S. K., Nehls, M., and Surendran, S., *et al.* (2000) Knock-out mouse for Canavan disease: a model for gene transfer to the central nervous system. *J. Gene Med.* **2,** 165–175

31. Moffett, J. R., Namboodiri, M. A., Cangro, C. B., and Neale, J. H. (1991) Immunohistochemical localization of N-acetylaspartate in rat brain. *Neuroreport.* **2,** 131–134

32. Birnbaum, S. M. (1955) Amino acid acylases I and II from hog kidney. *Methods Enzymol.* **2,** 115–119

33. Pushkin, A., Carpenito, G., Abuladze, N., Newman, D., Tsuprun, V., Ryazantsev, S., Motemoturu, S., Sassani, P., Solovieva, N., Dukkipati, R., and Kurtz, I. (2004) Structural characterization, tissue distribution, and functional expression of murine aminoacylase III. *Am. J. Physiol. Cell Physiol.* **286,** C848–856

34. Uttamsingh, V., Baggs, R. B., Krenitsky, D. M., and Anders, M. W. (2000) Immunohistochemical localization of the acylases that catalyze the deacetylation of N-acetyl-L-cysteine and haloalkene-derived mercapturates. *Drug Metab. Dispos.* **28,** 625–632

35. Cook, R. M., Burke, B. J., Buchhagen, D. L., Minna, J. D., and Miller, Y. E. (1993) Human aminoacylase-1. Cloning, sequence, and expression analysis of a chromosome 3p21 gene inactivated in small cell lung cancer. *J. Biol. Chem.* **268,** 17010–17017

36. Nigg, E. A. (1997) Nucleocytoplasmic transport: signals, mechanisms and regulation. *Nature* **386,** 779–787

37. Elpeleg, O. N., and Shaag, A. (1999) The spectrum of mutations of the aspartoacylase gene in Canavan disease in non-Jewish patients. *J. Inherit. Metab. Dis.* **22,** 531–534

38. Kaul, R., Gao, G. P., Aloya, M., Balamurugan, K., Petrosky, A., Michals, K., and Matalon, R. (1994) Canavan disease: mutations among Jewish and non-Jewish patients. *Am. J. Hum. Genet.* **55,** 34–41

39. Ma, Z., Chow, K. M., Yao, J., and Hersh, L. B. (2004) Nuclear shuttling of the peptidase nardilysin. *Arch. Biochem. Biophys.* **422,** 153–160

40. Sheng, Z., Lewis, J. A., and Chirico, W. J. (2004) Nuclear and nucleolar localization of 18-kDa fibroblast growth factor-2 is controlled by C-terminal signals. *J. Biol. Chem.* **279,** 40153–40160

41. Yang, Y., Ma, J., Chen, Y., and Wu, M. (2004) Nucleocytoplasmic shuttling of receptor-interacting protein 3 (RIP3): identification of novel nuclear export and import signals in RIP3. *J. Biol. Chem.* **279,** 38820–38829

42. Resendes, M. C., Dobransky, T., Ferguson, S. S., and Rylett, R. J. (1999) Nuclear localization of the 82-kDa form of human choline acetyltransferase. *J. Biol. Chem.* **274,** 19417–19421

43. Bird, C. H., Blink, E. J., Hirst, C. E., Buzza, M. S., Steele, P. M., Sun, J., Jans, D. A., and Bird, P. I. (2001) Nucleocytoplasmic distribution of the ovalbumin serpin PI-9 requires a nonconventional nuclear import pathway and the export factor Crm1. *Mol. Cell. Biol.* **21,** 5396–5407

44. Christophe, D., Christophe-Hobertus, C., and Pichon, B. (2000) Nuclear targeting of proteins: how many different signals? *Cell Signal* **12,** 337–341

45. Foletti, A., Vuadens, F., and Beermann, F. (2003) Nuclear localization of mouse fibroblast growth factor 2 requires N-terminal and C-terminal sequences. *Cell Mol. Life Sci.* **60,** 2254–2265

46. Matalon, R., and Michals-Matalon, K. (1999) Biochemistry and molecular biology of Canavan disease. *Neurochem. Res.* **24,** 507–513

47. Birnbaum, S. M., Levintow, L., Kingsley, R. B., and Greenstein, J. P. (1952) Specificity of amino acid acylases. *J. Biol. Chem.* **194,** 455–470

48. Besley, G. T., Elpeleg, O. N., Shaag, A., Manning, N. J., Jakobs, C., and Walter, J. H. (1999) Prenatal diagnosis of Canavan disease–problems and dilemmas. *J. Inherit. Metab. Dis.* **22,** 263–266

49. Clark, J. B. (1998) N-acetyl aspartate: a marker for neuronal loss or mitochondrial dysfunction. *Dev. Neurosci.* **20,** 271–276

50. Leone, P., Janson, C. G., Bilaniuk, L., Wang, Z., Sorgi, F., Huang, L., Matalon, R., Kaul, R., Zeng, Z., and Freese, A., *et al.* (2000) Aspartoacylase gene transfer to the mammalian central

nervous system with therapeutic implications for Canavan disease. *Ann. Neurol.* **48,** 27–38

51. Gill, S. K., Bhattacharya, M., Ferguson, S. S., and Rylett, R. J. (2003) Identification of a novel nuclear localization signal common to 69- and 82-kDa human choline acetyltransferase. *J. Biol. Chem.* **278,** 20217–20224

52. Munster, A. K., Weinhold, B., Gotza, B., Muhlenhoff, M., Frosch, M., and Gerardy-Schahn, R. (2002) Nuclear localization signal of murine CMP-Neu5Ac synthetase includes residues required for both nuclear targeting and enzymatic activity. *J. Biol. Chem.* **277,** 19688–19696

53. Rubenstein, P. A., and Martin, D. J. (1983) NH2-terminal processing of actin in mouse L-cells in vivo. *J. Biol. Chem.* **258,** 3961–3966

54. Rubenstein, P. A., and Martin, D. J. (1983) NH2-terminal processing of Drosophila melanogaster actin. Sequential removal of two amino acids. *J. Biol. Chem.* **258,** 11354–11360

55. Pederson, T., and Aebi, U. (2002) Actin in the nucleus: what form and what for? *J. Struct. Biol.* **140,** 3–9

56. Abe, A., Saeki, K., Yasunaga, T., and Wakabayashi, T. (2000) Acetyla-tion at the N-terminus of actin strengthens weak interaction between actin and myosin. *Biochem. Biophys. Res. Commun.* **268,** 14–19

57. Kuersten, S., Ohno, M., and Mattaj, I. W. (2001) Nucleocytoplasmic transport: Ran, beta and beyond. *Trends Cell Biol.* **11,** 497–503

58. Yoneda, Y. (2000) Nucleocytoplasmic protein traffic and its significance to cell function. *Genes Cells* **5,** 777–787

59. Dingwall, C., and Laskey, R. A. (1991) Nuclear targeting sequences–a consensus? *Trends Biochem. Sci.* **16,** 478–481

60. Makkerh, J. P., Dingwall, C., and Laskey, R. A. (1996) Comparative mutagenesis of nuclear localization signals reveals the importance of neutral and acidic amino acids. *Curr. Biol.* **6,** 1025–1027

61. Yamaki, A., Kudoh, J., Shimizu, N., and Shimizu, Y. (2004) A novel nuclear localization signal in the human single-minded proteins SIM1 and SIM2. *Biochem. Biophys. Res. Commun.* **313,** 482–488

Mutational Analysis of Aspartoacylase: Implications for Canavan Disease

Jeremy R. Hershfield*, Nagarajan Pattabiraman‡, Chikkathur N. Madhavarao*, and M.A. Aryan Namboodiri*

*Department of Anatomy, Physiology and Genetics, Uniformed Services University of the Health Sciences, Bethesda, Maryland, 20814

‡Department of Oncology, Lombardi Comprehensive Cancer Center, Georgetown University, Washington, DC 20057

Address correspondence to: M.A. Aryan Namboodiri, Department of Anatomy Physiology and Genetics, USUHS, 4301 Jones Bridge Rd, Bethesda, MD 20814, Tel. 301 295-9357; Fax. 301 295-3566; E-Mail: anamboodiri@usuhs.mil

Abbreviations used: CD, Canavan disease; ASPA, aspartoacylase; NAA, N-acetyl-L-aspartate; WT, wild-type; ZnCPA, zinc-dependent carboxypeptidase A; DMEM, Dulbecco's modified Eagle Medium; FBS, fetal bovine serum; PBS, phosphate buffered saline; pepASPA, sera against a conserved ASPA peptide; α-βT, monoclonal anti-β-tubulin antibody.

ABSTRACT

Mutations in aspartoacylase, which catalyzes the deacetylation of *N*-acetyl-L-aspartate in the CNS, correlate with Canavan Disease, a neurodegenerative disorder usually fatal during childhood. Although several mutations result in undetectable aspartoacylase activity, the underlying biochemical mechanisms are poorly understood. Therefore, we developed and tested a three-dimensional homology model of aspartoacylase based on zinc dependent carboxypeptidase A. Mutations of the putative zinc-binding residues (H21G, E24D/G, and H116G), the general proton donor (E178A), and mutants designed to switch the order of the zinc-binding residues (H21E/E24H and E24H/H116E) yielded wild-type aspartoacylase protein levels and undetectable ASPA activity. Mutations that affect substrate carboxyl binding (R71N) and transition state stabilization (R63N) also yielded wild-type aspartoacylase protein levels and undetectable aspartoacylase activity. Alanine substitutions of Cys124 and Cys152, residues indicated by homology modeling to be in close proximity and in the proper orientation for disulfide bonding, yielded reduced ASPA protein and activity levels. Finally, expression of several previously tested (E24G, D68A, C152W, E214X, D249V, E285A, and A305E) and untested (H21P, A57T, I143T, P183H, M195R, K213E/G274R, G274R, and F295S) Canavan Disease mutations resulted in undetectable enzyme activity, and only E285A and P183H showed wild-type aspartoacylase protein levels. These results show that aspartoacylase is a member of the caboxypeptidase A family and offer novel explanations for most loss-of-function aspartoacylase mutations associated with Canavan Disease.

Running Title: Aspartoacylase Homology Modeling

INTRODUCTION

Canavan Disease (CD), a neurodegenerative disorder most prevalent among Ashkenazi Jews, is linked to mutations in the gene encoding aspartoacylase (EC 3.5.1.15; abb. ASPA), which catalyzes deacetylation of *N*-acetyl-L-aspartate (NAA) in the central nervous system. Typical CD pathology is marked by early onset macrocephaly, head-lag, ataxia, severe psychomotor retardation, brain vacuolization, and dysmyelination resulting in death during childhood, though there are several reports of clinically protracted disease courses (Matalon et al. 1988; Zelnik et al. 1993; Elpeleg et al. 1994; Matalon et al. 1995; Shaag et al. 1995; Leone et al. 1999; Zafeiriou et al. 1999; Surendran et al. 2003; Tacke et al. 2005; Yalcinkaya et al. 2005; Janson et al. 2006). Considerable effort has been devoted to understanding the basis of CD by elucidating the function of ASPA in the CNS. Developmental increases in ASPA and NAA correlate with myelination (D'Adamo et al. 1968; D'Adamo et al. 1973; Bhakoo et al. 2001; Kirmani et al. 2002; Kirmani et al. 2003; Klugmann et al. 2003) and several studies have shown incorporation of acetate from NAA into myelin lipids (D'Adamo and Yatsu 1966; Benuck and D'Adamo 1968; Burri et al. 1991; Mehta and Namboodiri 1995; Chakraborty et al. 2001). Overall acetate levels and myelin lipid synthesis have recently been shown to be deficient in brains of CD knockout mice (Madhavarao et al. 2005), providing strong support for the hypothesis that NAA in the CNS supplies acetyl groups for lipid synthesis during myelination (Kirmani et al. 2002; Kirmani et al. 2003; Madhavarao et al. 2005). Furthermore, ASPA is found in cells within both cytoplasm and nucleus (Hershfield et al. 2006), though its role in nucleus is yet to be delineated. There are few reports, however, that describe the mechanistic reason for loss of ASPA activity due to mutations.

Currently, there are 56 mutations in the ASPA gene that correlate with CD, including 44 missense/nonsense mutations (Stenson et al. 2003; Zeng et al. 2006). Among Ashkenazi Jews, the E285A mutation is the most common (Elpeleg et al. 1994; Kaul et al. 1994; Kronn et al. 1995; Kaul et al. 1996; Feigenbaum et al. 2004), while the most common mutation among other populations is A305E (Kaul et al. 1994; Shaag et al. 1995; Kaul et al. 1996; Elpeleg and Shaag 1999; Sistermans et al. 2000; Zeng et al. 2002; Yalcinkaya et al. 2005; Janson et al. 2006; Zeng et al. 2006). However, only half of these mutations have been shown to result in inactive ASPA *in vitro*. In these experiments, CD mutant ASPA constructs were transfected into COS cells for comparison of ASPA activity with wild-type (WT) enzyme. It is unknown whether CD mutations result in a loss of ASPA protein or a loss of catalytic function.

Although its functional domains remain uncharacterized, ASPA has consistently been referred to as a serine hydrolase of the α/β-hydrolase superfamily of enzymes because of its enzymatic inhibition by diisopropyl fluorophosphates, which suggests a catalytic serine, and because of local sequence homology to catalytic cores in esterases (Cygler et al. 1993; Kaul et al. 1993; Matalon and Michals-Matalon 1999). However, alignment studies show that there is little homology of ASPA with serine proteases and that ASPA lacks an invariant serine, a candidate for a catalytic residue (Cygler et al. 1993; Makarova and Grishin 1999).

Meanwhile, sequence alignment has indicated that ASPA is similar in structure to members of the zinc carboyxpeptidase family (Makarova and Grishin 1999). Consistent with this possibility, divalent cation chelators have been shown to drastically reduce ASPA activity in bovine brain homogenates and in dialyzed recombinant human ASPA from *E. coli* (Kaul et al. 1991; Moore et al. 2003). Zinc chloride slightly increased purified bovine brain ASPA activity at low concentrations and inhibited activity at higher concentrations (Kaul et al. 1991). Following dialysis and denaturation of recombinant human ASPA expressed in *E. coli*, roughly two atoms of zinc were detected per enzyme subunit, though zinc-treated ASPA had the same activity as native enzyme refolded without additional metal ions (Moore et al. 2003). These results suggest that ASPA is a metalloenzyme, but the effects of zinc on its catalytic activity remain unclear.

The three-dimensional structure of ASPA, or any other aminoacylase, is currently unknown. Conversely, there are numerous structures of zinc-dependent carboxypeptidase family members (Rees et al. 1983; Shoham et al. 1984; Christianson and Lipscomb 1986; Bukrinsky et al. 1998; Jensen et al. 2002). The catalytic mechanism of these metalloenzymes involves a glutamate residue activating a water molecule for nucleophilic attack on the substrate carbonyl carbon and subsequent proton transfer with a single zinc ion involved in water polarization and stabilization of the tetrahedral substrate intermediate (Kim and Lipscomb 1990). Several residues in bovine zinc-dependent carboxypeptidase A (EC 3.4.17.1; abb. ZnCPA) are conserved in human and murine ASPA (Makarova and Grishin 1999; Namboodiri et al. 2000), equivalent to those involved in zinc coordination (His21, Glu24, His116), shaping the substrate-binding

cavity (Asp68), substrate binding (Arg71), transition state stability (Arg63), and catalysis (Glu178) (Makarova and Grishin 1999). Notably, missense mutations at His21, Glu24, Asp68, and Arg71 have been detected in CD patients (Sistermans et al. 2000; Zeng et al. 2002; Janson et al. 2006). While there are no existing CD mutations at Glu178, there are nearby CD mutations at Pro181, Pro183, and Val186 (Elpeleg and Shaag 1999; Sistermans et al. 2000; Zeng et al. 2002), suggesting Glu178 might be an important catalytic residue.

To test the hypothesis that ASPA is a zinc-dependent metalloenzyme, as well as to address the biochemical basis for undetectable ASPA activity in several CD-associated ASPA mutations, we have generated and tested a 3D homology-based active/binding site model of ASPA based on bovine ZnCPA. Specifically, mutations in this report include those that appear frequently in the literature (G274R, F295S, E285A, A305E), affect a putative active site residue (H21P, E24G, A57T, D68A), or those that assist in understanding the entire span of the ASPA gene (I143T, C152W, P183H, M195R, K213E, D249V). Finally, we analyzed a K213E/G274R double mutation previously associated with a mild phenotype of CD (Tacke et al. 2005).

MATERIALS AND METHODS

Homology Modeling of Aspartoacylase

Using the reported coordinates for the crystal structure of bovine (*Bos taurus*) pancreas carboxypeptidase A (PDB Code 8CPA) with the resolution of 2 Å (Kim and

Lipscomb 1991; Berman et al. 2000) as a template, as well as the reported alignment between human ASPA (ACY2_Human) and 8CPA (Makarova and Grishin 1999), a homology model of ASPA (hACY2) was generated. The sequence alignment between ACY2_Human and 8CPA used in this paper is shown in Figure 1. As there were several gaps between ASPA and carboxypeptidase A in this alignment, we used the fragment-based alignment approach to build a homology model. The coordinates for the 3D model of human ASPA protein were generated using the homology-modeling program, Modeler (v. 6.2; http://salilab.org/modeller/). A zinc ion was manually placed onto the homology model such that it favorably coordinates with His, Glu, and His. The homology model of ASPA with the Zn^{2+} ion was energy minimized using constrained minimization and the molecular mechanics program, AMBER6 (http://amber.scripps.edu/). The molecular visualization program, Chimera (http://www.cgl.ucsf.edu/chimera/), was used to analyze the quality of the final homology model, as well as to generate the figures reported in this paper.

Plasmid Constructs and Site-Directed Mutagenesis

Full-length human ASPA cDNA was subcloned by polymerase chain reaction (PCR) using primers ATGACTTCTTGTCACATTGCT (forward) and CTAATGTAAACAGCAGCGAAT (reverse) from pBAD/Thio-TOPO (Invitrogen, Carlsbad, CA) (Namboodiri et al. 2000) into the TOPO-T/A cloning site of pcDNA3.1/V5-His-TOPO such that the resulting hASPA plasmid expresses untagged, native ASPA. Individual point mutations were introduced in native untagged hASPA using Stratagene's Quick Change II Site-Directed Mutagenesis Kit (La Jolla, CA)

according to manufacturer's instructions (Table 1). Mutant plasmid DNA was then isolated and sequenced to confirm the desired mutation.

Cell Culture and Transient Transfections

COS-7 (ATCC, Manassas, VA) cells were grown at $37^{o}C$ with 5% CO_2, cultured in Dulbecco's modified Eagle Medium (DMEM) containing 10% fetal bovine serum (FBS), grown to confluence, and sub-cultured every 3-4 days. Transient transfections were performed using Lipofectamine 2000 (Invitrogen) with 1.2µg plasmid DNA added to 90% confluent cells in 12-well plates. COS-7 cells were harvested 24h post-transfection by treatment with 2mM EDTA (10 min, $37^{o}C$), spun down, and washed with phosphate buffered saline (PBS). Whole cell extracts were prepared by sonicating cell pellets in homogenization buffer (0.5mM DTT, 50mM Tris-HCl, pH 8.0, 50mM NaCl, 0.05% IGEPAL CA-630, 10% glycerol). Cellular debris was then removed (16,000g, 10 min, $4^{o}C$) and protein concentrations were determined using Bio-Rad's DC protein assay (Hercules, CA) based on the method of Lowry.

Aspartoacylase Enzyme Assay

A high-sensitivity radiometric assay involving TLC-based product separation and phosphor image-based quantification was followed as previously described (Madhavarao et al. 2002). ASPA activity in transiently transfected COS-7 cell extracts was determined with a fixed total NAA concentration of 0.454 mM.

Immunoblotting

Whole cell extracts were subjected to SDS-PAGE and immunoblotting as previously described (Hershfield et al. 2006). Following blocking, membranes were cut in half using the 45kDa protein standard of the High-Range Rainbow Molecular Weight Marker (Amersham, Piscatway, NJ) as a guide. Super Fast diaminobenzidine substrate (Sigma, St. Louis, MO) was used for colorimetric detection of separate immunoblot signals from rabbit polyclonal antibody (1:4000) raised against a partial ASPA peptide (pepASPA) and monoclonal β-tubulin (α-βT) (1:5000) antibodies (Upstate, Charlottesville, VA). ~50µg of protein were loaded per well.

Qualitative RT-PCR

Total RNA was extracted from COS-7 cells 24h post-transfection using the RNAqueous 4PCR kit (Ambion, Austin, TX). RNA was then treated with DNase I, concentrated, and quantified. Two-step reverse transcription with heat denaturation was then carried out using Ambion's RETROscript kit. The resulting cDNA was amplified by PCR using either ASPA-specific gene primers GGGTATAGAAGTTGGTCCTCA (forward) and CTAATGTAAACAGCAGCGAAT (reverse), or positive control primers against the housekeeping gene rig/S15 (Ambion), and analyzed by 2% agarose gel electrophoresis.

Statistical Analysis

Enzyme activities are presented as means ± SEM. The differences between groups were analyzed by ANOVA followed by the least significant difference post-hoc test at a significance level of $p < 0.05$.

Chemical Structures

All chemical structures and reactions were drawn using the MDL ISIS Draw 2.5 (Elsevier MDL, San Ramon, CA) program.

RESULTS

Homology-Based Modeling of ASPA

The BLAST program was used to identify sequences close to the ACY2_Human (ACY2-Human Swiss-Prot Identity P45381 (http://www.expasy.org/uniprot/P45381#seq)) sequence in the PDB structures, yielding the x-ray structure of Succinylglutamate Desuccinylase from *Vibrio parahaemolyticus* as the highest scoring structure. However, careful analysis of this alignment showed there was no alignment for the third zinc-binding ligand. Therefore, the complete active site of ASPA could not be constructed using the succinylglutamate desuccinylases. On the other hand, alignments of hACY2 sequence against carboxypeptidase A, carboxypeptidase G, and aminopeptidase have recently been reported (Makarova and Grishin 1999). Two zinc ions were reported to bind to aminopeptidase (Chevrier et al. 1994; Berman et al. 2000) and carboxypeptidase G2 (Rowsell et al. 1997; Berman et al. 2000). In these peptidases, the ligands were shared between the two zinc ions. In carboxypeptidase A, however, only one zinc ion is bound to the enzyme because the Glu ligand required for binding the second zinc ion has been replaced by Phe (Makarova and Grishin 1999). Similarly, for the ACY2_Human sequence, the region containing this glutamate is absent. Therefore,

from the sequence alignment and homology modeling it appears that human ASPA protein likely binds a single zinc atom.

The final homology model for ASPA is shown in Figure 2. The protein is represented by ribbons and the potentially critical catalytic and binding residues in the active site, His21, Glu24, His116, Glu178, Arg63, and Arg71 are shown by atom color coded ball and stick representation. A zinc atom (shown by cyan sphere) bound to His21, His116 and Glu24 is also shown. Four cysteine residues, Cys61, Cys67, Cys124, and Cys152, discussed in this report are also depicted using ball and stick. Even though the homology model of ASPA does not include the N-terminal 60 amino acid residues of the carboxypeptidase, the catalytic residues of the active sites correspond very well. Aspartoacylase and carboxypeptidase A both catalyze hydrolysis of a C-terminal peptide bond (Fig. 3A). Therefore, it is not surprising that there is a close superposition of these catalytic residues of the ASPA homology model (bonds shown by lines) onto the carboxypeptidase (bonds by thick lines and labeled) (Fig. 3B).

Characterization of Zinc-Coordination and ASPA Catalysis

The homology-based model suggests several residues that could potentially be involved in NAA binding and/or hydrolysis. Mutation of the conserved residues corresponding to bovine CPA's three putative zinc-binding ligands (His21, Glu24, His116) and the general proton donor (Glu178), to either Ala or Gly yielded WT levels of ASPA protein by immunoblotting with pepASPA (Hershfield et al. 2006) (Fig. 4A). These mutants yielded undetectable enzymatic activity by a high-sensitivity radiometric

ASPA assay (Madhavarao et al. 2002) (Fig. 4B) [see Fig. 6A for E24G]. Mutation of Glu24 to a conserved Asp, which shortens the length of the putative zinc ligand by ~1.5Å, also resulted in a catalytically defective enzyme (Fig. 4B). While aspartate is also a potential zinc ligand (Vallee and Auld 1990, 1990; Le Moual et al. 1991; Medina et al. 1991), we were unable to detect residual ASPA activity in E24D by alternate approaches such as tripling NAA concentration in the ASPA assay and analyzing partially nickel-affinity purified hASPA E24D expressed with a C-terminal V5-His tag (data not shown). In addition, double mutants designed to switch the order of the three putative zinc-binding ligands (H21E/E24H and E24H/H116E) resulted in catalytically defective enzymes (see Fig. 4C for illustration). Finally, arginines roughly aligned to those required for binding the C-terminal carboxyl group of the substrate (Arg145→Arg71) and stabilizing the gem diolate anion intermediate (Arg127→Arg63) in bovine ZnCPA (Makarova and Grishin 1999), were mutated to asparagines. This was done to maintain local geometry while losing positive charges. Expression of both R71N and R63N resulted in WT ASPA protein levels (Fig. 4A) and undetectable ASPA activity (Fig. 4B), suggesting catalytic roles for Arg71 and Arg63.

Indication of a Potential Disulfide Bond in ASPA

The homology model (Fig. 2) depicts the four cysteine residues in ASPA. Mutations at Cys152 have been associated with CD and undetectable ASPA activity *in vitro* (Kaul et al. 1995; Kaul et al. 1996; Zeng et al. 2002). Coupled with the observation that low concentrations of DTT are required to maintain ASPA activity and high concentrations destroy activity (Kaul et al. 1991; Madhavarao et al. 2002), it has been

suggested that there is an intramolecular disulfide bond in ASPA involving Cys152. Assuming that ASPA lacks the overall flexibility necessary for distal disulfide bonds, it appears likely that only the proximal cysteine pairs—Cys61/Cys67 and Cys124/Cys152—could reasonably form disulfide bridges *in vivo*. The homology model indicates that the reactive sulfhydryl groups of Cys61 and Cys67 face away from each other, making their bonding unlikely. Meanwhile, Cys124 and Cys152 are correctly orientated for disulfide bonding.

The potential of Cys124 and Cys152 to disulfide bond was analyzed using small, sterically non-interfering alanine substitutions (Fig. 5). Cys61 was also analyzed because it had been previously suggested to be the partner for Cys152 disulfide bonding (Kaul et al. 1995) and because of its proximity to the putative active site. A C61S mutation was also generated to mimic the possibility that the sulfhydryl group participates in catalysis via a proton donor/acceptor mechanism. Western blot analysis showed WT ASPA protein levels for C61A and C61S, versus diminished levels for C124A and C152A (Fig. 5A). Consistent with the relative amounts of ASPA protein, C61A and C61S had WT ASPA activity, while C124A and C152A had 50% and 25% activity, respectively (Fig. 5B). Similar to how a bulky Cys→Trp substitution at Cys152 appears to destabilize ASPA (see Fig. 6A), C61W was adequately transcribed (Fig. 6B, top panel), yet resulted in a nearly complete absence of ASPA protein and activity (Fig. 5A,B).

Protein Characteristics of CD Mutant ASPA

94

We tested the ASPA homology model using biologically relevant CD mutations that span the whole ASPA gene (see Table 2). It has been hypothesized that many non-conservative CD mutants exert deleterious effects due to a loss of structural integrity by a drastic conformational change, rather than directly disrupting catalytic events at the active site (Shaag et al. 1995; Zeng et al. 2002; Moore et al. 2003). Therefore, CD mutations resulting in nearly WT ASPA protein levels might suggest defective catalysis, while those drastically reducing ASPA protein might suggest defective protein integrity.

We first analyzed a subset of missense mutations in the ASPA gene that had previously been shown to result in undetectable enzyme activity upon *in vitro* expression (Fig. 6A). For each of six mutants, comparable levels of ASPA mRNA, when normalized to a loading control, were detected by RT-PCR (Fig. 6A, top panel). Western blot analysis for ASPA protein showed strong reductions for C152W, D249V, and A305E, mild reductions for E24G and D68A, and WT levels for E285A (Fig. 6A, middle panel). The E214X truncation mutant was used as a negative control for detection of full-length ASPA at ~36kDa. Finally, we confirmed that transfections of E24G, D68A, C152W, E214X, D249V, E285A, and A305E into COS-7 cells each resulted in undetectable ASPA activity(Kaul et al. 1994; Zeng et al. 2002) compared to ~20nmol/h/mg protein specific activity for WT ASPA (Fig. 6A, bottom panel). These results are consistent with the homology model (Fig. 2). Mutations affecting putative active-site residues (E24G, D68A) result in mildly reduced ASPA protein. Meanwhile, a non-conservative mutation affecting a site with no apparent catalytic role (C152W) results in drastically reduced ASPA protein levels. As the homology model does not

95

cover ASPA's C-terminus, we can only speculate that E285A is a catalytic mutation and that D249V and A305E affect protein integrity.

We next analyzed a subset of missense mutations in the ASPA gene that had previously been linked to CD but not tested *in vitro* (Fig. 6B). For each of eight mutants, comparable levels of ASPA mRNA, when normalized to a loading control, were detected by RT-PCR (Fig. 6B, top panel). Western blot analysis showed a nearly complete absence of ASPA protein for H21P, I143T, and F295S, strong reductions for M195R and G274R, a mild reduction for A57T, and WT levels for P183H and K213E (Fig. 6B, middle panel). Finally, there was WT activity for K213E, ~5% residual activity for G274R, and undetectable activity for H21P, A57T, I143T, P183H, M195R, and F295S (Fig. 6B, bottom panel). These results are consistent with our homology model (Fig. 2). The lone exception was the H21P protein phenotype, which affected protein integrity rather than enzyme catalysis, likely due to the contorted nature of the substituted proline. Mutations neighboring putative active-site and catalytic residues (A57T, P183H) resulted in slightly reduced or unaffected ASPA protein levels. Meanwhile, non-conservative mutations affecting residues with no apparent catalytic roles (I143T, M195R) resulted in drastically reduced ASPA protein levels. The reversal of charge at Lys213 did not affect ASPA activity (indicative of a silent mutation) and suggests that Lys213 is not crucial for catalytically active ASPA protein. Finally, with no knowledge of ASPA's C-terminal structure, we can only speculate that G274R and F295S affect protein integrity.

Lastly, it was postulated in a recent case report that K213E might serve a protective role in promoting a mild clinical phenotype (Tacke et al. 2005). To explore this possibility, we generated and analyzed the aforementioned K213E/G274R double mutant *in vitro* (Fig. 6C). Having determined that K213E is a silent mutation and that G274R appears to result in defective protein synthesis, folding, or stability (Fig. 6B), we observed that the K213E/G274R double mutant enzyme also shows a nearly complete absence of ASPA protein (Fig. 6C, top panel) and activity (Fig. 6C, bottom panel), in our expression system.

DISCUSSION

Since its purification from bovine brain in 1991 (Kaul et al. 1991), ASPA has been referred to as a member of the serine hydrolase superfamily of enzymes in CD literature (Kaul et al. 1993). However, a 1999 bioinformatics alignment study cast doubt upon this assumption, instead claiming that ASPA is a member of the zinc-peptidase superfamily of enzymes (Makarova and Grishin 1999). In our current report we explored this possibility using mutations to evaluate a homology model. This kind of approach has previously been used for identifying the metal ligands in endopeptidase (Cummins et al. 1999), insulin-regulated aminopeptidase (Laustsen et al. 2001), leukotriene A4 hydrolase (Medina et al. 1991), and aminopeptidase A (Vazeux et al. 1996). First, we generated an active/binding site model for ASPA based on homology to ZnCPA. Second, analysis of mutations of residues potentially involved in zinc coordination (His21, Glu24, His116), general proton donation (Glu178), substrate carboxyl binding (Arg71), and transition

state stabilization (Arg63) suggests that they have critical roles in ASPA catalysis. Third, an analysis of mutations of Cys61, Cys124, and Cys152 suggests that ASPA activity and stability might depend on an intramolecular disulfide bond between Cys124 and Cys152. Fourth, an analysis of several ASPA mutations associated with CD suggests that E24G, A57T, D68A, P183H, and E285A are catalytic mutations. Meanwhile, H21P, I143T, C152W, M195R, D249V, F295S, and A305E appear to be non-catalytic mutations. Furthermore, an analysis of K213E suggests that it is a silent mutation. Finally, an analysis of a K213E/G274R double mutation suggests that K213E does not play a protective role.

Mutations of ASPA residues equivalent to ZnCPA's zinc ligands (His21, Glu24, and His116), general proton donor (Glu178), substrate-binding determinant (Arg71), and substrate-cavity shaping residue (Asp68) result in catalytically defective ASPA protein. Analysis of the E24D mutation suggests that shortening the side chain by a single C-C bond drastically alters zinc binding that might polarize the zinc-coordinated water molecule for catalysis (Laustsen et al. 2001). Alternatively, the resulting distorted local geometry of the active site increases the distance between zinc and the carbonyl group of NAA and/or zinc-bond water, or provokes a small change in the spatial position of the catalytic glutamate through its linkage to one of the zinc-coordinating histidine residues (Le Moual et al. 1991). Although highly conserved Glu→Asp mutations have resulted in weakened zinc affinity and a lowered K_m in similar enzymes (Le Moual et al. 1991; Vazeux et al. 1996), we could not detect residual ASPA activity for the E24D mutant. While the E24G mutant could have resulted in a loss of activity due to structural

differences, the conserved E24D mutant still displayed a loss of activity, suggesting that this glutamate is directly involved in catalysis (Vazeux et al. 1996). In addition, the order of the three metal binding ligands was found to be crucial for zinc-promoted enzymatic catalysis. This is consistent with the notion that identity, spacing, and secondary interactions with neighboring amino acids are all crucial for zinc-mediated catalysis (Auld 2001).

The experimental results in this report suggest that ASPA follows a catalytic mechanism similar to that of ZnCPA (Fig. 7) (Wouters and Husain 2001; Jensen et al. 2002). Using carboxypeptidase-bound ligand inhibitor crystal structures as a template (Jensen et al. 2002), we propose that Arg71 binds the carboxylate group of the NAA, while the acetyl group is fitted into the active site by its affinity towards the zinc atom (Fig. 7A). At this stage, the zinc ion is five coordinated: Glu24 bidentate, His21, His116, and a water molecule, which is present in all catalytic zinc sites (Vallee and Auld 1990, 1990). The oxygen of the scissile carbonyl now interacts with Zn^{2+} and forms its sixth ligand. This interaction, and the approaching guanidine group of Arg63, then help zinc to activate the water ligand, as well as further polarize the scissile carbonyl group (Kim and Lipscomb 1990). Acidic zinc-activated water is able to donate a proton to Glu178 and leave a zinc-bound OH^- available for nucleophilic attack on the scissile carbonyl carbon of the acetyl group of NAA (Fig. 7B). This nucleophilic attack results in the formation of the negatively charged transition state, a gem-diolate anion that is primarily stabilized by its interaction with the guanidinium group of Arg63. The bidentate coordination to zinc and the electrostatic interaction with Glu178 also contribute to this stabilization (Fig. 7C).

The *gem*-diolate anion transition state is fundamentally unstable and inevitably breaks apart (Fig. 7C). Our mutational analysis is consistent with the notion that the positive charge of Arg63 is required to favor the formation/stabilization of the transition state. The eventual collapse of the transition state results in the formation of aspartate and acetate from NAA as Glu178 provides the proton required to form the primary amino group of aspartate. NAA hydrolysis concludes as the hydroxyl group from water becomes part of acetate and the proton becomes part of the primary amino group of aspartate (Fig. 7C, D). It appears that the electrostatic repulsion between Glu178 and the newly formed carboxyl group of acetate plays a role in its repulsion from the active site. Meanwhile, the electrostatic repulsion between the positively charged primary amino group of aspartate and those of the arginine residues at the active site helps release aspartate (Fig. 7D).

According to a published alignment, the equivalent of bovine ZnCPA Arg127, the primary role of which was determined via mutational analysis to be transition state stabilization (Phillips et al. 1990), is Lys60 in ASPA (Makarova and Grishin 1999). However, this lysine is unlikely to play the same role because, for ZnCPA, R127K resulted in an inactive enzyme (Phillips et al. 1990). It appears that hydrogen bonds, in addition to size and hydrophobicity, contribute to charge positioning relative to the scissile carbonyl bond and to stabilizing active site geometry. Therefore, though slightly misaligned, Arg63 (aligned with Arg130 in bovine ZnCPA) is more likely than Lys60 to be involved in transition state stabilization. Interestingly, Arg130 in bovine ZnCPA has

been implicated in substrate side chain binding (Jensen et al. 2002). Future studies are required to resolve this discrepancy in alignment and function of Lys60 and Arg63 in ASPA.

The assumptions in the literature pertaining to ASPA's catalytic mechanism are consistent with our proposed catalytic mechanism based on that of ZnCPA (Fig. 7). The carbon backbone of NAA has been suggested to interact with ASPA's active site because substrates with more electronegative carbonyl groups are better substrates for ASPA-mediated hydrolysis (Kaul et al. 1991; Matalon et al. 1993). A nucleophilic attack is then believed to occur at the carbonyl group, irrespective of the α and β-carboxyl groups (Moore et al. 2003).

By generating a partial homology model and a hypothetical catalytic mechanism for ASPA-mediated NAA hydrolysis, we can reasonably explain how several CD-associated mutations result in a loss of activity *in vivo*. Our initial hypothesis was that non-catalytic CD-associated mutations could alter ASPA's subcellular localization, which we recently determined to be nuclear-cytoplasmic (Hershfield et al. 2006). However, immunoblot analyses of mutations analyzed in this report quickly showed that CD-associated non-catalytic ASPA mutations tend to result in a nearly complete absence of ASPA protein. E285A was a lingering possibility for aberrant subcellular localization. However, it had previously been shown to result in an inactive enzyme when purified from *E. coli* (Moore et al. 2003), which lack organelles.

According to the homology model for ASPA, E24G precludes zinc-binding, while A57T and D68A disrupt the substrate binding cavity. The substitution to His at Pro183, the equivalent to the site of a type I reverse turn (Pro282) in bovine ZnCPA (Makarova and Grishin 1999), replaces a bend that is crucial for local geometry with a positive charge and misaligns the catalytic Glu178. The molecular basis of the E285A mutation remains unclear, though our data corroborate its putative catalytic role (Kaul et al. 1993), rather than a more recently proposed loss of protein integrity attributed to Ala and Asp substitutions at Glu285 (Moore et al. 2003). As mentioned previously, the homology model of ASPA does not include the first 60 amino acids of ZnCPA, residues believed to stabilize a part of the substrate binding pocket. ASPA's C-terminus might replace these 60 amino acids of ZnCPA and stabilize ASPA's substrate binding pocket. All other CD-associated ASPA mutations investigated in this report—including H21P, I143T, C152W, M195R, D249V, G274R, and A305E—appear to result in defective ASPA biosynthesis, processing, or stability through the introduction of a turn (H21P), loss of hydrophobicity (I143T, M195R, G274R and A305E), introduction of a bulky residue (C152W), or loss of charge (D249V).

Importantly, the resulting protein phenotype of a CD-associated ASPA mutation—non-catalytic versus catalytic—does not appear to influence a patient's physiological phenotype. This is in contrast to a previous suggestion that active site mutations result in a severe phenotype (Surendran et al. 2003). The most common mutation among non-Ashkenazi Europeans, A305E (non-catalytic), has been implicated in severe, classical, and mild CD cases (Shaag et al. 1995; Sistermans et al. 2000;

Yalcinkaya et al. 2005; Janson et al. 2006). Similarly, the most common mutation among Ashkenazim, E285A (catalytic), has also been implicated in multiple CD clinical courses (Shaag et al. 1995).

A typical course of CD results in death during childhood (Traeger and Rapin 1998). However, there are several examples of either particularly clinically severe (Zeng et al. 2002) or mild (Zafeiriou et al. 1999; Tacke et al. 2005; Yalcinkaya et al. 2005; Janson et al. 2006) CD courses wherein a particular missense mutation has been thought to correlate with the abnormal disease progression. Some of these correlations have been discredited by a contradictory course of CD resulting from either homozygosity or compound heterozygosity of the same mutation (Olsen et al. 2002). However, there are a few remaining examples of missense mutations that might contribute to a milder clinical course of CD. Such is the case of a child with 11.6% residual ASPA activity in cultured fibroblasts found to possess a K213E/G274R double mutation in the ASPA gene on each chromosome (Tacke et al. 2005). G274R had previously been associated with a more typical CD course (Shaag et al. 1995; Elpeleg and Shaag 1999). Therefore, it was postulated that K213E serves a protective role (Tacke et al. 2005). Since we detected neither ASPA activity nor ASPA protein for this double mutant, an alternative hypothesis that this mild disease course is due to one or several disease-modifying genes residing elsewhere in the genome (Tacke et al. 2005) needs to be considered. Coupled with our observation that the catalytic nature of a CD-associated ASPA mutation does not appear to correlate with a particular disease course, we conclude that it is very difficult to make accurate genotype-phenotype correlations for CD.

In conclusion, we have used mutational analyses to evaluate an active site homology model which shows that ASPA appears to follow a catalytic mechanism similar to bovine ZnCPA. During the preparation of this manuscript, a report was published which confirms our proposal that ASPA contains a single zinc atom (Le Coq et al. 2006). Future studies might utilize our homology model and the proposed catalytic mechanism for drug design with the goal of restoring ASPA activity in CD patients with catalytically mutant ASPA (Qiao et al. 2006).

ACKNOWLEDGMENTS

REFERENCES

Auld D. S. (2001) Zinc coordination sphere in biochemical zinc sites. *Biometals* **14,** 271-313.

Benuck M. and D'Adamo A. F., Jr. (1968) Acetyl transport mechanisms. Metabolism of N-acetyl-L-aspartic acid in the non-nervous tissues of the rat. *Biochim Biophys Acta* **152,** 611-618.

Berman H. M., Westbrook J., Feng Z., Gilliland G., Bhat T. N., Weissig H., Shindyalov I. N. and Bourne P. E. (2000) The Protein Data Bank. *Nucleic Acids Res* **28,** 235-242.

Bhakoo K. K., Craig T. J. and Styles P. (2001) Developmental and regional distribution of aspartoacylase in rat brain tissue. *J Neurochem* **79,** 211-220.

Bukrinsky J. T., Bjerrum M. J. and Kadziola A. (1998) Native carboxypeptidase A in a new crystal environment reveals a different conformation of the important tyrosine 248. *Biochemistry* **37,** 16555-16564.

Burri R., Steffen C. and Herschkowitz N. (1991) N-acetyl-L-aspartate is a major source of acetyl groups for lipid synthesis during rat brain development. *Dev Neurosci* **13,** 403-411.

Chakraborty G., Mekala P., Yahya D., Wu G. and Ledeen R. W. (2001) Intraneuronal N-acetylaspartate supplies acetyl groups for myelin lipid synthesis: evidence for myelin-associated aspartoacylase. *J Neurochem* **78,** 736-745.

Chevrier B., Schalk C., D'Orchymont H., Rondeau J. M., Moras D. and Tarnus C. (1994) Crystal structure of Aeromonas proteolytica aminopeptidase: a prototypical member of the co-catalytic zinc enzyme family. *Structure* **2,** 283-291.

Christianson D. W. and Lipscomb W. N. (1986) X-ray crystallographic investigation of substrate binding to carboxypeptidase A at subzero temperature. *Proc Natl Acad Sci U S A* **83,** 7568-7572.

Cummins P. M., Pabon A., Margulies E. H. and Glucksman M. J. (1999) Zinc coordination and substrate catalysis within the neuropeptide processing enzyme endopeptidase EC 3.4.24.15. Identification of active site histidine and glutamate residues. *J Biol Chem* **274,** 16003-16009.

Cygler M., Schrag J. D., Sussman J. L., Harel M., Silman I., Gentry M. K. and Doctor B. P. (1993) Relationship between sequence conservation and three-dimensional structure in a large family of esterases, lipases, and related proteins. *Protein Sci* **2,** 366-382.

D'Adamo A. F., Jr. and Yatsu F. M. (1966) Acetate metabolism in the nervous system. N-acetyl-L-aspartic acid and the biosynthesis of brain lipids. *J Neurochem* **13,** 961-965.

D'Adamo A. F., Jr., Gidez L. I. and Yatsu F. M. (1968) Acetyl transport mechanisms. Involvement of N-acetyl aspartic acid in de novo fatty acid biosynthesis in the developing rat brain. *Exp Brain Res* **5,** 267-273.

D'Adamo A. F., Jr., Smith J. C. and Woiler C. (1973) The occurrence of N-acetylaspartate amidohydrolase (aminoacylase II) in the developing rat. *J Neurochem* **20,** 1275-1278.

Elpeleg O. N. and Shaag A. (1999) The spectrum of mutations of the aspartoacylase gene in Canavan disease in non-Jewish patients. *J Inherit Metab Dis* **22,** 531-534.

Elpeleg O. N., Anikster Y., Barash V., Branski D. and Shaag A. (1994) The frequency of the C854 mutation in the aspartoacylase gene in Ashkenazi Jews in Israel. *Am J Hum Genet* **55,** 287-288.

Feigenbaum A., Moore R., Clarke J., Hewson S., Chitayat D., Ray P. N. and Stockley T. L. (2004) Canavan disease: carrier-frequency determination in the Ashkenazi Jewish population and development of a novel molecular diagnostic assay. *Am J Med Genet* **124A,** 142-147.

Hershfield J. R., Madhavarao C. N., Moffett J. R., Benjamins J., Garbern J. Y. and Namboodiri M. A. A. (2006) Aspartoacylase is a regulated nuclear-cytoplasmic enzyme. *FASEB J in press*.

Janson C. G., Kolodny E. H., Zeng B. J., Raghavan S., Pastores G., Torres P., Assadi M., McPhee S., Goldfarb O., Saslow B., Freese A., Wang D. J., Bilaniuk L., Shera D. and Leone P. (2006) Mild-onset presentation of Canavan's disease associated with novel G212A point mutation in aspartoacylase gene. *Ann Neurol* **59,** 428-431.

Jensen F., Bukrinsky T., Bjerrum J. and Larsen S. (2002) Three high-resolution crystal structures of cadmium-substituted carboxypeptidase A provide insight into the enzymatic function. *J Biol Inorg Chem* **7,** 490-499.

Kaul R., Gao G. P., Balamurugan K. and Matalon R. (1993) Cloning of the human aspartoacylase cDNA and a common missense mutation in Canavan disease. *Nat Genet* **5,** 118-123.

Kaul R., Casanova J., Johnson A. B., Tang P. and Matalon R. (1991) Purification, characterization, and localization of aspartoacylase from bovine brain. *J Neurochem* **56,** 129-135.

Kaul R., Gao G. P., Michals K., Whelan D. T., Levin S. and Matalon R. (1995) Novel (cys152 > arg) missense mutation in an Arab patient with Canavan disease. *Hum Mutat* **5,** 269-271.

Kaul R., Gao G. P., Aloya M., Balamurugan K., Petrosky A., Michals K. and Matalon R. (1994) Canavan disease: mutations among Jewish and non-jewish patients. *Am J Hum Genet* **55,** 34-41.

Kaul R., Gao G. P., Matalon R., Aloya M., Su Q., Jin M., Johnson A. B., Schutgens R. B. and Clarke J. T. (1996) Identification and expression of eight novel mutations among non-Jewish patients with Canavan disease. *Am J Hum Genet* **59,** 95-102.

Kim H. and Lipscomb W. N. (1990) Crystal structure of the complex of carboxypeptidase A with a strongly bound phosphonate in a new crystalline form: comparison with structures of other complexes. *Biochemistry* **29,** 5546-5555.

Kim H. and Lipscomb W. N. (1991) Comparison of the structures of three carboxypeptidase A-phosphonate complexes determined by X-ray crystallography. *Biochemistry* **30,** 8171-8180.

Kirmani B. F., Jacobowitz D. M. and Namboodiri M. A. (2003) Developmental increase of aspartoacylase in oligodendrocytes parallels CNS myelination. *Brain Res Dev Brain Res* **140,** 105-115.

Kirmani B. F., Jacobowitz D. M., Kallarakal A. T. and Namboodiri M. A. (2002) Aspartoacylase is restricted primarily to myelin synthesizing cells in the CNS: therapeutic implications for Canavan disease. *Brain Res Mol Brain Res* **107,** 176-182.

Klugmann M., Symes C. W., Klaussner B. K., Leichtlein C. B., Serikawa T., Young D. and During M. J. (2003) Identification and distribution of aspartoacylase in the postnatal rat brain. *Neuroreport* **14,** 1837-1840.

Kobayashi K., Tsujino S., Ezoe T., Hamaguchi H., Nihei K. and Sakuragawa N. (1998) Missense mutation (I143T) in a Japanese patient with Canavan disease. *Hum Mutat* **Suppl 1,** S308-309.

Kronn D., Oddoux C., Phillips J. and Ostrer H. (1995) Prevalence of Canavan disease heterozygotes in the New York metropolitan Ashkenazi Jewish population. *Am J Hum Genet* **57,** 1250-1252.

Laustsen P. G., Vang S. and Kristensen T. (2001) Mutational analysis of the active site of human insulin-regulated aminopeptidase. *Eur J Biochem* **268,** 98-104.

Le Coq J., An H. J., Lebrilla C. and Viola R. E. (2006) Characterization of human aspartoacylase: the brain enzyme responsible for canavan disease. *Biochemistry* **45,** 5878-5884.

Le Moual H., Devault A., Roques B. P., Crine P. and Boileau G. (1991) Identification of glutamic acid 646 as a zinc-coordinating residue in endopeptidase-24.11. *J Biol Chem* **266,** 15670-15674.

Leone P., Janson C. G., McPhee S. J. and During M. J. (1999) Global CNS gene transfer for a childhood neurogenetic enzyme deficiency: Canavan disease. *Curr Opin Mol Ther* **1,** 487-492.

Madhavarao C. N., Hammer J. A., Quarles R. H. and Namboodiri M. A. (2002) A radiometric assay for aspartoacylase activity in cultured oligodendrocytes. *Anal Biochem* **308,** 314-319.

Madhavarao C. N., Arun P., Moffett J. R., Szucs S., Surendran S., Matalon R., Garbern J., Hristova D., Johnson A., Jiang W. and Namboodiri M. A. (2005) Defective N-

acetylaspartate catabolism reduces brain acetate levels and myelin lipid synthesis in Canavan's disease. *Proc Natl Acad Sci U S A* **102,** 5221-5226.

Makarova K. S. and Grishin N. V. (1999) The Zn-peptidase superfamily: functional convergence after evolutionary divergence. *J Mol Biol* **292,** 11-17.

Matalon R. and Michals-Matalon K. (1999) Recent advances in Canavan disease. *Adv Pediatr* **46,** 493-506.

Matalon R., Kaul R. and Michals K. (1993) Canavan disease: biochemical and molecular studies. *J Inherit Metab Dis* **16,** 744-752.

Matalon R., Michals K. and Kaul R. (1995) Canavan disease: from spongy degeneration to molecular analysis. *J Pediatr* **127,** 511-517.

Matalon R., Michals K., Sebesta D., Deanching M., Gashkoff P. and Casanova J. (1988) Aspartoacylase deficiency and N-acetylaspartic aciduria in patients with Canavan disease. *Am J Med Genet* **29,** 463-471.

Medina J. F., Wetterholm A., Radmark O., Shapiro R., Haeggstrom J. Z., Vallee B. L. and Samuelsson B. (1991) Leukotriene A4 hydrolase: determination of the three zinc-binding ligands by site-directed mutagenesis and zinc analysis. *Proc Natl Acad Sci U S A* **88,** 7620-7624.

Mehta V. and Namboodiri M. A. (1995) N-acetylaspartate as an acetyl source in the nervous system. *Brain Res Mol Brain Res* **31,** 151-157.

Moore R. A., Le Coq J., Faehnle C. R. and Viola R. E. (2003) Purification and preliminary characterization of brain aspartoacylase. *Arch Biochem Biophys* **413,** 1-8.

Namboodiri M. A., Corigliano-Murphy A., Jiang G., Rollag M. and Provencio I. (2000) Murine aspartoacylase: cloning, expression and comparison with the human enzyme. *Brain Res Mol Brain Res* **77,** 285-289.

Olsen T. R., Tranebjaerg L., Kvittingen E. A., Hagenfeldt L., Moller C. and Nilssen O. (2002) Two novel aspartoacylase gene (ASPA) missense mutations specific to Norwegian and Swedish patients with Canavan disease. *J Med Genet* **39,** e55.

Phillips M. A., Fletterick R. and Rutter W. J. (1990) Arginine 127 stabilizes the transition state in carboxypeptidase. *J Biol Chem* **265,** 20692-20698.

Qiao Y., Molina H., Pandey A., Zhang J. and Cole P. A. (2006) Chemical rescue of a mutant enzyme in living cells. *Science* **311,** 1293-1297.

Rees D. C., Lewis M. and Lipscomb W. N. (1983) Refined crystal structure of carboxypeptidase A at 1.54 A resolution. *J Mol Biol* **168,** 367-387.

Rowsell S., Pauptit R. A., Tucker A. D., Melton R. G., Blow D. M. and Brick P. (1997) Crystal structure of carboxypeptidase G2, a bacterial enzyme with applications in cancer therapy. *Structure* **5,** 337-347.

Shaag A., Anikster Y., Christensen E., Glustein J. Z., Fois A., Michelakakis H., Nigro F., Pronicka E., Ribes A., Zabot M. T. and et al. (1995) The molecular basis of canavan (aspartoacylase deficiency) disease in European non-Jewish patients. *Am J Hum Genet* **57,** 572-580.

Shoham G., Rees D. C. and Lipscomb W. N. (1984) Effects of pH on the structure and function of carboxypeptidase A: crystallographic studies. *Proc Natl Acad Sci U S A* **81,** 7767-7771.

Sistermans E. A., de Coo R. F., van Beerendonk H. M., Poll-The B. T., Kleijer W. J. and van Oost B. A. (2000) Mutation detection in the aspartoacylase gene in 17 patients with Canavan disease: four new mutations in the non-Jewish population. *Eur J Hum Genet* **8,** 557-560.

Stenson P. D., Ball E. V., Mort M., Phillips A. D., Shiel J. A., Thomas N. S., Abeysinghe S., Krawczak M. and Cooper D. N. (2003) Human Gene Mutation Database (HGMD): 2003 update. *Hum Mutat* **21,** 577-581.

Surendran S., Bamforth F. J., Chan A., Tyring S. K., Goodman S. I. and Matalon R. (2003) Mild elevation of N-acetylaspartic acid and macrocephaly: diagnostic problem. *J Child Neurol* **18,** 809-812.

Surendran S., Michals-Matalon K., Quast M. J., Tyring S. K., Wei J., Ezell E. L. and Matalon R. (2003) Canavan disease: a monogenic trait with complex genomic interaction. *Mol Genet Metab* **80,** 74-80.

Tacke U., Olbrich H., Sass J. O., Fekete A., Horvath J., Ziyeh S., Kleijer W. J., Rolland M. O., Fisher S., Payne S., Vargiami E., Zafeiriou D. I. and Omran H. (2005) Possible genotype-phenotype correlations in children with mild clinical course of Canavan disease. *Neuropediatrics* **36,** 252-255.

Traeger E. C. and Rapin I. (1998) The clinical course of Canavan disease. *Pediatr Neurol* **18,** 207-212.

Vallee B. L. and Auld D. S. (1990) Zinc coordination, function, and structure of zinc enzymes and other proteins. *Biochemistry* **29,** 5647-5659.

Vallee B. L. and Auld D. S. (1990) Active-site zinc ligands and activated H2O of zinc enzymes. *Proc Natl Acad Sci U S A* **87,** 220-224.

Vazeux G., Wang J., Corvol P. and Llorens-Cortes C. (1996) Identification of glutamate residues essential for catalytic activity and zinc coordination in aminopeptidase A. *J Biol Chem* **271,** 9069-9074.

Wouters M. A. and Husain A. (2001) Changes in zinc ligation promote remodeling of the active site in the zinc hydrolase superfamily. *J Mol Biol* **314,** 1191-1207.

Yalcinkaya C., Benbir G., Salomons G. S., Karaarslan E., Rolland M. O., Jakobs C. and van der Knaap M. S. (2005) Atypical MRI findings in Canavan disease: a patient with a mild course. *Neuropediatrics* **36,** 336-339.

Zafeiriou D. I., Kleijer W. J., Maroupoulos G., Anastasiou A. L., Augoustidou-Savvopoulou P., Papadopoulou F., Kontopoulos E. E., Fagan E. and Payne S. (1999) Protracted course of N-acetylaspartic aciduria in two non-Jewish siblings: identical clinical and magnetic resonance imaging findings. *Brain Dev* **21,** 205-208.

Zelnik N., Luder A. S., Elpeleg O. N., Gross-Tsur V., Amir N., Hemli J. A., Fattal A. and Harel S. (1993) Protracted clinical course for patients with Canavan disease. *Dev Med Child Neurol* **35,** 355-358.

Zeng B. J., Pastores G. M., Leone P., Raghavan S., Wang Z. H., Ribeiro L. A., Torres P., Ong E. and Kolodny E. H. (2006) Mutation analysis of the aspartoacylase gene in non-Jewish patients with Canavan disease. *Adv Exp Med Biol* **576,** 165-173; discussion 361-163.

Zeng B. J., Wang Z. H., Ribeiro L. A., Leone P., De Gasperi R., Kim S. J., Raghavan S., Ong E., Pastores G. M. and Kolodny E. H. (2002) Identification and characterization of novel mutations of the aspartoacylase gene in non-Jewish patients with Canavan disease. *J Inherit Metab Dis* **25,** 557-570.

Table 1. Table of forward primers used for site-directed mutagenesis of hASPA cDNA.

Amino Acid	Base Pair	Forward Mutagenic Primer
H21E / E24H	CAT61GAG, GAG70CAC	5' GCTATCTTTGGAGGAACCGAGGGGAATCACCTAACCGG 3'
H21G	CA61GG	5' CTATCTTTGGAGGAACCGGTGGGAATGAGCTAACCG 3'
H21P	A62C	5' CTATCTTTGGAGGAACCCCTGGGAATGAGCTAACCG 3'
E24D	G72C	5' GGAACCCATGGGAATGACCTAACCGGAGTATTTC 3'
E24G	A71G	5' GGAACCCATGGGAATGGGCTAACCGGAGTATTTC 3'
E24H	GAG70CAC	5' GGAGGAACCCATGGGAATCACCTAACCGGAGTATTTCTGG 3'
A57T	G169A	5' CATTTATTACTAACCCCAGAACAGTGAAGAAGTGTACCAG 3'
C61A	TG181GC	5' CCCAGAGCAGTGAAGAAGGCTACCAGATATATTGACTG 3'
C61S	T181A	5' CCCAGAGCAGTGAAGAAGAGTACCAGATATATTGACTG 3'
C61W	T183G	5' CAGAGCAGTGAAGAAGTGGACCAGATATATTGACTGTG 3'
R63N	GA188AC	5' GAGCAGTGAAGAAGTGTACCAACTATATTGACTGTGACCTG 3'
D68A	A203C	5' CCAGATATATTGACTGTGCCCTGAATCGCATTTTTGAC 3'
R71N	CG211AA	5' CCAGATATATTGACTGTGACCTGAATAACATTTTTGACCTTGAAAATCTTGGC 3'
H116E	CAC346GAG	5' CTATGACATTATTTTTGACCTTGAGAACACCACCTCTAACATGGGGTG 3'
H116G	CA346GG	5' CTATGACATTATTTTTGACCTTGGCAACACCACCTCTAACATGGG 3'
C124A	TG370GC	5' CCACCTCTAACATGGGGGCCACTCTTATTCTTGAGG 3'
I143T	T428C	5' CTTTTTAATTCAGATGTTTCATTACACTAAGACTTCTCTGGCTCCACTACCC 3'
C152A	TG454GC	5' CTCTGGCTCCACTACCCGCCTACGTTTATCTGATTG 3'
C152W	C456G	5' CTGGCTCCACTACCCTGGTACGTTTATCTGATTG 3'
E178A	A533C	5' GTATCCTGTGGGTATAGCAGTTGGTCCTCAGCCTC 3'
P183H	C548A	5' GAAGTTGGTCCTCAGCATCAAGGGGTTCTGAG 3'
M195R	T584G	5' GAGAGCTGATATCTTGGATCAAAGGAGAAAATGATTAAACATGCTC 3'
D204H	G610C	5' CAAATGAGAAAAATGATTAAACATGCTCTTCATTTTATACATCATTTCAATGAAGGAAAAG 3'
K213E	A637G	5' CATCATTTCAATGAAGGAGAAGAATTTCCTCCCTGCGC 3'
E214X	G640T	5' CATTTCAATGAAGGAAAATAATTTCCTCCCTGCGCC 3'
D249V	A746T	5' CCATCCTAATCTGCAGGTTCAAGACTGGAAACCAC 3'
G274R	G820A	5' GACGATCCCACTGGGCAGAGACTGTACCGTGTAC 3'
E285A	A854C	5' GTACCCCGTGTTTGTGAATGCGGCCGCATATTACGAAAAG 3'
F295S	T884C	5' CATATTACGAAAAGAAAGAAGCTTCTGCAAAGACAACTAAACTAACGC 3'
A305E	C914A	5' CTAAACTAACGCTCAATGAAAAAAGTATTCGCTGCTG 3'

Table 2. Summary table of CD missense mutations analyzed in this report.

DNA Mutation	Protein Mutation	Relative ASPA Activity	Ethnicity	Citations
A62C	H21P	Untested	Dutch	(Sistermans et al. 2000)
A71G	E24G	Undetectable	German	(Zeng et al. 2002)
G169A	A57T	Untested	German	(Sistermans et al. 2000)
A203C	D68A	Undetectable	British	(Zeng et al. 2002)
T428C	I143T	Untested	Japanese	(Kobayashi et al. 1998)
C456G	C152W	Undetectable	Yemenite	(Zeng et al. 2002)
C548A	P183H	Untested	French	(Elpeleg and Shaag 1999)
T584G	M195R	Untested	Algerian	(Elpeleg and Shaag 1999)
A637G	K213E	Untested	Greek	(Tacke et al. 2005)
A746T	D249V	Undetectable	British, Norwegian, Swedish	(Olsen et al. 2002; Zeng et al. 2002)
G820A	G274R	Untested	Turkish, Greek	(Shaag et al. 1995; Elpeleg and Shaag 1999; Tacke et al. 2005)
A854C	E285A	2.5%	Ashkenazi Jewish	(Kaul et al. 1993; Kaul et al. 1994; Kaul et al. 1996; Zeng et al. 2002; Zeng et al. 2006)
T884C	F295S	Untested	Greek, Turkish	(Shaag et al. 1995; Elpeleg and Shaag 1999; Tacke et al. 2005)
C914A	A305E	Undetectable	Pan-European	(Kaul et al. 1994; Shaag et al. 1995; Kaul et al. 1996; Elpeleg and Shaag 1999; Zeng et al. 2002; Yalcinkaya et al. 2005; Janson et al. 2006; Zeng et al. 2006)

While CD predominantly afflicts Ashkenazi Jews through 3 possible mutations, including the E285A missense mutation, it has been increasingly detected in a wide variety of ethnicities. In these cases, the mutations are highly variable and span the entire ASPA gene (http://www.hgmd.cf.ac.uk/ac/gene.php?gene=ASPA). ASPA activities relative to WT enzyme for CD mutations that have been previously recreated *in vitro* are listed.

FIGURE LEGENDS

Fig. 1. **Sequence alignment between ACY2_Human (ASPA) and bovine zinc-dependent carboxypeptidase (PDB structure 8CPA).** The numbers indicated in parenthesis for the ASPA gene begin with the glutamine residue that aligns with proline 60 of 8CPA. The conserved residues that are possibly involved in a zinc-dependent catalytic mechanism for ASPA are shown white in black boxes with the putative zinc ligands highlighted by asterisks. There is a break in the polypeptide for 8CPA for the following sequences: ENLD, GFWR, RSVG, and KNH-.

Fig. 2. **Partial 3D homology model of ASPA based on crystal structures of bovine ZnCPA.** Some of the loops are shown for clarity. The residues of interest in this report are depicted as ball-and-stick. A single zinc atom has been placed in the active site as a cyan sphere.

Fig. 3. **Comparison of reactions and active sites of ASPA and bovine ZnCPA.** *A,* Chemical reactions catalyzed by ASPA and ZnCPA. The arrows point to hydrolyzed peptide bonds. *B,* Superposition of critical active site residues between ASPA and 8CPA. The ASPA residues are depicted in atom color-coded ball-and-stick. The bovine ZnCPA residues are overlayed in thick yellow lines. Labeling corresponds to ZnCPA numbering.

Fig. 4. **Mutational analysis of ASPA residues that align with those involved in bovine ZnCPA's catalytic mechanism.** Whole cell extracts prepared from COS-7 cells transiently transfected with the indicated constructs were analyzed by immunoblotting

and radiometric ASPA assay (see Materials and Methods). The enzyme activities are presented as mean +/- SEM for triplicate transfections. *A,* Western blot analysis using pepASPA and α-βT. *B,* Each putative catalytic mutation resulted in undetectable ASPA activity relative to WT. *C,* Changing the order of the putative Zn-binding ligands results in undetectable ASPA activity.

Fig. 5. **Cysteine mutational analysis indicates a possible disulfide bond in hASPA.** Whole cell extracts prepared from COS-7 cells transiently transfected with the indicated constructs were analyzed by immunoblotting and radiometric ASPA assay (see Materials and Methods). The enzyme activities are presented as mean +/- SEM for six transfections. *A*, Western blot analysis using pepASPA and α-βT. *B*, Expression of C61A and C61S resulted in WT ASPA activity, expression of C124A and C152A resulted in statistically significantly reduced activity levels relative to WT (*; $p < 0.05$), and expression of C61W and C152W resulted in undetectable activity.

Fig. 6. **CD mutations give insight into hASPA structure.** Whole cell extracts prepared from COS-7 cells transiently transfected with the indicated constructs were analyzed by immunoblotting and radiometric ASPA assay (see Materials and Methods). The enzyme activities are presented as mean +/- SEM for triplicate transfections. *ND*, No DNA mock transfection. *WT*, wild-type hASPA. *A,* Analysis of select previously *in vitro* tested CD mutations. *Top panel:* RT-PCR confirmed that each mutant construct was expressed comparably to WT hASPA. *Middle panel:* Western blot analysis using a polyclonal peptide antibody (pepASPA) and β-tubulin loading control (α-βT). The ASPA band is

38kDa and the beta-tubulin band is 50kDa. *Bottom panel: In vitro* expression of each CD mutant resulted in undetectable ASPA activity compared to WT. *B,* Analysis of select previously *in vitro* untested CD mutations. *Top panel:* RT-PCR confirmed that each construct was expressed comparably to WT. *Middle panel:* Western blot analysis using pepASPA and α-βT. *Bottom panel:* Each mutant resulted in undetectable activity, with the following exceptions: WT activity for K213E and ~5% residual activity for G274R. *C,* Analysis of a case report of clinically mild CD. *Top panel:* Western blot analysis using pepASPA and α-βT. K213E/G274R is a double mutant expressed from a single plasmid (see Materials and Methods). *Bottom panel:* Expression of both G274R and the K213E/G274R double mutant in this set of triplicate transfections resulted in undetectable ASPA activity compared to WT and K213E.

Fig. 7. **Proposed catalytic mechanism for NAA hydrolysis by ASPA.** *A*, NAA binding. *B*, Nucleophilic attack. *C*, Transition-state intermediate. *D*, Product formation

FIGURE 1

```
                          *   *
ACY2-Human  (12) MTSCHIAEEHIQKVAIFGGTHGNELTGVFLVKHWLENGAEIQRTGLEVKPFITNPRAVKKCTRYIDCDLN
8cpa        (60) -----------PAIWIDLGIHSREWITQATGVWFAKKFTENLDSMDIFLEIVTNPNGFWRKTRSVGVDAN

                                                            *
ACY2-Human  (71) RIFDLENLGKKMSEDLPYEVRRAQEINHLFGPKDSEDSYDIIFDLHNTTSNMGCTLILEDSRNNFLIQMF
8cpa       (145) RNWDAGFG--GKYANSEVEVKSIVDFVKNH-------NFKAFLSIHSY---SQLLLYPYGY----QVAKS

ACY2-Human (141) HYIKTSLAPLPCYVYLIEHPSLKYATTRSIAKYPVGIEVGPQPQGVLRADILDQMRKMIKHALDFIHHFN
8cpa       (221) AVAALGTSYKYGSIIQASGGSIDWSYNQGI-KYSFTFELRDLPASQII-PTAQETWLGVLTIMEH
```

119
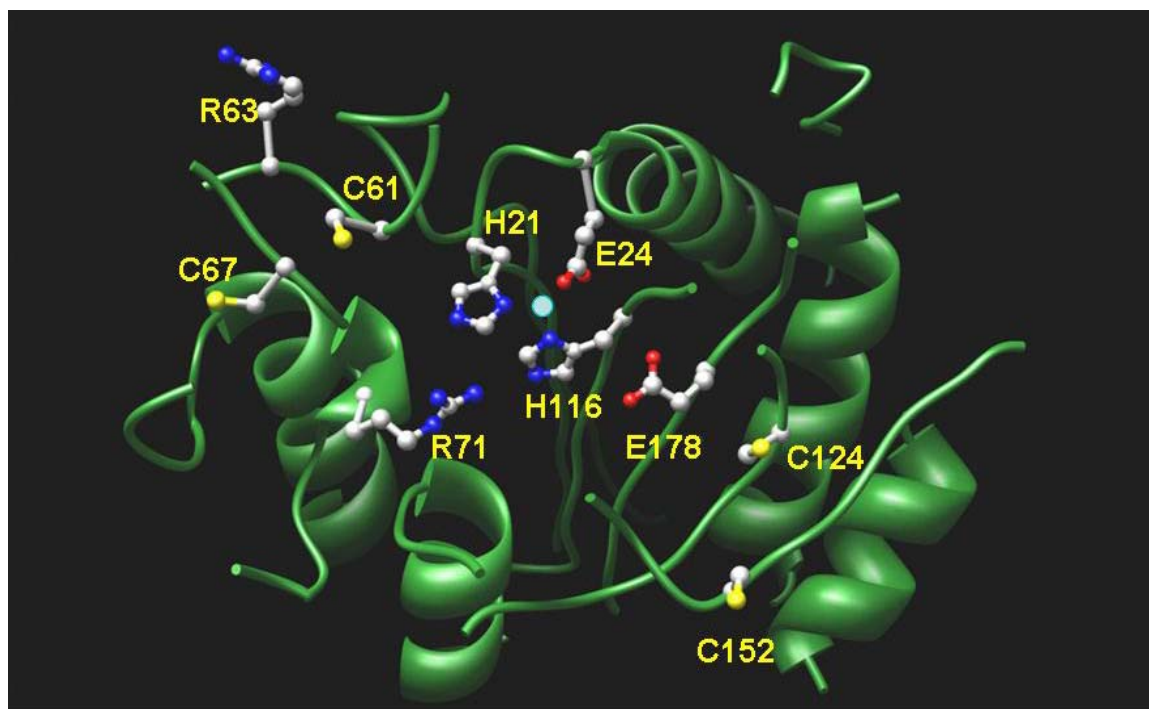
FIGURE 2

FIGURE 3

A

B

FIGURE 4

A

B

C

122
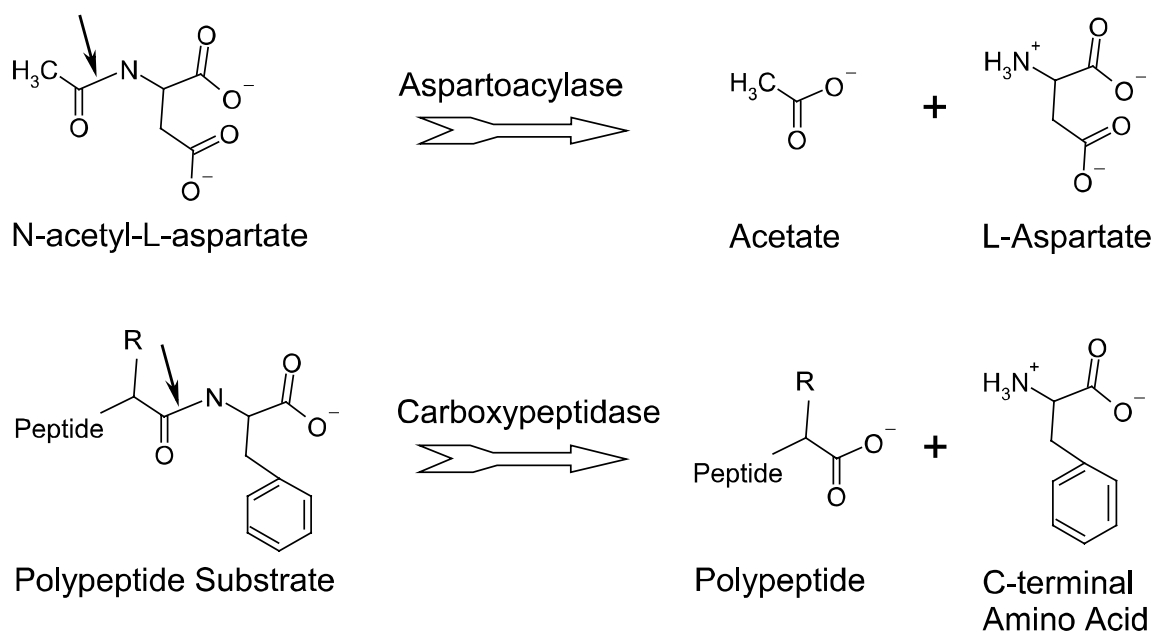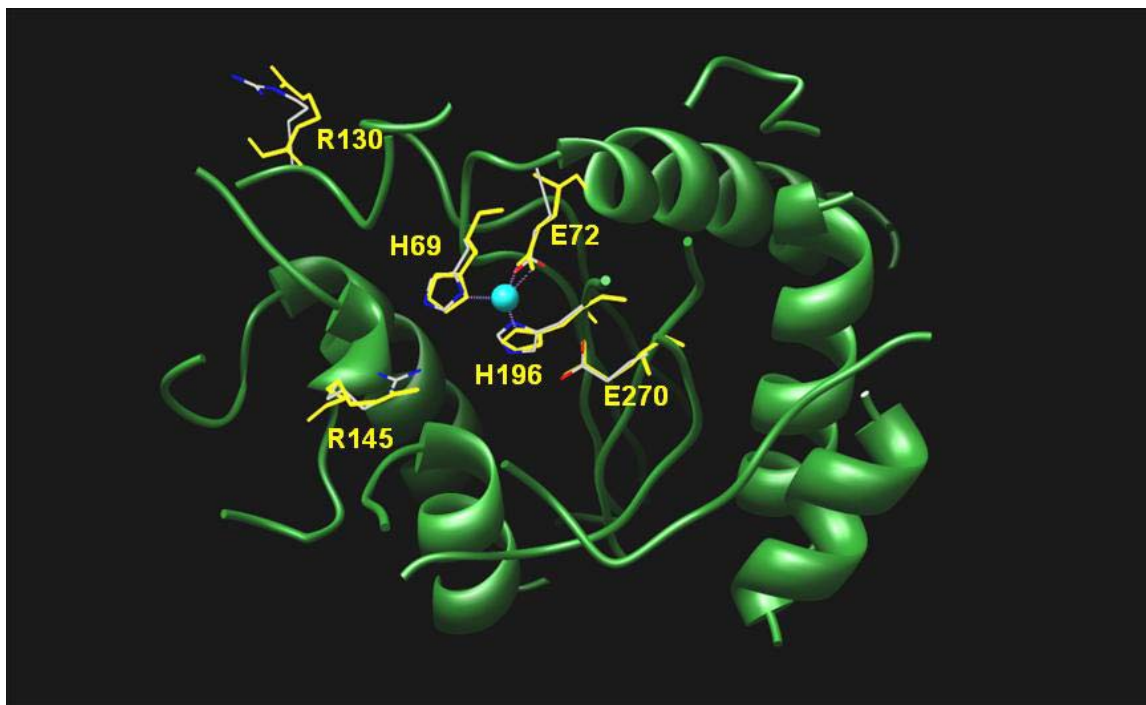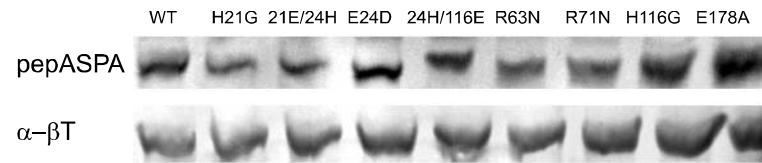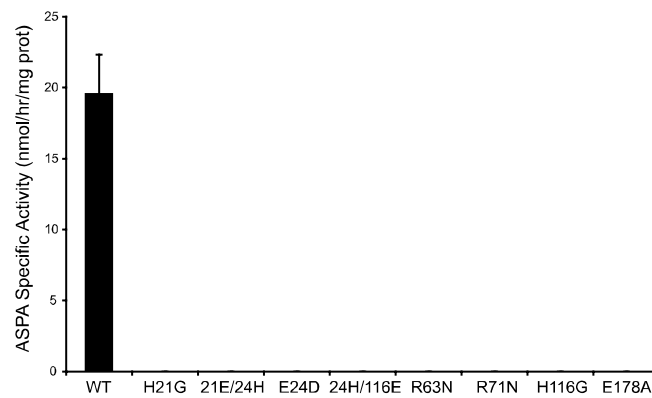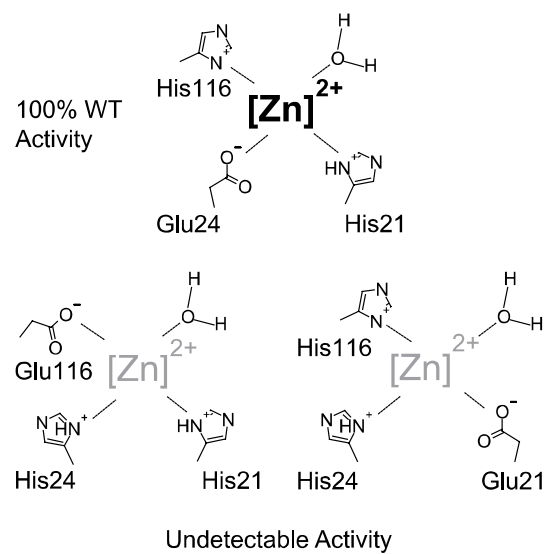
FIGURE 5

A
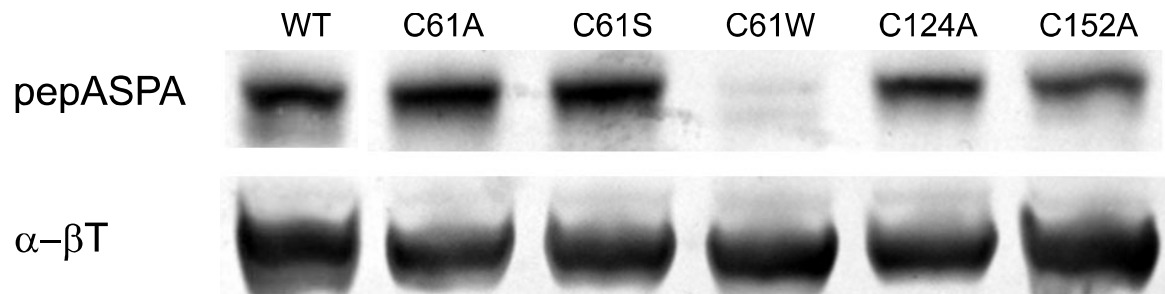
B
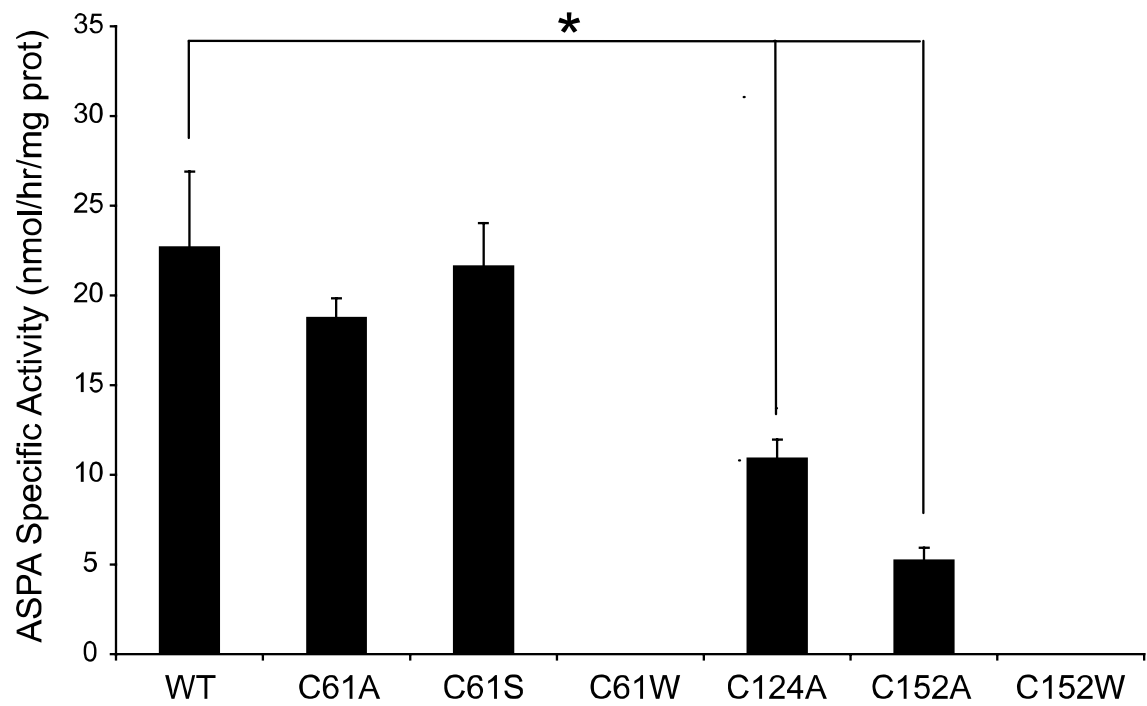
FIGURE 6

A

B

C
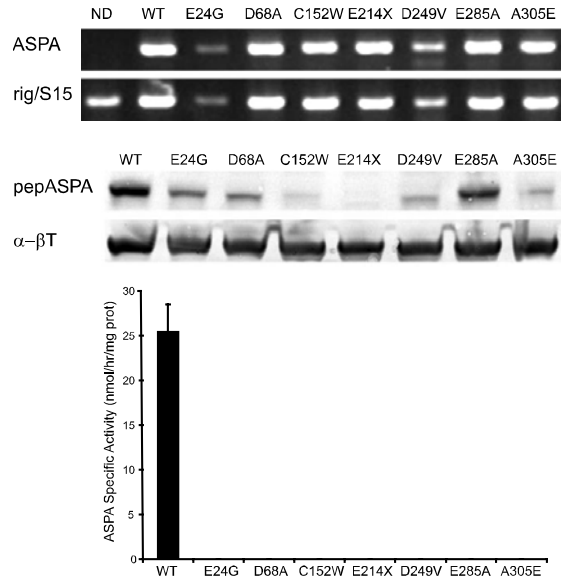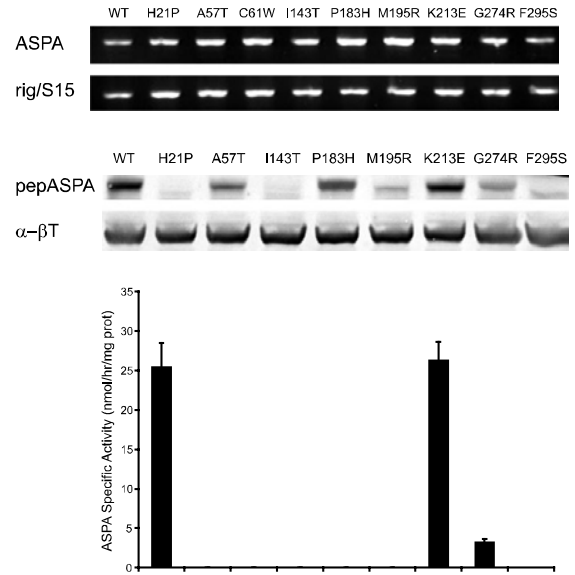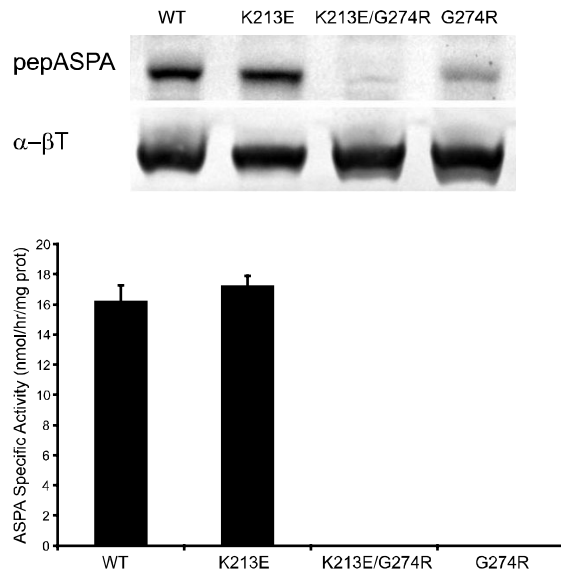
FIGURE 7

CHAPTER 4

Discussion
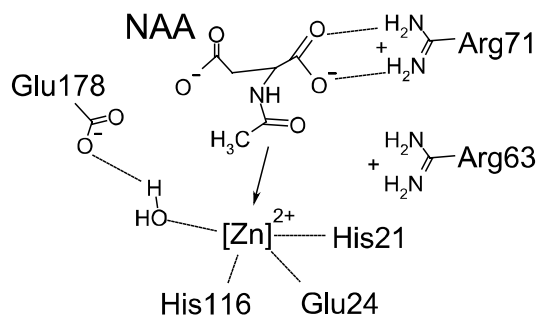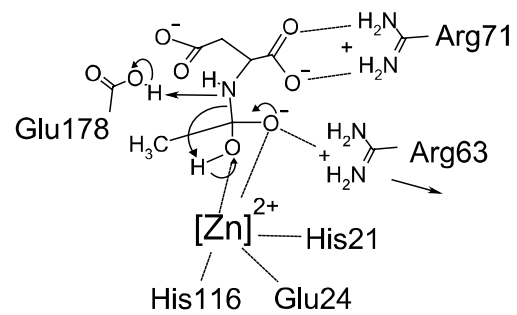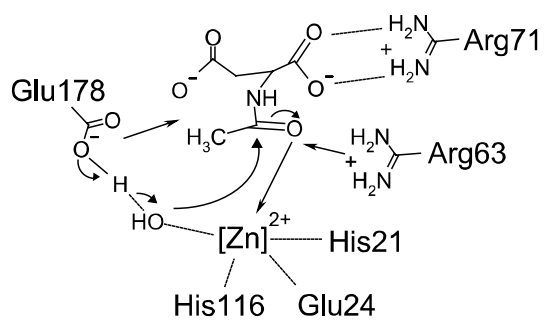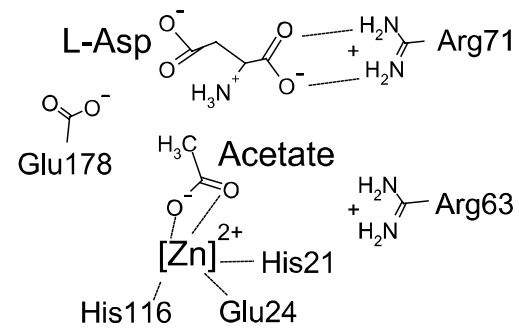
Summary of Findings

CD, which is also known as spongy degeneration of the CNS, is a fatal neurodegenerative autosomal recessive disorder that is correlated with defects in the ASPA enzyme, which catalyzes the deacetylation of NAA to generate acetate and aspartate (1, 2). Although the biochemical link between CD and ASPA deficiency is well-established (2-4), much work needs to be done in order to elucidate the physiological role of ASPA and its role in CD etiology. Even though purified ASPA protein has been well-characterized (5-9), there is limited evidence to support regulation of the ASPA protein.

The goal of this dissertation was to show how regulation of the ASPA enzyme by its localization, multimeric state, and structure help to elucidate its roles in the normal phsyiology and etiology of CD.

The ASPA protein is likely regulated by its localization within tissues and within cells. Several studies have shown that the ASPA reaction is localized to OLs within the CNS (10-13), but the basis of this restriction is unknown. In this dissertation, the OL-specific localization of ASPA was confirmed using immunohistochemistry of cultured rodent OLs and rat brain slices. The high abundance of ASPA in the kidney makes this an important model for characterizing ASPA, for studying its enzymatic functions, and for elucidating the possible functions of ASPA outside the CNS. Here,

immunohistochemistry, immunoblotting, and activity analysis were used to confirm that ASPA is very abundant in the kidney and that it is much more active there than in the CNS. These techniques were also used to describe the localization of ASPA within specific kidney cells.

More so than its cellular localization, the subcellular localization of the ASPA enzyme has remained unclear. Previous activity analyses had shown that ASPA is strictly cytoplasmic (14) or partially membrane-bound (6, 15). In this dissertation, the combination of *in vitro* and *in vivo* immunohistochemical staining with *in vitro* subcellular fractionation and subsequent immunoblotting and activity analysis were used to demonstrate that the ASPA enzyme can be found as predominantly cytoplasmic, nuclear-cytoplasmic, or predominantly nuclear. In addition, fluorescence microscopy analysis of a 69 kDa N-terminal green fluorescent protein-human ASPA fusion protein (GFP-hASPA) provided evidence that the subcellular localization of ASPA is regulated.

It is possible that the subcellular localization of the ASPA enzyme is regulated by its multimeric state. While there is some evidence to suggest that ASPA exists as a dimer (7, 8, 10), it is unknown whether it is active as a dimer. In this dissertation, we provided evidence that rat kidney ASPA is active as a monomer in both sucrose density gradient-purified nuclear fractions and in cytoplasmic subcellular fractions. Strong immuno-histochemical staining for ASPA was detected within rat kidney nuclei *in situ*, but weak immunoblotting staining and low ASPA activity were detected within rat kidney nuclear fractions. These findings suggest dimerization might play a role in sequestering the ASPA enzyme within the nucleus.

127

While much research has focused on treating CD-associated ASPA deficiency, efforts to elucidate the molecular basis of the disease have been scarce. Although ASPA had consistently been referred to as a serine hydrolase of the α/β-hydrolase superfamily of enzymes (16-18), an alignment study suggested that ASPA is functionally and structurally similar to the CPA enzyme family (19). To test this hypothesis, we generated and analyzed a homology model for ASPA based on CPA and showed that several active site residues are functionally conserved between ASPA and CPA. Moreover, the ASPA deficiency inherent to CD appears to result from mutations in the ASPA gene that either disrupt catalysis or protein integrity. Finally, the phenotypical outcome of CD does not appear to correlate with specific ASPA mutation types.

Regulation of the ASPA Enzyme by Localization

ASPA in the Kidney

Before using the kidney as a model system to analyze various biochemical properties of ASPA in subcellular fractions, we investigated the localization of the ASPA enzyme in the kidney, the tissue from which it was initially purified and in which ASPA is highly abundant (14, 15).

Although ASPA is more abundant and more active against NAA in the kidney than in the CNS (14, 17), it is thought to have a scavenging function outside of the CNS (17). Kidney ASPA might catalyze a reaction other than NAA hydrolysis because NAA substrate is virtually undetectable within the kidney (20-22) and because it is an efficient

use of metabolic energy to express and translate an enzyme without a function. Within the kidney, ASPA was selectively localized to the cortex, where it was strongly expressed only in the proximal tubule cells (Manuscript 1, Figure 4). This localization is similar to that of aminoacylases I and III, which serve crucial functions for removing xenobiotics and recycling other acetylated amino acids in the kidney (23, 24). Therefore, a possible function of ASPA in these kidney regions is the retention of amino acids.

One way to evaluate the role of ASPA in the kidney and in other peripheral tissues is through the creation and analysis of aminoacylases I and III knockout mice. In CD patients, dysfunctional ASPA in the proximal tubules of the kidney might result in an impaired ability to deacetylate NAA that is retained from circulation. This would explain why NAA accumulates in the urine of CD patients. Curiously, kidney pathology is rarely reported in CD patients (3, 25). The activities of aminoacylases I and III might compensate for the loss of functional ASPA in the kidney (5, 23). Therefore, analysis of acetylated amino acids and ASPA activity in aminoacylase I and III knockout mice would help clarify the function of kidney ASPA

The investigation of ASPA protein regulation by localization within the kidney provides a basis for investigating the ASPA enzyme in other peripheral tissues where it is highly abundant, such as the skeletal muscle (26). It is unclear whether muscle deterioration in CD is a secondary result of dysfunctional ASPA in peripheral tissues (27) or a tertiary result of the breakdown of the entire motor nervous system due to rampant dysmyelination and brain vacuolization. Future studies could focus on the cellular and subcellular localizations, as well as the substrate specificity, of ASPA in these peripheral

tissues in order to gain more insight into the etiology of CD.
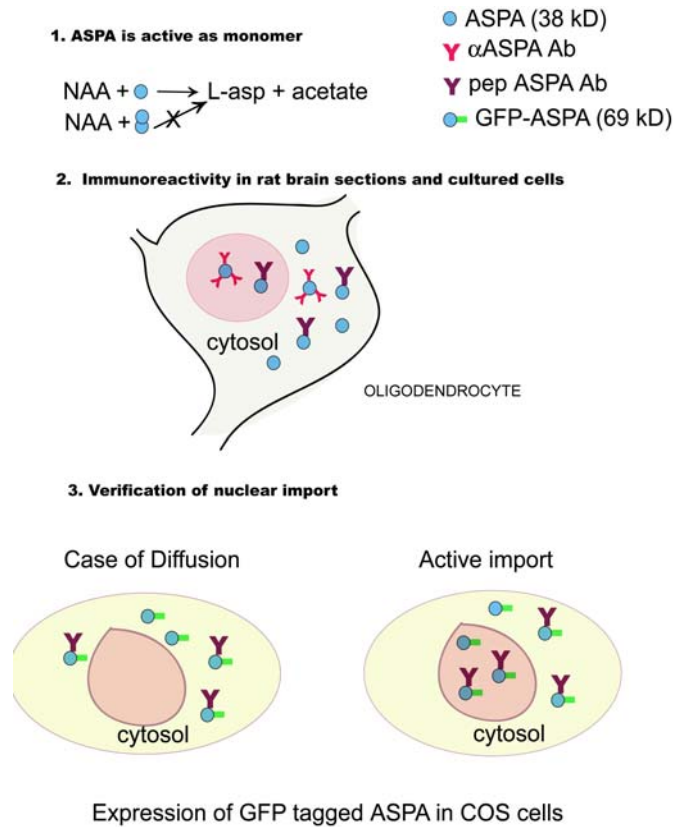
Figure 1. Subcellular localization and multimeric state of ASPA.

ASPA Is a Nuclear-Cytoplasmic Enzyme

This dissertation in part aimed to elucidate the *in vivo* subcellular localization of ASPA, a novel means for regulating the ASPA enzyme. Previous studies had shown that ASPA is located mostly in the cytoplasm (14) and is partially bound to a membrane (6, 15, 28). However, these studies only followed ASPA activity; detailed antibody-based experiments were needed to clarify where ASPA resides within cells.

Using several techniques (Figure 1), we have confirmed a recent observation that ASPA is found throughout OLs in both the cytoplasm and the nucleus (12). In cultured primary rat and mouse OLs, *in vitro* staining for ASPA using indirect immunofluorescence with newly generated polyclonal antibodies against a conserved ASPA peptide (pepASPA) and against full-length recombinant murine ASPA (αASPA) was counter-stained with a nuclear stain, DAPI (Manuscript 1, Figure 1). The αASPA antibody had been previously used in immunohistochemistry and immunoblotting (12). The pepASPA antibody was useful because it minimizes epitope sites (Figure 1) and because it is less cross-reactive than αASPA in immunoblotting (Manuscript 1, Figure 5). While ASPA has been shown to be glycosylated at Asn117 (7), which suggests that ASPA is processed in the lumen of the endoplasmic reticulum (ER), we did not co-stain for ER markers to distinguish between staining for ASPA within the nucleus versus the ER, which is contiguous with the nuclear membrane.

The results of *in vitro* staining with two antibodies did not rule out the possibility that ASPA co-localized with DAPI due to cytoplasmic overlay or due to cross-reactivity with a different nuclear antigen. To confirm that *in vitro* ASPA nuclear staining did not reflect cytoplasmic overlay, *in vivo* analysis using a confocal microscopy Z-series that captured multiple depths of a rat brain section showed staining for ASPA that counter-stained with DAPI in the same longitude planes (Manuscript 1, Figure 2). In addition, this analysis showed that ASPA is found in three distinct configurations within OLs: predominantly nuclear, nuclear-cytoplasmic, and predominantly cytoplasmic (Manuscript 1, Figure 2). To demonstrate that nuclear staining was specific for ASPA protein, *Tremor* rat tissues were utilized as an ASPA null control. There was no detectable

staining for ASPA protein using immunohistochemistry of *Tremor* rat versus WT rat brain slices (Manuscript 1, Figure 3).

Investigations of ASPA protein regulation by a nuclear-cytoplasmic localization were extended to rat brain and kidney subcellular fractions. There was strong ASPA staining in the nuclei of kidney proximal tubule cells, which suggests that ASPA has a nuclear-cytoplasmic localization in the kidney (Manuscript 1, Figure 4). In previous fractionation studies, ASPA activity was enhanced in cytoplasm (14) and membrane fractions (28). Using a highly sensitive radiometric ASPA assay (29), we showed that the percentage of ASPA activity in the sucrose density gradient-purified nuclear fraction relative to ASPA activity in the cytoplasmic fraction was ~3% in kidney extracts (120 nmol/h/mg protein in cytoplasmic versus 3.3 nmol/h/mg protein in nuclear) and ~6% in brain extracts (20 nmol/h/mg protein in cytoplasmic versus 1.2 nmol/h/mg protein in nuclear) (Manuscript 1, Figure 5). Immunoblotting with both αASPA and pepASPA antibodies detected ASPA protein in nuclear fractions at a lower level than in cytoplasmic fractions (Manuscript 1, Figure 5). No cross-reactive bands were detected in the nuclear fraction, which further suggests that staining for ASPA in the nucleus was not the result of cytoplasmic contamination.

The confirmed nuclear-cytoplasmic localization of the ASPA protein provides insight into regulation of the ASPA reaction by its location within cells. It is well known that the ASPA reaction is regulated at the cellular level within the CNS and that the cytoplasmic role of the ASPA enzyme is to provide acetyl groups for fatty acid synthesis during myelination (11, 30, 31). In this dissertation, there was reduced ASPA activity

against NAA in nuclear fractions, suggesting that a possible function of nuclear ASPA is sequestration via compartmentalization. As further support for the possibility that ASPA's subcellular localization is regulated during OL development and / or myelination, staining for nuclear ASPA was found in a subpopulation of predominantly immature cultured OLs (Manuscript 1, Figure 1). Future antibody-based studies could analyze ASPA expression within OLs during rodent development, addressing whether nuclear ASPA follows the same expression pattern as cytoplasmic ASPA and whether pools of ASPA protein are sequestered in the nucleus in order to regulate the use of free acetyl groups for myelin lipid synthesis. In parallel, *in vitro* studies to determine ASPA's subcellular localization could involve co-culturing OLs with neurons in order to recreate the communication that occurs between cell types before and during myelination.

Regulation of the ASPA reaction by its subcellular localization also raises the possibility that nuclear ASPA is modified in such a way as to lose specificity for NAA and acquire specificity against other *N*-acetylated amino acid substrates. Moreover, nuclear ASPA might be active against *N*-acetylated proteins such as actin, which is also found in the nucleus (34) and has an acetylated aspartate as its N-terminal residue (32, 33). Two experimental observations support this hypothesis. First, the analysis of anion-exchange chromatography of rat kidney extracts showed that nuclear ASPA displays different ionic behavior than cytoplasmic ASPA (Manuscript 1, Figure 6). This difference might be attributable to a post-translational modification of ASPA in one fraction, but not the other. The ASPA enzyme has recently been shown to be glycosylated at Asn117 (7), so this modification might explain different ionic behaviors of ASPA in the nucleus versus the cytoplasm. Second, ASPA activity against NAA was

relatively low in nuclear extracts, while ASPA immunoreactivity was generally strong in the nuclei of rat kidneys and OLs. This suggests that ASPA might be modified in such a way as to alter antibody reactivity in the cytoplasm versus the nucleus. It has been suggested that recombinant ASPA is partially active against *N*-acetyl-L-asparagine (8). Therefore, future studies could use amino acid analysis of enzyme assays with partially purified ASPA from rat kidney extracts to explore whether nuclear ASPA is active against other *N*-acetylated amino acids.

Nuclear Import of ASPA Protein

In addition to demonstrating that the ASPA enzyme is regulated by its subcellular localization in the brain and the kidney, we determined whether ASPA can be actively imported into the nucleus. Because ASPA is small enough to passively diffuse through the 40-60 kDa size cutoff of the nuclear pore complex (NPC), we generated and analyzed GFP-hASPA, a 69 kDa fusion protein (Figure 1). The distribution of transiently transfected GFP-hASPA in formalin-fixed COS-7 cells was 22.6% predominantly nuclear, 41.5% nuclear-cytoplasmic, and 35.8% predominantly cytoplasmic (Manuscript 1, Figure 9).

Future studies are necessary to support our assertion that ASPA can be actively imported into the nucleus. First, the localization of a larger fusion protein (i.e., β-galactosidase fused to the ASPA protein) should be investigated because it is possible that 69 kDa proteins might be able to passively diffuse through the NPC. Second, an *in vitro* assay using wheat germ agglutin, which by binding to *O*-glycosylated nucleoporins blocks the active nuclear import of proteins through the NPC (35), and digitonin, which is

a detergent that lyses the plasma membrane and leaves the nuclear envelope intact (36), could further assess whether ASPA can be actively imported into the nucleus. In addition, the localization of GFP-hASPA and other fusion proteins should be investigated in primary OLs or immortalized OL cell lines in order to understand the physiological importance of ASPA's subcellular localization. One cell line that is commonly used to study OL biology is the spontaneously immortalized, non-transformed Central Glia-4 cell line (37). Primary culture comparisons have established how this cell line accurately recreates natural conditions (38-44). Since ASPA activity has been detected in the Central Glia-4 cell line (29), determining the subcellular localization of an ASPA fusion protein would depend on detection of the fused element (i.e., GFP fluorescence or β-galactosidase activity).

In this dissertation, the biochemical and molecular mechanisms of putative ASPA nuclear import were not investigated. Traditional protein nuclear import relies on a classical nuclear localization signal (NLS; based on the SV40 large T antigen), the critical lysine residues of which facilitate binding of the transported protein to importin α and importin β for movement through the NPC (45, 46). Although online computer prediction programs do not identify a classical NLS in ASPA protein, there are several poorly characterized NLSs that have been shown to assist in nuclear targeting (47). After failing to find a putative or functional NLS, visual inspection has identified a non-classical C-terminal bipartite NLS in other proteins (48).

A search of ASPA's primary amino acid sequence for clusters of conserved basic amino acids identified a conserved KKEAFAKTTK C-terminal sequence. This putative

NLS loosely resembles a functional non-classical NLS, PAAKRVKLD (49), and is a condensed version of a non-classical bipartite NLS that is found in SIM1 and SIM2 proteins (50). Monitoring the fluorescence of GFP fusion proteins, in which the basic residues of a putative NLS have been mutated to neutral residues, is a common way to assess the functionality of an NLS (48, 50-56). Therefore, a future study could analyze the effects of single and double lysine mutations on the subcellular localization of GFP-hASPA. Alternatively, a mutagenic approach using yeast expression and DNA sequencing of mutants that have lost nuclear localization could identify regions of the ASPA protein that are critical for nuclear import, assuming ASPA is targeted to the nucleus in yeast.

While it is beneficial to investigate whether ASPA possesses a functional NLS, some proteins do not require an NLS for entry into the nucleus, because they enter the nucleus via interactions with other proteins that have an NLS (57). Therefore, future studies could use yeast two-hybrid screens to identify proteins that bind to ASPA and subsequently analyze the ability of an ASPA-binding protein to actively enter the nucleus. Epitope masking, glycosylation and phosphorylation are other ways for proteins that lack an NLS to enter the nucleus (58). Maximum ASPA stability and activity require glycosylation at Asn117 (7), so analysis of an Asn117 mutant might elucidate whether this post-translational modification affects the subcellular localization of ASPA. In this dissertation, nuclear ASPA displayed less affinity toward positively charged column resins than cytoplasmic ASPA, which suggests there are differential post-translational modifications between nuclear and cytoplasmic ASPA. Future studies should address whether phosphorylation influences the subcellular localization of ASPA protein.

Regulation of the ASPA Enzyme by Multimerization

In addition to post-translational modification of ASPA, the multimeric state of the enzyme might play a role in regulating its subcellular localization. While the ASPA enzyme can enter the nucleus as a 69 kDa GFP-hASPA fusion protein, it remains possible that the multimeric state of ASPA influences its localization. Specifically, dimerization is a common mechanism for regulating nuclear import of protein, notably of the STAT and BRCA proteins (59, 60). Therefore, we sought to determine whether the multimeric state of ASPA affects its location within subcellular fractions.

There is some controversy as to whether ASPA exists as a monomer or a dimer. Although the predicted size of the ASPA enzyme has been confirmed as 36-38 kDa by SDS-PAGE and immunoblotting (9, 10, 12), reports of its multimeric state have varied. A recent immunoblot analysis using polyclonal antiserum against human ASPA suggested that ASPA exists as both a ~37 kDa monomer and a ~80 kDa covalent dimer (10). In this dissertation, immunoblotting of rat kidney extracts with both αASPA and pepASPA antibodies detected an ASPA monomer band at 38 kDa that was absent from *Tremor* rat extracts (Manuscript 1, Figure 5). In addition, immunoblotting detected the aforementioned putative ASPA dimer band (10) in *Tremor* rat kidney and untransfected COS-7 cell extracts (Manuscripts 1 & 2). Therefore, this ~80 kDa band was more likely the result of cross-reactivity with another antigen, rather than covalent dimerization.

Two recent analyses using mass spectroscopy and dynamic light scattering showed that the majority of purified, recombinant human ASPA from both *E. coli* and *P. pastoris* exists in solution as a dimer (7, 8). While the latter study demonstrated that the kinetics of purified ASPA are sigmoidal with respect to NAA concentration (7), which is characteristic of a multi-subunit enzyme, there was no direct evidence to suggest that ASPA is active as a dimer. The analysis of fractions from HPLC size-exclusion chromatography showed that maximum specific and total ASPA activities from cytoplasmic and nuclear rat kidney extracts correspond to the size of the ASPA monomer (Manuscript 1, Figure 7). Therefore, it is unlikely that activity against NAA in the nuclear fraction was due to an ASPA dimer.

However, there was residual ASPA activity in both cytoplasmic and nuclear extracts that was detected in the dimer range, which suggests that ASPA activity can be regulated by dimerization (Figure 1). A possible explanation for why ASPA staining as detected by immunohistochemistry was much higher than the relative intensity of the ASPA band in nuclear extracts to cytoplasmic extracts is that the majority of nuclear ASPA exists as an inactive dimer. This dimerization might enhance the immunoreactivity for ASPA under the native conditions of immunohistochemistry versus the denaturing conditions of SDS-PAGE and immunoblotting. A future experiment to address this hypothesis could be to transfect COS-7 cells with HA-tagged and untagged ASPA, then immunoprecipitate the HA-tagged enzyme and determine whether the untagged enzyme has co-immunoprecipitated.

Although the ASPA enzyme might be regulated by dimerization, it is possible that

ASPA dimers are an *in vitro* artifact that results from purification conditions and a reported tendency of the ASPA protein to aggregate (7). Size-exclusion chromatography and subsequent enzyme activity analysis of ASPA that has been purified from bacteria or yeast and shown to exist in solution as a dimer (7, 8) would address whether ASPA from an *in vitro* source can function as a dimer. Finally, the ASPA gene could be cloned into a vector to express a dimerization domain at either terminus. If *in vitro* expression of this artificial dimer yielded WT levels of ASPA protein with undetectable activity, it would confirm the hypothesis that dimerization of the protein inactivates the ASPA enzyme. In addition, the subcellular localization of a transiently transfected artificial ASPA dimer could be determined to assess a possible mechanism for regulation of ASPA's subcellular localization by its multimeric state.

Regulation of the ASPA Enzyme by Structure

ASPA Is a CPA Family Member

The possibility of ASPA activity regulation by multimerization raises the question of the method by which the structure of individual ASPA monomers facilitates the catalysis of NAA hydrolysis. The ASPA enzyme had been referred to as a member of the serine hydrolase superfamily (17) until an alignment study indicated that its structure is similar to that of CPA (19). This guidance was used to generate an active site homology model for ASPA based on its homology to CPA (Manuscript 2, Figures 2 & 3). During the course of this dissertation, the hypothesis that ASPA binds a single zinc atom that is

139

essential for catalysis was confirmed (7). Mutations of residues predicted by the homology model to be involved in zinc coordination (His21, Glu24, His116), general proton acceptance / donation (Glu178), substrate carboxyl binding (Arg71), and transition state stabilization (Arg63) resulted in undetectable ASPA activity upon transient transfection in COS-7 cells (Manuscript 2, Figure 4). Furthermore, the data suggested a zinc-dependent catalytic mechanism for the ASPA reaction (Manuscript 2, Figure 7), that is similar to the accepted catalytic mechanism for CPA (Introduction, Figure 6).

	ASPA	CPA
Chemical Reaction	NAA→L-Aspartate + acetate	Polypeptide→ C-terminal amino acid + Polypeptide (n-1)
Critical Location	CNS	Liver
Substrate Size	Very small	Very large
Enzyme Size	313 amino acids	307 amino acids
Molecular Weight	36.5 kDa	34.5 kDa
Catalytic Zinc Atom	Single	Single
Inhibition by Excess Zinc	Yes	Yes
Zinc Ligands	His21, Glu24, His116	His69, Glu72, His169
Catalytic Residue	Glu178	Glu270

Table 1. Comparison of ASPA and CPA characteristics.

In addition to conserved active site and catalytic residues, there are several other similarities between ASPA and CPA (Table 1). Both reactions catalyze the hydrolysis of a peptide bond to yield a free C-terminal amino acid, both enzymes have similar sizes, and both enzymes use a single catalytic zinc atom that inhibits activity when in excess (7, 61, 62). Short of solving ASPA's crystal structure, one possible future experiment could assess the effects of various CPA active site inhibitors on ASPA activity. Small CPA

inhibitors designed to block proton donation by Glu270 (Glu178 in ASPA) or interfere with zinc ligation (63, 64) should also inhibit ASPA activity.

To identify further similarities between ASPA and CPA, another future study could be a more extensive mutational analysis of other amino acid substitutions of the putative catalytic residues analyzed in this dissertation. The study could also analyze other residues conserved between the two enzymes. For example, drastic effects on ASPA activity of conserved His→Lys mutations at residues 21 and 116 would confirm their catalytic importance. Further mutational analysis of Arg63 and Lys60 would also help to resolve which residues are involved in transition state stabilization.

Although they share several characteristics, ASPA and CPA catalyze different physiological reactions. The ASPA enzyme catalyzes the deacetylation of NAA in the CNS, and CPA catalyzes the breakdown of food-derived polypeptides in the liver. It is interesting to speculate as to the structural differences that account for these different substrate specificities. Unlike polypeptide substrates and food proteins of carboxypeptidases (65), NAA is a very small hydrophilic molecule. Therefore, its substrate-binding pocket is probably much smaller than the one in CPA. Several key residues in CPA catalysis, such as Leu202, Gly207, Ile243, Tyr248, Ile255, and Thr268, do not structurally align with ASPA (19, 66). In particular, the role of Tyr248 in enhancing the active site flexibility of CPA in order to bind bulky substrates (66) is probably not required by the ASPA enzyme.

Finally, another difference between ASPA and CPA is that the primary amino acid sequence of ASPA only partially aligns with that of CPA (Manuscript 2, Figure 1).

Our homology model for ASPA does not include the first 60 amino acids of CPA that are believed to stabilize a part of the CPA substrate binding pocket. The C-terminus of ASPA, which does not align well with CPA, might replace this part of CPA and be involved in stabilizing ASPA's substrate binding pocket. Alternatively, this C-terminal region could be involved in regulation of the ASPA enzyme through influencing nuclear localization, dimerization, or both. Future experiments could focus on differentiating between NAA binding and NAA hydrolysis. Various pieces or mutations of the ASPA protein could be incubated with [^{3}H]-NAA at 0^oC, then separated by size-exclusion chromatography. Substrate that has bound enzyme would be easily distinguished from unbound substrate (a size difference of 36 kDa) and monitored by radiolabel counts. The E285A mutation results in dysfunctional ASPA enzyme and shows that the C-terminus is required for catalysis. Therefore, C-terminal truncations of ASPA might bind NAA without catalyzing its hydrolysis.

Zinc-Binding Ligands of ASPA

Several studies suggest that, at the structural level, the ASPA enzyme appears to regulated by zinc (6-8, 19). The data in this dissertation suggest that the zinc-binding ligands in human ASPA are His21, Glu24, and His116. Therefore, future experiments could investigate whether catalytically inactive H21G, E24G, and H116G purified proteins are zinc-deficient. The zinc-binding ligands in various other proteins were identified by showing that the zinc content per mole of purified mutant protein was much lower than WT using flame atomic absorption spectroscopy (67-69). Alternatively, the zinc-binding capability of WT ASPA and various putative zinc ligand mutants could be

assessed by incubating transfected cells in medium containing ^{65}Zn (70). Immunoprecipitated H21G, E24G, and H116G mutant ASPA proteins might have negligible radioactive counts relative to WT ASPA. Finally, the analysis of the E24D mutation in this dissertation suggests that shortening the side chain by a single CH$_2$ bond drastically alters zinc binding and polarization of the zinc-coordinated water molecule for efficient NAA hydrolysis. Highly conserved Glu→Asp mutations have resulted in weakened zinc affinity and a lowered K_M in other zinc metalloenzymes (70, 71). Therefore, future studies could assess the kinetics and zinc content of purified E24D protein to determine whether Asp24 is a weak zinc ligand.

Cys124-Cys152 Disulfide Bond in ASPA

Regulation of the ASPA protein at the structural level also appears to depend on disulfide bonding. Based on how DTT affects ASPA activity (6, 29) and how mutations at Cys152 result in undetectable ASPA activity *in vitro* (72-74), there might be an intramolecular disulfide bond in ASPA that involves Cys152. Our homology model indicated that the Cys124-Cys152 proximal pair is correctly orientated for disulfide bonding (Manuscript 2, Figure 2). Expression of Cys→Ala mutations at residues 124 and 152, respectively, yielded reduced ASPA activity and protein levels relative to WT ASPA (Manuscript 2, Figure 5). These results suggested there is an intramolecular disulfide bond between Cys124 and Cys152 that is required for optimal ASPA activity and stability, though further mutational and biophysical experimentation is required to support this hypothesis. Specifically, the analysis of a Cys124/Cys152 double mutant and the effects of altering the oxidation / reduction environment of the WT and Cys124

and Cys152 mutant ASPA enzyme might clarify the significance of this bond to ASPA structure and function. Furthermore, the use of chemicals that selectively modify sulfhydryl groups that are not in disulfide bonds might also clarify whether there is a Cys124-Cys152 disulfide bond in ASPA.

ASPA Mutations and CD

The regulation of the ASPA enzyme by its localization, multimeric state, and structure helps to elucidate its physiological role. As ASPA deficiency is linked to CD, the analysis of several CD-associated ASPA mutations helps clarify the molecular basis of CD based on their effects on ASPA protein structure and catalysis.

Molecular Basis of CD Based on ASPA Missense Mutations

Although there are 44 known missense / nonsense mutations in the ASPA gene that are correlated with CD (Introduction, Table 3), few of these mutations have been shown to result in reduced ASPA activity upon *in vitro* expression (72-77). Therefore, while CD has been linked to dysfunctional ASPA for almost 20 years (2), the mechanisms through which certain ASPA mutations ablate enzymatic activity are unclear. According to most CD literature, ASPA has three highly conserved putative catalytic cores similar to those conserved among esterases: 18-GGTHGNE-24, 275-DCTV-278, and 283-VNEAAYY-289 (9, 16, 17, 26). Citing this hypothesis, the H21P, E24G, and E285A mutations in the first and third of these proposed regions, respectively, have been suggested to ablate ASPA activity *in vitro* by disrupting a single critical

144

catalytic domain (17, 74, 78).

In contrast, this dissertation elucidated a possible molecular basis for how ASPA deficiency and CD results from missense / nonsense mutations in the ASPA gene by using homology modeling for ASPA based on CPA. We confirmed that the E24G, D68A, C152W, D249V, E285A, and A305E CD-associated ASPA mutations result in undetectable ASPA activity when expressed *in vitro* and showed for the first time that the H21P, A57T, I143T, P183H, M195R, G274R, and F295S mutations result in undetectable ASPA activity when expressed *in vitro* (Manuscript 2, Figure 6). Furthermore, the data distinguished between two types of CD-associated ASPA mutations. Various non-bulky amino acid substitutions (E24G, A57T, D68A, P183H, and E285A) appear to interfere with catalysis, and various non-conserved substitutions (H21P, I143T, C152W, M195R, D249V, F295S, and A305E) appear to interfere with ASPA protein integrity (Manuscript 2, Figure 6).

Specifically, the homology model provides explanations for how individual ASPA missense mutations result in dysfunctional enzyme. The E24G mutation appears to preclude zinc-binding, whereas the A57T and D68A mutations appear to disrupt the substrate binding cavity. Changing Pro183, the equivalent to the site of a type I reverse turn (Pro282) in bovine CPA (19), to His causes a substitution against a bend crucial for local geometry due to a positive charge, which misaligns the putative catalytic residue, Glu178. All other CD-associated ASPA mutations in this dissertation appear to disrupt ASPA protein integrity through the introduction of a turn (H21P), the introduction of a bulky residue (C152W), the loss of a negative charge (D249V), or the disruption of local

145

hydrophobicity (I143T, M195R, G274R and A305E). These mutations might signify critical structural residues by the loss of ASPA protein and activity.

The homology model and putative catalytic mechanism for ASPA offer explanations for how other ASPA missense mutations not investigated in this dissertation might result in non-functional enzyme (Introduction, Table 3 & Figure 4). Mutations affecting residues in close proximity to putative catalytic sites (His21, Glu24, His116, Glu178, Glu285), and residues with side chains that protrude into the active site probably disrupt ASPA catalysis. All of the remaining CD-associated ASPA missense mutations probably destabilize the ASPA enzyme.

Putative Genotype / Phenotype Correlation for CD

The disruption of normal ASPA physiology due to various mutations in the ASPA gene has been shown to correlate with CD (2, 17, 76). Although the typical progression for CD results in childhood mortality (79), there are mild (75, 80-82) and severe (74) progressions that have been linked to specific ASPA missense mutations. While some of these correlations have been discredited by a contradictory disease course resulting from either homozygosity or compound heterozygosity of the same mutation (83), there are a few examples of missense mutations that might contribute specifically to a mild clinical course. Evidence in this dissertation suggests that the K213E mutation, which had been previously implicated in promoting a mild CD phenotype (80), rescues neither ASPA activity nor ASPA protein and does not appear to be a protective mutation (Manuscript 2, Figure 6). However, more *in vivo* analysis is required to support this conclusion. In addition, the Y288C mutation was not investigated. One report concluded from the *in*

146

vitro expression of the Y288C mutation resulting in 100% ASPA activity relative to WT that the Y288C mutation is a benign polymorphism (77). Meanwhile, another report suggested that the Y288C mutation is a protective mutation (80). The homology model does not include the C-terminus of ASPA, so there is no structural explanation for how the Y288C mutation could facilitate a mild clinical phenotype.

Conclusions and Implications

Defects in the ASPA enzyme, which catalyzes the deacetylation of NAA to generate acetate and aspartate, are correlated with CD (1, 2). The goal of this dissertation was to show how regulation of the ASPA enzyme by its localization, multimeric state, and structure help to elucidate its roles in the normal physiology and etiology of CD.

The localization of the ASPA enzyme within OLs of the CNS is consistent with the hypothesis that the function of ASPA in the CNS is to provide acetate for fatty acid synthesis during myelination (31). Meanwhile, the localization of the ASPA enzyme within proximal tubule cells of the kidney suggests that one peripheral function of ASPA might be the retention of amino acids. Alternatively, ASPA might have different substrate specificity in the kidney.

The subcellular localization of the ASPA enzyme appears to be regulated, though future studies are necessary to uncover the mechanism and significance of ASPA nuclear localization. The multimeric state of ASPA might play a role in its subcelllular

localization.   Although the ASPA enzyme appears to be active as a monomer, dimerization might negatively regulate its activity.

As an active monomer, ASPA catalyzes the hydrolysis of NAA similar to the way in which CPA catalyzes the hydrolysis of food-derived polypeptides.   Mutational evaluation of a homology model provided insight into how zinc might regulate the catalytic mechanism of the ASPA enzyme.   Furthermore, we provided explanations for how several ASPA missense mutations that are associated with CD result in dysfunctional or absent enzyme.

Collectively, these studies provided insight into the physiological role of ASPA and its role in the molecular basis of CD.

References

1.	Birnbaum, S. M., Levintow, L., Kingsley, R. B., and Greenstein, J. P. (1952) Specificity of amino acid acylases. *J Biol Chem* **194**, 455-470
2.	Matalon, R., Michals, K., Sebesta, D., Deanching, M., Gashkoff, P., and Casanova, J. (1988) Aspartoacylase deficiency and N-acetylaspartic aciduria in patients with Canavan disease. *Am J Med Genet* **29**, 463-471
3.	Kitada, K., Akimitsu, T., Shigematsu, Y., Kondo, A., Maihara, T., Yokoi, N., Kuramoto, T., Sasa, M., and Serikawa, T. (2000) Accumulation of N-acetyl-L-aspartate in the brain of the tremor rat, a mutant exhibiting absence-like seizure and spongiform degeneration in the central nervous system. *J Neurochem* **74**, 2512-2519
4.	Matalon, R., Rady, P. L., Platt, K. A., Skinner, H. B., Quast, M. J., Campbell, G. A., Matalon, K., Ceci, J. D., Tyring, S. K., Nehls, M., Surendran, S., Wei, J., Ezell, E. L., and Szucs, S. (2000) Knock-out mouse for Canavan disease: a model for gene transfer to the central nervous system. *J Gene Med* **2**, 165-175
5.	Birnbaum, S. M. (1955) Amino acid acylases I and II from hog kidney. *Methods in Enzymology* **2**, 115-119
6.	Kaul, R., Casanova, J., Johnson, A. B., Tang, P., and Matalon, R. (1991) Purification, characterization, and localization of aspartoacylase from bovine brain. *J Neurochem* **56**, 129-135
7.	Le Coq, J., An, H. J., Lebrilla, C., and Viola, R. E. (2006) Characterization of human aspartoacylase: the brain enzyme responsible for canavan disease. *Biochemistry* **45**, 5878-5884
8.	Moore, R. A., Le Coq, J., Faehnle, C. R., and Viola, R. E. (2003) Purification and preliminary characterization of brain aspartoacylase. *Arch Biochem Biophys* **413**, 1-8
9.	Namboodiri, M. A., Corigliano-Murphy, A., Jiang, G., Rollag, M., and Provencio, I. (2000) Murine aspartoacylase: cloning, expression and comparison with the human enzyme. *Brain Res Mol Brain Res* **77**, 285-289
10.	Klugmann, M., Symes, C. W., Klaussner, B. K., Leichtlein, C. B., Serikawa, T., Young, D., and During, M. J. (2003) Identification and distribution of aspartoacylase in the postnatal rat brain. *Neuroreport* **14**, 1837-1840
11.	Kirmani, B. F., Jacobowitz, D. M., Kallarakal, A. T., and Namboodiri, M. A. (2002) Aspartoacylase is restricted primarily to myelin synthesizing cells in the CNS: therapeutic implications for Canavan disease. *Brain Res Mol Brain Res* **107**, 176-182
12.	Madhavarao, C. N., Moffett, J. R., Moore, R. A., Viola, R. E., Namboodiri, M. A., and Jacobowitz, D. M. (2004) Immunohistochemical localization of aspartoacylase in the rat central nervous system. *J Comp Neurol* **472**, 318-329
13.	Baslow, M. H., Suckow, R. F., Sapirstein, V., and Hungund, B. L. (1999) Expression of aspartoacylase activity in cultured rat macroglial cells is limited to oligodendrocytes. *J Mol Neurosci* **13**, 47-53
14.	D'Adamo, A. F., Jr., Smith, J. C., and Woiler, C. (1973) The occurrence of N-acetylaspartate amidohydrolase (aminoacylase II) in the developing rat. *J Neurochem* **20**, 1275-1278
15.	D'Adamo, A. F., Jr., Wertman, E., Foster, F., and Schneider, H. (1978) A radiochemical assay for N-acetyl-L-aspartate amidohydrolase (EC 3.5.1.15) and its occurrence in the tissues of the chicken. *Life Sci* **23**, 791-795
16.	Cygler, M., Schrag, J. D., Sussman, J. L., Harel, M., Silman, I., Gentry, M. K., and Doctor, B. P. (1993) Relationship between sequence conservation and three-dimensional structure in a large family of esterases, lipases, and related proteins. *Protein Sci* **2**, 366-382

17.   Kaul, R., Gao, G. P., Balamurugan, K., and Matalon, R. (1993) Cloning of the human aspartoacylase cDNA and a common missense mutation in Canavan disease. *Nat Genet* **5**, 118-123

18.   Matalon, R., and Michals-Matalon, K. (1999) Recent advances in Canavan disease. *Adv Pediatr* **46**, 493-506

19.   Makarova, K. S., and Grishin, N. V. (1999) The Zn-peptidase superfamily: functional convergence after evolutionary divergence. *J Mol Biol* **292**, 11-17

20.   Tsai, G., and Coyle, J. T. (1995) N-acetylaspartate in neuropsychiatric disorders. *Prog Neurobiol* **46**, 531-540

21.   Tallan, H. H., Moore, S., and Stein, W. H. (1956) N-Acetyl-L-aspartic acid in brain. *J Biol Chem* **219**, 257-264

22.   Truckenmiller, M. E., Namboodiri, M. A., Brownstein, M. J., and Neale, J. H. (1985) N-Acetylation of L-aspartate in the nervous system: differential distribution of a specific enzyme. *J Neurochem* **45**, 1658-1662

23.   Pushkin, A., Carpenito, G., Abuladze, N., Newman, D., Tsuprun, V., Ryazantsev, S., Motemoturu, S., Sassani, P., Solovieva, N., Dukkipati, R., and Kurtz, I. (2004) Structural characterization, tissue distribution, and functional expression of murine aminoacylase III. *Am J Physiol Cell Physiol* **286**, C848-856

24.   Uttamsingh, V., Baggs, R. B., Krenitsky, D. M., and Anders, M. W. (2000) Immunohistochemical localization of the acylases that catalyze the deacetylation of N-acetyl-L-cysteine and haloalkene-derived mercapturates. *Drug Metab Dispos* **28**, 625-632

25.   Leone, P., Janson, C. G., Bilaniuk, L., Wang, Z., Sorgi, F., Huang, L., Matalon, R., Kaul, R., Zeng, Z., Freese, A., McPhee, S. W., Mee, E., During, M. J., and Bilianuk, L. (2000) Aspartoacylase gene transfer to the mammalian central nervous system with therapeutic implications for Canavan disease. *Ann Neurol* **48**, 27-38

26.   Kaul, R., Balamurugan, K., Gao, G. P., and Matalon, R. (1994) Canavan disease: genomic organization and localization of human ASPA to 17p13-ter and conservation of the ASPA gene during evolution. *Genomics* **21**, 364-370

27.   Francois, J., and Manaligod, J. M. (2002) Upper airway abnormalities in Canavan disease. *Int J Pediatr Otorhinolaryngol* **66**, 303-307

28.   Chakraborty, G., Mekala, P., Yahya, D., Wu, G., and Ledeen, R. W. (2001) Intraneuronal N-acetylaspartate supplies acetyl groups for myelin lipid synthesis: evidence for myelin-associated aspartoacylase. *J Neurochem* **78**, 736-745

29.   Madhavarao, C. N., Hammer, J. A., Quarles, R. H., and Namboodiri, M. A. (2002) A radiometric assay for aspartoacylase activity in cultured oligodendrocytes. *Anal Biochem* **308**, 314-319

30.   Kirmani, B. F., Jacobowitz, D. M., and Namboodiri, M. A. (2003) Developmental increase of aspartoacylase in oligodendrocytes parallels CNS myelination. *Brain Res Dev Brain Res* **140**, 105-115

31.   Madhavarao, C. N., Arun, P., Moffett, J. R., Szucs, S., Surendran, S., Matalon, R., Garbern, J., Hristova, D., Johnson, A., Jiang, W., and Namboodiri, M. A. (2005) Defective N-acetylaspartate catabolism reduces brain acetate levels and myelin lipid synthesis in Canavan's disease. *Proc Natl Acad Sci U S A* **102**, 5221-5226

32.   Rubenstein, P. A., and Martin, D. J. (1983) NH2-terminal processing of actin in mouse L-cells in vivo. *J Biol Chem* **258**, 3961-3966

33.   Rubenstein, P. A., and Martin, D. J. (1983) NH2-terminal processing of Drosophila melanogaster actin. Sequential removal of two amino acids. *J Biol Chem* **258**, 11354-11360

34.   Pederson, T., and Aebi, U. (2002) Actin in the nucleus: what form and what for? *J Struct Biol* **140**, 3-9

35. Fagotto, F., Gluck, U., and Gumbiner, B. M. (1998) Nuclear localization signal-independent and importin/karyopherin-independent nuclear import of beta-catenin. *Curr Biol* **8**, 181-190

36. Bird, C. H., Blink, E. J., Hirst, C. E., Buzza, M. S., Steele, P. M., Sun, J., Jans, D. A., and Bird, P. I. (2001) Nucleocytoplasmic distribution of the ovalbumin serpin PI-9 requires a nonconventional nuclear import pathway and the export factor Crm1. *Mol Cell Biol* **21**, 5396-5407

37. Louis, J. C., Magal, E., Muir, D., Manthorpe, M., and Varon, S. (1992) CG-4, a new bipotential glial cell line from rat brain, is capable of differentiating in vitro into either mature oligodendrocytes or type-2 astrocytes. *J Neurosci Res* **31**, 193-204

38. Bichenkov, E., and Ellingson, J. S. (1999) Temporal and quantitative expression of the myelin-associated lipids, ethanolamine plasmalogen, galactocerebroside, and sulfatide, in the differentiating CG-4 glial cell line. *Neurochem Res* **24**, 1549-1556

39. Baumann, N., and Pham-Dinh, D. (2001) Biology of oligodendrocyte and myelin in the mammalian central nervous system. *Physiol Rev* **81**, 871-927

40. Blasi, F., Riccio, M., Brogi, A., Strazza, M., Taddei, M. L., Romagnoli, S., Luddi, A., D'Angelo, R., Santi, S., Costantino-Ceccarini, E., and Melli, M. (1999) Constitutive expression of interleukin-1beta (IL-1beta) in rat oligodendrocytes. *Biol Chem* **380**, 259-264

41. Gallo, V., and Armstrong, R. C. (1995) Developmental and growth factor-induced regulation of nestin in oligodendrocyte lineage cells. *J Neurosci* **15**, 394-406

42. Sock, E., Leger, H., Kuhlbrodt, K., Schreiber, J., Enderich, J., Richter-Landsberg, C., and Wegner, M. (1997) Expression of Krox proteins during differentiation of the O-2A progenitor cell line CG-4. *J Neurochem* **68**, 1911-1919

43. Stariha, R. L., and Kim, S. U. (2001) Mitogen-activated protein kinase signalling in oligodendrocytes: a comparison of primary cultures and CG-4. *Int J Dev Neurosci* **19**, 427-437

44. Yim, S. H., Farrer, R. G., and Quarles, R. H. (1995) Expression of glycolipids and myelin-associated glycoprotein during the differentiation of oligodendrocytes: comparison of the CG-4 glial cell line to primary cultures. *Dev Neurosci* **17**, 171-180

45. Kuersten, S., Ohno, M., and Mattaj, I. W. (2001) Nucleocytoplasmic transport: Ran, beta and beyond. *Trends Cell Biol* **11**, 497-503

46. Yoneda, Y. (2000) Nucleocytoplasmic protein traffic and its significance to cell function. *Genes Cells* **5**, 777-787

47. Christophe, D., Christophe-Hobertus, C., and Pichon, B. (2000) Nuclear targeting of proteins: how many different signals? *Cell Signal* **12**, 337-341

48. Sheng, Z., Lewis, J. A., and Chirico, W. J. (2004) Nuclear and nucleolar localization of 18-kDa fibroblast growth factor-2 is controlled by C-terminal signals. *J Biol Chem* **279**, 40153-40160

49. Makkerh, J. P., Dingwall, C., and Laskey, R. A. (1996) Comparative mutagenesis of nuclear localization signals reveals the importance of neutral and acidic amino acids. *Curr Biol* **6**, 1025-1027

50. Yamaki, A., Kudoh, J., Shimizu, N., and Shimizu, Y. (2004) A novel nuclear localization signal in the human single-minded proteins SIM1 and SIM2. *Biochem Biophys Res Commun* **313**, 482-488

51. Wang, P., Wu, Y., Ge, X., Ma, L., and Pei, G. (2003) Subcellular localization of beta-arrestins is determined by their intact N domain and the nuclear export signal at the C terminus. *J Biol Chem* **278**, 11648-11653

52. Munster, A. K., Weinhold, B., Gotza, B., Muhlenhoff, M., Frosch, M., and Gerardy-Schahn, R. (2002) Nuclear localization signal of murine CMP-Neu5Ac synthetase

includes residues required for both nuclear targeting and enzymatic activity. *J Biol Chem* **277**, 19688-19696

53.   Ma, Z., Chow, K. M., Yao, J., and Hersh, L. B. (2004) Nuclear shuttling of the peptidase nardilysin. *Arch Biochem Biophys* **422**, 153-160

54.   Holmes, K. D., Mattar, P., Marsh, D. R., Jordan, V., Weaver, L. C., and Dekaban, G. A. (2002) The C-terminal C1 cassette of the N -methyl-D-aspartate receptor 1 subunit contains a bi-partite nuclear localization sequence. *J Neurochem* **81**, 1152-1165

55.   Vandenbroucke, I., Van Oostveldt, P., Coene, E., De Paepe, A., and Messiaen, L. (2004) Neurofibromin is actively transported to the nucleus. *FEBS Lett* **560**, 98-102

56.   Delgermaa, L., Hayashi, N., Dorjsuren, D., Nomura, T., Thuy le, T. T., and Murakami, S. (2004) Subcellular localization of RPB5-mediating protein and its putative functional partner. *Mol Cell Biol* **24**, 8556-8566

57.   Nigg, E. A. (1997) Nucleocytoplasmic transport: signals, mechanisms and regulation. *Nature* **386**, 779-787

58.   Dingwall, C., and Laskey, R. A. (1991) Nuclear targeting sequences--a consensus? *Trends Biochem Sci* **16**, 478-481

59.   Henderson, B. R. (2005) Regulation of BRCA1, BRCA2 and BARD1 intracellular trafficking. *Bioessays* **27**, 884-893

60.   Imada, K., and Leonard, W. J. (2000) The Jak-STAT pathway. *Mol Immunol* **37**, 1-11

61.   Gomez-Ortiz, M., Gomis-Ruth, F. X., Huber, R., and Aviles, F. X. (1997) Inhibition of carboxypeptidase A by excess zinc: analysis of the structural determinants by X-ray crystallography. *FEBS Lett* **400**, 336-340

62.   Hirose, J., Ando, S., and Kidani, Y. (1987) Excess zinc ions are a competitive inhibitor for carboxypeptidase A. *Biochemistry* **26**, 6561-6565

63.   Ghosh, S. S., Dakoji, S., Tanaka, Y., Cho, Y. J., and Mobashery, S. (1996) Properties of analogues of an intermediate in the process of mechanism-based inactivation of carboxypeptidase A. *Bioorg Med Chem* **4**, 1487-1492

64.   Lee, K. J., and Kim, D. H. (1998) Design of mechanism-based carboxypeptidase A inactivators on the basis of the X-ray crystal structure and catalytic reaction pathway. *Bioorg Med Chem* **6**, 1613-1622

65.   Auld, D. S. (2001) Zinc coordination sphere in biochemical zinc sites. *Biometals* **14**, 271-313

66.   Jensen, F., Bukrinsky, T., Bjerrum, J., and Larsen, S. (2002) Three high-resolution crystal structures of cadmium-substituted carboxypeptidase A provide insight into the enzymatic function. *J Biol Inorg Chem* **7**, 490-499

67.   Medina, J. F., Wetterholm, A., Radmark, O., Shapiro, R., Haeggstrom, J. Z., Vallee, B. L., and Samuelsson, B. (1991) Leukotriene A4 hydrolase: determination of the three zinc-binding ligands by site-directed mutagenesis and zinc analysis. *Proc Natl Acad Sci U S A* **88**, 7620-7624

68.   Smith, A. A., Carlow, D. C., Wolfenden, R., and Short, S. A. (1994) Mutations affecting transition-state stabilization by residues coordinating zinc at the active site of cytidine deaminase. *Biochemistry* **33**, 6468-6474

69.   Burgisser, D. M., Thony, B., Redweik, U., Hess, D., Heizmann, C. W., Huber, R., and Nar, H. (1995) 6-Pyruvoyl tetrahydropterin synthase, an enzyme with a novel type of active site involving both zinc binding and an intersubunit catalytic triad motif; site-directed mutagenesis of the proposed active center, characterization of the metal binding site and modelling of substrate binding. *J Mol Biol* **253**, 358-369

70.   Vazeux, G., Wang, J., Corvol, P., and Llorens-Cortes, C. (1996) Identification of glutamate residues essential for catalytic activity and zinc coordination in aminopeptidase A. *J Biol Chem* **271**, 9069-9074

71. Le Moual, H., Devault, A., Roques, B. P., Crine, P., and Boileau, G. (1991) Identification of glutamic acid 646 as a zinc-coordinating residue in endopeptidase-24.11. *J Biol Chem* **266**, 15670-15674

72. Kaul, R., Gao, G. P., Matalon, R., Aloya, M., Su, Q., Jin, M., Johnson, A. B., Schutgens, R. B., and Clarke, J. T. (1996) Identification and expression of eight novel mutations among non-Jewish patients with Canavan disease. *Am J Hum Genet* **59**, 95-102

73. Kaul, R., Gao, G. P., Michals, K., Whelan, D. T., Levin, S., and Matalon, R. (1995) Novel (cys152 > arg) missense mutation in an Arab patient with Canavan disease. *Hum Mutat* **5**, 269-271

74. Zeng, B. J., Wang, Z. H., Ribeiro, L. A., Leone, P., De Gasperi, R., Kim, S. J., Raghavan, S., Ong, E., Pastores, G. M., and Kolodny, E. H. (2002) Identification and characterization of novel mutations of the aspartoacylase gene in non-Jewish patients with Canavan disease. *J Inherit Metab Dis* **25**, 557-570

75. Janson, C. G., Kolodny, E. H., Zeng, B. J., Raghavan, S., Pastores, G., Torres, P., Assadi, M., McPhee, S., Goldfarb, O., Saslow, B., Freese, A., Wang, D. J., Bilaniuk, L., Shera, D., and Leone, P. (2006) Mild-onset presentation of Canavan's disease associated with novel G212A point mutation in aspartoacylase gene. *Ann Neurol* **59**, 428-431

76. Kaul, R., Gao, G. P., Aloya, M., Balamurugan, K., Petrosky, A., Michals, K., and Matalon, R. (1994) Canavan disease: mutations among Jewish and non-jewish patients. *Am J Hum Genet* **55**, 34-41

77. Surendran, S., Bamforth, F. J., Chan, A., Tyring, S. K., Goodman, S. I., and Matalon, R. (2003) Mild elevation of N-acetylaspartic acid and macrocephaly: diagnostic problem. *J Child Neurol* **18**, 809-812

78. Sistermans, E. A., de Coo, R. F., van Beerendonk, H. M., Poll-The, B. T., Kleijer, W. J., and van Oost, B. A. (2000) Mutation detection in the aspartoacylase gene in 17 patients with Canavan disease: four new mutations in the non-Jewish population. *Eur J Hum Genet* **8**, 557-560

79. Traeger, E. C., and Rapin, I. (1998) The clinical course of Canavan disease. *Pediatr Neurol* **18**, 207-212

80. Tacke, U., Olbrich, H., Sass, J. O., Fekete, A., Horvath, J., Ziyeh, S., Kleijer, W. J., Rolland, M. O., Fisher, S., Payne, S., Vargiami, E., Zafeiriou, D. I., and Omran, H. (2005) Possible genotype-phenotype correlations in children with mild clinical course of Canavan disease. *Neuropediatrics* **36**, 252-255

81. Yalcinkaya, C., Benbir, G., Salomons, G. S., Karaarslan, E., Rolland, M. O., Jakobs, C., and van der Knaap, M. S. (2005) Atypical MRI findings in Canavan disease: a patient with a mild course. *Neuropediatrics* **36**, 336-339

82. Zafeiriou, D. I., Kleijer, W. J., Maroupoulos, G., Anastasiou, A. L., Augoustidou-Savvopoulou, P., Papadopoulou, F., Kontopoulos, E. E., Fagan, E., and Payne, S. (1999) Protracted course of N-acetylaspartic aciduria in two non-Jewish siblings: identical clinical and magnetic resonance imaging findings. *Brain Dev* **21**, 205-208

83. Olsen, T. R., Tranebjaerg, L., Kvittingen, E. A., Hagenfeldt, L., Moller, C., and Nilssen, O. (2002) Two novel aspartoacylase gene (ASPA) missense mutations specific to Norwegian and Swedish patients with Canavan disease. *J Med Genet* **39**, e55

APPENDIX A

Modulation of Aspartoacylase Activity by Constitutive Phosphorylation

Introduction

CD, also known as spongy degeneration of the CNS, is a fatal neurodegenerative autosomal recessive disorder linked to defects in the ASPA enzyme, which catalyzes the deacetylation of NAA to generate acetate and aspartate (2, 3).

There are limited reports of regulation of the ASPA protein. In addition to its subcellular localization, multimeric state, and structure, the ASPA enzyme might be regulated by phosphorylation. There are 5 putative phosphorylation sites—Ser83, Ser105, Ser108, Ser146, and Thr264—in the ASPA protein (1). Two of these putative phosphorylated residues (Ser83, Ser105) are conserved among human, bovine, murine, and rat species, and further analysis reveals at least 3 other highly conserved or probable sites of phosphorylation (Table 1). Therefore, the residues chosen for mutational analysis in this report were Ser83, Ser105, Ser108, Ser146, Thr264, Thr277, Thr298, and Ser307.

In this report, we investigated the effects of constitutive phosphorylation on ASPA activity using mutations of several potentially phosphorylated serine and threonines. Mutations of the 5 putative phosphorylated residues (S83A, S83D, S105A, S105D, S108A, S108D, S146A, T264A), as well as 3 additional residues that were predicted by NetPhos 2.0 (T277A, T298A, S307A), were created and expressed in COS-7 cells. Preliminary results showed that expression of the S83A and S105A mutations resulted in reduced ASPA activity relative to WT, expression of the S108A mutation

154

resulted in elevated ASPA activity relative to WT, and that expression of the S146A and

T264A mutations resulted in WT ASPA activity. However, poor transfection and ASPA

assay conditions caused overall low activities and spurious trends. Upon correcting these

factors, only expression of the S108D mutation resulted in ASPA activity that was

significantly different from WT ASPA activity. Meanwhile, phosphatase treatment and

phosphatase inhibition did not affect human or murine ASPA activity. Therefore, we

conclude that there is no evidence for an effect of constitutive phosphorylation on ASPA

activity in COS-7 cells and that the S108D mutation affects ASPA catalysis, not a

phosphorylation site. Future experiments could use these preliminary results to further

explore ASPA activity regulation by site-specific phosphorylation.

Amino Acid	Kaul et al 1993?[1]	NetPhos 2.0 Score[2]	Highly Conserved?[3]	NetPhosK 1.0 Kinase[4]
Ser83	Y	0.053	Y	PKA[5]
Ser105	Y	0.838	Y	CKII
Ser108	Y	0.779	N	CKI/CKII
Ser146	Y	0.012	N	PKA
Thr264	Y	0.710	N	PKC
Thr277	N	0.585	Y	None predicted
Thr298	N	0.890	Y	PKC
Ser307	N	0.742	Y	None predicted

[1] Was the residue in question predicted upon initial cloning of the ASPA gene?
[2] Bioinformatic prediction program based on known kinase target sequences. Scores higher than 0.5 indicate likely phosphorylation.
[3] Is this residue conserved among human, mouse, bovine, and rat ASPA proteins?
[4] Bioinformatic prediction program based on known kinases and their consensus target sequences. Higher scores indicated likely phosphorylation by the indicated kinase. Scores ranged from 0.50 to 0.76.
[5] Abbreviations: PKA = protein kinase A; CK = casein kinase; PKC = protein kinase C

Table 1. Putative phosphorylated serines and threonines investigated in this report.

EXPERIMENTAL APPROACH

Plasmid Constructs

Full-length human ASPA cDNA was subcloned by polymerase chain reaction (PCR) using primers ATGACTTCTTGTCACATTGCT (forward) and CTAATGTAAACAGCAGCGAAT (reverse) from pBAD/Thio-TOPO (Invitrogen) (4) into the TOPO-T/A cloning site of pcDNA3.1/NT-GFP-TOPO. The resulting GFP-hASPA plasmid expresses a fusion protein of cycle 3 GFP fused to the N-terminus of ASPA. Full-length human ASPA cDNA was also subcloned into the TOPO-T/A cloning site of pcDNA3.1/V5-His-TOPO such that the resulting hASPA plasmid expresses native untagged ASPA. Control plasmid expressing GFP alone was obtained from Invitrogen.

Site-Directed Mutagenesis

Individual point mutations were introduced in either native untagged hASPA or in GFP-hASPA using Stratagene's Quick Change II Site-Directed Mutagenesis kit according to manufacturer's instructions (Table 2). S108A double mutants with S83A, S105A, and T298A were made by mutagenizing hASPA S108A plasmid. Mutant plasmid DNA was subsequently isolated and sequenced to confirm the desired mutation. Mutant constructs were subcloned by PCR to yield native untagged and GFP-hASPA constructs that expressed full-length ASPA including its stop codon. Alternatively, ASPA was subcloned by PCR using a reverse primer that lacked the stop codon such that when ligated into pcDNA3.1/V5-His-TOPO the resulting hASPA-V5-His plasmid expresses ASPA fused to the V5 epitope and a 6x-His tag at its C-terminus.

156

Amino Acid	Base Pair	Forward Mutagenic Primer
S83A	T247G	5' GAAAATCTTGGCAAAAAAATGGCAGAAGATTTGCCATATGAAGTG 3'
S105A	AG313GC	5' CATTTATTTGGTCCAAAAGACGCTGAAGATTCCTATGACATTAT 3'
S105A*	AG313GC	5' GAAATAAATCATTTATTTGGTCCAAAAGACGCTGAAGATGCCTATGACATTATTTTTGACC 3'
S108A	T322G	5' GGTCCAAAAGACAGTGAAGATGCCTATGACATTATTTTTGACC 3'
S146A	T436G	5' GTTTCATTACATTAAGACTGCTCTGGCTCCACTACCCTG 3'
T264A	A790G	5' GGGATCCCATGTTTTTAGCTCTTGATGGGAAGACG 3'
T277A	A829G	5' CTGGGCGGAGACTGTGCCGTGTACCCCGTG 3'
T298A	A892G	5' GAAAGAAGCTTTTGCAAAGGCAACTAAACTAACGCTC 3'
S307A	AG919GC	5' CTAACGCTCAATGCAAAAGCTATTCGCTGCTGTTTAC 3'
S83D	TCA247GAC	5' GACCTTGAAAATCTTGGCAAAAAAATGGACGAAGATTTGCCATATGAAGTGAGAAG 3'
S105D	AGT313GAC	5' CAAGAAATAAATCATTTATTTGGTCCAAAAGACGACGAAGATTCCTATGACATTATTTTTGACCTTCAC 3'
S108D	TC322GA	5' GGTCCAAAAGACAGTGAAGATGACTATGACATTATTTTTGACC 3'
T298D	ACA892GAC	5' CGAAAAGAAAGAAGCTTTTGCAAAGGACACTAAACTAACGCTCAATGCAAAAAG 3'

* Generation of the S105A/S108A double mutant required special mutagenic primers to compensate for the inclusive mutation within the primers' target region of the plasmid.

Table 2. Forward primers used for site-directed mutagenesis of hASPA cDNA.

Cell Culture and Transient Transfections

COS-7 (ATCC) cells were grown at 37°C with 5% CO$_2$, cultured in DMEM containing 10% fetal bovine serum, grown to confluence, and sub-cultured every 3-4 days. Transient transfections were performed using Lipofectamine 2000 (Invitrogen). Transfected COS-7 cells were harvested roughly 24 h post-transfection by treatment with 2 mM EDTA (15 min, 37°C), spun down, and washed with PBS. Whole cell extracts were generated by sonicating cell pellets in homogenization buffer (*HB*; 0.5 mM DTT, 50

mM Tris-HCl, pH 8.0, 50 mM NaCl, 0.05% IGEPAL CA-630), with or without 8-10% glycerol. Cellular debris was then removed (16,000 g, 10 min, 4°C) and protein concentrations were determined by BioRad's DC protein assay.

ASPA Enzyme Assay

A coupled spectrophotometric ASPA activity assay based on β-NADH oxidation of ASPA-liberated aspartate (5) and a high-sensitivity radiometric assay involving thin-layer chromatography (TLC)-based product separation and phosphor image-based quantification were followed as previously described (6).

SDS-PAGE and Immunoblotting

Samples were diluted in 5X loading buffer (Quality Biological), reduced with 10 mM DTT, and heated (90°C, 5 min) prior to loading onto 10% pre-cast Tris-Glycine gels (Invitrogen). Following electrophoresis, samples were transferred to Immobilon-P PVDF (Millipore) membranes using the XCell II blotting module (Invitrogen). Membranes were blocked (PBS, 0.05% v/v Tween-20, and 5% NGS) for 1 h at room temperature, followed by overnight 4°C incubation with either a polyclonal antibody against a conserved ASPA peptide (pepASPA), a monoclonal GFP antibody (Chemicon), a monoclonal β-tubulin antibody (Upstate), or a polyclonal antibody against the V5 epitope (Invitrogen). Following brief washing, horseradish peroxidase-conjugated goat anti-rabbit or anti-mouse secondary antibody was added at a dilution of 1:5,000. Membranes were washed and developed in Super Fast diaminobenzidine substrate (Sigma).

Statistical Analysis

Enzyme activities are presented as means ± SEM. Differences between groups were analyzed by ANOVA followed by Dunnett's Post-Hoc T-Test, which referenced WT samples as a control group, at a significance level of $p < 0.05$.

Figure	Dish Size (mm)	# of Cells[1]	Time	Glycerol in Buffer?[2]	ASPA DNA (µg)[3]	Lipo (µL)[4]	ΔM?	Source (cpm/µL)	S.A.	Spot Vol. (µL)	Protein / Assay (µg)
1	60	1x10^7	varied	?	4	15	N	194,311	8.4	10	varied
1	35	4x10^5	22	?	2	7	N	194,311	8.4	10	20
2A	60	High	23	?	5	14	N	194,311	8.4	10	varied
2C	35	80%	23	N	2.5	7	Y	194,311	8.4	10	90
3	60	1.5x10^6	24	N	3	14	Y	194,311	20.7	10	varied
4	35	7.5x10^5	24	N	1.5[3]	7	Y	varied	varied	10	90-150
5	35	7.5x10^5	24	N	3	7	Y	194,311	20.7	12.5	varied
6	35	7.5x10^5	24	Y	1.5[3]	7	N	232,000	21.2	20	100
7	35	1x10^6	24	Y	3	7	N	232,000	14.83	20	varied
8	35	1x10^6	24	Y	3	7	N	232,000	8.71	10	varied
9A	35	1x10^6	24	Y	3	7	N	232,000	14.83	?	varied
9C	35	1x10^6	24	Y	3	7	N	232,000	8.71	20	varied
10	35	1x10^6	24	varied	varied	7	N	232,000	8.71	15	varied
11	12-well	80%	24	Y	1.2	2.8	N	232,000	8.71	10	varied
12	12-well	80%	24	Y	1.2	2.8	N	232,000	8.71	10	varied

1 In some instances, cells were not counted for seeding. Relative density is presented instead.
2 Transfected cells were harvested in HB, with or without 8-10% glycerol.
3 Plasmid DNA containing ASPA constructs. Where indicated, ASPA plasmid DNA was mixed 1:1 with GFP plasmid DNA.
4 Abbreviations: Lipo = Lipofectamine; S.A. = specific activity; Vol = volume; ΔM = changed medium

Table 3. Transfection and radiometric ASPA assay conditions.

RESULTS

Preliminary Trend: Serine Substitutions Affect ASPA Activity

Conserved alanine substitutions of serine and threonine residues were made in order to lose the possibility of covalent phosphorylation at the serine hydroxyl group without significantly altering local geometry or charge. The initial analysis compared WT ASPA to S83A, S105A, and S83A/S105A mutations generated in the GFP-hASPA plasmid. Transfection and assay conditions for each experiment in this report are summarized in Table 3.
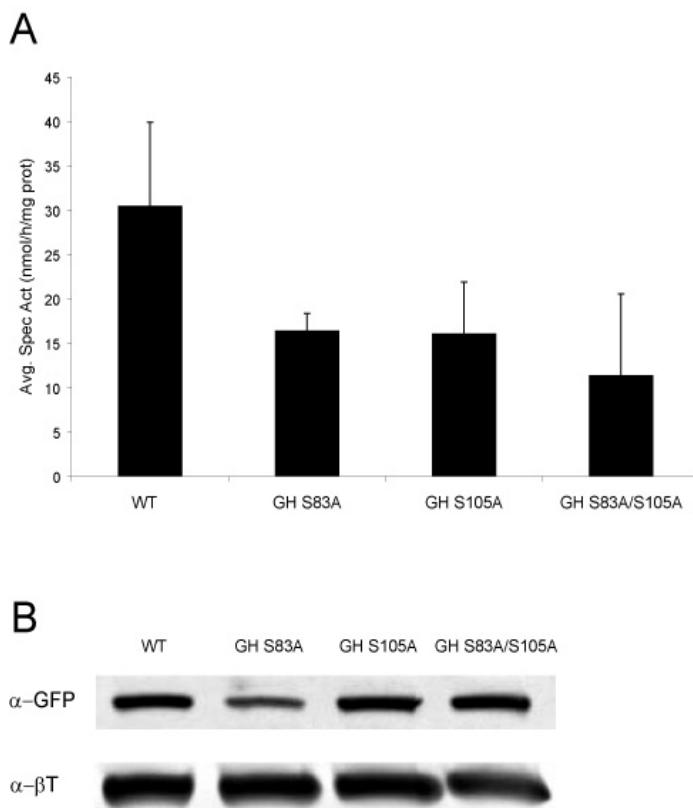

Figure 1. Preliminary analysis of Ser83 and Ser105 mutations. Whole cell extracts prepared from COS-7 cells transiently transfected with GFP-hASPA constructs. Enzyme activities are presented as mean +/- SEM for triplicate transfections. *A,* Single and double alanine substitutions of Ser83 and Ser105 resulted in notably decreased ASPA activity levels relative to WT. *B,* Immunoblot analysis using α-GFP (1:3,500) and α-βT (1:3,500) antibodies detecting GFP-hASPA fusion proteins at 67 kDa and β-tubulin at 50 kDa. 25 µg protein per lane.

The first set of transfections was harvested ~25 h post-transfection, and double

mutant transfections were harvested ~46 h post-transfection.   Total protein per

radiometric ASPA assay varied between samples, with ~100 μg and ~50 μg for WT and

mutants, respectively. Overall, the specific activity of WT ASPA was roughly twice that

of the S83A, S105A, and S83A/S105A mutants (Figure 1A), but these differences were

not statistically significant. Immunoblotting showed comparable levels of GFP-hASPA

protein for WT, S105A, and S83A/S105A and a slight reduction for the S83A mutant

(Figure 1B).
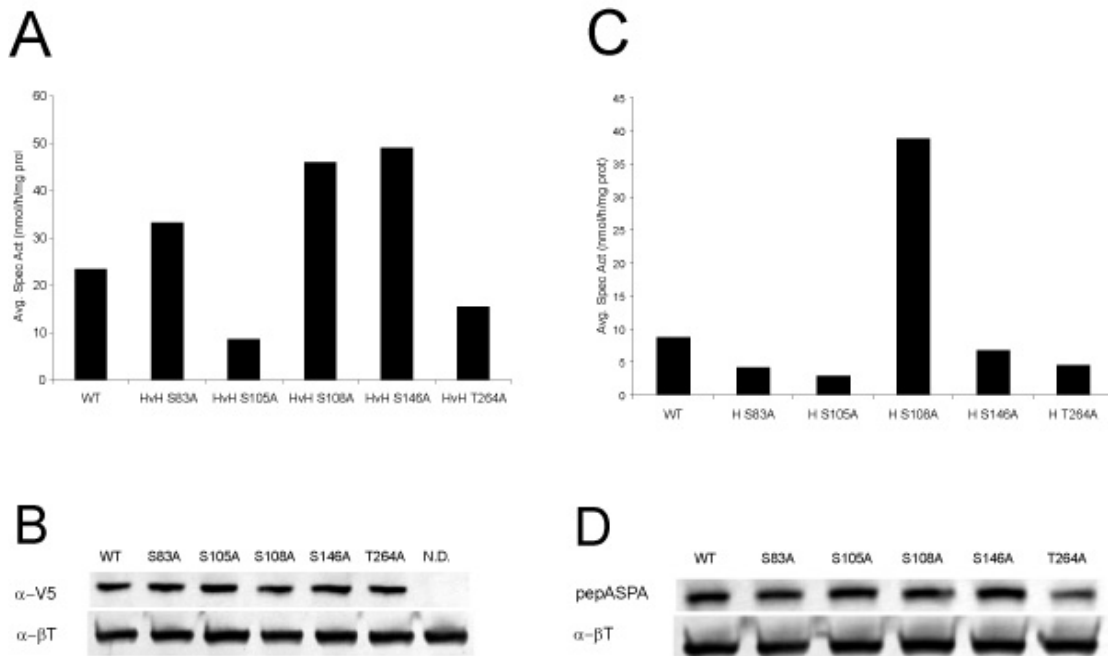
Figure 2.   **Serine and threonine substitutions of published predicted phosphorylated residues (1).**   Whole cell extracts prepared from COS-7 cells transiently transfected with indicated constructs.   Enzyme activities of single transfections.   *A,* Ser/Thr→Ala mutations generated in hASPA-V5-His result in activities different from WT. *B,* Immunoblot analysis using α-V5 (1:5,000) and α-βT (1:5,000) antibodies detecting hASPA-V5-His proteins at 42 kDa and β-tubulin at 50 kDa. 50 μg protein per lane. N.D., No DNA mock transfection. *C*, Ser/Thr→Ala mutations generated in hASPA result in activities different from WT. *D*, Immunoblot analysis using pepASPA (1:4,000) and α-βT (1:5,000) antibodies detecting ASPA at 37 kDa and β-tubulin at 50 kDa. 25 μg protein per lane.

The next set of transfections compared WT ASPA to mutations of the 5 published potential phosphorylation sites (1) generated such that native hASPA was expressed with V5 and 6x-His tags at its C-terminus (hASPA-V5-His). Different amounts of protein were used per radiometric ASPA assay: ~95 µg protein each for WT, S105A, S108A, and T264A compared with ~50 µg protein each for the S83A and S146A mutants.

Figure 3. **Determining the linear range of enzyme per ASPA assay.** Whole cell extracts prepared from transiently transfected COS-7 cells. *A,* hASPA activity is linear between 75 µg and 120 µg protein. *B,* mASPA activity is linear between 5 µg and 25 µg protein.

A

B

y = 0.1765x - 0.104
R^2 = 0.9712
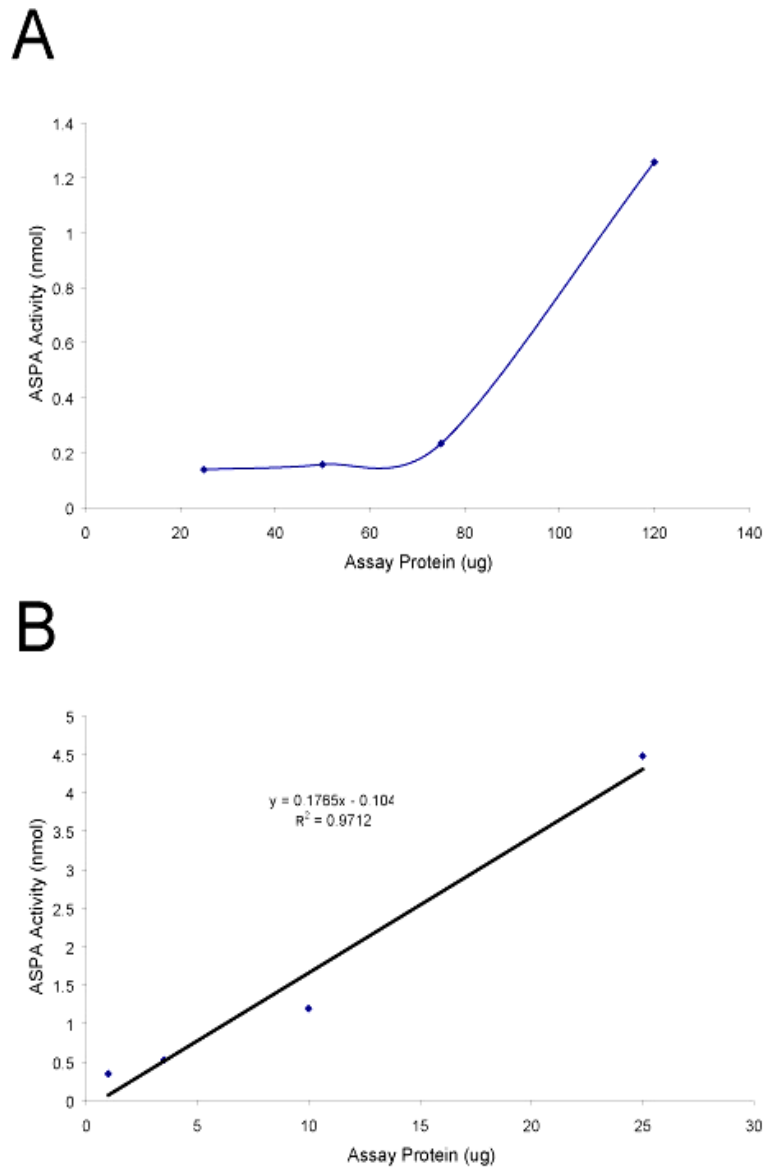
A comparison of samples from which similar amounts of protein were used per assay shows that the specific activities of the S105A, S108A, and T264A mutants were ~3-fold elevated, ~2-fold reduced, and unchanged relative to WT ASPA (Figure 2A). The specific activities of S83A and S146A mutants were comparable. Immunoblots using an antibody against the C-terminal V5 epitope showed there were comparable levels of ASPA protein for each construct (Figure 2B). Meanwhile, the specific activities of hASPA S83A and S105A mutants were ~2-4-fold lower than WT ASPA, and the specific activity of the S108A mutant was ~4-5-fold higher than WT ASPA (Figure 2C). Notably, there was a 2-fold reduction in the specific activity of native WT hASPA compared with hASPA-V5-His (Figure 2A). Immunoblotting showed there were comparable ASPA protein levels for each construct (Figure 2D). These results collectively supported the hypothesis that constitutive phosphorylation at Ser83 and Ser105 enhances ASPA activity, while constitutive phosphorylation at Ser108 reduces ASPA activity.

Establishing a Trend: Implied Phosphorylation at Ser83, Ser105, and Ser108

In order to monitor transfection efficiency, total plasmid DNA was mixed 1:1 with ASPA and GFP plasmid DNA. Immunoblotting showed an optimum transfection ratio of 3 μg total plasmid DNA to 7 μL of Lipofectamine (data not shown). The next set of experiments determined a linear range for ASPA protein per radiometric assay. We had previously noted that transient transfections of murine ASPA resulted in higher activity than those of human ASPA (spectrophotometric ASPA assays, data not shown). Radiometric assays of transfected cells that were contaminated by bacteria, yeast, or

fungus showed low activity for WT hASPA that rose sharply between 75 µg and 120 µg

protein (Figure 3A). Mouse ASPA showed considerably higher activity and a linear

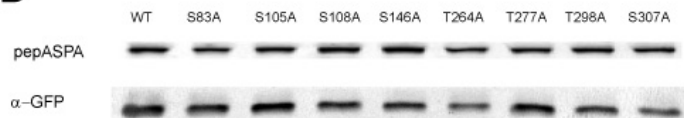range between 5 µg and 25 µg protein (Figure 3B).

A
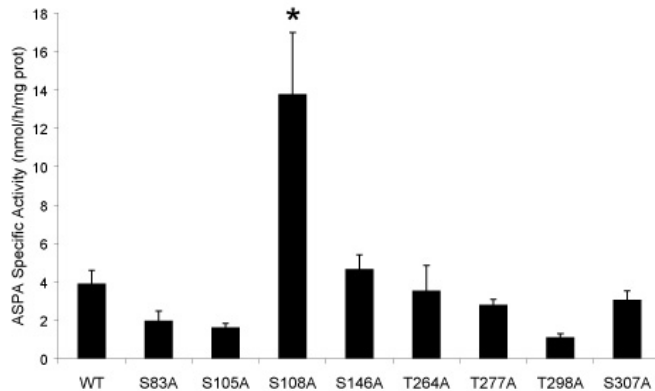
B

Figure 4. Serine and threonine substitutions of predicted phosphorylated residues. Whole cell extracts prepared from COS-7 cells transiently transfected with hASPA constructs. Enzyme activities are presented as mean +/- SEM for triplicate transfections. *A,* Expression of S108A resulted in statistically significantly elevated activity levels relative to WT (*; $p < 0.05$). Other Ser/Thr→Ala mutants result in activities different from WT. *B,* Immunoblot analysis using pepASPA (1:4,000) and α-GFP (1:5,000) antibodies. 35 µg protein per lane.

The full set of serine and threonine substitutions (Table 1) was subsequently

analyzed. The first set of samples was analyzed as before, and the remaining two sets

used 290,000 cpm/µL [^{14}C]-NAA at a 28.4 specific activity in the radiometric assay. All

specific activities were very low (Figure 4A). The specific activity of the S108A mutant

was ~5-fold higher than WT ASPA, and the specific activities of the S83A and S105A

mutants were reduced ~2- and ~4-fold, respectively, compared with WT ASPA.

Immunoblotting showed there were comparable amounts of ASPA protein per construct
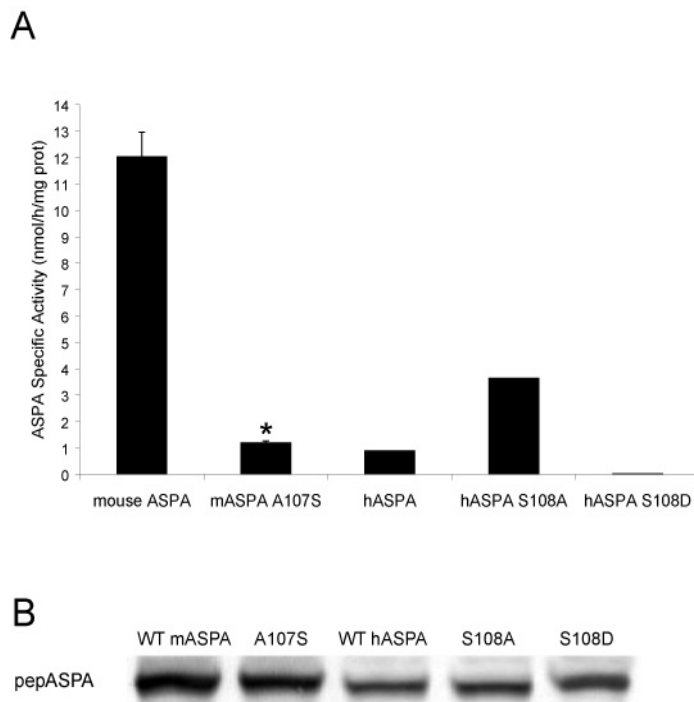
(Figure 4B).

Figure 5. Analysis of human Ser108 and Murine Ala107. Whole cell extracts prepared from COS-7 cells transiently transfected with indicated constructs. Enzyme activities are presented as either mean +/- SEM for triplicate transfections or as single values for individual transfections. *A,* Expression of mASPA A107S resulted in statistically significantly decreased activity levels relative to WT (*; $p < 0.05$). S108A activity was higher than WT. Expression of S108D resulted in virtually undetectable activity. *B,* Western blot analysis using pepASPA (1:5,000) and α-GFP (1:5,000) antibodies. 35 μg protein per lane.

As the specific activity of the S108A mutant was consistently higher than WT, the focus shifted to the Ser108 mutant and its equivalent residue, Ala107, in murine ASPA. For enzyme assays, ~25 μg and ~125 μg of protein were used for murine and human samples, respectively. Although the specific activities were very low, the activity of the S108A mutant remained elevated compared with WT ASPA (Figure 5A). The expression of an S108D mutant generated to mimic the negative charge of phosphorylation resulted in virtually undetectable activity. The expression of an mASPA A107S mutant generated to allow for the possibility of serine phosphorylation at this residue resulted in ~5-fold reduced activity compared with WT mASPA (Figure 5A).

Immunoblotting showed there were comparable levels of ASPA protein for WT hASPA, S108A, and S108D, and it also revealed a slight shift in size for S108D protein (Figure 5B) due to its extra negative charge. Immunoblotting also showed greater reactivity for each mASPA construct than for hASPA. Therefore, activity differences between human and murine ASPA might be because of higher expression upon transfection or innate difference, rather than differential post-translational modification. These results supported the hypothesis that phosphorylation at Ser108 inhibits human ASPA activity.

The analysis of mutants generated in hASPA-V5-His (Figure 6A) showed similar results to those presented in Figure 4A. However, the overall specific activities were much lower than before (Figure 2A). Immunoblotting showed there were comparable amounts of ASPA protein per construct (Figure 6B).

At this point, overall trends began to change. The S83A/S108A and S105A/S108A double mutants were generated and analyzed to evaluate how the simultaneous loss of two putative phosphorylation events would affect ASPA activity. Native untagged WT hASPA activity was higher than before (~25 nmol/h/mg versus 1-10 nmol/h/mg) and was comparable to that of S83A/S108A and S105A/S108A double mutants (Figure 6C). In addition, the S83D and S105D mutants and alanine substitutions for each previously speculated phosphorylated serine were generated and analyzed. The specific activity of WT hASPA was now ~14 nmol/h/mg (Figure 6D) and was significantly higher than before (Figures 2B, 4, & 5A). There was no longer a difference between WT and S108A activities. Although the activities of S83A and S105A mutants

remained lower than WT hASPA, the activities of the S105D and S105A mutants were

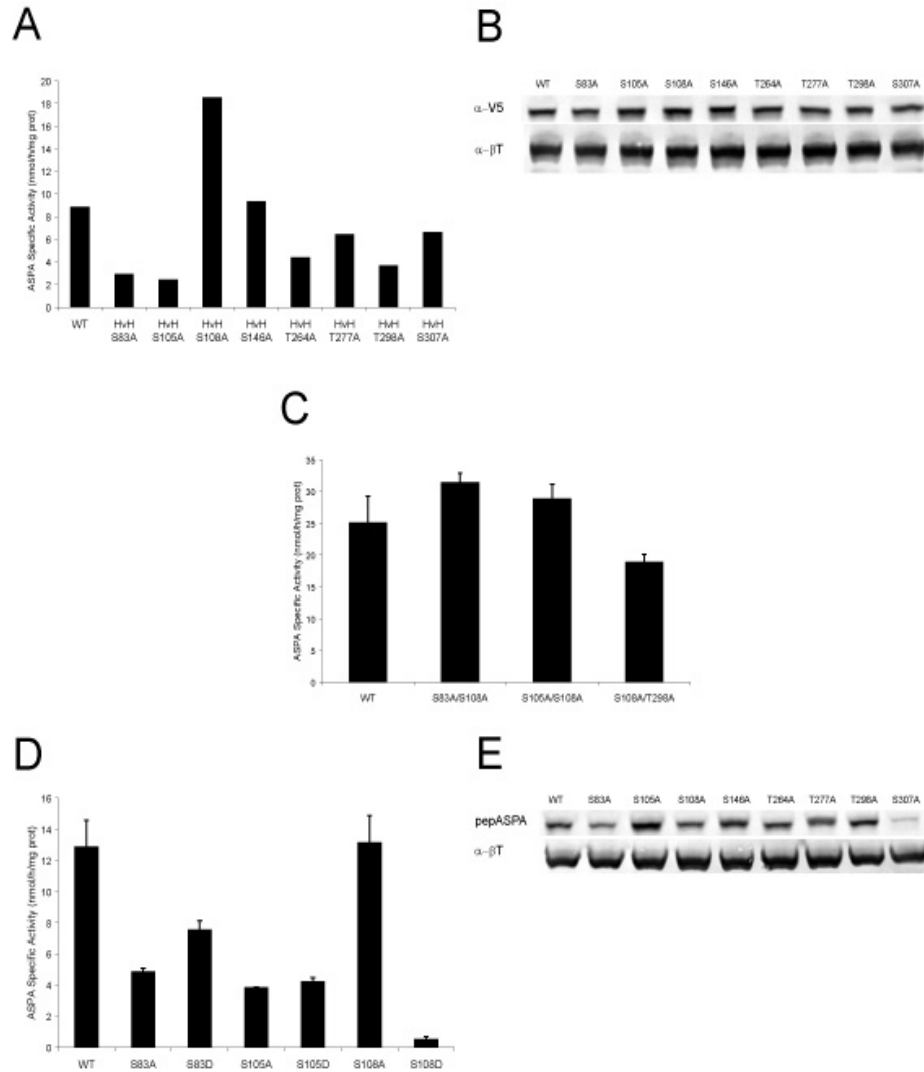comparable, which suggests Ser105 is not phosphorylated.

Figure 6. **Various mutational analyses reveal higher activities.** Whole cell extracts prepared from COS-7 cells transiently transfected with indicated constructs. Enzyme activities are presented as either mean +/- SEM for triplicate transfections or as single values for individual transfections. *A,* Ser/Thr→Ala mutations generated in hASPA-V5-His result in activities different from WT. *B,* Western blot analysis using α-V5 (1:5,000) and α-βT (1:5,000) antibodies. 35 µg protein per lane. *C,* Expression of double mutants with S108A resulted in activity levels comparable to WT. *D,* Expression of S108D resulted in statistically significantly decreased activity levels relative to WT (*; $p < 0.05$). All other differences were not significant. *E,* Western blot analysis using pepASPA (1:5,000) and α-βT (1:5,000). 35 µg protein per lane.

Notably, the activity of the S108D mutant remained virtually undetectable. It now appeared that Ser108 is not constitutively phosphorylated and that the S108D mutation results in reduced ASPA activity by another mechanism. Finally, the activity of the S83D mutant was higher than that of the S83A mutant but lower than that of WT ASPA. While this supports the hypothesis that negative charges due to phosphorylation at Ser83 enhance ASPA activity, S83D protein levels were elevated compared with other constructs (Figure 6E), which might explain the elevated enzyme activity.

Questioning Trends: Which Experimental Factors Led to Erroneous Data?

There was now confusion as to the reliability of most data. Activity assays (using ~75 µg and ~15 µg of protein for mASPA and hASPA, respectively) now showed that WT hASPA and mASPA activities were higher than before (Figure 7).

Figure 7. Analysis of Human Ser108 and Murine Ala107 using improved transfection conditions. Whole cell extracts prepared from COS-7 cells transiently transfected with indicated constructs. Enzyme activities are presented as mean +/- SEM for triplicate transfections. Expression of S108D resulted in statistically significantly decreased activity levels relative to WT (*; $p < 0.05$). Other hASPA mutant activities were comparable to WT. Expression of mASPA A107S resulted in statistically significantly decreased activity levels relative to WT (**; $p < 0.05$).
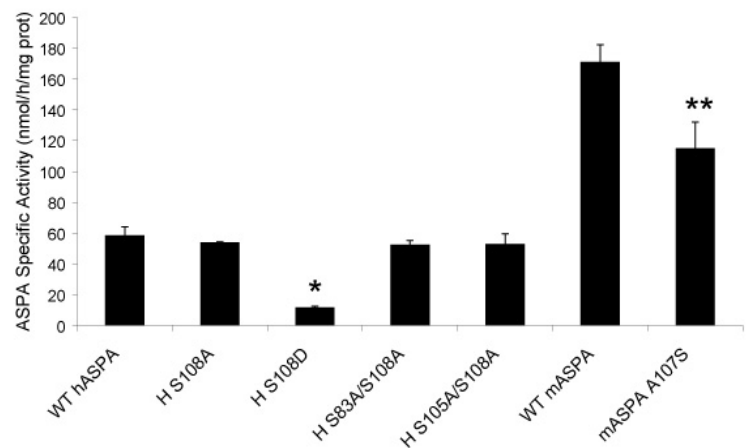
Meanwhile, the activity of the S108A mutant was comparable to WT, and the activity of the S108D mutant was lower than WT. Activities of S83A/S108A and S105A/S108A double mutants were comparable to WT (Figure 6C). Finally, the activity of the A107S mutation in mASPA was significantly reduced compared with WT mASPA.
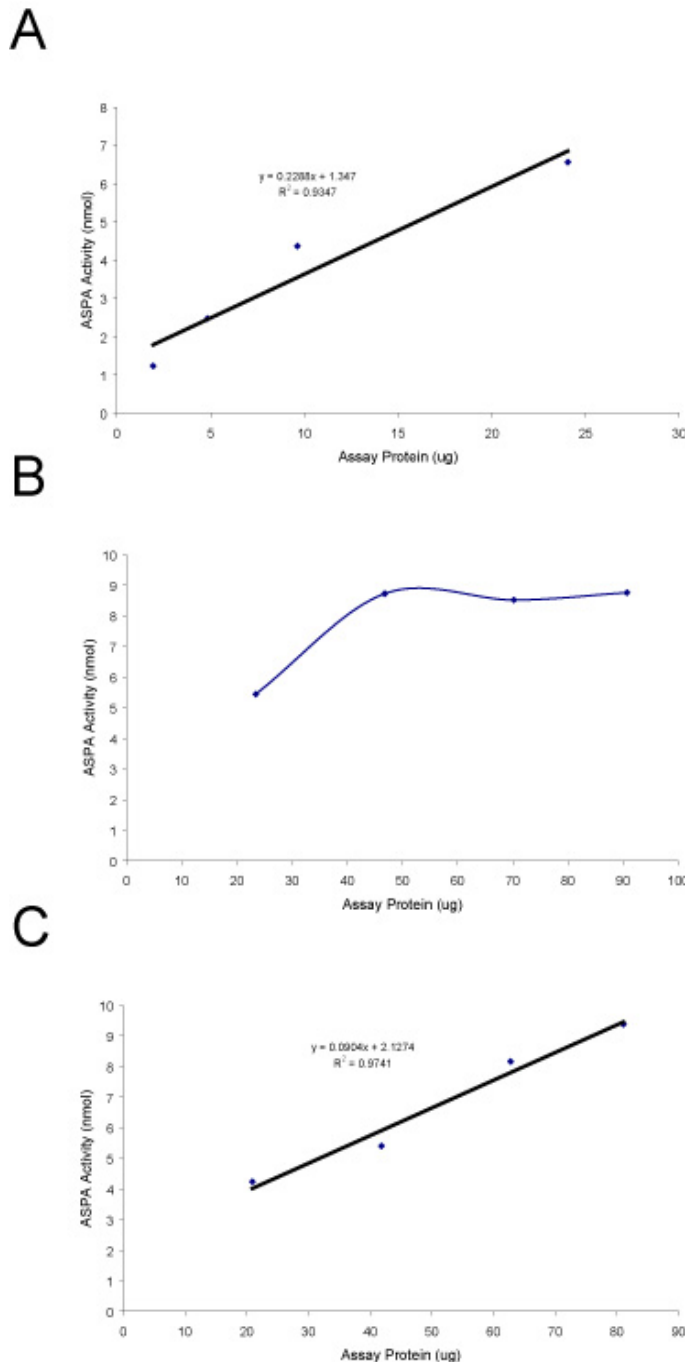
A

Figure 8. **Determining the linear range of enzyme per ASPA assay using improved transfection conditions.** Whole cell extracts prepared from transiently transfected COS-7 cells. *A*, mASPA activity is linear between 5 µg and 20 µg protein. *B,* hASPA activity is linear between 20 µg and 50 µg protein. *C*, S108A activity is linear between 30 µg and 70 µg protein.

B

C

Linear ranges of ASPA per assay were re-established because overall activities were much higher than before. The activity of WT mASPA was again linear between 5 µg and 20 µg protein and at higher levels than before (Figure 8A). Meanwhile, the activity of WT hASPA was very high and linear between 20 µg and 50 µg protein (Figure 8B), and much lower than before (see Figure 3A). Finally, the activity of the S108A mutant was slightly lower than WT and was linear between 30 µg and 70 µg protein (Figure 3C).

**Figure 9.** **CIAP treatment has little effect on activity of various hASPA and mASPA constructs.** Whole cell extracts prepared from COS-7 cells transiently transfected with indicated constructs. Enzyme activities reflect single transfections. *A,* CIAP pre-treatment slightly decreases WT mASPA activity and has little effect on other constructs. *B,* Immunoblot analysis using pepASPA (1:4,000) and α-βT (1:5,000). 20 µg protein per lane. *C*, CIAP pre-treatment using more protein slightly decreases WT mASPA activity and has little effect on other constructs.
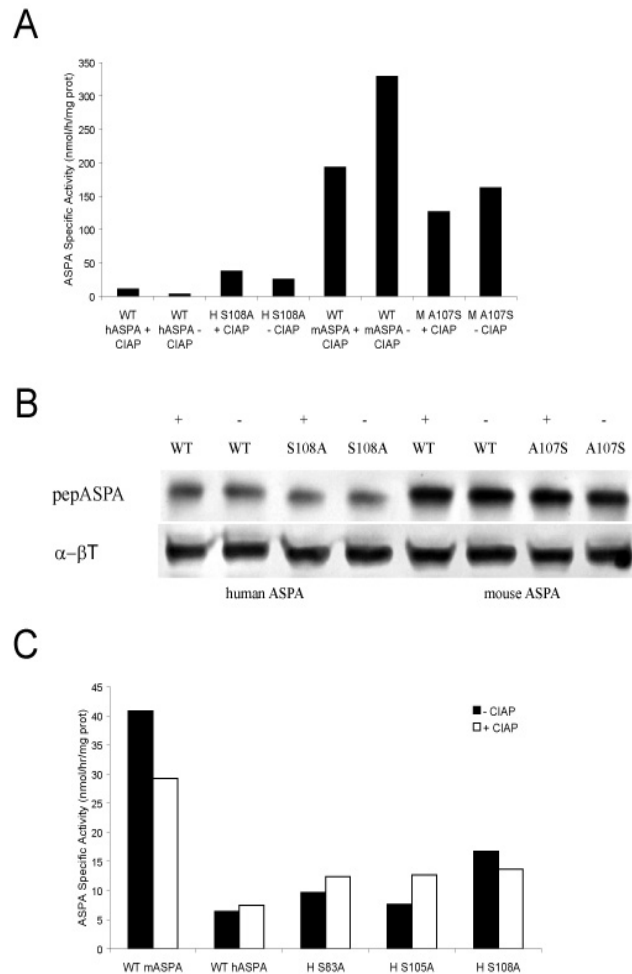
The purpose of this study was to demonstrate regulation of ASPA protein by phosphorylation in COS-7 cells. With this in mind, samples were pre-treated *in vitro* with calf alkaline intestine phosphatase (CIAP), which helped to indirectly assess the effects of phosphorylation on ASPA activity. Analysis of CIAP pre-treated samples used 10 μg and 17.5 μg of protein per ASPA assay for mASPA and hASPA samples, respectively. The activity of WT hASPA was very low, while the activities of WT mASPA and mASPA A107S were very high (Figure 9A). The activity of the S108A mutant was greatly elevated compared with WT hASPA. Treatment with CIAP increased WT and S108A activities and decreased WT and mASPA A107S activities. Immunoblotting did not show a shift for any ASPA band due to CIAP treatment (Figure 9B).

Figure 10. **Transfection condition details.** Whole cell extracts prepared from COS-7 cells transiently transfected with indicated constructs. Enzyme activities reflect single transfections. Cells harvested in HB with 8-10% glycerol displayed no difference in activity from cells harvested in HB without glycerol. Splitting total DNA 1:1 with ASPA and GFP plasmid apparently halved ASPA activity. Pre-incubation at 37°C did not affect ASPA activity.
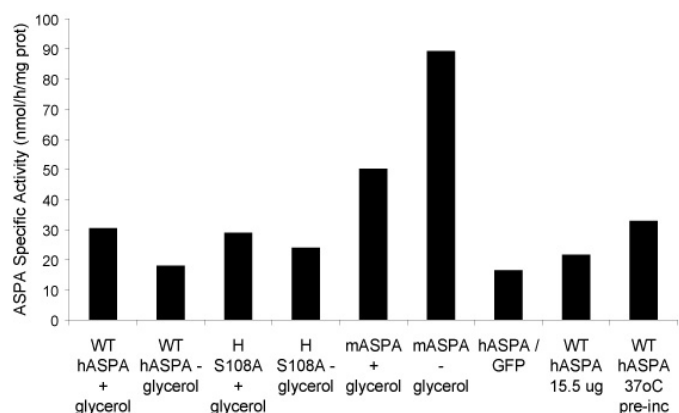
This approach was repeated using more protein per CIAP assay and 10 μg and 26.25 μg protein per ASPA assay for mASPA and hASPA, respectively. Now, the

activities of the S83A, S105A, and S108A mutants were comparable to WT and treatment with CIAP reduced WT mASPA and S108A activities and slightly increased WT hASPA, S83A, and S105A activities (Figure 9C). Treatment with CIAP decreased WT mASPA activity in both cases, though these trends were probably spurious due to overall low activities.
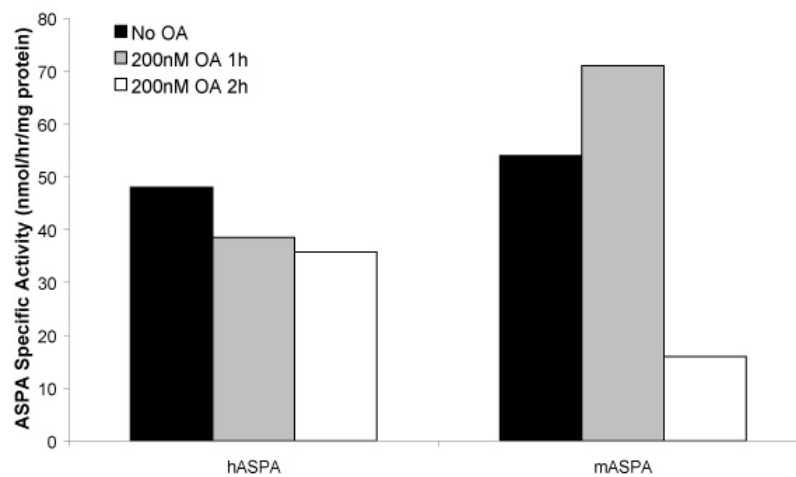

Figure 11. Okadaic acid (OA) treatment has little effect on activity of WT hASPA and mASPA. Medium was replaced ~23 h post-transfection with medium containing 200 nM OA and incubated further for 1 h or 2 h at 37°C. Whole cell extracts were prepared from COS-7 cells transiently transfected with indicated constructs. Enzyme activities reflect single transfections. OA had no consistent effect on either WT hASPA or WT mASPA activity.

Other factors subsequently were explored as causative reasons for low activities. The effects of 8-10% glycerol in the homogenization buffer and the amount of ASPA plasmid DNA used per transfection were investigated. Neither of these two factors was found to significantly affect activity (Figure 10). In contrast, a 1:1 ratio of ASPA and GFP plasmid DNA caused a ~2-fold reduction in ASPA activity. There was comparable

ASPA activity using 15.5 µg or 30 µg of WT hASPA protein. Finally, pre-incubation at 37°C, which was a negative control for CIAP treatment, did not affect ASPA activity. In general, mASPA activity was higher than hASPA, and S108A and WT hASPA activities were comparable.

If an enzyme is susceptible to endogenous protein phosphatase activity, then the effects of phosphorylation on its activity should be enhanced following treatment with okadaic acid (OA), a cell-permeable phosphatase inhibitor. Treatment with OA had no effect on WT hASPA activity, increased mASPA activity after 1 h, and drastically reduced mASPA activity after 2 h (Figure 11).
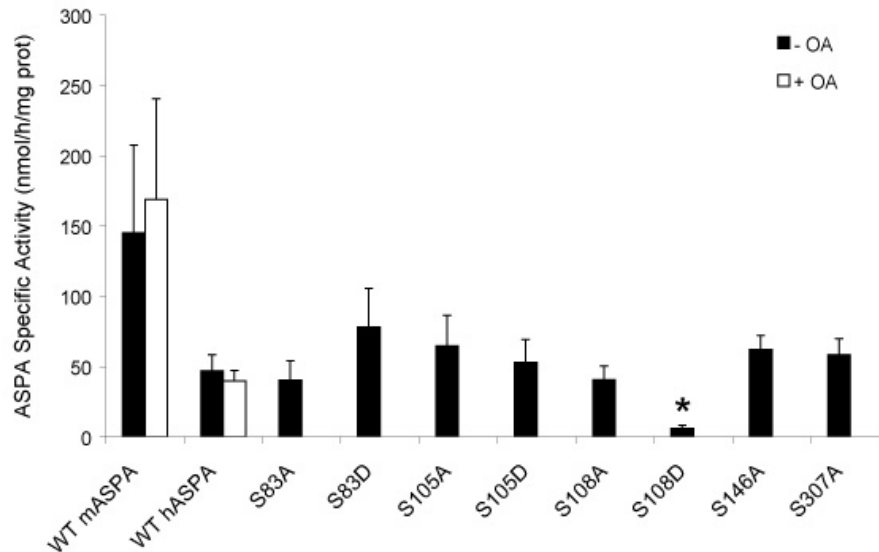

Figure 12. **Analysis of serine substitutions using optimized transfection conditions.** Whole cell extracts prepared from COS-7 cells transiently transfected with indicated constructs. Enzyme activities are presented as mean +/- SEM for triplicate transfections. *A,* Expression of S108D resulted in statistically significantly decreased activity levels relative to WT (*; *p < 0.05*). Other Ser→Ala/Asp mutants resulted in activities comparable to WT.

The final analysis of all serine substitutions used optimized transfection and assay conditions. The specific activities of WT hASPA and WT mASPA were ~50 nmol/h/mg and ~100 nmol/h/mg, respectively (Figure 12). There was no effect of OA treatment on either WT hASPA or WT mASPA activity. In addition, there were no significant differences between WT and S83A, S83D, S105A, S105D, S108A, S146A, and S307A activities, and the activity of the S108D mutant was significantly reduced relative to WT (Figure 12). Once there was no longer any evidence in support of overall or site-specific phosphorylation of hASPA protein, it became more plausible that the S108D mutation affects ASPA catalysis.

DISCUSSION

This report explored whether phosphorylation affects ASPA activity, using COS-7 cells as a model system. A few tentative conclusions were made following the analysis of Ser→Ala and Ser→Asp mutations of residues that might be phosphorylated (Table 1). Briefly, the S108D mutation appears to affect catalysis, while the S83A, S83D, S105A, S105D, S108A, S146A, and S307A mutations appear to be silent. Preliminary results from *in vitro* phosphatase treatment and *in vivo* phosphatase inhibition suggest there is no effect of constitutive phosphorylation on ASPA activity in COS-7 cells. However, this report was not able to conclusively determine whether ASPA is constitutively phosphorylated in COS-7 cells, whether ASPA activity can be modulated via phosphorylation, or whether specific serine and threonines can be phosphorylated.

The initial analysis suggested a phosphate at Ser83 and Ser105 is needed to achieve full activity. In addition, preliminary experiments suggested phosphorylation at Ser108 inhibits hASPA activity and mASPA activity is higher than hASPA activity, in part, because of the loss of an inhibitory phosphate at residue 107/108. The preliminary hypotheses were based on radiometric ASPA assays that were done without first establishing a protein linear range. Because too little ASPA enzyme does not hydrolyze enough NAA for detection and because too much ASPA enzyme no longer produces product due to enzyme saturation, assays conducted outside the linear range do not reflect enzyme efficiency. Too much protein was used in assays upon which initial hypotheses were based (Figures 1 & 2). Furthermore, the first linear range was established used contaminated cells. Subsequently, samples that were harvested from uncontaminated cells showed that much less protein was required per assay.

Further analysis showed that these trends were established using results from poor transfections. The results presented in Figures 3, 4, 5, & 6 were based on transfections in which fresh DMEM/FBS had been added to over-crowded COS-7 cells immediately prior to transfection (Table 3). Therefore, there were two possible experimental flaws: the use of fresh medium prior to transfection and cell over-crowding. The overall activities were lower when the medium was replaced before transfection. The variance in transfection conditions should have been controlled by seeding cells at a consistent density, by optimizing the ratio of plasmid DNA to Lipofectamine, by monitoring transfection efficiency using a co-transfected protein that is easy to assay, by consistently harvesting cells 24 h post-transfection in fresh HB containing glycerol, and by utilizing an absolute positive control. Briefly, assays of an abundant ASPA source using fixed concentrations

of total NAA, specific activity of radiolabeled NAA, and volume spotted per TLC plate would establish a value for this sample that might reveal assay variance over time if used in each subsequent assay.

While initial hypotheses were based on low specific activities, they were contradicted by further analysis of transfected samples in which the medium had not been changed. Once a linear range was established for optimized transfection and assay conditions, S83A, S105A, and S108A activities were comparable to WT (Figure 12). Therefore, S83A, S83D, S105A, S105D, S108A, S146A, and S307A appear to be silent mutations. In contrast, alanine substitutions of threonines predicted to be phosphorylated (Thr264, Thr277, and Thr298) were not analyzed after transfection and assay conditions were improved. The initial analyses showed significant ASPA activity for each T$\rightarrow$A mutant, which suggests that T264A, T277A, and T298A are not catalytic mutations. Specifically, though Thr277 is an invariant residue contained in one of ASPA's three putative catalytic cores (1) ($_{275}$DCTV$_{278}$), considerable T277A activity (Figures 4A & 6A) implies that Thr277 is not critical for ASPA catalysis.

Bacterial expression is one way to discern whether an effect of serine and threonine substitutions on ASPA activity is due to the loss of a phosphate versus the disruption of catalysis or protein integrity. Since phosphorylation does not occur in bacteria, bacterially-expressed mutants with different activities than WT ASPA would signify different innate protein properties. On the other hand, mutants with different activities than WT ASPA in COS-7 cells, but with unchanged activities in bacteria,

would signify sites of post-translational modification. This approach was recently used to demonstrate glycosylation at Asn117 of ASPA (7).

In this report, the S108D mutant was the only one with ASPA activity that significantly differed from WT ASPA after optimizing transfection and assay conditions. This non-conservative substitution appears to disrupt catalysis because there was undetectable ASPA activity with a sufficient amount of ASPA protein. According to the homology model for ASPA structure (Manuscript 2, Figure 2), the side chain of Ser108 protrudes into the active site. Serine and alanine are small uncharged residues that are unlikely to interfere with nearby catalysis, whereas negatively charged aspartate might interfere with zinc coordination or water-activation required for catalysis.

In conclusion, the main flaw of this investigation was its experimental approach. There is no evidence that ASPA is phosphorylated under any condition, so future approaches should begin with *in vitro* phosphorylation assays using various kinases. A positive result would signify a kinase that can phosphorylate ASPA. The effects of various kinase agonists and inhibitors on ASPA activity in cell culture could subsequently be tested, incorporating various serine substitutions to implicate residues for site-specific phosphorylation. Although this approach would reveal only the indirect effects of activating or inhibitory kinases, a combination of *in vitro* assays and *in vivo* drug treatments might implicate kinases and ASPA residues involved in ASPA regulation by phosphorylation. Subsequently, *in vivo* radiolabeling of COS-7 cells transfected with WT ASPA and various serine and threonine substitutions using activating conditions could be used to best demonstrate site-specific ASPA phosphorylation.

REFERENCES

1. Kaul, R., Gao, G. P., Balamurugan, K., and Matalon, R. (1993) Cloning of the human aspartoacylase cDNA and a common missense mutation in Canavan disease. *Nat Genet* 5, 118-123

2. Birnbaum, S. M., Levintow, L., Kingsley, R. B., and Greenstein, J. P. (1952) Specificity of amino acid acylases. *J Biol Chem* 194, 455-470

3. Matalon, R., Michals, K., Sebesta, D., Deanching, M., Gashkoff, P., and Casanova, J. (1988) Aspartoacylase deficiency and N-acetylaspartic aciduria in patients with Canavan disease. *Am J Med Genet* 29, 463-471

4. Namboodiri, M. A., Corigliano-Murphy, A., Jiang, G., Rollag, M., and Provencio, I. (2000) Murine aspartoacylase: cloning, expression and comparison with the human enzyme. *Brain Res Mol Brain Res* 77, 285-289

5. Fleming, M. C., and Lowry, O. H. (1966) The measurement of free and N-acetylated aspartic acids in the nervous system. *J Neurochem* 13, 779-783

6. Madhavarao, C. N., Hammer, J. A., Quarles, R. H., and Namboodiri, M. A. (2002) A radiometric assay for aspartoacylase activity in cultured oligodendrocytes. *Anal Biochem* 308, 314-319

7. Le Coq, J., An, H. J., Lebrilla, C., and Viola, R. E. (2006) Characterization of human aspartoacylase: the brain enzyme responsible for canavan disease. *Biochemistry* 45, 5878-5884
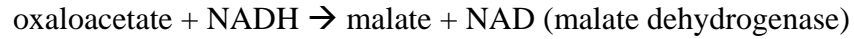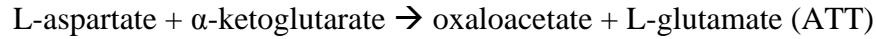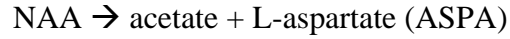
APPENDIX B

ASPA Tools and Techniques

Antibodies

While there is no commercial antibody against ASPA protein, various polyclonal antibodies have been used over the years, with varying degrees of reliability. The first published use of an antibody against ASPA involved rabbit polyclonal antiserum against purified bovine ASPA (1). This antibody, which was later tested in an immunoblot analysis to confirm the absence of ASPA in extracts from CD knockout mice (2, 3), worked poorly for immunohistochemical detection (2). Several years later, the use of polyclonal antiserum against recombinant 6x His-tagged human ASPA purified from *E. coli* that was generated in Wistar rats confirmed the absence of ASPA in *Tremor* rat cerebellum by immunohistochemistry and in mock-transfected human embryonic kidney (HEK) 293 cells by immunocytochemistry (4). Around the same time, a protein G-purified polyclonal antibody raised in rabbits against purified recombinant 6x His-tagged murine ASPA (αASPA) was generated and has since been extensively used in immunohistochemistry and immunoblotting (5, 6).

Enzyme Assays

The activity of ASPA against NAA has been monitored in several ways. The original coupled spectrophotometric ASPA assay (7), which is still in use (1, 8-14), is based on the reaction series:

NAA → acetate + L-aspartate (ASPA)

L-aspartate + α-ketoglutarate → oxaloacetate + L-glutamate (ATT)

oxaloacetate + NADH → malate + NAD (malate dehydrogenase)

The amount of aspartate product is quantified by the decrease in OD_{340}, which corresponds to NADH oxidation by malate dehydrogenase activity. The spectrophotometric assay is subject to high variability due to endogenous aspartate and NADH auto-oxidation and is, therefore, most effective in tissues with high ASPA activity, such as the kidney (15-18). Other ASPA assays that do not use radiolabeled substrate include a separate coupled assay based on aspartase activity (13) and an assay based on NAA depletion as quantified by reverse-phase high performance liquid chromatography (HPLC) (19).

There are several more precise radiometric assays based on the detection of product from radiolabeled NAA substrate (15-18, 20). Arguably the most sensitive assay to date uses [14C]-aspartyl labeled NAA substrate for direct quantification of rabiolabeled L-aspartate product enabled by thin-layer chromatography separation (5, 18). This radiometric assay is characterized by low variability and high sensitivity, which can be improved by increasing the specific activity of the substrate and reducing the total volume of the assay, minimizing the background by reducing the total radioactivity in the reaction blank (18). Another radiometric assay is plagued by higher background activity (15) and contaminations inherent to the use of [3H]-acetic anhydride for substrate synthesis, as well as ion-exchange chromatography to separate the [3H]-acetate product

from the [^{3}H]-NAA substrate (18). By comparison, the [^{14}C]-NAA-based radiometric assay can detect 10 pmol of product while the [^{3}H]-NAA-based assay can detect only 5 nmol of product (15, 18). A third, more laborious and contamination-prone radiometric assay uses [^{14}C]-aspartyl labeled NAA substrate and ion-exchange chromatography (16).

Although the [^{14}C]-NAA-based radiometric assay is currently the most precise ASPA activity assay, the spectrophotometric assay remains the best assay for high-throughput analysis.

Recombinant ASPA

There are relatively few molecular studies involving the expression of recombinant ASPA. Most of these studies have used ASPA cDNA for the *in vitro* analysis of CD-associated ASPA mutations, or for developing vectors for gene delivery. Full-length human and mouse ASPA cDNA have been cloned into vectors such as pEUK-C1 (21, 22), pBAD/Thio-TOPO (8), pcDNA3.1 (20), and pET-3a (4). For mutational analyses of human ASPA cDNA, site-directed mutagenesis has been performed using Clontech's Transformer (20), Invitrogen's GeneTailer (23), and Stratagene's Quick Change II (12) kits. Finally, ASPA has been transfected using Lipofectin (21), DOTAP liposomes (20), and Fugene (4) into COS-1 and COS-7 green monkey kidney cells (20-24), HeLa cells (25), and HEK 293 cells (4, 26).

References

1.	Kaul, R., Casanova, J., Johnson, A. B., Tang, P., and Matalon, R. (1991) Purification, characterization, and localization of aspartoacylase from bovine brain. *J Neurochem* 56, 129-135

2.	Matalon, R., Surendran, S., Rady, P. L., Quast, M. J., Campbell, G. A., Matalon, K. M., Tyring, S. K., Wei, J., Peden, C. S., Ezell, E. L., Muzyczka, N., and Mandel, R. J. (2003) Adeno-associated virus-mediated aspartoacylase gene transfer to the brain of knockout mouse for canavan disease. *Mol Ther* 7, 580-587

3.	Surendran, S., Campbell, G. A., Tyring, S. K., and Matalon, R. (2005) Aspartoacylase gene knockout results in severe vacuolation in the white matter and gray matter of the spinal cord in the mouse. *Neurobiol Dis* 18, 385-389

4.	Klugmann, M., Symes, C. W., Klaussner, B. K., Leichtlein, C. B., Serikawa, T., Young, D., and During, M. J. (2003) Identification and distribution of aspartoacylase in the postnatal rat brain. *Neuroreport* 14, 1837-1840

5.	Madhavarao, C. N., Moffett, J. R., Moore, R. A., Viola, R. E., Namboodiri, M. A., and Jacobowitz, D. M. (2004) Immunohistochemical localization of aspartoacylase in the rat central nervous system. *J Comp Neurol* 472, 318-329

6.	McPhee, S. W., Francis, J., Janson, C. G., Serikawa, T., Hyland, K., Ong, E. O., Raghavan, S. S., Freese, A., and Leone, P. (2005) Effects of AAV-2-mediated aspartoacylase gene transfer in the tremor rat model of Canavan disease. *Brain Res Mol Brain Res* 135, 112-121

7.	Fleming, M. C., and Lowry, O. H. (1966) The measurement of free and N-acetylated aspartic acids in the nervous system. *J Neurochem* 13, 779-783

8.	Namboodiri, M. A., Corigliano-Murphy, A., Jiang, G., Rollag, M., and Provencio, I. (2000) Murine aspartoacylase: cloning, expression and comparison with the human enzyme. *Brain Res Mol Brain Res* 77, 285-289

9.	Chakraborty, G., Mekala, P., Yahya, D., Wu, G., and Ledeen, R. W. (2001) Intraneuronal N-acetylaspartate supplies acetyl groups for myelin lipid synthesis: evidence for myelin-associated aspartoacylase. *J Neurochem* 78, 736-745

10.	Bhakoo, K. K., Craig, T. J., and Styles, P. (2001) Developmental and regional distribution of aspartoacylase in rat brain tissue. *J Neurochem* 79, 211-220

11.	Hagenfeldt, L., Bollgren, I., and Venizelos, N. (1987) N-acetylaspartic aciduria due to aspartoacylase deficiency--a new aetiology of childhood leukodystrophy. *J Inherit Metab Dis* 10, 135-141

12.	Le Coq, J., An, H. J., Lebrilla, C., and Viola, R. E. (2006) Characterization of human aspartoacylase: the brain enzyme responsible for canavan disease. *Biochemistry* 45, 5878-5884

13.	Moore, R. A., Le Coq, J., Faehnle, C. R., and Viola, R. E. (2003) Purification and preliminary characterization of brain aspartoacylase. *Arch Biochem Biophys* 413, 1-8

14.	Matalon, R., Michals, K., Sebesta, D., Deanching, M., Gashkoff, P., and Casanova, J. (1988) Aspartoacylase deficiency and N-acetylaspartic aciduria in patients with Canavan disease. *Am J Med Genet* 29, 463-471

15.	Barash, V., Flhor, D., Morag, B., Boneh, A., Elpeleg, O. N., and Gilon, C. (1991) A radiometric assay for aspartoacylase activity in human fibroblasts: application for the diagnosis of Canavan's disease. *Clin Chim Acta* 201, 175-181

16.	D'Adamo, A. F., Jr., Wertman, E., Foster, F., and Schneider, H. (1978) A radiochemical assay for N-acetyl-L-aspartate amidohydrolase (EC 3.5.1.15) and its occurrence in the tissues of the chicken. *Life Sci* 23, 791-795

17. D'Adamo, A. F., Jr., Smith, J. C., and Woiler, C. (1973) The occurrence of N-acetylaspartate amidohydrolase (aminoacylase II) in the developing rat. *J Neurochem* 20, 1275-1278

18. Madhavarao, C. N., Hammer, J. A., Quarles, R. H., and Namboodiri, M. A. (2002) A radiometric assay for aspartoacylase activity in cultured oligodendrocytes. *Anal Biochem* 308, 314-319

19. Baslow, M. H., Suckow, R. F., Sapirstein, V., and Hungund, B. L. (1999) Expression of aspartoacylase activity in cultured rat macroglial cells is limited to oligodendrocytes. *J Mol Neurosci* 13, 47-53

20. Zeng, B. J., Wang, Z. H., Ribeiro, L. A., Leone, P., De Gasperi, R., Kim, S. J., Raghavan, S., Ong, E., Pastores, G. M., and Kolodny, E. H. (2002) Identification and characterization of novel mutations of the aspartoacylase gene in non-Jewish patients with Canavan disease. *J Inherit Metab Dis* 25, 557-570

21. Kaul, R., Gao, G. P., Aloya, M., Balamurugan, K., Petrosky, A., Michals, K., and Matalon, R. (1994) Canavan disease: mutations among Jewish and non-jewish patients. *Am J Hum Genet* 55, 34-41

22. Kaul, R., Gao, G. P., Michals, K., Whelan, D. T., Levin, S., and Matalon, R. (1995) Novel (cys152 > arg) missense mutation in an Arab patient with Canavan disease. *Hum Mutat* 5, 269-271

23. Surendran, S., Bamforth, F. J., Chan, A., Tyring, S. K., Goodman, S. I., and Matalon, R. (2003) Mild elevation of N-acetylaspartic acid and macrocephaly: diagnostic problem. *J Child Neurol* 18, 809-812

24. Kaul, R., Gao, G. P., Matalon, R., Aloya, M., Su, Q., Jin, M., Johnson, A. B., Schutgens, R. B., and Clarke, J. T. (1996) Identification and expression of eight novel mutations among non-Jewish patients with Canavan disease. *Am J Hum Genet* 59, 95-102

25. Seki, T., Matsubayashi, H., Amano, T., Kitada, K., Serikawa, T., Sakai, N., and Sasa, M. (2002) Adenoviral gene transfer of aspartoacylase into the tremor rat, a genetic model of epilepsy, as a trial of gene therapy for inherited epileptic disorder. *Neurosci Lett* 328, 249-252

26. Leone, P., Janson, C. G., Bilaniuk, L., Wang, Z., Sorgi, F., Huang, L., Matalon, R., Kaul, R., Zeng, Z., Freese, A., McPhee, S. W., Mee, E., During, M. J., and Bilianuk, L. (2000) Aspartoacylase gene transfer to the mammalian central nervous system with therapeutic implications for Canavan disease. *Ann Neurol* 48, 27-38

APPENDIX C

Contributions

Dr. Joyce A. Benjamins:

   Chapter 2, Figure 1

Dr. James Y. Garbern:

   Chapter 2, Figure 1

Dr. Chikkathur N. Madhavararo:

   Chapter 1, Figure 2

   Chapter 2, Figures 1, 2, and 9

   Chapter 4, Figure 1

Dr. John R. Moffett:

   Chapter 2, Figures 3 and 4

Dr. Nagarajan Pattabiraman:

   Chapter 3, Figures 1, 2, and 3